ISTANBUL TECHNICAL UNIVERSITY ★ GRADUATE SCHOOL OF SCIENCE ENGINEERING AND TECHNOLOGY

CHARACTERIZATION OF NFI TRANSCRIPTION FACTORS, NFIB TARGETS AND miRNAS THAT REGULATE NFIB IN HUMAN NEURAL STEM CELLS

M.Sc. THESIS

Gökçe CESUR

Department of Molecular Biology-Genetics and Biotechnology

Molecular Biology-Genetics and Biotechnology Programme

AUGUST 2015

ISTANBUL TECHNICAL UNIVERSITY ★ GRADUATE SCHOOL OF SCIENCE ENGINEERING AND TECHNOLOGY

CHARACTERIZATION OF NFI TRANSCRIPTION FACTORS, NFIB TARGETS AND miRNAS THAT REGULATE NFIB IN HUMAN NEURAL STEM CELLS

M.Sc. THESIS

Gökçe CESUR
(521121138)

Department of Molecular Biology-Genetics and Biotechnology

Molecular Biology-Genetics and Biotechnology Programme

Thesis Advisor: Assist. Prof. Dr. Aslı KUMBASAR

AUGUST 2015

İSTANBUL TEKNİK ÜNİVERSİTESİ ★ FEN BİLİMLERİ ENSTİTÜSÜ

İNSAN NÖRAL KÖK HÜCRELERİNDE NFI TRANSKRİPSİYON FAKTÖRLERİNİN, NFIB HEDEF GENLERİNİN VE NFIB EKSPRESYONUNU DÜZENLEYEN miRNA'LARIN KARAKTERİZASYONU

YÜKSEK LİSANS TEZİ

Gökçe CESUR
(521121138)

Moleküler Biyoloji-Genetik ve Biyoteknoloji Anabilim Dalı

Moleküler Biyoloji-Genetik ve Biyoteknoloji Programı

Tez Danışmanı: Yrd. Doç. Dr. Aslı KUMBASAR

AĞUSTOS 2015

Gökçe CESUR, a M.Sc. student of ITU Graduate School of Science, Engineering and Technology student ID 521121138, successfully defended the thesis entitled ”CHARACTERIZATION OF NFI TRANSCRIPTION FACTORS, NFIB TARGETS AND miRNAS THAT REGULATE NFIB IN HUMAN NEURAL STEM CELLS”, which she prepared after fulfilling the requirements specified in the associated legislations, before the jury whose signatures are below.

Thesis Advisor :	**Assist. Prof. Dr. Aslı KUMBASAR** Istanbul Technical University	.....
Jury Members :	**Prof. Dr. Arzu KARABAY KORKMAZ** Istanbul Technical University	.....
	Assist. Prof. Dr. İbrahim YAMAN Boğaziçi University	.....

Date of Submission : 25 August 2015
Date of Defense : 31 August 2015

To my family and my aunt,

FOREWORD

I would like to start by acknowledging people who made it possible for me to study in this project. My advisor, Assist. Prof. Dr. Aslı Kumbasar was supported and challenged me with her scientific expertise. I would like to sincerely thank for everything that I have learned during the past three years and for her guidance during my practical work and writing of my thesis. I would also like to thank my jury members Prof. Dr. Arzu Karabay Korkmaz and Assist. Prof. Dr. İbrahim Yaman for their time and helpful suggestions.

I would like to thank TUBITAK (KBAG Project Number: 212T017) and Istanbul Technical University Research Fund (ITU BAP) for financial support for the project.

It would be impossible for me go through the project without the learning from Betul Uluca. She provided me her guidance in this work for the duration of my thesis. Also, I would like to express my honest gratitude to all Kumbasar lab members (Varol, Sinem, Cemre, Eda) for their constructive and motivational atmosphere and the kind helpfulness that made the practical work on this thesis a wonderful experience. Especially, I want to thank our undergraduate students (İsmail, Fidan, Tolga, Yusuf, Özlem and Sezgi) for their time we have spent together.

I want to thank ASY lab members for the help at flow cytometry. Additionally, I would like to thank to Cyto lab, especially Koray for sharing their knowledge and reagents during my experiments.

Throughout my thesis, I worked with wonderful friends (Ilgın, Mehtap, Ceren, Oğuzhan, Okan) who make Mobgam easy to study with their smiles. I would like to thank also all Mobgam members for their helpful discussions, advice and support at various time points.

I would like to send my biggest thank to my friends, my aunt, my uncle and my family for never ending support, encouragement and for always believing in me.

August 2015

Gökçe CESUR
(Molecular Biologist & Geneticist)

TABLE OF CONTENTS

Page

FOREWORD ..... **ix**

ABBREVIATIONS ..... **xv**

SYMBOLS ..... **xix**

LIST OF TABLES ..... **xxi**

LIST OF FIGURES ..... **xxiii**

1. INTRODUCTION **33**

1.1 Nuclear Factor One (NFI) Transcription Factors **33**

1.1.1 Discovery of NFI 33

1.1.2 The Evolution of gene regulation by NFI transcription factors 34

1.1.3 Mechanisms of NFI function 36

1.1.4 Roles of NFIs in central nervous system development 38

1.1.4.1 Loss of function studies of NFI members in mice 38

1.1.4.2 Cortex development 39

1.1.4.3 Development of the cerebellum 41

1.1.4.4 Development of the spinal cord 42

1.1.4.5 Development of the hindbrain 43

1.1.5 Role of NFIs during adult neurogenesis 43

1.2 Small non-coding RNAs **44**

1.2.1 Biogenesis of microRNAs 44

1.2.2 miRNA mediated regulation 46

1.2.3 Regulation of NFIs by miRNAs 47

1.3 Putative NFIB Target Genes **48**

1.3.1 CAM-related/down-regulated by oncogenes (CDO) 48

1.3.2 Fibroblast growth factors (FGF19/FGF15) 49

1.3.3 Type II Collagen (COL2A1) 50

1.4 Aim of the Study **51**

2. MATERIALS AND METHODS **53**

2.1 Materials **53**

2.1.1 Equipment 53

2.1.2 Commercial Kits 53

2.1.3 Chemicals 53

2.1.4 Reagents 53

2.1.5 Cell types 54

2.1.6 Growth and freezing Media 54

2.1.6.1 HEK 293T and SH-SY5Y complete medium 54

2.1.6.2 GIBCO complete human neural stem cells (hNSCs) culture medium 54

2.1.6.3 GIBCO human neural stem cells (hNSCs) differentiation medium 54

2.1.6.4 2X Freezing medium for GIBCO hNSCs 55
2.1.6.5 Freezing medium for HEK293T and SH-SY5Y cell lines.....55
2.1.7 Reagents, chemicals, small molecules, buffers for cell culture 55
2.1.8 Bacterial strains 55
2.1.9 Bacterial culture media.....55
2.1.9.1 LB medium and LB-agar medium 55
2.1.9.2 SOC medium 56
2.1.9.3 NZY Broth.....56
2.1.10 Vectors 56
2.1.10.1 pCR-Blunt II-TOPO vector 56
2.1.10.2 pmiRGLO Dual-luciferase miRNA target expression vector 57
2.1.11 Buffers in SDS-PAGE and Western blotting 57
2.1.11.1 5X SDS sample buffer.....57
2.1.11.2 Components of SDS-PAGE gel 58
2.1.11.3 10X Running buffer 58
2.1.11.4 Blocking buffer 58
2.1.11.5 Ponceau-S staining solution 58
2.1.11.6 1X Running buffer and 1X Transfer buffer 58
2.1.11.7 1X TBS and 1X TBS-T 59
2.1.12 Buffers for preparation of whole cell and nuclear protein extracts.....59
2.1.12.2 1X Sample buffer 59
2.1.12.3 Nuclear extract buffer A (NEB-A) and nuclear extract buffer C (NEB-C) (Ravichandran, 2006) 60
2.1.13 Primers 60
2.1.14 Antibodies 62
2.2 Methods 63
2.2.1 Cell culture methods.....63
2.2.1.1 Coating culture vessels for preparing matrix for hNSCs 63
2.2.1.2 Thawing and subculturing GIBCO hNSCs 63
2.2.1.3 Cryopreservation of hNSCs 64
2.2.1.4 Differentiation protocol of hNSCs 65
2.2.1.5 Thawing and subculturing SH-SY5Y and HEK293T cell lines.....65
2.2.1.6 Freezing procedure of SH-SY5Y and HEK293T cell lines 66
2.2.2 Characterization of GIBCO hNSCs 66
2.2.2.1 Immunocytochemistry.....66
2.2.2.2 Flow cytometry 67
2.2.3 Analysis of RNA expression 67
2.2.3.1 Total RNA isolation 67
2.2.3.2 Reverse transcription reaction for total RNA expression analysis...67
2.2.3.3 Expression analysis by Quantitative Reverse Transcriptase PCR (qRT-PCR) 68
2.2.4 Analysis of miRNA expression.....69
2.2.4.1 Total RNA isolation by using mirVana miRNA isolation kit.....69
2.2.4.2 Reverse transcription reaction for microRNA expression analysis .70
2.2.4.3 microRNA expression analysis by quantitative reverse transcriptase PCR (qRT-PCR).....70
2.2.5 Identification of isoforms of NFIB expression in hNSCs.....71
2.2.5.1 Polymerase chain reaction (PCR) 71
2.2.5.2 Agarose gel electrophoresis for the detection of PCR product 74
2.2.6 Analysis of protein expression 74

2.2.6.1 Preparation of whole cell extracts 74
2.2.6.2 Preparation of nuclear extracts 75
2.2.6.3 Determination of protein concentrations 75
2.2.6.4 Sodium dodecyl sulfate-polyacrylamide gel electrophoresis (SDS-PAGE) 76
2.2.6.5 Western blotting 77
2.2.7 Cloning of 3'UTR of NFIB into pCR II_Blunt-TOPO vector 77
2.2.7.1 Primer design for the amplification of fragments of 3'UTR of NFIB for cloning 78
2.2.7.2 Isolation of genomic DNA from SH-SY5Y cell line 78
2.2.7.3 Polymerase chain reaction (PCR) 78
2.2.7.4 Cloning of PCR products into pCR II_Blunt-TOPO vector 79
2.2.7.5 Transformation protocol for NEB 5-alpha competent *E.coli* cells 79
2.2.7.6 Quantitation of DNA 80
2.2.7.7 Restriction enzyme digestion 80
2.2.7.8 Sequencing of selected constructs 80
2.2.7.9 Plasmid preparation 80
2.2.8 Clonining of NFIB 3'UTR fragments from pCR Blunt II_TOPO vector to pmiRGLO Dual-Luciferase miRNA target expression vector 82
2.2.8.1 First strategy for the cloning of PCR products 82
2.2.8.2 Second strategy for the cloning of PCR products 84
2.2.9 QuikChange site-directed mutagenesis for the reporter constructs 85
2.2.9.1 Mutant strand synthesis 85
2.2.9.2 Transformation of ultracompetent XL10-Gold *E.coli* competents 88
2.2.10 Dual luciferase assay 89
2.2.10.1 miRNA mimic and/or inhibitor and reporter construct tranfection using DharmaFECT 1 transfection reagent 89
2.2.10.2 Luciferase assay 89
2.2.11 Statistical analyses 90

3. RESULTS 91
3.1 hNSCs Differentiate into Neurons in Cell Culture 91
3.1.1 Expression of Nestin and neural differentiation marker, TUJ1 91
3.1.2 Flow cytometry analyses of hNSCs progenitors and differentiated hNSCs 92
3.2 Characterization of NFI Expression during Differentiation 93
3.3 NFIB Protein Levels Decrease during hNSC Differentiation 97
3.4 Expression of Putative Downstream Targets of NFIB (CDO, COL2A1, FGF19) are Regulated during hNSC Differentiation 103
3.5 Several miRNAs that can Bind NFIB 3'UTR are Upregulated during hNSC Differentiation 106
3.6 Identification of miRNA Binding Sites on NFIB 3'UTR in Silico 109
3.7 NFIB 3'UTR-Reporter Constructs 110
3.8 Activity of Luc-NFIB 3'UTR Constructs in HEK293T Cells 115
3.8.1 Activity of Luc-NFIB 3'UTR_A and Luc-NFIB 3'UTR_B is repressed by endogenous miRNAs in HEK293T cells 115
3.8.2 Identification of miRNAs that regulate post-transcriptional expression of NFIB 117

4. DISCUSSION AND CONCLUSION 123

REFERENCES **131**
APPENDICES **145**
CURRICULUM VITAE **173**

ABBREVIATIONS

ACC	: Agenesis of corpus callosum
Ad	: Adenovirus
AGO	: Argonaute
Amp	: Ampicillin
BCA	: Bicinchoninic acid
BDNF	: Brain-derived neurotrophic factor
B-FABP	: Brain fatty acid-binding protein
BOC	: Biregional CDON-binding region
BSA	: Bovine serum albumin
CaN	: Calcineurin
CDC2	: Cell division cycle 2
cDNA	: Complementary DNA
CDO	: CAM-related/down-regulated by oncogenes
C. elegans	: *Caenorhabditis elegans*
chr	: Chromosome
COL2A1	: Type II collagen
Ct	: Cycle threshold
CTD	: C terminal domain
CTF	: CAAT box transcription factor
CNS	: Central nervous system
DMEM	: Dulbecco's Modified Eagle Medium
DMSO	: Dimethyl sulfoxide
DNA	: Deoxyribonucleic acid
DNMT1	: DNA methyltransferase I
dNTP	: Deoxyribonucleotide triphosphate
dsRBD	: Double-stranded RNA-binding domain
DTT	: Dithiothreitol
E	: Embryonic day
ECM	: Extracellular matrix
ECN	: External cuneate nucleus
EDTA	: Ethylenediaminetetraacetic acid
EGF	: Epidermal growth factor
EGL	: External granule layer
EGTA	**:** Ethylene glycol tetraacetic acid
eIF4E	: Eukaryotic translation initiation factor 4E
ELU	: Elution buffer
EQU	: Equilibrium buffer
EZH2	: Enchancer of zaste homolog 2
FBS	**:** Fetal bovine serum

FGF : Fibroblast growth factor
Fluc : Firefly luciferase
GABRA6 : α-6 subunit of the $GABA_A$ receptor
GAS-1 : Growth arrest-specific 1
GCP : Granule cell progenitor
GFAP : Glial fibriallry acidic protein
GNP : Granule neural progenitor
GW182 : Glycine-tryptophan repeat-containing protein 182
HEK : Human embryonic kidney
HES : Hairy-enchancer-of-split genes
hESC : Human embryonic stem cell
HL-60 : Human promyelocytic cell line
HRP : Horse redoxperoxidase
IGL : Internal granule layers
IO : Isthmus organizer
iPSCs : Induced pluripotent stem cells
IRES : Internal ribosome entry Site
JAK2 : Janus kinase 2
Kan : Kanamycin
KO : Knockout
LARII : Luciferase assay reagent II
LB : Luria-Bertani broth
LDBR : Lariat-Debranching enzyme
Luc : Luciferase
LRN : Lateral reticular nucleus
LYS : Lysis buffer
Matn1 : Matrillin-1
MAPK : Mitogen activated protein kinase
MH-1 : Mad homology domain
mRNA : Messenger Ribonucleic Acid
miRNA : microRNA
NEB : Nuclear extraction buffer A
NEU : Neutralization buffer
NFATc : Nuclear factor of activated T-cells
NFI : Nuclear factor one
NFIB-S : Short isoform of NFIB
OB : Olfactory bulb
OLIG2 : Oligodendrocyte transcription factor 2
PABP : Poly(A) binding protein
PBS : Phosphate-buffered saline
PCR : Polymerase chain reaction
PFA : Paraformaldehyde
pH : Power of hydrogen
pi : Phosphotase inhibitor cocktail
PML : Premigratory layer
PN : Pontine nuclei

pre-miRNA : Precursor miRNA
pri-miRNA : Primary miRNA
PTBP1 : Polypyrimidine tract-binding protein
qRT-PCR : Quantitative revere transcriptase polymerase chain reaction
RES : Resuspension buffer
Rluc *: Renilla* luciferase
RMS : Rostral migratory system
RNA : Ribonucleic acid
RNAPII : RNA polymerase II
rpm : Revolutions per minute
rSAP : Shrimp alkaline phosphatase
RT : Room temperature
SB : Sample buffer
SDS-PAGE : Sodium dodecyl sulfate-polyacrylamide gel electrophoresis
SHH : Sonic Hedgehog
SOC : Super optimal broth with catabolite repression
SOX9 : Sry-related HMG box 9
SVZ : Subventricular zone
TAE : Tris-acetate-EDTA
TE : Tris-EDTA
TF : Transcription factor
Tm : Melting temperature
UTR : Untranslated region
UV : Ultraviolet
VZ : Ventricular zone
WAP : Whey acidic protein
WR : Working reagent

SYMBOLS

µg	: Microgram
µL	: Microliter
bp	: Base pair
cm	: Centimeter
g	: Gram
h	: Hour
kbp	: Kilo base pair
kDa	: Kilo dalton
L	: Liter
M	: Molar
mA	: Miliamper
min	: Minute
mL	: Mililiter
mM	: Milimolar
mm	: Milimeter
nt	: Nucleotide
sec	: Second
V	: Volt

LIST OF TABLES

		Page
Table 1.1 :	Several miRNAs regulate post-translational expression of NFIs…….	**47**
Table 2.1 :	Reagents……..	**53**
Table 2.2 :	Antibiotics and their stock and working concentrations….	**56**
Table 2.3 :	Formulation of 5X Sample buffer……...	**57**
Table 2.4 :	Formulations of SDS-PAGE gels……	**58**
Table 2.5 :	Formulation of 10X Running buffer……...	**58**
Table 2.6 :	Formulation of Ponceau-S staining solution……...	**58**
Table 2.7 :	Formulations of 1X Running buffer and 1X Transfer buffer……...	**59**
Table 2.8 :	Formulations of 1X TBS and 1X TBS-T……	**59**
Table 2.9 :	Formulation of 1X Sample buffer……...	**60**
Table 2.10 :	Buffers used in preparation of nuclear extracts……...	**60**
Table 2.11 :	Primers for the cloning of 3'UTR of NFIB from SH-SY5Y gDNA……...	**61**
Table 2.12 :	Primers for qRT-PCR……..	**61**
Table 2.13 :	Sequencing primers for pCR II_Blunt-TOPO vector and pmiRGLO Dual-Luciferase miRNA target expression vector……...	**62**
Table 2.14 :	Primers for the In-Fusion cloning of NFIB 3'UTR from TOPO vector to pmiRGLO vector……..	**62**
Table 2.15 :	Antibodies for immunocytochemistry, flow cytometry…..	**62**
Table 2.16 :	Antibodies for Western blotting……..	**63**
Table 2.17 :	Contents of the first part of the cDNA synthesis……	**68**
Table 2.18 :	Contents of the second part of the cDNA synthesis……	**68**
Table 2.19 :	Components of qRT-PCR reaction…….	**69**
Table 2.20 :	RT-Mastermix for one reaction……...	**70**
Table 2.21 :	Parameter values to program thermal cycler……...	**70**
Table 2.22 :	Complete qPCR reaction mix for one reaction and duplicates……	**71**
Table 2.23 :	Thermal cycler parameter for TaqMan assays……	**71**
Table 2.24 :	Primers used to identify isoforms of NFIB expressed in hNSCs…….	**73**
Table 2.25 :	PCR components to identify the expression of alternative splicing forms of NFIB by using C*rimson Taq* DNA polymerase……..	**73**
Table 2.26 :	Thermal cycler parameters with *Crimson Taq* polymerase…….....	**73**
Table 2.27 :	PCR components to identify the expression of alternative splicing forms of NFIB by using *One Taq* DNA polymerase……..	**74**

Table 2.28 : Thermal cycler parameters with *One Taq* DNA polymerase..... **74**
Table 2.29 : Components of the BCA standards..... **76**
Table 2.30 : PCR components for amplification of NFIB 3'UTR by using CloneAmp HiFi PCR Premix..... **79**
Table 2.31 : Components of TOPO reaction..... **79**
Table 2.32 : PCR components by using CloneAmp Hi-Fi PCR Premix. **84**
Table 2.33 : In-Fusion cloning reaction components..... **85**
Table 2.34 : Reagents used for QuikChange multi site-directed mutagenesis kit of desired miRNAs binding sites in NFIB 3'UTR and respective control..... **86**
Table 2.35 : Primers to mutate binding sites of selected miRNAs on NFIB 3'UTR..... **87**
Table 2.36 : Thermocycling parameters for mutant strand synthesis reaction for QuikChange multi site-directed kit..... **87**
Table 2.37 : Reagents used for QuikChange II XL site-directed mutagenesis kit of desired miRNAs binding sites in NFIB 3'UTR and respective control..... **87**
Table 2.38 : Thermocycling parameters for mutant strand synthesis reaction for QuikChange II XL site-directed kit..... **89**
Table 3.1 : Fold changes of *NFIA, NFIB, NFIC* and *NFIX* expression levels between proliferative and differentiating hNSCs in three independent assays. Negative fold change values indicate lower expression in differentiating hNSCs..... **96**
Table 3.2 : Normalized expression of NFIB-1 and NFIB-3 in three independent differentiation assays. Expression is expressed as percentage of proliferative hNSCs..... **103**
Table A.1 : Laboratory equipment used in this study..... **146**
Table B.1 : Commercial kits that are used in this thesis are listed..... **147**
Table C.1 : Chemicals that are used in this study are listed..... **148**
Table D.1 : List of reagents, chemicals, small molecules and buffers used for cell culture..... **149**

LIST OF FIGURES

		Page
Figure 1.1 :	Schematic representation of known alternative splice forms of human NFIB proteins and their domains. ……..	**34**
Figure 1.2 :	Schematic representation of mechanisms of NFIs for cell- or tissue-specific functions. …….....	**37**
Figure 1.3 :	NFIs promote gliogenesis during cortex development……	**40**
Figure 1.4 :	NFIs promote late-neurogenesis during the development of cerebellum……	**41**
Figure 1.5 :	The role of NFIs during the development of the spinal cord and their potential downstream targets…….....	**43**
Figure 1.6 :	Model for miRNA biogenesis……..…	**45**
Figure 2.1 :	pCR-Blunt II-TOPO vector circular map ……..…..	**56**
Figure 2.2 :	pmiRGLO Dual-luciferase miRNA target expression vector circular map…….……	**57**
Figure 2.3 :	Schematic representation of mRNAs that are known as alternative splice forms of NFIB…….…….……	**72**
Figure 2.4 :	Primers were designed to mutate putative miRNA binding sites on 3'UTR of NFIB…….…….….	**86**
Figure 3.1 :	Expression of neural stem cell and differentiation markers in progenitor and differentiated human neural stem cells……	**91**
Figure 3.2 :	The ratio of Nestin^{+} hNSCs decreases upon differentiation....	**92**
Figure 3.3 :	Upon differentiation of hNSCs *NFIB, NFIC* and *NFIX* are downregulated while *NFIA* is upregulated (I)…….……	**93**
Figure 3.4 :	Upon differentiation of hNSCs *NFIB, NFIC* and *NFIX* are downregulated while *NFIA* is upregulated (II)……..…..	**94**
Figure 3.5 :	Upon differentiation of hNSCs *NFIB, NFIC* and *NFIX* are downregulated while *NFIA* is upregulated (III)……..….	**95**
Figure 3.6 :	*NFIA* is upregulated while *NFIB, NFIC* and *NFIX* are downregulated in differentiating hNSCs in a time-dependent manner……..	**96**
Figure 3.7 :	*NFIB-1* and/or *NFIB-3* and *NFIB-4* isoforms are expressed in progenitor hNSCs……..……..	**97**
Figure 3.8 :	NFIB-3 is expressed by hNSCs (I)……..……	**98**
Figure 3.9 :	NFIB-3 is expressed by hNSCs (II)……..……...	**99**
Figure 3.10 :	Characterization of NFIB expression in hNSCs upon differentiation (I)……..…….....	**100**
Figure 3.11 :	Characterization of NFIB expression in hNSCs upon differentiation (II)…….……...	**101**
Figure 3.12 :	Characterization of NFIB expression in hNSCs upon differentiation (III)……..…….....	**101**

Figure 3.13 : Expression of two alternative splicing forms of NFIB decrease during differentiation of hNSCs (III)…….…….. **102**
Figure 3.14 : Characterization of expression of putative NFIB downstream targets (*CDO*, *COL2A1*) in hNSC during differentiation…… **104**
Figure 3.15 : Characterization of expression of putative NFIB downstream targets (*CDO*, *COL2A1, FGF19*) in hNSC during differentiation……... **104**
Figure 3.16 : Characterization of expression of putative NFIB downstream targets (*CDO*, *COL2A1, FGF19*) in hNSC during differentiation in a time-dependent manner……. **105**
Figure 3.17 : Characterization of NFIB targeting miRNAs on mRNA level……..…… **107**
Figure 3.18 : Characterization of NFIB targeting miRNAs on mRNA level during differentiation of hNSCs in a time-dependent manner……..…... **108**
Figure 3.19 : Predicted binding sites of potential NFIB targeting miRNAs on 3'UTR of NFIB……..……. **109**
Figure 3.20 : Fragments of 3'UTR of NFIB was cloned into luciferase reporter vector according to predicted miRNA binding sites.. **110**
Figure 3.21 : NFIB 3'UTR fragments amplified from SH-SY5Y gDNA…. **111**
Figure 3.22 : NFIB 3'UTR_A and NFIB 3'UTR_B fragments were cloned into luciferase reporter vector (pmiRGLO)……. **112**
Figure 3.23 : NFIB 3'UTR_C and NFIB 3'UTR_D fragments were cloned into luciferase reporter vector (pmiRGLO)……..… **112**
Figure 3.24 : Luc-NFIB 3'UTR_B-124M mutant reporter vectors were generated by site-directed mutagenesis…….…….. **113**
Figure 3.25 : Luc-NFIB 3'UTR_D-153M mutant vectors were generated by site-directed mutagenesis…….. **114**
Figure 3.26 : Luc-NFIB 3'UTR_A-124M and Luc-NFIB 3'UTR_A_21 M mutant vectors were generated by site-directed mutagenesis.. **115**
Figure 3.27 : Endogenously expressed miRNAs in HEK293T cells repress (translation of) Luc-NFIB 3'UTR_A and Luc-NFIB 3'UTR_B…… **116**
Figure 3.28 : miR-21 represses Luc-NFIB 3'UTR_A……. **117**
Figure 3.29 : Repression of NFIB 3'UTR_A by miR-21is rescued by anti-miR-21……. **118**
Figure 3.30 : miR-124a represses Luc-NFIB 3'UTR_B, but not Luc-NFIB 3'UTR_A……. **119**
Figure 3.31 : Binding of miR-124 does not repress Luc-NFIB 3'UTR-B_124M……..…… **119**
Figure 3.32 : miR-30a cannot repress translation from Luc-NFIB 3'UTR_A, Luc-NFIB 3'UTR_C or Luc-NFIB 3'UTR_D….. **120**
Figure 3.33 : miR-153 repressed Luc-NFIB 3'UTR_D but not Luc-NFIB 3'UTR_B…… **121**
Figure 3.34 : Binding of miR-153 does not repress Luc-NFIB 3'UTR_D-153M…….. **122**
Figure 4.1 : miR-124 is a key regulator during neurogenesis in embryo and adult brains..... **125**

Figure E.1 : *NFIA* is upregulated while *NFIC* and *NFIX* are downregulated upon differentiation of hNSCs in a time-dependent manner…… **150**
Figure F.1 : Characterization of expression of putative NFIB downstream targets (*CDO*, *COL2A1, FGF19*) in hNSC during differentiation in a time-dependent manner……. **151**
Figure G.1 : Characterization of NFIB targeting miRNAs on mRNA level…….. **152**
Figure H.1 : Characterization of NFIB targeting miRNAs on mRNA level during differentiation of hNSCs in a time-dependent manner**.**..... **153**
Figure L.1 : miR-21 represses Luc-NFIB 3'UTR_A..... **164**
Figure M.1 : Binding of miR-21 on Luc-NFIB 3'UTR_A is reversed by anti-pre-miR-21..... **165**
Figure N.1 : miR-124a represses Luc-NFIB 3'UTR_B, but not Luc-NFIB 3'UTR_A**.**..... **166**
Figure O.1 : Binding of miR-124 does not repress Luc-NFIB 3'UTR_B-124M..... **167**
Figure P.1 : miR-30a cannot repress translation from Luc-NFIB 3'UTR_A, Luc-NFIB 3'UTR_C or Luc-NFIB 3'UTR_D..... **168**
Figure R.1 : miR-153 repressed Luc-NFIB 3'UTR_D but not Luc-NFIB 3'UTR_B……..…… **169**
Figure S.1 : Binding of miR-153 does not repress Luc-NFIB 3'UTR_D-153M..... **170**
Figure T.1 : Predicted binding sites of potential NFIB targeting miRNAs in human, mouse and human……..….. **171**

CHARACTERIZATION OF NFI TRANSCRIPTION FACTORS, NFIB TARGETS AND miRNAS THAT REGULATED NFIB ON HUMAN NEURAL STEM CELLS

SUMMARY

The transcription factors of the nuclear factor one (NFI) family play an important role in regulation of gene expression during nervous system development. NFI family has four members (NFIA, NFIB, NFIC and NFIX) that are highly homologous in their N-terminal DNA binding domains, but vary in their C terminal transcription activation/repression domains. NFIs can induce or repress transcription of different genes in different cell types in a context dependent manner. Each NFI member has multiple alternative splicing isoforms; however, functions of these isoforms of NFIs have not been well described. NFI proteins recognize consensus sequence TTGGC(N5)GCCAA and bind double strand DNA as homo- or heterodimers. In addition, the post-translational modifications (glycosylation or phosphorylation) of NFI proteins can potentially affect or modulate their function.

NFIs are expressed in an overlapping but distinct expression pattern in the developing embryo suggesting a role in regulation of development. All NFIs except for NFIC are expressed in the embryonic central nervous system while expression is restricted to stem cell niches in the adult brain. Deletion of *NFIA*, *NFIB* and *NFIX* leads to distinct phenotypes involving different brain regions such as neocortex, hippocampus, and hindbrain, altering different developmental processes like axonal outgrowth and guidance, differentiation, neurogenesis or gliogenesis.

Previously, we have found that while all three neural NFI proteins are expressed in the precerebellar systems of the hindbrain, only the absence of NFIB lead to a delay in the development of precerebellar nuclei. To understand how NFIB affected neurogenesis in the precerebellar system, potential NFIB target genes were identified in precerebellar neuroprogenitors by mRNA expression profiling. Here, we set out to study regulation of downstream targets of NFIB as well as upstream regulators of NFIB in the human neural stem cell culture system derived from H9 human embryonic stem cell line. To this end, we first characterized the expression of NFI family members and three target genes (*CDO, COL2A1* and *FGF19*) selected according to their expression patterns and known functions. Expression of *NFIB*, *NFIC*, *NFIX*, *CDO* and *COL2A1* was significantly reduced while *NFIA* and *FGF19* were up-regulated during neuronal differentiation. NFIB-4, NFIB-3 and/or NFIB-1 isoform mRNA expression was detected in this cell line. We found that NFIB-3 and NFIB-1 protein expression also decreased in differentiated hNSCs.

To identify novel upstream regulators of NFIB, we first determined miRNA binding sites on the NFIB 3'UTR and looked for those miRNAs that are upregulated in hNSCs during neural differentiation. We analyzed expression of miR-153, miR-30a, miR-124a, miR-92b, miR-130a and miR-363 and found miR-153, miR-124a and miR-30a expression increased while miR-363 decreased in differentiating hNSCs.

Upregulated miRNAs were selected for further study. 3'UTR fragments carrying binding sites of these miRNAs were fused to a reporter gene and screened for inhibition by miRNA mimics. Preliminary data indicate that miR-153 and miR-124a can directly repress translation of NFIB by interacting with 3'UTR_D (6418-6425) and 3'UTR_B (1842-1848) regions on the NFIB. Site directed mutagenesis of miR-153 and miR-124a binding sites appear to render these sites resistant to miRNA mimics, underlining the specificity of this repression.

İNSAN SİNİR KÖK HÜCRELERİNDE NFI TRANSKRİPSİYON FAKTÖRLERİNİN, NFIB HEDEF GENLERİNİN VE NFIB EKSPRESYONUNU DÜZENLEYEN miRNA'LARIN KARAKTERİZASYONU

ÖZET

Nükleer faktör I (NFI) transkripsiyon faktörü ailesi sinir sisteminin gelişimi sırasında gen ifadesinin önemli regülatörlerinden biridir. *C.elegans* ve *Drosophilia* genomunda tek bir NFI geni bulunurken, omurgalılarda N-ucu DNA bağlama bölgesi homolog olan dört farklı NFI üyesi (*NFIA, NFIB, NFIC ve NFIX*) vardır. Bunun yanı sıra NFI genlerinin basit prokaryot ve ökaryotların genomunda bulunmamasından dolayı metazoanlara özgü olduğu söylenilebilir. Ayrıca alternatif kesilim sonucunda her bir NFI proteinin pek çok izoformunun varlığı gösterilmiştir. Ancak izoformların NFI proteinlerinin fonksiyonlarına olan etkisi tam olarak bilinmemektedir.

NFI proteinleri, hedef genlerinin promotor bölgelerinde bulunan palindromik TTGGC(N5)GCCAA dizisini tanıyarak çift iplikli DNA'ya N-ucu domeni aracılığıyla bağlanmaktadır. Bu nedenle N-ucu DNA bağlanma ve dimer oluşturma domeni olarak bilinmekte ve yaklaşık olarak 200-220 aminoasitten oluşmaktadır. Bu bölgede SMAD proteinlerinin DNA'ya bağlanmasında fonksiyonel olduğu bilinen Mad Homoloji 1 (MH1) domenini bulunmaktadır. MH1 domeni içindeki, NFI'larda korunmuş olan dört sistein aminoasidinden üçünün DNA'ya bağlanmada rol aldığı bilinmektedir. Bu domeninin bilinen diğer DNA bağlanma domenleri ile homolojisi bulunmamaktadır. C-ucu domeni ise transkripsiyonel aktivasyon/represyon domeni olarak bilinmektedir. N-ucu domeninde görülen homolojinin aksine, C-ucu domeni NFI izoformlarında farklılık göstermektedir. Bu bölgede yer alan ve sekansın ~ %25'ini oluşturan prolince zengin bölge NFI'ların fonksiyonunda önemlidir. NFI proteinleri arasında C-ucu domenindeki farklılıklaşmaya ek olarak, alternative kırpılma mekanizmaları da izoformlar arasındaki çeşitliliği artırmaktadır ve bu çeşitliliğin NFI izoformlarının farklı fonksiyonları gerçekleştirmesini sağlayabileceği düşünülmektedir.

NFI'ların hücre ya da doku spesifik olarak gen ekspresyonunu: (1) promotorun metilasyon paternini değiştirmesi; (2) nükleozom yapısını değiştirmesi ve/veya RNA polimerazın bağlanmasını etkilemesi; (3) NFI ile rekabet edebilen farklı transkripsiyon faktörlerinin hedef dizisine bağlanmasının engellemesi; (4) genel transkripsiyon faktörleriyle etkileşmesi; (5) hücreye spesifik olarak koaktivatör/korepresörlerle etkileşmesi gibi beş farklı mekanizma yoluyla düzenlemektedir.

Merkezi sinir sisteminde embriyonik dönemde NFIA, NFIB ve NFIX nöral progenitor hücrelerinin bulunduğu ventriküler bölgelerde, nöronlarda ve glialarda ifade edilirken, yetişkin dönemde ise nöral kök hücrenin ve projenitor hücrelerinin lokalize olduğu subventriküler zonda bulunmaktadır. NFIC ifadesinin ise düşük

düzeylerde bulunması sebebiyle nöronal gelişimde önemli bir rol oynamadığı düşünülmektedir.

In vivo çalışmalar sonucunda, bu genlerin ifadesinin susturulmasının, beynin farklı bölgelerinin (hipokampüs, neokorteks, arka beyin, gibi) gelişimini, farklı gelişimsel süreçlerde (nöronal farklılaşma, nörogenez, gliogenez, akzonal uzama ve hücre migrasyonu) etkilediği gösterilmiştir. NFI proteinleri tarafından transkripsiyonu aktive olan genler farklılaşma, gliogenez, dendrit ve akson oluşumu veya hücre taşınımı ile ilgili mekanizmlarda rol oynarken; transkripsiyonu represyona uğrayan genlerin kök hücrenin kendini yenilemesi veya projenitör hücrenin kendini sürdürmesi ile ilgili olduğu görülmüştür. Embriyonik kök hücrelerdeki işlevinin aksine, yetişkin kök hücrelerde NFI proteinleri farklılaşmayı sağlamak yerine kök hücrelerin çoğalmadan sessiz kalmasını ve/veya hayatta kalmasını teşvik etmektedir.

NFI transkripsiyon faktörlerinin beynin farklı kısımlarında farklı fonksiyonları bulunmaktadır. Ön beyinde NFI'ların astrosit oluşumunda önemli olduğu bilinen *GFAP* geninin promotoruna bağlanarak ifadesini arttırdığı ve gliogenezi tetiklediği, bunun yanı sıra kök hücre yenilenmesini aktifleştirecek genlerin (*EZH2, SOX9, HES1)* ifadesini baskıladığı görülmüştür. Beyincik gelişiminde ise NFI'ların erken nörogenez sonrasındaki aşamalarda rol oynadıkları, akson ve dendrit oluşumu ile birlikte hücre migrasyonuyla ilişkili olan genlerin (*TAG1, GABRA6, N-CAD, EPHRIN-B1, WNT7A)* ifadesini kontrol ettikleri bilinmektedir. Omurilik gelişiminde, NFI proteinleri erken nörogenezde farklılaşmayı engelleyerek nöral prekürsör hücre sayısının artmasını sağlarken, geç nörogenez süresince astrosit oluşumu ile ilişkili genleri *(GFAP, MMD2, APCDD1, ZCCHC24, GLAST, FGFR3)* kontrol ederek gliogenez oluşumunu teşvik etmektedir. Buna ek olarak, NFI'lar ile oligodendrosit oluşumu ile ilgili olduğu bilinen OLIG2 transkripsiyon faktörünün ifadelerinin birbiri ile rekabet ettiği görülmüştür. Bu nedenle NFI proteinleri oligodendrit ve astrosit oluşumu arasındaki dengeyi sağlamaktadır.

Daha önceki çalışmalarımızda, NFIA, NFIB ve NFIX proteinlerinin üçünün de arka beyindeki preserebellar sistemde ifade edildiği ve bu proteinlerden sadece NFIB ifadesinin yokluğunda preserebellar çekirdek nöronlarının gelişiminde azalma ve gecikme görülmüştür. Bu sebeple NFIB'nin arka beyin gelişimindeki rolünün nörogenez ile ilişkili olabileceği düşünülmektedir.

Ön araştırmalarda, *NFIB* ifadesinin yokluğunda mRNA ekspresyon analizi yapılarak preserebellar nöroprojenitörlerde NFIB'nin hedef genleri tespit edilmiştir. Bu hedef genlerin içerisinden merkezi sinir sistemindeki fonksiyonları ve ekspresyonları sebebiyle üç hedef genin (*CDO*, *FGF19*, *COL2A1*) öncelikli olarak incelenmesi uygun bulunmuştur.

Nörogenezde temel bir rolünün olduğu düşünülen CDO bir hücre membran proteinidir ve merkezi sinir sisteminde ventriküler bölgelerde ifade edildiği görülmüştür. CDO'nun beyin korteksinde sinyal kompleksi kurarak, bazik heliks-loop-heliks (Neurogenin-1) ve E protein (E47) heterodimerlerinin oluşumuna yol açıp, nöronal farklılaşmayı teşvik etmektedir. Ayrıca SHH yolağında koreseptör olarak da rol almaktadır.

Büyüme faktörü ailesine ait olan FGF19 farede ifade edilen FGF15'in insanda ifade edilen formudur. FGF15'in beyin korteks gelişimi sırasında hücre çoğalmasını durdurarak nöronal farklılaşmayı tetiklediği ve hücre döngüsünü kısalttığı görülmüştür.

COL2A1 ise hücrenin ekstra-hücresel matriksinin (ECM) oluşumunda rol oynayan bir proteindir. ECM proteinlerinin ifadesinin değişimi hücresel farklılaşmada önemli olduğu bilinmektedir. COL2A1'in merkezi sinir sistemi gelişiminde fonksiyonu bilinmemektedir. İlginç olarak, kondrosit gelişiminde NFIB'nin COL2A1 ekspresyonunu kontrol ettiği bulunmuştur.

Bu tez kapsamında, H9 insan embriyonik kök hücre hattından elde edilen nöral kök hücrelerinin (Gibco) farklılaşması sırasında NFI transkripsiyon faktörleri ve hedef genlerin ekspresyonu karakterize edilmiştir. Nöronal farklılaşma sürecinde *NFIA* ve *FGF19* ifadesinin arttığı görülürken; *NFIB, NFIC, NFIX, CDO* ve *COL2A1* genlerinin ifadesinde önemli ölçüde azalma gözlenmiştir. Ayrıca, NFIB'nin ekspresyonunun protein düzeyinde de azaldığı tespit edilmiştir.

Son zamanlarda yapılan çalışmalar miRNA'ların transkripsiyon sonrası düzenlemelerle merkezi sinir sistemi gelişimi sürecinde (hücre kaderinin belirlenmesinde, nöronal farklılaşma, kök hücre/projenitör hücrelerin proliferasyonunda ya da ölümü) rol aldığını göstermektedir. Nöronal farklılaşma sürecinde, NFIB'nin miRNA'lar tarafından post-transkripsiyonel düzenlemeye tabi tutulup tutulmadığını tespit edebilmek amacıyla, NFIB 3'UTR'ını hedeflediği düşünülen miRNA'lar belirlenmiştir. İnsan nöral kök hücrelerinin nöronal farklılaşması sırasında, seçilen miRNA'ların (miR-153, miR-30a, miR-124a, miR-92b, miR-130a ve miR-363) ekspresyon analizleri yapılmıştır. Bu analiz sonucunda da miR-153, miR-124a ve miR-30a ifadelerinin arttığı, miR-363 ifadesinin ise azaldığı bulunmuştur.

Ekspresyon analizleri doğrultusunda, hücre farklılaşması sırasında ekspresyonları artan miRNA'ların NFIB 3'UTR'ına bağlanmasının NFIB'nin ifadesi üzerindeki etkisini belirlemek için bildirici gen (lusiferaz) analizi yapılmak istenilmiştir. Bu amaçla bu miRNA'ların NFIB 3'UTR'ındaki tahmini bağlanma bölgelerini içeren 4.5 kb kısmı, dört farklı bölüme ayrılıp (3'UTR_A, 3'UTR_B, 3'UTR_C ve 3'UTR_D) insan genomik DNA'sından çoğaltılarak pmiRGLO lusiferaz vektörüne klonlanmıştır. Ön veriler sonucunda miR-153 ve miR-124a'nın 3'UTR_D (6418-6425) ve 3'UTR_A (1842-1848) bölgeleri ile doğrudan etkileşime girerek NFIB'nin ifadesini kontrol ettiği bulunmuştur. Ayrıca, miR-153 ve miR-124a bağlanma bölgelerine özgü olarak yapılan mutasyon analizlerinin sonucunda, NFIB ifadesinin bu miRNA'lar tarafından spesifik olarak düzenlendiği tespit edilmiştir.

Bizim çalışmamızla eş zamanlı olarak, fetal sıçan akciğer epitel hücrelerinin olgunlaşması sırasında miR-124a'nın NFIB 3'UTR'ına bağlanarak NFIB ekspresyonunu kontrol ettiği gösterilmiştir. Yine aynı çalışmada miR-124a'nın NFIB 3'UTR'ındaki iki potansiyel bağlanma bölgesine de bağlandığı (214-418 bp ve 1481-1487 bp) tespit edilmiştir. Bunun aksine, bizim çalışmamızın sonucunda bu bağlanma bölgelerinden sadece birine (1481-1487 bp) fonksiyonel olarak bağlandığı gözlemlenmiştir.

Ayrıca çalışmamızla eş zamanlı olarak gerçekleştirilen farklı bir araştırma sonucuna göre, etanole maruz kalınması durumda miR-153 ekspresyonunun arttığı ve nöronal farklılaşmanın daha erken gerçekleştiği görülmüştür. Yine aynı araştırmada miR-153'ün NFIB 3'UTR'ında bulunan iki potansiyel bağlanma bölgesinden birisine (6418-6425 bp) bağlandığı bulunmuştur ve bu bulgular bu tezin sonuçlarını desteklemektedir. Çalışmalarımız sonucunda insan nöral kök hücrelerinin farklılaşması sırasında NFIB ekspresyonu azalırken miR-153 ifadesinin arttığı gözlemlenmiştir. Son olarak yayınlanan başka bir çalışmada ise erken nörogenezde

miR-153 ekspresyonunun dışsal etmenlerin (LIF, BMP2) etkisi ile arttığı ve NFIB ekspresyonunu baskıladığı görülürken, geç nörogenez sürecinde ise miR-153 ekspresyonunun azaldığı ve NFIB ekspresyonunun arttığı gözlemlenmiştir. Bunun sonucunda gliogenez ile ilişkili genlerin ifadesinin arttığı tespit edilmiştir. Bu çalışmalarda elde edilen verilerin, bu tezde sunulan bulgular ile tutarlı olması, insan nöral kök hücre hattında gerçekleştiğimiz farklılaşmanın erken nörogenez sürecine örnek oluşturabileceğini göstermektedir.

1. INTRODUCTION

1.1 Nuclear Factor One (NFI) Transcription Factors

1.1.1 Discovery of NFI

Nuclear Factor One (NFI) family was first identified in and isolated from HeLa cells as a factor required for the *in vitro* replication of Adenovirus DNA (Nagata et al., 1982). Further studies demonstrated that NFI proteins bind as a dimer to a site-specific dyad symmetric consensus sequence TTGGC(N5)GCCAA with high affinity (Gronostasjki et al., 1985; Hennighausen et al., 1985; Leegwater et al., 1985; Nowock et al., 1985). Equilibrium binding constants of the interaction of NFI with different sites of DNA were determined by gel retardation assays indicating that NFI could also bind specifically individual half sites (TTGGC or GCCAA) (Meisterernst et al., 1988). However, binding affinity was reduced (Kd ~ 10^{-9} M) compared to that of dyad symmetric site (Kd ~ 10^{-11} M). NFI-like nuclear proteins were also identified as TGGCA-binding proteins that recognize and bind a symmetrical sequence on the enhancer region of the chicken lysozyme gene (Borgmeyer et al., 1984; Leegwater et al., 1986; Rupp et al., 1990).

NFIs have several alternatively spliced forms. Studies about NFI proteins demonstrated that alternative splicing has a significant role in the regulation of the transcription of viral and cellular gene expression. Differences in transactivation domains play an essential role in cell-specific regulation of promoters (Apt et al., 1994). Recently, a short isoform of NFIB (NFIB-S) that lacks DNA binding domain was detected by using RNA-seq and 5'RACE. Interestingly, this NFIB-S isoform, with NFIC, specifically functions as an important regulator of megakaryocyte differentiation (Chen et al., 2014). Known alternative spliced forms of NFIB are shown in Figure 1.1.

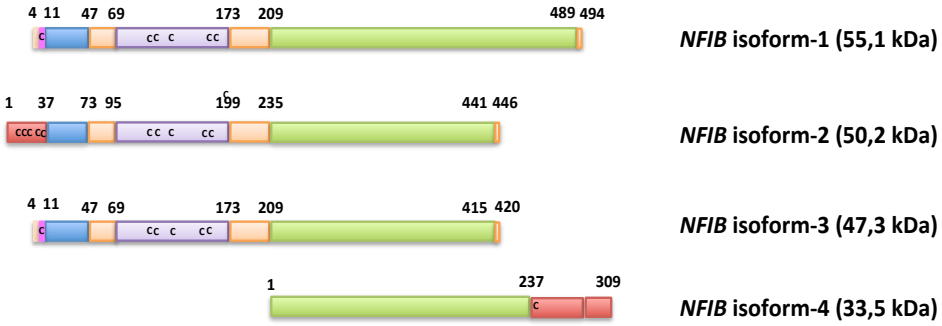


Figure 1.1 : Schematic representation of known alternative splice forms of human NFIB proteins and their domains. Generally, NFIB isoforms contain two major domains: N-terminal DNA binding and dimerization domain and C-terminal transactivation/ repression domain. All known isoforms contain the C-terminal domain while Type IV lacks the N-terminal DNA binding domain. (Blue: Pre-N-terminal subdomain; lilia: MH-1 domain (Mad homology domain discussed below), green: NFI transcriptional modulation region). Molecular weights of proteins were calculated by using SerialCloner 2-6. (NCBI reference codes: NFIB-1, NP_001177666.1; NFIB-2, NP_001177667.1; NFIB-3, NP_005587.2; NFIB-4, NP_001269716.1).

1.1.2 The Evolution of gene regulation by NFI transcription factors

Four different genes (*NFIA*, *NFIB*, *NFIC* and *NFIX)* that encode NFI transcription factors were identified in vertebrates from Xenopus to mouse and humans while a single NFI gene was detected in *C. elegans* and *Drosophila* genomes. However, genome sequencing identified no NFI genes in simple eukaryotes and prokaryotes (Fletcher et al., 1999). The fact that NFI genes are only found in metazoans may be because either these genes evolved later in evolution or have been lost in simple eukaryotes and prokaryotes.

NFI genes are dispersed across three chromosomes in vertebrates. In the mouse genome, *NFIA* and *NFIB* are found on chr 4, *NFIC* is on chr 10 and *NFIX* is located on chr 8 while NFI genes are found on chr 1 (*NFIA*), chr 9 (*NFIB*) and chr 19 (*NFIC* and *NFIX*) in the human genome. NFI family members in vertebrates share structural homologies including a highly conserved N-terminal DNA binding/dimerization domain and C-terminal transcriptional activation/repression domain.

N-terminal DNA binding domain is composed of ~ 200-220 amino acids and includes four cysteine residues that are conserved between all DNA binding domains of NFI. Three of four cysteine residues are essential for the specific DNA-binding activity, while the fourth cysteine residue renders NFI proteins subject to redox

regulation (Bandyopadhyay and Gronostasjki, 1994; Bandyopadhyay, 1998). NFI proteins bind DNA as homo/heterodimers and the N terminal domain is necessary for dimerization as well as DNA binding (Mermod et al., 1989; Gounari et al., 1990). NFI DNA-binding domain contains MH1 (Mad homology) domain first identified in SMAD proteins. The presence of this domain suggests that NFI proteins may contain a similar DNA binding segment as MH1 (Sadreyev and Grishin, 2003). In addition NFIs contain the Cys-His box motif of three cysteine residues and a histidine, suggesting these residues are Zinc binding as in Smad proteins. As mentioned above, these conserved metal binding cysteine residues are essential for DNA binding of NFI proteins (Sadreyev and Grishin, 2003). No other sequence homology with other DNA binding domains has been reported.

In contrast with the highly conserved N-terminal domain, C-terminal domain varies between the NFI members and isoforms. C-terminal domain includes a proline rich region (~ 25% of its sequence). This proline rich region is implicated in gene regulation by NFI proteins. Alternative splicing leads to further variation in the C terminal domains of NFI proteins. Differences between NFI isoforms may determine their specific function in transcriptional regulation. Moreover, NFIs can activate or repress gene expression depending on the cellular context and target promoter (reviewed in Gronostajski et al., 2000).

In addition to NFI dimerization, post-translational modifications (glycosylation or phosphorylation) can potentially control NFI function. 74 kDa N-glycosylated NFIC protein is expressed during early involution in the mouse mammary gland and putative glycosylation sites found in the C terminal domain may potentially affect transcriptional activity (Kane et al., 2002). Additionally, O-linked-glycosylation of the C-terminus of NFIB-2 may be involved in interaction and co-regulative action with STAT-5 in controlling whey acidic protein (WAP) expression in JEG choriocarcinoma cells, a cell line commonly used in the NFI field because of their lack of endogenous NFI expression (Mukhopadhyay and Rosen, 2007). Modifications may change the DNA-binding affinity of NFIs and allow NFIs to compete with other transcription factors for binding to regulatory DNA regions. However, the effect of glycosylation on NFI function has not been yet elucidated. Finally, NFI proteins are also modified by phosphorylation. Cyclin dependent kinase-2 (CDC2) can phosphorylate NFI proteins in phosphorylation assays *in vitro*

*(*Kawamura et al., 1993). Another study showed that prolactin signaling pathway activates receptor-associated tyrosine kinase Janus kinase 2 (JAK2) leading to tyrosine phosphorylation of NFIC-2 preventing its proteasomal degradation and causing transcriptional activation in mammary epithelial cells (Nilsson et al., 2006). Interestingly, Bisgrove et al. (2000) found that the degree of NFI phosphorylation correlated with the expression level of a glial differentiation marker, brain fatty acid-binding protein (B-FABP), in malignant glioma cell lines. NFI phosphorylation appeared to be controlled by a serine/threonine phosphatase, calcineurin (Brun et al., 2013).

1.1.3 Mechanisms of NFI function

NFIs act as homo- or hetero-dimers to modulate transcription by repression or activation of promoters of specific genes suggesting that there are multiple mechanisms by which they perform their cell- or tissue- specific function ((Gronostajski, 2000), summarized in Figure 1.2).

First mechanism involves changes in the methylation status of the promoter: NFIA is induced by Notch signaling pathway, binds glial fibrillary acidic protein *(GFAP)* promoter and causes dissociation of DNA methyltransferase I (DNMT1), leading to demethylation of the promoter and activation of transcription (Namihira et al. 2009). A second mechanism of transcriptional activation by NFIs involves rearrangement of nucleosome structure. Namely, proline-rich transactivation domain of NFIs competes with the structural components (such as histones) for DNA binding or directly interacts with these components (Gao et al., 1998; Alevizopoulos et al., 1995). Specifically, NFIX-3 splice variants activate *GFAP* expression by changing the nucleosome structure and allowing RNA polymerase to bind the *GFAP* promoter (Singh et al. 2011).

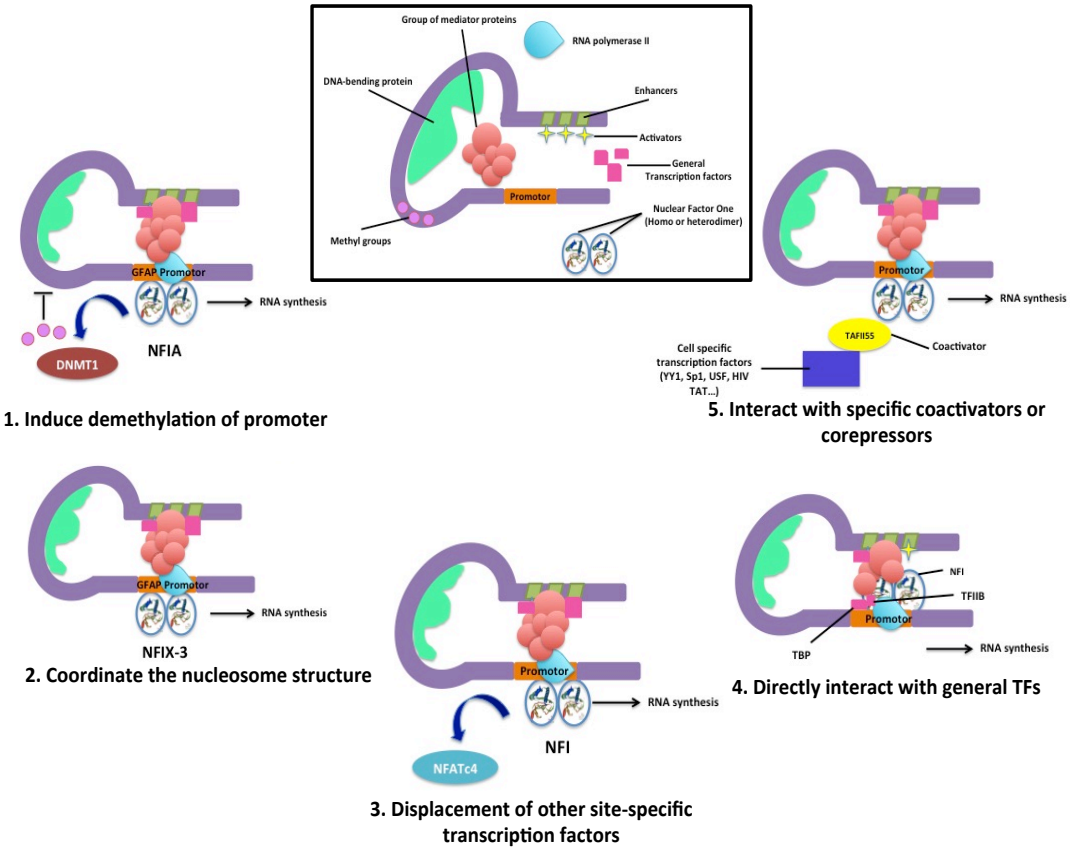


Figure 1.2 : Schematic representation of mechanisms of NFIs for cell- or tissue-specific functions. First mechanism involves the changes in the methylation status of the promoter (Namihira et al., 2009), second mechanism is based on nucleosome rearrangement and interaction with RNA polymerase components (Gao et al., 1998; Alevizopoulos et al., 1995; Singh et al., 2011). In the third mechanism, NFI competes with other site-specific transcription factors for its DNA binding site on the regulatory region (Ding et al., 2013). Fourth regulatory mechanism entails the direct interaction of NFI with the general transcription factors (Kim and Roeder, 1994; Xiao et al., 1994). Last mechanism involves the interaction of NFIs with co-activator and/or co-repressor proteins (Chiang and Roeder, 1995).

A third mechanism has NFIs to compete with other transcription factors for binding to site-specific binding sites on regulatory regions. For example, during development of cerebellar granule neurons, temporal regulation of NFI activated late maturation genes is achieved when another transcription factor, NFATc occupies promoters of these genes and prevents NFI from binding (Ding et al., 2013). A fourth mechanism for NFI function may be through direct interaction with the general transcription factors such as TFIIB (Kim and Roeder, 1994) and TBP (Xiao et al., 1994). Interestingly, some isoforms of NFIA and NFIC carry a single copy of the heptapeptide repeat of C terminal domain (CTD) of RNA polymerase (Xiao et al.,

1994). The CTD repeat is required for NFIs to bind TFIIB (Xiao et al., 1994). Since, all NFI isoforms do not contain this repeat, it is not clear if NFIs regulate gene expression through their interaction with TFIIB (Apt et al., 1993 and Chaudhry et al., 1997). Fifth mode of modulation entails interaction of NFI proteins with specific co-activator or co-repressor proteins. For example, coactivator proteins p300/CBP and SRC-1 interact with truncated NFIC to prevent its repressive effect on the MMTV promoter (Chaudhry et al., 1999).

1.1.4 Roles of NFIs in central nervous system development

Three kinds of cell types (neurons, astrocytes and oligodendrocytes) generate the mature mammalian central nervous system (CNS). Early in neural development, neuroepithelial cells populate the neural plate that folds to give rise to the neural tube. Initially, these cells undergo two different divisions: asymmetric and symmetric. As the CNS will be made of millions of neural cells, expansion of stem cell population is required to create large numbers of cells of many different cell types. Neural stem cell population expands through symmetric cell divisions, while intermediate progenitor cells that generate neurons are formed as a result of asymmetric cell division. Neurogenesis is followed by gliogenesis, where neural progenitors now generate astrocytes and then oligodendrocytes.

Three NFI family members, NFIA, NFIB and NFIX are expressed in the developing CNS within the ventricular zones by progenitor cells and also they are expressed in neurons and glia. The phenotypes of knockout (KO) mice for these genes show that they play important roles in neural development. Specifically, loss of each neural specific NFI gene has distinct effects on the development of different brain regions such as neocortex, hippocampus, cerebellum and hindbrain involving different processes like axonal outgrowth and guidance, differentiation, neurogenesis or gliogenesis.

1.1.4.1 Loss of function studies of NFI members in mice

Each NFI gene is widely expressed with overlapping but unique expression patterns in distinct organ systems during mouse embryonic development (Chaudhry et al., 1997). Also targeted knockout studies of the four NFI genes in mice indicate that *NFIA, NFIB, NFIC* and *NFIX* are important regulators in CNS, lung, musculoskeletal and teeth development.

Ablation of *NFIA, NFIB,* or *NFIX* genes has revealed distinct neurological defects in different brain regions during development (das Neves et al., 1999; Grunder et al., 2002; Steele-Perkins et al., 2005; Plachez et al., 2008; Heng at al., 2012). Interestingly, *NFIA* and *NFIB* KO mice display remarkably similar phenotypes including agenesis of the corpus callosum (ACC) and enlarged lateral ventricles. Agenesis of the corpus callosum is probably due to disruption of midline glia populations in *NFIA* KO mice (Shu et al, 2003). *NFIB* KO mouse also exhibits a similar phenotype, with similar defects in the development of glia along the midline (Steele-Perkins et al., 2005). *NFIX*-null mice do not exhibit ACC, but enlargement of the lateral ventricles of the brain is one of the observed defects similar to those in *NFIA* and *NFIB* KO mice. *NFIC*-null mice do not appear to have an abnormal neurological phenotype and this result is consistent with the low-levels of NFIC expression in the developing telencephalon (Chaudhry et al., 1997).

Outside the nervous system, *NFIB* gene is an important regulator of lung development and *NFIB*$^{-/-}$ mice exhibit perinatal lethality due to lung hypoplasia (Steele-Perkins et al., 2005). Thus, *NFIB* null mice cannot be inspected postnatally for developmental defects. Additionally, *NFIC* expression regulates the thooth root formation during embryonic and postnatal development (Steele-Perkins et al., 2003) and *NFIX*-null mice exhibit musculoskeletal system defects suggesting a crucial role in myogenesis (Messina et al., 2010).

1.1.4.2 Cortex development

Expression of NFIA, NFIB and NFIX is detected within the ventricular zone from embryonic day 12 (E12) to the end of the cortical development (Plachez et al., 2008; Campbell et al., 2008). Moreover, knockout of NFI genes results in the expansion of the neural stem cell population in the ventricular zone of neocortex and hippocampus at the expense of astrocytes and intermediate progenitor cells (Piper et al, 2010; Betancourt et al., 2014; Heng et al., 2012). Specifically, *NFIB* null mice show defects in axon formation and migration of neurons and downregulation of the number of progenitor cells. Lack of NFIB leads to defects in both neurogenesis and terminal differentiation of cortical neurons (Betancourt et al., 2014). NFIA and NFIB repress hairy and enchancer split-1 (*HES1*) expression, a Notch effector, and promote neurogenesis (Piper et al, 2010). In the hippocampus, NFIX represses Sry-related

HMG box 9 (SOX9) expression, a progenitor cell self-renewal mediator, and induces neuronal differentiation, (Heng et al. 2012).

Several pieces of evidence implicate NFI proteins as regulators in gliogenesis. First, NFI proteins bind to the promoter of *GFAP* (astrocyte marker) and are important for expression of this gene in rat cortical precursors (Cebolla and Vallejo, 2006). Notch induced regulation of *GFAP* promoter by NFIA was described above (Namihira et al., 2009). Consistent with this result, NFIX-3, an NFIX splice variant, activates *GFAP* expression in primary human astrocytes (Singh et al. 2011). Chromatin modifying protein, Enhancer of zaste homolog 2 (*EZH2*) was shown to be transcriptionally repressed by NFIB in the cerebral cortex where some of the developmental defects observed in the absence of *NFIB* may be due to removal of repression of *EZH2* (Piper et al., 2014). *SOX9*, a key factor for stem cell maintenance, is also repressed by NFIX during hippocampal development (Heng et al., 2012). Notch pathway is mainly involved in progenitor cell self-renewal, inhibiting genes required for neurogenesis and gliogenesis (Shimojo et al., 2008). NFIA directly binds and represses expression of HES1, a Notch effector (Piper et al., 2010) thus inhibiting progenitor self-renewal and facilititating differentiation during telencephalon development. Elsewhere, in the spinal cord NFIA and NFIB activate *HES5*, another Notch effector and keep neural progenitors from differentiating until later where they activate astrocytogenesis (Deneen et. al, 2006).

These observations are consistent with the key role of NFIs in the timing of the switch between neurogenesis and gliogenesis during development of the neocortex and a summary of their role and the other key players are presented in Figure 1.3.

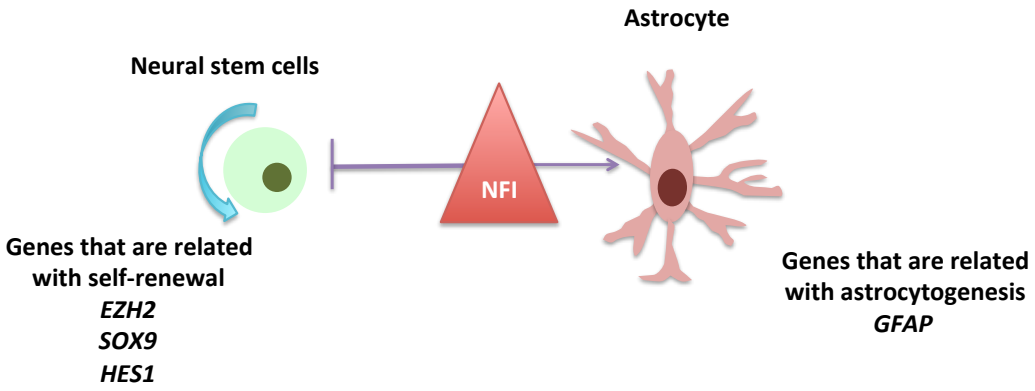


Figure 1.3 : NFIs promote gliogenesis during cortex development.

Figure 1.3 (cont'd) : NFIs promote gliogenesis during cortex development. (*GFAP)* is directly activated by NFIs and is involved in astrocytogenesis (Cebolla and Vallejo et al., 2006). Moreover, genes associated with self-renewal of neural stem cells (*EZH2, SOX9* and *HES1* ((Piper et al., 2014; Heng et al., 2012; Scott et al., 2010)) are other downstream NFI targets and are repressed by NFIs.

1.1.4.3 Development of the cerebellum

During the differentiation of cerebellum, granule neural progenitors (GNPs) proliferate in the outer external granule layer (EGL) before they differentiate into mature granule cells. During the differentiation process, GNPs begin to migrate tangentially to form premigratory (PML) and internal granule layers (IGL), GNPs stop proliferation and terminally differentiate within the IGL. In contrast with their role in neurogenesis and gliogenesis during telencephalon development, NFI transcription factors play a role in the terminal differentiation and migration stages of granule cells. NFI proteins regulate expression of α-6 subunit of the $GABA_A$ receptor (*GABRA6*), cell adhesion molecules (*EPHRIN B1, N-Cadherin* and *TAG1*) and an extracellular signaling molecule (*WNT7A*) in differentiated cerebellar granule neurons (Wang et al., 2004; 2007; 2010 and Kilpatrick et al., 2012). Interestingly, NFIA, NFIB and NFIX expression is upregulated in the nuclei of the granule cells as they become postmitotic within the EGL and expression persists in the IGL, indicating that these proteins are involved in regulation of postmitotic granule cells (Wang et al., 2007).

A summary of current findings on NFI function and expression pattern during post-mitotic maturation of cerebellar granule progenitors and NFI downstream targets, are shown in Figure 1.4.

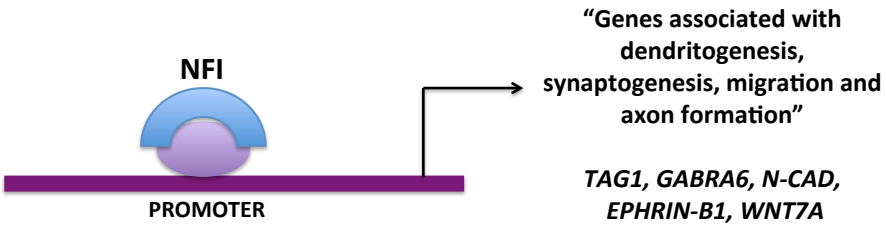


Figure 1.4 : NFIs promote late-neurogenesis during the development of cerebellum. NFIs regulate transcriptional targets (*TAG1, GABRA6, N-Cadherin, EPHRIN-B1* and *WNT7A*) that are required for terminal differentiation, migration, synapse and dendrite formation (Wang et al., 2004; Wang et al., 2007; Wang et al., 2010 and Kilpatrick et al., 2012).

In addition to cerebellar granule cell culture, P17 *NFIA*-null mice exhibit a delay in migration and dendritogenesis of granule cells. Axon formation is also reduced in EGL/PMZ of *NFIB*-null mice. NFIX is also expressed in cerebellar progenitors and cerebellar granule cells. Development of cerebellar granule neurons, as well as Purkinje neurons and astrocytes is delayed in *NFIX*$^{-/-}$ mice (Piper et al. 2011). In a recent study, NFIs were found to play a role in the switch to late maturation gene expression program in GNP development. NFI temporally upregulates genes that are late expressed in CGNs and required for precise GABA receptor maturation and dendrite and synapse formation. NFI occupancy of these genes may be inhibited and delayed by calcineurin activity in depolarized conditions through the binding of NFATc4 to late-expressed gene promoters (Ding et al., 2013).

1.1.4.4 Development of the spinal cord

During the development of the spinal cord, NFIs play an essential role in determination of glial lineages. At early stages, during neurogenesis, NFIs inhibit differentiation by inducing expression of Notch effector (*HES5*) to maintain a pool of precursors that can later differentiate into glia. Induction of gliogenesis is regulated by NFI binding to the promoters of early glial specification genes (*GLAST, FGFR3, OLIG2)*. At later stages, NFIA and NFIB promote astrocytogenesis that can be antagonized by actions of oligodendrocyte transcription factor 2 (OLIG2), the basic helix-loop-helix transcription factor, which directs precursors to differentiate into oligodendrocytes (Deneen et al., 2006). Moreover, while NFIX represses SOX9 during telencephalon differentiation (Heng et al., 2012), in the spinal cord SOX9 induces NFIA expression and these two proteins form a complex to regulate a set of genes expressed after onset of the gliogenesis (Kang et al., 2012).

In contrast to the synergistic effects of SOX9 and NFIA, NFIA and SOX10 mutually antagonize each other during spinal cord development in chick and mouse, creating a balance between oligodendrocyte and astrocyte fates (Glasgow et al., 2014) by regulating myelin genes and astrocyte related genes. In short, during the development of the spinal cord, NFIs function to maintain a population of precursors by repressing neurogenesis. Later, they promote astrocytogenesis and also regulate gliogenic fate (summarized in Figure 1.5).

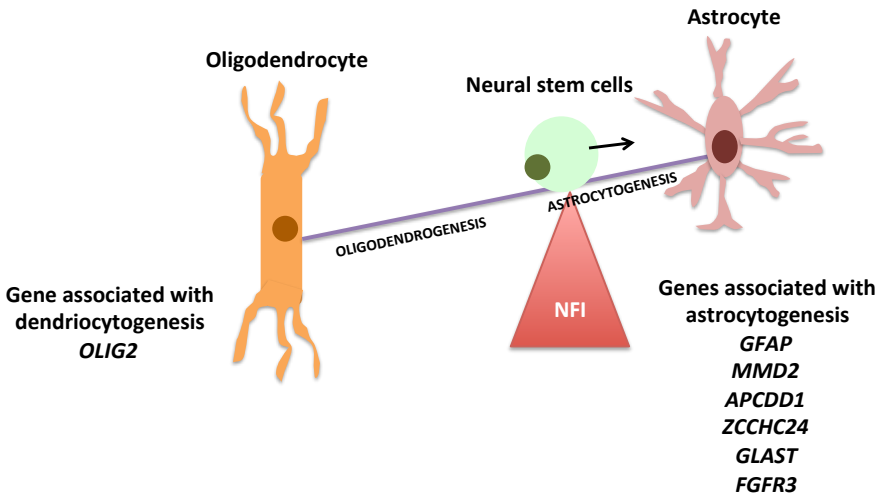


Figure 1.5 : The role of NFIs during the development of the spinal cord and their potential downstream targets. NFIs regulate gliogenesis and also function as a balance between the oligodendrite and astrocyte generation by regulating related genes expression (*OLIG2, GLAST, FGFR3, APCDD1, ZCCHC24* and *MMD2* (Deneen et al., 2006; Kang et al., 2012)).

1.1.4.5 Development of the hindbrain

The precerebellar system of the hindbrain comprises several nuclei that relay input from the cerebral cortex to the cerebellum. These neurons are generated from the rhombic lip, the neuroepithelium that lines the opening of the fourth ventricle of the hindbrain, and migrate tangentially to their final locations to form their respective nuclei (Gallego et al., 2005). While all three neural NFIs are present in the precerebellar progenitors of the hindbrain (Chaudhry et al., 1998), only deletion of *NFIB* leads to a delay in development of precerebellar nuclei (Steele-Perkins et al., 2005). Closer look at the *NFIB*$^{-/-}$ phenotype showed a decrease in generation of pontine neurons with no effect on migration or survival indicating a role in neurogenesis (Kumbasar et al, 2009). Other precerebellar nuclei including the lateral reticular nucleus (LRN) and the external cuneate nucleus (ECN), like the pontine nuclei (PN), also exhibit developmental defects in *NFIB* deficient mice.

1.1.5 Role of NFIs during adult neurogenesis

As the generation of neurons in the adult is a rare event, most of the neural stem cells are thought to be in a quiescent state. In the adult, NFIs are also expressed in ventricular zones that are populated by stem cells and occupy quiescence specific enhancers in adult neural stem cells (Plachez et al., 2008; Plachez et al., 2012; Campbell et al., 2008; Martynoga et al. 2013). Specifically NFIX was found to

induce the quiescent state in cultured NSCs, but the analysis of NFI null adult stem cells *in vivo* awaits generation of conditional NFI knockout mice. However, data from studying other, melanocyte and hematopoietic adult stem cells, supports the idea that NFIs promote quiescence and/or cell survival rather than differentiation in the adult (Chang et al., 2013; Holmfeldt et al., 2013; Martynoga et al., 2013).

1.2 Small non-coding RNAs

Until the discovery of lin-4 transcripts in *C. elegans* (Lee et al., 1993), it was generally believed that RNA functioned only in protein synthesis. In this study, 22 nt and 61 nt transcripts of lin-4 were identified as non-coding RNAs that regulate the translation of lin-14 via interaction with its 3'untranslated region (UTR) thus controlling timing of transition between larval stages in *C. elegans* (Chalfie et al., 1981). A genetic screen for heterochronic genes in *C.elegans* led to discovery of stage-specific expression of a novel class small RNAs (let-7) during the development of larva (Reinhart et al., 2000). After the rise of next generation sequencing, small RNA sequencing combined with bioinformatics identified hundreds of small RNAs from plants to humans (Lau et al., 2001; Lee and Ambros, 2001; Llave et al., 2002; Lagos-Quintana et al., 2001; Rhoades et al., 2002). Biogenesis of non-coding RNAs and their functions in development, disease and physiology have been characterized in more detail recently.

1.2.1 Biogenesis of microRNAs

miRNAs are single-stranded RNAs of about 21 nucleotides (nt) and based on their location in the genome are classified into two subgroups: intergenic or intragenic (Bartel et al., 2004). Intragenic microRNAs are located within the introns or exons of protein coding gene and transcribed within the same orientation by RNA Polymerase II (RNAPII). On the other hand, intergenic microRNAs are independent from the coding genes and expressed by RNA Polymerase III.

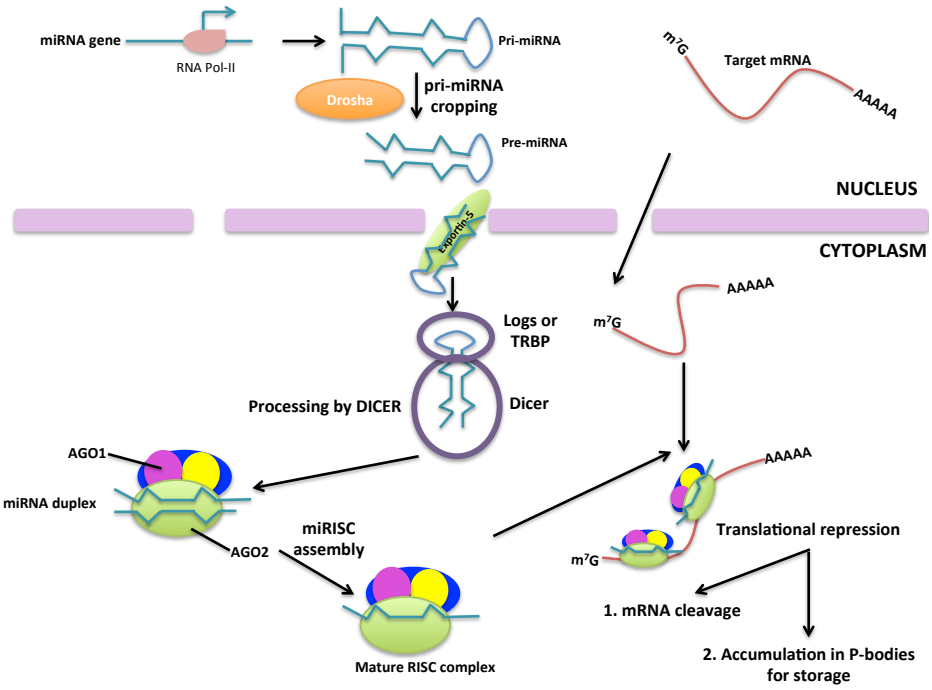


Figure 1.6 : Model for miRNA biogenesis. miRNAs are transcribed by RNAP II and cropped by DROSHA and DGCR8 complex. pre-miRNA is translocated to cytoplasm by exportin-5 and mature miRNA is generated by DICER enzyme. Mature miRNA is assembled into the RISC complex and binds seed region on 3'UTR of target gene for post-transcriptional modulation.

Generally, primary miRNAs (pri-miRNAs) are transcribed from the genomic DNA by RNA polymerase II/III and 5'-7-methylguanosine capped and 3'polyadenylated like mRNAs (reviewed in Maciotta et al., 2013). pri-miRNAs form hairpin structures and can range from several hundred nucleotides to tens of kilobases in size. RNase III enzyme (DROSHA) and double-stranded RNA-binding domain (dsRBD) protein "DGCR8" generate a multi-protein complex called as "microprocessor complex" and this complex cleaves at the stem of the hairpin structure. This shorter (~65 nt long) precursor miRNA (pre-miRNA) is released and translocated to the cytoplasm in a Ran-GTP-dependent manner by exportin-5. Another RNAse III enzyme (DICER) cleaves pre-miRNA to generate a 19-25 nt double stranded mature miRNA duplex. A single strand (guide strand) is loaded onto Argonaute proteins and other protein factors to form effector complexes. This complex is mostly directed to the 3'UTR of target mRNA to carry out post-transcriptional regulation. However, 5'UTR and/or coding regions of some mRNAs can also be targeted by miRNAs (reviewed in Ha & Kim, 2014). Biogenesis of miRNAs is summarized in Figure 1.6.

1.2.2 miRNA mediated regulation

The specificity of the regulation by miRNAs is based on the target recognition sequence known as the seed region (2-8 nt). The extent of the match between miRNA seed region and mRNA is the main factor to determine the strength and effect of the translational control of gene expression (Wang, 2014). Complete complementarity between miRNA and mRNA sequence match is needed for mRNA degradation to control translation. On the other side, formation of translation complex is inhibited for post-transcriptional control whether pairing of miRNA and mRNA match is nearly complementary. Additionally, other factors such as the accessibility of the binding site, RNA secondary structure, the number of the target sites for the same miRNA can also influence the outcome of the miRNA-mRNA interaction (reviewed in Valinezhad et al., 2014).

Most animal miRNAs promote translational repression rather than cleavage or degradation of mRNA. miRNAs function as a nucleic acid core to form complexes with argonaute proteins (AGO1-4) and argonaute-bound glycine-tryptophan repeat-containing protein 182 (GW182) to repress protein expression. Kiriakidoui et al. (2007) showed that Ago2 protein contains a motif similar to that found on the m(7)G-cap binding domain of eIF4E (eukaryotic translation initiation factor 4E). This structural similarity allows Ago2 proteins to compete with eIF4E for binding to the cap structure**.** Evidence for the repression by miRNAs early in the translation process comes from another study found that Ago2 proteins also interact with the large ribosomal subunits and eIF6 (Chendrimada et al., 2007). As eIF6 catalyzes the association of 40S and 60S ribosomal subunits, Ago2 would then prevent the joining of ribosomal subunits to initiate the translation. Nevertheless, the mechanisms by which miRNAs inhibit translation initiation are not known in greater detail. However, other data suggest that miRNAs inhibit translation at post-initiation steps rather than initiation (Kim et al., 2004; Nelson et al., 2004). Repression by small RNAs may be at the level of elongation causing more rapid dissociation of ribosomes from the mRNA (Petersen et al., 2006). Furthermore, let-7a interferes with the growing polypeptide chain and promotes the degradation of nascent polypeptides (Nottrott et al., 2006). Moreover, when hepatitis C virus internal ribosome entry site (IRES) was placed upstream of a reporter construct to circumvent steps involved in initiation on capped mRNAs, translation was still repressed (Lytle et al. (2007).

Thus, translational regulation by miRNAs seems to involve steps downstream from initiation.

1.2.3 Regulation of NFIs by miRNAs

Several pieces of evidence support a role for miRNAs in the regulation of NFIs during progenitor cell differentiation. NFIA is in a negative feedback loop with miR-223, a miRNA that is upregulated during granulocytic differentiation (Fazi et al., 2005). NFIA expression keeps levels of miR-223 expression low in myeloid precursor cells and is later repressed by miR-223 upon differentiation. This regulatory relationship between miR-223 and NFIA in granulopoiesis is reproduced in the CNS (Glasgow et al., 2013). As described earlier NFIA is a key regulator of gliogenesis; miR-223 suppresses NFIA and inhibits glial precursor proliferation during spinal cord development and glioma tumorigenesis. Studies on granulocytic differentiation that followed up on findings by Fazi et al found that miR-107 was also upregulated during granulocytic differentiation, and targets NFIA (Garzon et al., 2007). In addition, there is a similar double negative feedback loop between NFIB and miR-21 where NFIB has to dissociate from the miR-21 promoter in HL-60 cell line (human promyelocytic cell line) to enable its expression during macrophage differentiation (Fujita et al., 2008). Studies of regulation of NFIs by miRNAs during progenitor cell differentiation are summarized in Table 1.1.

Table 1.1 : Several miRNAs regulate post-translational expression of NFIs.

miRNAs	Target gene	Function	References
miR-223	*NFIA*	Granulocytic differentiation of myeloid precursor cells	Fazi et al., 2005
miR-107	*NFIA*	Granulocytic differentiation of myeloid precursor cells	Garzon et al., 2007
miR-21	*NFIB*	Macrophage differentiation in HL-60 cells	Fujita et al., 2008
miR-223	*NFIA*	Granulocytic differentiation in the spinal cord	Glasgow et al., 2013

In a recent study (Tsai et al., 2014), miR-153 was identified as a translational regulator of NFIA/NFIB. Two predicted binding sites of miR-153 were identified on NFIB 3'UTR, however translation of NFIB is regulated by binding only one of those sites (Target 6559-6566). Moreover, two of three predicted binding sites on NFIA 3'UTR (Target 7285-7306 and Target 9451-9469) were identified as functional.

NFIB expression is controlled by miR-153 and miR-153 is downregulated in mouse neural stem cells under ethanol exposure. Decrease in miR-153 expression upon ethanol exposure lead to increased amounts of NFIA/NFIB expression, which resulting in premature neuronal differentiation.

Finally, NFIB has also been showed as a direct target of miR-124 in rat lung epithelial cells. Mutations of the predicted miR-124 binding sites in the 3'UTR of NFIB showed that both sites are functional and miR-124 inhibits lung maturation in part by repressing NFIB (Wang et al., 2015).

1.3 Putative NFIB Target Genes

While all NFI proteins are present in the precerebellar neuroepithelium of the hindbrain (Chaudhry et al., 1998), only deletion of *NFIB* leads to a delay in the development of pontine neurons of the precerebellar system (Kumbasar et al., 2009). Molecular mechanisms behind the regulation of neurogenesis by NFIB in the pecerebellar development have not yet been studied. In order to identify potential NFIB target genes, mRNA expression profile of precerebellar neuroprogenitors was performed and thirty-three candidate genes were identified (Kumbasar et al., unpublished data). According to their known functions and expression profiles, three of them (*CDO, COL2A1* and *FGF19*) were selected for further study in this thesis.

1.3.1 CAM-related/down-regulated by oncogenes (CDO)

Cell adhesion molecules play important roles in development, since they can regulate cellular structure, growth, and cell motility. CDO (CAM-related/down-regulated by oncogenes) was first defined as a member of the Ig superfamily that contains extracellular five Ig-like domains and three trans-membrane FNIII-like repeats. CDO may play an essential role in neurogenesis. First of all, CDO is expressed in the ventricular zones in the telencephalon, diencephalon and midbrain as well as the cerebellar and precerebellar neuroepithelium (rhombic lip) of the hindbrain in the mouse embryo while its expression becomes restricted in the adult (Mulieri et al., 2000). Second, mice lacking CDO show defects in brain development including thinned neocortex, holoprosencephaly, hydrocephaly and decreased differentiation (Zhang et al. 2006). Further experiments showed that CDO promotes neuronal differentiation by facilitating heterodimerization of bHLH protein neurogenin1 with E protein E47 in the cerebral cortex. Interestingly, the signaling pathway by which

CDO promotes neuronal differentiation in cell culture (C17.2 neural precursor cell line and P19 embryonal carcinoma cell line) is similar to that found for myogenic differentiation (Oh et al., 2009).

The role of CDO has been investigated in different pathways CDO functions with GAS1 (Growth arrest-specific 1) and BOC (Biregional Cdon-binding region) as coreceptors of SHH signalling pathway during neural development (Tenzen et al., 2006). Moreover, CDO acts as a corepressor of Wnt signaling by interacting with LRP6 during neuronal differentiation in the dorsal forebrain (Jeong et al., 2014). Thus, CDO functions as a coordinator between WNT and SHH signalling pathways during the dorsal forebrain development (Jeong et al., 2014).

In addition to its role in neurogenesis, CDO also regulates the differentiation of myoblasts in multifunctional mechanisms such as SHH-dependent or p38-MAPK dependent pathways. It directly interacts with SHH and serves a corepressor during differentiation of cultured myoblasts (Tenzen et al., 2006; Yao et al., 2006). However, CDO is also involved in SHH independent p38-dependent kinase pathway (Lu and Krauss, 2010). CDO forms a complex with N-Cadherin on the cell-surface which induces CDO to bind to BNIP-2 and JLP, which further interacts with CDC42, resulting in p38-MAPK dependent differentiation of myoblasts (Kang et al., 1998; 2003; 2008).

1.3.2 Fibroblast growth factors (FGF19/FGF15)

The family of fibroblast growth factors (FGFs) functions as a signaling molecule by interacting with FGF-tyrosine-kinase receptors and activates two major phosphorylation cascades (Ras/mitogen activated protein kinase (MAPK) and the phosphatidylinositol 3-kinase/AKT pathways) to mediate proliferation, differentiation and survival (Mason, 2007). This family comprises at least twenty-two distinct members that are grouped into seven subfamilies that are highly conserved and share greater than 90% amino acid identity throughout the various species (Itoh and Ornitz, 2004). In contrast to other members, *FGF15/ FGF19*, *FGF21* and *FGF23* subfamily is known as the endocrine FGFs enabling them to enter into the bloodstream and act on distant tissues (Goetz et al., 2007). *FGF15* was firstly identified as a novel FGF of the central nervous system (McWhirter et al., 1997). *FGF19* is the human, chicken and zebrafish orthologs of mouse *FGF15* (Nishimura et al., 1999). Although, human *FGF19* and mouse *FGF15* share only

approximately 50% amino acid identity, they are seen as structurally and functionally orthologous (Miyake et al., 2005; Nishimura et al., 1999; Wright et al., 2004). The function of *FGF15* in CNS is not clearly defined; however, its role in neurogenesis is revealed in several studies, in contrast to other members of FGF family that promote proliferation. *FGF15* induces neural differentiation by suppressing proliferation and reduces cell cycle length and exit during cortical development (Borello et al., 2008). Interestingly, here expression of *FGF15* is regulated by SHH. SHH pathway is also involved in regulation of the orthologs in the mouse and chick midbrain and as well as zebrafish hindbrain (Saitsu et al., 2005; Miyake et al., 2005; Gimeno and Martinez, 2007). Further study showed that *FGF15* has an effect on the expression of helix-loop-helix proneural transcription factors that are involved in neurogenesis during the dorsolateral midbrain development (Fischer et al., 2011). Removal of *FGF15* results in the upregulation and expanded expression of proneural genes (*ID1, ID3* and *HES5*) as well as downregulation or complete loss of expression of genes that are related with neurogenesis (*NEUROG1, NEUROG2, ASCL1, NEUROD1*). Interestingly, FGF19 facilitates development of polarized cerebellar neuroepithelium from hESCs in 3D culture (Mugurama et al., 2015); when added with other signaling molecules it can induce formation of continuous neuroepithelium with rostral hindbrain neuronal-tube like structure indicating that FGF19 may play a yet uncharacterized role in patterning and growth in the hindbrain.

1.3.3 Type II Collagen (COL2A1)

Extracellular matrix (ECM) is a complex and dynamic microenvironment. Not only it serves cells as structural scaffolds, but also acts as a storage reservoir for growth factors, cytokines and other small molecules (Watt & Huck, 2013). Components of ECM can act as probes to which cells respond to detect if the conditions are suitable for differentiation (Puklin-Faucher & Sheetz, 2009). ECM and its receptors (laminin, cadherin, integrin, collagen, fibronectin etc.) determine cell fate by promoting proliferation or differentiation into specific cell lineages (Hayashi et al., 2007 and Chen et al., 2013). Collagen-II is expressed in the developing mouse brain, in the ventricular zones (E9.5 to E14.5) (Lui et al., 1995; Cheah et al., 1991). Brain specific localization during development suggests that COL2A1 could be important for stem cell niches or neuronal differentiation. Also, its expression is shown in hippocampus

and thalamus (Leung et al., 1998). However, there is no evidence so far showing any function of Collagen-II during the development of the central nervous system.

However, regulation of *COL2A1* by NFIB has been investigated by Uchihashi et al. (2007). NFIB dominant negative study in murine mesenchymal (ATDC5) cell line by transfection of truncated NFIB leads to delayed or decreased expression of early chondrocyte marker genes such as type II collagen (*COL2A1*). Additionally, NFIB regulates activation of *COL2A1* gene expression and this indicates a role for NFIB during the early differentiation of chondrocytes.

1.4 Aim of the Study

NFI proteins appear to regulate neural differention in the CNS by promoting neurogenesis and gliogenesis while repressing stem cell renewal. In the hindbrain NFIB specifically regulates neurogenesis in the precerebellar neuroepithelium and controls expression of many target genes involved in several developmental signaling pathways (Kumbasar, unpublished data). Putative NFIB targets (*CDO*, *FGF19* and *COL2A1)* were chosen for further study, as they were highly upregulated in the *NFIB* null precerebellar neuroepithelium, also confirmed by in situ hybridization analysis. The aim of this study is to elucidate new gene regulation mechanisms upstream and downstream of NFIB in human neural stem cells (hNSCs, Gibco). In order to study genes downstream from NFIB, we characterized expression profiles of NFIs and putative NFIB target genes (*CDO, FGF19* and *COL2A1*) by qRT-PCR and Western blotting during neural differentiation and compared these with those found *in vivo*. To identify new upstream regulators of NFIB, we looked for microRNAs that potentially target NFIB 3'UTR and screened for those that are upregulated during neural differentiation. We then used reporter assays to distinguish those miRNAs that can directly target the 3'UTR of NFIB in HEK293T cells.

2. MATERIALS AND METHODS

2.1 Materials

2.1.1 Equipment

The equipment used in this study is shown in Appendix A.

2.1.2 Commercial Kits

Commercial kits used in this thesis project are given in Appendix B.

2.1.3 Chemicals

The chemicals used in this study are listed in Appendix C.

2.1.4 Reagents

The reagents including enzymes and buffers used in this study are listed below in Table 2.1.

Table 2.1 : Reagents.

Product	Supplier
CloneAmp HiFi PCR Premix	ClontechTM, 639298
ColorPlus™ Prestained Protein Marker	NEB, P7712
Crimson Taq DNA Polymerase	NEB, M0324
10X CutSmart Buffer	NEB, B7204
HindIII restriction endonuclease	NEB, R3104
MassRuler DNA Ladder Mix	Life Technologies, SM0403
100X Protease inhibitor cocktail	CST-E, 5871S
One Taq DNA Polymerase	NEB, M0480
Shrimp Alkaline Phosphatase	NEB, M0371
SacI-HF restriction endonuclease	NEB, R3156
XhoI restriction endonuclease	NEB, R0146

2.1.5 Cell types

Human embryonic kidney (HEK) 293T cells (America Type Culture Collection): HEK 293T cells are easy to culture and transfect. These cells are highly transfectable by various techniques and they have a high expansion rate. In this study, this cell line was used for overexpression and luciferase assays.

SH-SY5Y Cells (America Type Culture Collection): SH-SY5Y cell line is a human derived neuroblastoma cell line. It is used as a positive control for neural differentiation and its genomic DNA was isolated for the cloning of NFIB 3'UTR.

GIBCO Human Neural Stem Cells (hNSCs) (H9 derived) (Life Technologies, Grand Island, NY, USA): The human neural stem cells are pluripotent and derived from NIH-approved H9 (WA09) hESCs. In this study, hNSCs cell line was mainly used in expression studies during neural differentiation analysis..

2.1.6 Growth and freezing Media

2.1.6.1 HEK 293T and SH-SY5Y complete medium

Complete medium for HEK293T and SH-SY5Y cell lines consists of DMEM (high glucose without L-glutamine) with 2 mM L-Glutamine, 10% (v/v) Fetal Bovine Serum (FBS), 500 μg/ml Penicilin/Streptomycin liquid.

2.1.6.2 GIBCO complete human neural stem cells (hNSCs) culture medium

Cells were cultured according to the manufacturer's instructions. Additionally EmbryoMax penicilin-streptomycin solution (Millipore) was added to avoid contamination. StemPro NSC SFM complete medium consists of Knockout D-MEM/F12 with 2% StemPro Neural Supplement, GlutaMAX-I Supplement (2mM) and 500 μg/ml EmbryoMax Penicilin-Streptomycin solution and then filter sterilized with 0.22 μm filter. EGF (20 ng/ml), bFGF (20 ng/ml), were freshly added into the medium before use.

2.1.6.3 GIBCO human neural stem cells (hNSCs) differentiation medium

For induction of neuronal differentiation of GIBCO hNSCs, differentiation medium composed of StemPro NSC SFM complete medium without the growth factors (bFGF and EGF), and then sterilized with 0.22 μm filter. Fresh BDNF (20 ng/ml) and NT-3 (20 ng/ml) were added into medium before use.

2.1.6.4 2X Freezing medium for GIBCO hNSCs

2X Freezing medium composed of 80% complete StemPro NSC SFM medium and 20% DMSO and kept on ice until use.

2.1.6.5 Freezing medium for HEK293T and SH-SY5Y cell lines

Freezing medium for HEK293T and SH-SY5Y cell lines composed of 40% FBS, 10% DMSO and 50% DMEM. It was sterilized with 0.22 μm filter before use.

2.1.7 Reagents, chemicals, small molecules, buffers for cell culture

Reagents, chemicals, small molecules, buffers for the cell culture are listed in Appendix D.

2.1.8 Bacterial strains

1. Chemical competent *E. coli* cells (strain **NEB 5-alpha)** were purchased from New England Biolabs (NEB) and used for transformation of pCR-Blunt II_TOPO vector because of its high transformation efficiency.

2. Stellar competent cells (*E. coli* HST04) were purchased from Clontech and were used for the cloning of fragments of NFIB 3'UTR from pCR-Blunt II_TOPO vector to pmiRGLO Dual-Luciferase miRNA target expression vector after In-Fusion Cloning reaction.

3. XL1-Blue *E. coli* strain was used for the transformation of pmiRGLO vector after ligation of sticky-ended fragments of 3'UTR of NFIB.

4. XL10-Gold Ultracompetent cells were purchased from Agilent Technologies. This strain contains Hte genotype to increase the transformation efficiency of large and ligated DNA molecules and is used for transformation of mutated single strand plasmid DNA after site-directed mutagenesis cycle and DpnI treatment.

2.1.9 Bacterial culture media

2.1.9.1 LB medium and LB-agar medium

Luria Bertani (LB) medium was prepared by dissolving 10 g tryptone, 5 g yeast extract and 10 g NaCl in dH_2O and final volume was adjusted to 1 L with dH_2O. LB-Agar Medium was prepared by dissolving 10 g tryptone, 5 g yeast extract and 10 g NaCl and 15 g agar in dH_2O and final volume was adjusted to 1 L. The resulting solutions were sterilized by autoclaving for 15 min at 121°C. Selective medium was

prepared by addition of relevant antibiotics after solutions cooled down. Stock and working concentrations of antibiotics are listed below in Table 2.2.

Table 2.2 : Antibiotics and their stock and working concentrations.

Antibiotic	Stock concentration	Final concentration
Ampicilin	10 mg/ml in dH_2O	100 µg/L
Kanamycin	10 mg/ml in dH_2O	50 µg/L

2.1.9.2 SOC medium

SOC medium was prepared by adding 20 g tryptone, 5 g yeast extract, 2 ml of 5M NaCl, 2.5 ml of 1M KCl, 10 ml of 1M $MgCl_2$, 10 ml of 1M $MgSO_4$ and 20 ml of 1 M glucose in 900 ml of distilled H_2O. After the components were dissolved, final volume was adjusted to 1 L with dH_2O. It was sterilized by autoclaving before use.

2.1.9.3 NZY Broth

To prepare NZY Broth,10 g NZ amine (casein hydrolysate), 5 g yeast extract, 5 g NaCl were dissolved in 900 ml dH_2O and final volume was adjusted to 1L with dH_2O (pH 7,5). Then the solution was sterilized by autoclaving for 15 min at 121°C. Filter sterilized supplements 12,5 ml of 1M $MgCl_2$, 12,5 ml of 1 M $MgSO_4$ and 20 ml of 20% (w/v) glucose were added before use.

2.1.10 Vectors

2.1.10.1 pCR-Blunt II-TOPO vector

pCR-Blunt II_TOPO vector (Invitrogen) is specifically designed to clone blunt-end PCR products generated by thermostable proofreading polymerases. In this study, this vector was used to clone blunt end PCR products of 3'UTR of NFIB. Its circular map is shown in Figure 2.1.

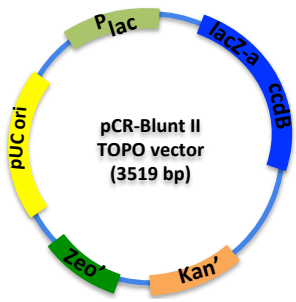


Figure 2.1 : pCR-Blunt II-TOPO vector circular map.

Figure 2.1 (cont'd) : pCR-Blunt II-TOPO vector circular map. TOPO vector was used for the cloning of blunt-end PCR products

2.1.10.2 pmiRGLO Dual-luciferase miRNA target expression vector

The pmiRGLO Dual-luciferase miRNA target expression vector (pmiRGLO vector) containing both firefly luciferase gene and Renilla luciferase gene was purchased from Promega. Four different fragments of 3'UTR of NFIB were cloned into pmiRGLO vector separately for luciferase assay analysis. Circular map of pmiRGLO is shown in Figure 2.2.

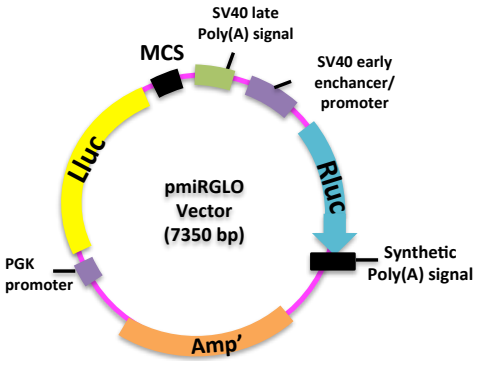


Figure 2.2 : pmiRGLO Dual-luciferase miRNA target expression vector circular map. Fragments of 3'UTR of NFIB were cloned into 3'UTR of luciferase gene into the multiple cloning site (MCS).

2.1.11 Buffers in SDS-PAGE and Western blotting

2.1.11.1 5X SDS sample buffer

5X SDS sample buffer was used to denature protein samples that were loaded on SDS-PAGE. Its formulation is shown in Table 2.3.

Table 2.3 : Formulation of 5X Sample buffer.

5X Sample buffer	Amount
0.5 M Tris pH 6.8	600 µl
SDS (stock)	0.1 g
Bromophenol blue (10 mg/ml)	50 µl
Glycerol (100% stock)	0,4 ml
dH_2O	Up to 1 ml

25 µl DTT (20X) was freshly before use.

2.1.11.2 Components of SDS-PAGE gel

7.5% separating and 4% stacking gels were used for SDS-PAGE and their formulations are given in Table 2.4.

Table 2.4 : Formulations of SDS-PAGE gels.

Stock solution	7.5% Separating Gel	4% Stacking Gel
0.375 M Acrylamide (40%)	1.88 ml	0.5 ml
1.5 M Tris-HCl pH 8.8	2.5 ml	-
0.5 M Tris-HCl pH 6.8	-	1.25 ml
10% SDS	100 µl	50 µl
10% APS	100 µl	50 µl
TEMED	4 µl	5 µl
dH_2O	Up to 10 ml	Up to 5 ml

2.1.11.3 10X Running buffer

Stock solution 10X running buffer was diluted to 1X as a working solution and used in SDS-PAGE (Table 2.5).

Table 2.5 : Formulation of 10X Running buffer.

Content	Amount	Final Concentration
Tris-Base (MW: 121.1g)	30.3 g	250 mM
Glycine	144.0 g	1.92 M
dH_2O	Up to 1000 ml	

2.1.11.4 Blocking buffer

Blocking buffer contains 3% skim milk powder (Cell Signaling) in TBS-T and is used for blocking of nitrocellulose membrane.

2.1.11.5 Ponceau-S staining solution

Ponceau-S staining was used for visualizing proteins on nitrocellulose membrane after electrophoretic transfer and components of the Ponceau-S staining solution are listed in Table 2.6.

Table 2.6 : Formulation of Ponceau-S staining solution.

Content	Amount	Final Concentration
Ponceau S	0.1 g	1% (w/v)
Glacial Acetic Acid	5 ml	5%
dH_2O	Up to 100 ml	

2.1.11.6 1X Running buffer and 1X Transfer buffer

Stock solution 10X Running buffer was diluted to 1X as a working solution and used in SDS-PAGE. 1X Transfer buffer was prepared by diluting 10X Running buffer.

Formulations of these buffers are shown in Table 2.7.

Table 2.7 : Formulations of 1X Running buffer and 1X Transfer buffer.

Content	1X Running buffer		1X Transfer buffer	
	Amount	**Final concentration**	**Amount**	**Final concentration**
10X Running buffer	100 ml	25 mM Tris-Base, 192 mM glycine	100 ml	25 mM Tris-Base, 192 mM glycine
10% SDS	10 ml	0.01%	-	-
Methanol	-	-	200 ml	20% (v/v) methanol
dH_2O	Up to 1000 ml		Up to 1000 ml	

2.1.11.7 1X TBS and 1X TBS-T

Blocking buffer was prepared in TBS. TBS-T was used as washing buffer during Western blotting and antibodies were diluted in TBST. The formulations for these buffers are shown in Table 2.8.

Table 2.8 : Formulations of 1X TBS and 1X TBS-T.

Components	1X TBS		1X TBS-T	
	Amount	**Final Concentration**	**Amount**	**Final Concentration**
1 M Tris-Base pH 7.5	50 ml	50 mM	50 ml	50 mM
5 M NaCl	30 ml	150 mM	30 ml	150 mM
20% Tween-20	-	-	5 ml	0.1%
dH_2O	Up to 1000 ml		Up to 1000 ml	

Supplied at pH 7.5.

2.1.12 Buffers for preparation of whole cell and nuclear protein extracts

2.1.12.2 1X Sample buffer

1X Sample buffer was used for preparation of whole cell lysates and components of this buffer are shown in Table 2.9.

Table 2.9 : Formulation of 1X Sample buffer.

Components	1X Sample buffer	
	Amount	**Final concentration**
0.5 M Tris pH 6.8	1.25 ml	6.25 mM
10% SDS	2 ml	%2
Glycerol (100% stock)	1 ml	% 10
dH_2O	Up to 10 ml	

2.1.12.3 Nuclear extract buffer A (NEB-A) and nuclear extract buffer C (NEB-C) (Ravichandran, 2006)

Concentration and amounts of components of NEB-A and NEB-C buffers were used in extraction of nuclear proteins from cell pellets are listed in Table 2.10.

Table 2.10 : Buffers used in preparation of nuclear extracts.

Components	NEB-A buffer (Nuclear extract buffer-A)		NEB-C buffer (Nuclear extract buffer-C)	
	Amount	**Final concentration**	**Amount**	**Final concentration**
1 M HEPES, pH 7.9	100 µl	10 mM	100 µl	20 mM
1 M NaCl	400 µl	10 mM	400 µl	0.4 mM
0.5 M EDTA	1 µl	0.1 mM	10 µl	1 mM
0.5 M EGTA	1 µl	0.1 mM	10 µl	1 mM
dH_2O	4.5 ml		4.5 ml	

Dithiothreitol and protease inhibitor cocktail were added freshly into buffers.

2.1.13 Primers

All primers used in PCR, In-Fusion cloning, sequencing and qRT-PCR are shown in Table 2.11, 2.12, 2.13 and 2.14.

Table 2.11 : Primers for the cloning of 3'UTR of NFIB from SH-SY5Y gDNA.

Amplicon	Primer Name	Sequence	Binding sites	Amplicon length
NFIB 3'UTR_A	NFIB 3'UTR_10	AGGCTGCAGCTAAACCAACA	3102-3121	1071 bp
	NFIB 3'UTR_1	CACCCATCTTACCGGCCAAT	2050-2069	
NFIB 3'UTR_B	NFIB 3'UTR_9	TCCTTCAGCCCTTGGACTCT	2941-2960	1204 bp
	NFIB 3'UTR_8	ATCTCAGGGTGCACTGCTTC	4126-4145	
NFIB 3'UTR_C	NFIB 3'UTR_7	TGTCGAAGCACCACTGTCTT	6345-6364	1159 bp
	NFIB-3'UTR_12	CCACATCAGTCCCTGTAGCA	7485-7504	
NFIB 3'UTR_D	NFIB 3'UTR_11	TCCTTCAGCCCTTGGACTCT	7379-7398	1107 bp
	NFIB 3'UTR_2	CAGAGTCGTAGCATAGCTCATTT	8463-8486	

Table 2.12 : Primers for qRT-PCR.

Species	Target gene	PrimerName	Primer	Sequence
Human	**GAPDH**	qGAPDH-F	Forward	AGCCACATCGCTCAGACA
		qGAPDH-R	Reverse	GCCCAATACGACCAAATCC
Human	**NFIA**	hNFIA_1Q	Forward	CAGCATCACCGACCTGTCAT
		hNFIA_2Q	Reverse	TGAAGAGTCGATGGTGTTGCA
Human	**NFIB**	hNFIB_3Q	Forward	TCTCCACCAAGCAGCAAAAGA
		hNFIB_4Q	Reverse	GCAGCTGGTGAACTTGGAGAG
Human	**NFIC**	hNFIC_3Q	Forward	CAAGTCACCATTCAACAGCCC
		hNFIC_4Q	Reverse	CGTAGGGAAATGCAGAGCG
Human	**NFIX**	hNFIX_1Q	Forward	TGCCTGTGCTTGCTGGAGT
		hNFIX_2Q	Reverse	TGGATGATGGACGTGGAGG
Human	**CDON**	hCdon_3	Forward	AGTGAATGGTGGTGGAATGTACACG
		hCdon_4	Reverse	TGCTGAAAGTGCTGTTGGTTTTGGT
Human	**COL2A1**	hCol2a1_5	Forward	CCCAATGGGTCCTCGTGGCCTG
		hCol2a1_6	Reverse	GCTGACCATCGTTGCCTCGGG
Human	**FGF19**	hFGF19_5	Forward	GCGCACAGTTTGCTGGAGAT
		hFGF19_6	Reverse	AAAGCACAGTCTTCCTCCGAGTA

Table 2.13 : Sequencing primers for pCR II_Blunt-TOPO vector and pmiRGLO Dual-Luciferase miRNA target expression vector.

Vector name	Sequencing primers	Sequence
TOPO vector	**M13F**	GTAAAACGACGGCCAGT
	M13R-pUC(-40)	CAGGAAACAGCTATGAC
pmiRGLO vector	**T7 terminator**	GCTAGTTATTGCTCAGCGG
	pmirGlo F	GAGGTGCCTAAAGGACTGAC
	EBV-RP	GTGGTTTGTCCAAACTCATC

Table 2.14 : Primers for the In-Fusion cloning of NFIB 3'UTR from TOPO vector to pmiRGLO vector.

Primer Name	Sequence
pmiRGLO_F	CTAGTTGTTTAAACGATCTGCAGAATTCGCCCTT
pmiRGLO_R	CGACTCTAGACTCGAGTGCTGGAATTCGCCCTT

Highlighted sequences show the regions homologous to the vector sequence.

2.1.14 Antibodies

List of antibodies that were used in immunocytochemistry, flow cytometry and Western blotting experiments are listed in Table 2.15 and Table 2.16.

Table 2.15 : Antibodies for immunocytochemistry, flow cytometry.

Antibody name	Supplier Company	Working dilutions
Rabbit monoclonal anti-Nestin antibody	Abcam, ab105389	1:500
Mouse monoclonal Anti-Tubulin Beta III isoform (Tuj-1)	Millipore, MAB1637	1:100
Mouse monoclonal neuronal class III Beta-Tubulin isoform (Tuj-1), Alexa Fluor® 488 labeled antibody	Covance, A488-435L	1:100
Cy3-AffiniPure Donkey Anti-Mouse IgG (H+L)	Jackson ImmunoResearch, 715-165-150	1:500
Alexa Fluor® 488 Goat Anti-Rabbit IgG (H+L) Antibody	Molecular Probes, A11008	1:200
Alexa Fluor® 488 Goat Anti-Mouse IgG (H+L) Antibody	Molecular Probes, A11001	1:200

Table 2.16 : Antibodies for Western blotting.

Antibody name	Supplier Company	Working dilutions
Rabbit polyclonal anti-NFIB (middle region) antibody	Aviva Biosystems Biology, ARP32716	1:1000
Rabbit polyclonal anti-NFIB antibody	Sigma, HPA003956	1:5000
Rabbit polyclonal NFI antibody	Santa Cruz Biotechnology, 5567	1:1000
Mouse monoclonal Anti-Lamin B1 antibody	Abcam, ab8982	1:1000
Stabilized Peroxidase Conjugated Goat Anti-Rabbit (H+L)	Thermo Scientific, 32430	1:500
Stabilized Peroxidase Conjugated Goat Anti-Mouse (H+L)	Thermo Scientific, 32460	1:500

2.2 Methods

2.2.1 Cell culture methods

2.2.1.1 Coating culture vessels for preparing matrix for hNSCs

For culturing hNSCs, culture vessels were coated with poly-L-ornithine and laminin. Stock solutions were prepared and treated as follows: Poly-L-ornithine (Sigma) was dissolved with distilled water to make 500X stock solution (10 mg/ml). 1mg/ml laminin (Sigma) was thawed slowly at 4°C to prevent polymerization and frozen into 50 µl aliquots to avoid multiple freeze/thaw cycles.

Then, poly-L-ornithine stock solution was diluted 1:500 in distilled water to make 2 µg/ml working solution. The surface of the culture vessels were coated with the working solutions, 3 ml for T75 flask; 2 ml for 100-mm dish; 1 ml for T25 flask. Culture vessels were incubated for at least 1 h at 37°C and subsequently washed twice with sterile water. The plates were kept at 4°C until further use.

To coat the culture vessels with laminin, aliquoted solutions were diluted 1:100 in cold 1X DPBS to make 1 µg/ml working solution. Culture vessels were coated with the working solutions 3 ml for T75 flask; 2 ml for 100-mm dish; 1 ml for T25 flask and incubated for 1 h at 37°C. Finally, the culture vessels were rinsed with DPBS and stored with DPBS until use at 4°C. Then, they were washed twice with DPBS and replaced DPBS with StemPro NSC SFM to prevent the plates from drying out.

2.2.1.2 Thawing and subculturing GIBCO hNSCs

Cells were removed from liquid nitrogen storage. They were immediately transferred to a 37°C water bath and thawed quickly by swirling. Thawed cells were immediately transferred into 15-ml sterile centrifuge tube. 4 ml pre-warmed

complete StemPro NSC SFM was added carefully drop-wise. An additional 5 ml pre-warmed complete StemPro NSC SFM was added into the same tube. Subsequently, cells were centrifuged for 300x*g* (1100 rpm) for 5 min and the supernatant was aspirated to remove the cryoprotectant. Then, cells were resuspended with 2 ml complete StemPro NSC SFM and counted in a hemacytometer. Viable cell number was determined by trypan blue exclusion. Finally, resuspended cells were plated at a seeding density of 1.0 x 10^5 cells/cm^2 on poly-L-ornithine/laminin coated culture vessel. Cells were incubated at 37°C, 5% CO_2, and 90% humidity incubator. Next day, the medium was changed with the fresh pre-warmed complete StemPro NSC SFM. The culture was re-fed with fresh medium every two days. When the culture was seen to be 90% confluent under the microscope, cells were passaged. For that purpose, StemPro Accutase and the complete StemPro NSC SFM were pre-warmed to 37°C. First, the spent complete medium was removed from the cells by aspiration. Cells were washed once by adding 5ml DPBS to the side of the vessel opposite the attached cell layer, and gently swirling. Then, DPBS was discarded. StemPro Accutase was added to cover the attached cell layer and cells were incubated for 3-5 min at 37°C. When cell detachment was observed, (app. 9 ml) fresh medium was added onto the cells to stop cell-disassociation reaction and the cells were gently pipetted up and down to break the larger clumps. Cells were transferred to a 15 or 50 ml centrifuge tube and centrifuged at 300x*g* (1100 rpm) for 5 min at RT and medium was removed. The pellet was resuspended in a minimal volume of the complete StemPro NSC SFM and the number of viable cells was counted. $5x10^4$ cells/cm^2 were transferred into the coated and fresh medium and growth factors added culture vessels. Cells were incubated at 37°C, 5% CO_2, and 90% humidity incubator.

2.2.1.3 Cryopreservation of hNSCs

Detached cells were transferred into a 15 or 50 ml centrifuge tube by following the same steps described for subculturing. Then, cells were centrifuged at 300x*g* (1100 rpm) for 5 min at RT and the medium was discarded. The pellet was resuspended using the complete StemPro NSC SFM to half the final freezing volume. The same amount of 2X freezing medium was added to the resuspended cells in a drop-wise manner. The final cell concentration was $2x10^6$ cell/ml. 1 ml of the cell suspension was aliquoted into each cryovial. The vials were placed in an isopropanol freezing

container and stored at –80°C overnight. The next day, frozen vials were transferred to a liquid nitrogen tank for long-term storage.

2.2.1.4 Differentiation protocol of hNSCs

To differentiate GIBCO hNSCs into neurons, oligodendrocytes, and astrocytes, hNSCs were plated on poly-L-ornithine/laminin coated culture vessels at $2.5x10^4$ cells/cm^2 according to the protocol for passaging GIBCO hNSCs. After 2 days, medium was changed to complete StemPro NSC SFM without growth factors. To increase cell survival during growth factor withdrawal, the culture medium included fresh BDNF (20 ng/ml) and NT-3 (20 ng/ml). The medium was replaced with fresh medium every two days. The differentiation procedure lasted seven days.

2.2.1.5 Thawing and subculturing SH-SY5Y and HEK293T cell lines

Cells were removed from liquid nitrogen storage and immediately transferred to a 37°C water bath and thawed quickly with agitation. Then, thawed cells were transferred into 15-ml sterile centrifuge tube. 4 ml pre-warmed complete StemPro NSC SFM was added carefully drop-wise. An additional 5 ml pre-warmed complete StemPro NSC SFM was added into the same tube. Subsequently, cells were centrifuged for 300x*g* (1100 rpm) for 5 min and the supernatant was aspirated to remove the cryoprotectant. Then, cells were resuspended with 2 ml complete medium and counted in a hemacytometer. Viable cell number was determined by trypan blue exclusion. Finally, resuspended cells were plated at a seeding density of 4.0×10^5 cells/cm^2 on culture vessels. Cells were incubated at 37°C, 5% CO_2, and 90% humidity incubator. Next day, the medium was changed with the fresh pre-warmed complete medium. Then, the culture was re-fed with fresh medium every two days. When the culture was seen 90% confluent under microscope, cells were passaged. For that purpose, Cell-dissociation reagent (0.25% Trypsin-EDTA solution) and the complete medium were pre-warmed to 37°C. Firstly, the spent complete medium was removed from the cells by aspiration. Cells were washed once by adding 5 ml PBS to the side of the vessel opposite the attached cell layer, with gentle swirling. Then, PBS was discarded and 0.25% Trypsin-EDTA solution was added to cover the attached cell layer and cells were incubated cells incubated for 2 min at 37°C. When cell detachment was observed, (app. 9 ml) fresh medium was added onto the cells to stop this reaction and the cells were gently pipetted up and down to break the larger clumps. Cells were transferred to a 15 ml centrifuge tubes

and centrifuged at 300x*g* (1100 rpm) for 5 min at RT and medium was removed. The pellet was resuspended in a minimal volume of the complete medium and the number of viable cells was counted. $5x10^4$ cells/cm^2 were transferred into the culture vessels. Cells were incubated at 37°C, 5% CO_2, and 90% humidity incubator.

2.2.1.6 Freezing procedure of SH-SY5Y and HEK293T cell lines

Detached cells were transferred into 15 or 50 ml centrifuge tube by following the same procedure described for subculturing. Then, cells were centrifuged at 300x*g* (1100 rpm) for 5 min at RT and the medium was discarded. The pellet was resuspended using the freezing medium for SH-SY5Y and HEK293T cells at ~ $4x10^6$ cell/ml. 1 ml of the cell suspension was aliquoted into cryovials. Cryopreservation was achieved overnight in a controlled-rate freezing apparatus following standard procedure. The next day, frozen vials were transferred to a liquid nitrogen tank for long-term storage.

2.2.2 Characterization of GIBCO hNSCs

2.2.2.1 Immunocytochemistry

For immunofluorescence staining, progenitor or differentiated hNSCs were grown on poly-L-ornithine and laminin coated glass coverslips in 24 well plates. Cells were fixed in PBS containing 4% paraformaldehyde (PFA), 5% sucrose for 10 min, rinsed with PBS twice and permeabilized with 0.2% Triton-X in PBS for 5 min. Then, cells were blocked with 10% goat serum (blocking solution) in PBS for 1 h. Coverslips were incubated with primary antibodies (listed in Table 2.1.18) diluted in blocking solution for 1 h at RT. Excess antibody on the cells was washed with PBS for three times with 5 min of incubation. Cells were further incubated in fluorescent-labelled secondary antibodies (listed in Table 2.15) in blocking solution for 1 h at RT with DAPI (used concentration: 100ng/ml) for counterstaining, followed again by three washes in PBS. A drop of Vectashield Mounting Media was placed on a glass slide and the glass coverslip was placed on top of the mounting media drop keeping the cells upside down position. Sections were examined by using Leica confocal microscope equipped with ultraviolet, helium/neon/argon lasers and the slides were stored at 4°C.

Immunocytochemistry analysis was set up in parallel to flow cytometry analysis.

2.2.2.2 Flow cytometry

Cells were harvested with accutase and washed once with PBS. Subsequent steps in the procedure were carried out at 4°C. Cells were fixed with 1% PFA in PBS for 20 min on ice, rinsed with PBS. Cells were then permeabilized in PBS supplemented with 0.7% Tween-20 for 15 min. Primary and secondary antibodies (Table 2.15) were diluted in PBS/0.7%Tween-20 with 3% goat serum. Primary antibody was incubated for 3 h while secondary antibody incubation was for 1 h in the dark. Two washing steps were performed after antibody incubations in PBS/0.7%Tween-20. For flow cytometry, cells were resuspended in FACS solution (2% FBS in PBS) and filtered through nylon mesh and analysed in a BD Accuri C6 FACS-Area cell sorter (Becton, Dickinson and Company).

2.2.3 Analysis of RNA expression

2.2.3.1 Total RNA isolation

Total RNA was isolated and purified using PureLink RNA Mini Kit (Invitrogen) according to the manufacturer's instructions. After RNA was bound to the membrane of the Spin Cartridge (during washing step 1), RNase free DNase treatment (Qiagen) was performed to remove contaminating DNA. Procedure for wash and elution steps were then performed according to the protocol. RNA was eluted with 50 µl RNase free water three times for maximum recovery. The concentration and purity of RNA samples were measured by UV spectroscopy (Nanodrop). Samples were then combined into one aliquot and final RNA concentration was determined as before. Finally, samples were divided into appropriate aliquots to avoid freeze-thaw cycles and stored at -80°C.

2.2.3.2 Reverse transcription reaction for total RNA expression analysis

cDNA was prepared from 2 µg total RNA by reverse transcription using a High-Capacity cDNA Reverse Transcription Kit (Applied Biosystems, Carlsbad, CA). The procedure for cDNA synthesis is described below. First of all, the components listed in Table 2.17 were mixed gently and spun down. The resulting solution was incubated at 70°C for 5 min. Then, it was immediately chilled on ice.

Table 2.17 : Contents of the first part of the cDNA synthesis.

Components	Volume/Reaction	Negative control Volume/Reaction
Total RNA	Conc. of RNA 2 µg	Conc. of RNA 2 µg
10X RT Random primers	2.0 µl	2.0 µl
Nuclease free water	Up to 12 µl	Up to 12 µl

Following components listed in Table 2.18 were added to RNA-primer solution, mixed gently and spun down. The cDNA reactions were carried out at 25°C for 10 min; at 37°C for 2 h and stopped at 85°C for 5 min in the thermal cycler, cDNAs were stored at -20°C before use.

Reactions were diluted 2.5 times with dH_2O for all quantitative real-time PCR (qRT-PCR) experiments.

Table 2.18 : Contents of the second part of the cDNA synthesis.

Components	Volume/Reaction (µl)	Negative control Volume/Reaction (µl)
10X RT Buffer	2.0	2.0
dNTP mix (40 mM)	2.0	2.0
MultiScribe™ Reverse Transcriptase	1.0	-
Rnase inhibitor	1.0	1.0
Nuclease free water	Up to 20	Up to 20

2.2.3.3 Expression analysis by Quantitative Reverse Transcriptase PCR (qRT-PCR)

Even though qRT-PCR is based on the principle of conventional polymerase chain reaction, it allows the quantification of the obtained DNA template. Fluorescent dyes (e.g. SybrGreen, EtBr) that bind to double stranded DNA fragment are often used in detection of products in qPCR. Amplification of the DNA target correlates with the increase of fluorescence from cycle to cycle. To analyze the expression of *NFIA*, *NFIB*, *NFIC*, *NFIX*, *FGF19*, *CDO* and *COL2A1* genes, SYBR Green was used as a fluorometric dye. Reactions were carried out with Power SYBR® Green PCR Master Mix (Applied Biosystems).

Primers were designed using Primer Express version 3 (PE Applied Biosystems) and are listed in Table 2.15. All primers were designed either to cross-large expanses of intronic sequence or to span an intron-exon boundary. Annealing temperatures were chosen as 60°C and length of the amplicons about 100 nucleotides. Genomic DNA contamination was also tested by the inclusion of no RT controls (omitted the reverse

transcriptase enzyme from the cDNA synthesis reaction). The components of each reaction are listed in Table 2.19.

Five fold serial cDNA dilutions were used to construct standart curves for validation of PCR reaction efficiencies of different targets. cDNA from hNSCs progenitor cells were used for *NFIB, NFIC, NFIX, CDO, COL2A1* primer sets; cDNA from differentiated hNSCs was used for *NFIA* primers and cDNA from SH-S5Y5 cell line was used for *FGF19* primers. After validation of primer efficiencies between 96-100% and with R^2=0.99, ΔΔCt method was used for further measurements.

Table 2.19 : Components of qRT-PCR reaction.

Components	Volume/Reaction (µl)	Final Concentration
Power SYBR Green PCR Master Mix, (2X)	5	1X
1.25 µM Forward and Reverse Primer Mix	1.2	0.15 µM
Template	2.5	
Nuclease free water	Up to 10	

Amplification cycles were started with initial step at 95°C for 10 min. 40 cycles of 95°C for 10 sec and 58°C for 30 sec followed; for melting curve analysis, samples were heated up to 95°C again for 15 sec. Afterwards samples were cooled to 60°C for 1 min and re-heated again up to 95°C for 15 sec. Reactions were carried out in an Applied Biosystems StepOnePLus™ Real-Time PCR System.

All PCR reactions were performed in duplicate and the average value was used for data analysis. The quantitation of the marker gene was compared to amplification of *GAPDH* as a reference gene and subsequently expressed relative to progenitor cells.

2.2.4 Analysis of miRNA expression

2.2.4.1 Total RNA isolation by using mirVana miRNA isolation kit

Total RNA was isolated and purified using mirVana miRNA isolation kit (Invitrogen) according to manufacturer's protocol. RNase free DNase treatment (Qiagen) was performed after binding RNA to the membrane of the spin cartridge (during washing step 1) to purify DNA-free total RNA. Then, washing steps and elution steps were continued. Purified total RNA was eluted in 50 µl RNase free water. Nanodrop measurement was performed to detect the concentration and purity of RNA samples. Finally, samples were divided into appropriate aliquots to avoid freeze-thaw and stored at -80°C.

2.2.4.2 Reverse transcription reaction for microRNA expression analysis

To analyze the amount of pre-miR-21, pre-miR-153, pre-miR-124a, pre-miR-30a-5p, pre-miR-130a, pre-miR-363, pre-miR-92b and housekeeping genes (snRNA U6, pre-miR-140 and pre-miR-103), 1 µg total RNA (including small RNAs) was reverse transcribed into cDNA using TaqMan Small RNA Assays (Applied Biosystems; hsa-miR-124-3p, assay no: 001182; hsa-miR-130a, assay no: 000454, hsa-miR-363, assay no: 001271; hsa-miR-30a-5p, assay no: 000417; hsa-miR-140, assay no: 001187; U6, assay no: 001973, hsa-miR-21, assay no: 000397, hsa-miR-153, assay no: 000476, hsa-miR-92b, assay no: 007028_mat, hsa-miR-103, assay no: 000439).

Table 2.20 : RT-Mastermix for one reaction.

Component	Volume
100mM dNTPs	0.15 µl
MultiScribeTM Reverse Transcriptase, 50 U/µl	1.00 µl
10X Reverse Transcription Buffer	1.50 µl
Rnase Inhibitor, 20U/µl	0.19 µl
Nuclease-free water	4.16 µl

First of all, RT master mix was prepared on ice by combining the components (listed in Table 2.20 for one reaction) for the desired number of RT reactions and mixed gently. 7 µl RT master mix were mixed with 1 µg RNA (5 µl) and placed on ice. Then, 3 µl of 5X RT primers were added into specified tubes and spun down. Tubes were incubated on ice for 5 min before the reverse transcription reaction. This reaction was performed in Thermal Cycler (BIORAD) by using following parameters in Table 2.21.

Table 2.21 : Parameter values to program thermal cycler.

Step	Time	Temperature
Hold	30 min	16°C
Hold	30 min	42°C
Hold	5 min	85°C
Hold	∞	∞

Reaction mixture was diluted 3 times with dH_2O for use in quantitative real-time PCR (qRT-PCR) experiments.

2.2.4.3 microRNA expression analysis by quantitative reverse transcriptase PCR (qRT-PCR)

miR-21, miR-153, miR-124a, miR-30a, miR-363, miR-92b, miR-130a, snRNA U6, miR-103 and miR-140 expressions were quantified in duplicates in qRT-PCR

TaqMan MicroRNA Assays (Applied Biosystems), namely assay hsa-miR-124-3p, assay no: 001182; hsa-miR-130a , assay no: 000454, hsa-miR-363, assay no: 001271; hsa-miR-30a-5p, assay no: 000417; hsa-miR-140, assay no: 001187; U6, assay no: 001973, hsa-miR-21, assay no: 000397, hsa-miR-153, assay no: 000476, hsa-miR-92b, assay no: 007028_mat, hsa-miR-103, assay no: 000439. Components were added into each tube for each duplicate listed in Table 2.22 and inverted tubes several times and centrifuged briefly. 10 µl of the complete qPCR reaction mix was transferred into each of two wells on 96-well plate.

Table 2.22 : Complete qPCR reaction mix for one reaction and duplicates.

Component	Volume per 10 µl reaction	
	Single Reaction	Two replicates
TaqMan Small RNA Assay (20X)	0.5	1.2
Product from RT Reaction	1	2.4
TaqMan Universal PCR Master Mix II (2X), no UNG	5	12
Nuclease free water	3.5	8.4
Total volume	10 µl	24 µl

The comparative cycle threshold (Ct) method was used to analyze the expression levels and normalized by using U6, pre-miR-103 and pre-miR-140 assays (Applied Biosystems) as internal controls. qRT-PCR reactions for microRNA expression analysis were carried out in the same Applied Biosystems StepOnePLus™ Real-Time PCR System. Temperature profile for qRT-PCR reaction was shown in Table 2.23.

Table 2.23 : Thermal cycler parameter for TaqMan Assays.

Step	Optional AmpErase UNG activity	Enzyme activation	PCR CYCLE (40 Cycles)	
	HOLD	HOLD	Denature	Anneal/Extend
Temperature	50°C	95°C	95°C	60°C
Time	2 min	10 min	15 sec	60 sec

2.2.5 Identification of isoforms of NFIB expression in hNSCs

2.2.5.1 Polymerase chain reaction (PCR)

To characterize expression levels of NFIB protein in hNSCs, it is necessary to identify, which isoforms of NFIB are expressed by hNSCs. For that purpose, PCR was performed to amplify the isoforms that are expressed in this cell line. Four

different alternative splicing forms of NFIB are reported in the literature and schematic representation of their exons are shown in Figure 2.3.



Figure 2.3 : Schematic representation of mRNAs that are known as alternative splice forms of NFIB. hNFIB 1/4 primers amplify a region between exon 5 to exon 9 and are specific for NFIB-1 and NFIB-4. hNFIB 2 primers are specific for NFIB-2 and amplify the region between exon X and exon 2. hNFIB 1/3 primers amplify the region between exon 1 and exon 2 and are specific for NFIB-1 and NFIB-3 isoforms. hNFIB 4 primers amplify the region between exon Y and exon 6 and are specific for NFIB-4. Also, universal primers were designed to amplify the region between exon 8 and exon 11 in all isoforms. Different isoforms yield amplicons of different sizes, indicating the particular isoforms that are expressed in hNSCs (amplicon sizes: NFIB-1: 367 bp; NFIB-2 and NFIB-3: 145 bp and NFIB-4: 483 bp).

We could not design primers that were specific for each isoform because of the high level of homology between isoforms. Therefore, we designed a set of primers that detect a combination of isoforms (Table 2.24).

Two different *Taq* polymerases (*Crimson Taq* DNA polymerase (NEB) and *One Taq* DNA polymerase (NEB) were used to amplify cDNA samples of hNSCs. Components of PCR reactions (Table 2.25 and Table 2.27) and thermal cycling conditions (Table 2.26 and Table 2.28) are shown below. SH-SY5Y cell line was used as a positive control.

Table 2.24 : Primers used to identify isoforms of NFIB expressed in hNSCs.

Amplicon	Primer name	Sequence	Length
1. and 4. isoforms	hNFIB1/4_F	CACCAAGCAAAAGACCC	466 bp
	hNFIB1/4_R	ACTTGACCACTGCCGTTAGG	
2. isoform	hNFIB2_F	CGAGTGTACAGGACCCCTTT	381 bp
	hNFIB2_R	TTGCACGGACATGTGGAAGA	
1. and 3. isoforms	hNFIB1/3_F	CTCGGACTGCAAGAGGGTT	476 bp
	hNFIB1/3_R	CCTGGATGCCCACTTCTGTT	
4. isoform	hNFIB4_F	GCACACTGAGGAGGACACAA	380 bp
	hNFIB4_R	GGTCTTTTGCTGCTTGGTGG	
Universe primer for all isoforms	hNFIBU_F	CAGCCCCATCGAGCTACTTT	NFIB_1 367 bp, NFIB_4 483 bp, NFIB_2 and 3 145 bp
	hNFIBU_R	GAACCAAGCTAGCCCAGGTA	

Table 2.25 : PCR components to identify the expression of alternative splicing forms of NFIB by using C*rimson Taq* DNA polymerase.

Content	Volume	Final Concentration
5X Crimson Taq Reaction Buffer	5 µl	1X
10 mM dNTP	0.5 µl	200 µM
10 µM Forward primer	0.5 µl	0.2 µM
10 µM Reverse primer	0.5 µl	0.2 µM
Template DNA	1 µg	40 ng/µl
Crimson Taq DNA Polymerase	0.125 µl	0.625 units/25 µl
Nuclease-free water	Up to 25 µl	
Total	25 µl	

Table 2.26 : Thermal cycler parameters with *Crimson Taq* polymerase.

Step	Cycle	Temperature	Time
1	1 cycle	95°C	30 sec
2	30 cycles	95°C	30 sec
		Tm for specific primers for isoforms	30 sec
		68°C	1 min
3	1 cycle	68°C	5 min
4	Hold	4°C	

Table 2.27 : PCR components to identify the expression of alternative splicing forms of NFIB by using *One Taq* DNA polymerase.

Content	Volume	Final Concentration
5X *One Taq* Standard Reaction Buffer	5 µl	1X
10 mM dNTP	0.5 µl	200 µM
10 µM Forward primer	0.5 µl	0.2 µM
10 µM Reverse primer	0.5 µl	0.2 µM
Template DNA	1 µg	40 ng/µl
One *Taq* DNA Polymerase	0.125 µl	0.625 units/25 µl
Nuclease-free water	Up to 25 µl	

Table 2.28 : Thermal cycler parameters with *One Taq* DNA polymerase.

Step	Cycle	Temperature	Time
1	1 cycle	94°C	30 sec
2	30 cycles	94°C	30 sec
		Tm for universe primer (50°C, 52°C, 55°C)	30 sec
		68°C	1 min
3	1 cycle	68°C	5 min
4	Hold	4°C	

2.2.5.2 Agarose gel electrophoresis for the detection of PCR product

Agarose gel electrophoresis was performed in order to analyse PCR products. 1% agarose gel was prepared by dissolving 400 mg agarose (SeaKem® LE Agarose, Lonza) in 40 ml 1X TAE buffer and heated in the microwave for 90 sec. After the gel material cooled down, 2 µl of Pronosafe nucleic acid staining dye (20000X, Conda Lab) was added and the gel was poured into the tray. When the gel was ready for use, 10 µl of PCR products were mixed with 2 µl 6X loading dye and loaded into the wells of the gel. In addition, 3 µl MassRuler DNA Ladder Mix (Life Tech.) were mixed with 1 µl 6X loading dye and 2 µl dH_2O and loaded into well. Gel was run at 100V for 30 min in 1X TAE buffer. Pronosafe stained DNA bands were visualized with UV trans-illuminator.

2.2.6 Analysis of protein expression

2.2.6.1 Preparation of whole cell extracts

Cells were washed with 1X PBS (5 ml for 100 mm plate) and added 200 µl pre-heated (95°C) 1X sample buffer. Cell lysate was scraped off the plate, the plate was rinsed with 200 µl 1X SB, the remaining solution was collected and combined with

initial cell lysate. Combined lysate samples were boiled at 95°C for 10 min, genomic DNA was sheared by passing through a 22G syringe 5 times and samples were centrifuged at 12300x*g* for 10 min. Supernatants were transferred into a new centrifuge tubes and aliquoted for future use; pellets were discarded. Whole cell extracts were stored at -80°C.

2.2.6.2 Preparation of nuclear extracts

Nuclear extract were prepared according to the protocol described by Ravichandran (2006). Cells were washed with ice-cold TBS (6 ml TBS for T75 flask), scraped in 600 ul TBS and collected into eppendorf tubes. Samples were centrifuged at 1100 rpm for 5 min at 4°C. Supernatant was discarded and pellet was washed in 600 µl ice-cold TBS. 10 µl phosphatase inhibitor cocktail (pi) and 1 µl dithiothreitol (DTT) were added into 1 ml Nuclear extract buffer-A (NEB-A) and Nuclear extract buffer-C (NEB-C). Subsequently, the pellet was resuspended in 400 µl NEB-A (pi and DTT added) and incubated at 4°C for 15 min and vortexed briefly. 25 µl (10%) nonylphenoxypolyethoxyethanol (NP-40) was added into the mixture and centrifuged at 16000x*g* for 30 sec at 4°C. Supernatant (cytosolic proteins) were collected into a centrifuge tube and stored at -80°C. Nuclear pellet was resuspended in 50 µl ice-cold NEB-C (pi and DTT added). Mixture was rocked for 15 min at 4°C, and centrifuged at 16000x*g* for 5 min at 4°C. Resulted supernatant containing nuclear proteins were transferred into centrifuge tubes and aliquoted for the future use to avoid freeze-thaw. Aliquots were stored at -80°C.

2.2.6.3 Determination of protein concentrations

Protein concentrations were measured by using the bicinchoninic acid (BCA) protein assay kit (Pierce). This quantification method depends on the conversion of Cu^{+2} ions to Cu^{+} ions by the presence of four amino acid residues (cysteine, tyrosine, tryptophan and cystine) in peptide molecules in an alkaline solution and this reaction occurs in a temperature dependent manner. NEB-C buffer was used as a diluent for measurements of nuclear extract samples while 1X Sample buffer was added for the measurement of whole cell extracts. BCA standards were prepared as described in Table 2.29.

Table 2.29 : Components of the BCA standards.

Vial	Volume of diluent (µl)	Volume and source of BSA (µl)	Final BSA concentration
A	0	300 of Stock	2000 µg/µl
B	125	375 of Stock	1500 µg/µl
C	325	325 of Stock	1000 µg/µl
D	175	175 of vial B dilution	750 µg/µl
E	325	325 of vial C dilution	500 µg/µl
F	325	325 of vial E dilution	250 µg/µl
G	325	325 of vial F dilution	125 µg/µl
H	400	100 of vial G dilution	25 µg/µl
I	400	0	0 µg/µl = blank

Working reagent (WR) was prepared by diluting BCA reagent B in BCA reagent A at 1:50 ratio. In a 96-well microplate, first 200 µl working solution was pipetted into each well and then 25 µl of BCA standards or unknown samples were added; samples were shaken for 30 sec. Then, microplate was incubated within a humidified chamber at 37°C for 30 min. After incubation, absorbance at 562 nm was measured on plate reader spectrophotometer (Shimadzu, UV-1601).

2.2.6.4 Sodium dodecyl sulfate-polyacrylamide gel electrophoresis (SDS-PAGE)

SDS-PAGE is a widely used technique to separate proteins according to electrophoretic mobility. SDS, which is an anionic detergent, is used to disrupt the tertiary structures of proteins and reducing agents such as β-mercaptoethanol and dithiothreitol (DTT) was used to reduce all di-sulfide bonds. Lysates were first resolved by SDS-PAGE before Western blot analysis. In this study, 7.5% separating gel was poured between SDS-glasses and overlayed with 0.1% SDS to facilitate polymerization and prevent bubbles. After allowing polymerization, 4% stacking gel was poured onto the separating gel and the comb was inserted straight on down and left for polymerization. Then, the gel was placed into tank. The proteins to be analyzed were mixed with 5X SDS loading dye and 1M DTT and incubated at 95°C for 5 min to denature secondary and non-disulfide-linked tertiary structures. Then, samples and ColorPlus Protein Marker resolved by 7.5 % SDS-PAGE (5 µg for whole cell lysates; 50-70 µg for nuclear extracts). Denatured protein samples were separated by size in SDS-PAGE at constant 90 V (initial current 32 mA) in 1X

Running Buffer. Once samples were in the stacking gel, voltage was increased to 110 V.

2.2.6.5 Western blotting

Western Blot analysis is used to detect specific proteins in a sample. For Western blotting, denatured proteins were first resolved in the separating gel according to their size and then were transferred onto nitrocellulose membranes using wet transfer system (Biorad). Nitrocellulose membrane and gel were equilibrated with 1X transfer buffer for 5 min. Then, the gel and membrane were sandwiched between sponges and filter papers (Whatman) according to manufacturer's instructions; air bubbles were removed during this process. Sandwich was inserted into the tank and run overnight at 4°C, 16V in 1X Transfer Buffer. After blotting, membrane bound proteins were visualized by Ponceau-S staining and lanes and positions of protein molecular weight markers were marked on the membrane. Then, the membrane was blocked with 3% skim milk powder in TBS-T for 1 h at RT to prevent non-specific binding. Subsequently, the membrane was washed twice with TBS-T for 5 min at RT before incubation with primary antibody. Concentrations of primary antibodies are listed in Table 2.18. Antibody dilutions were prepared in %10 FBS /TBS-T and incubated overnight at 4°C with gentle agitation. The following day, the membrane was washed three times with TBS-T for 5 min at RT with gentle agitation. Concentrations of primary antibodies are listed in Table 2.18. Secondary antibody dilutions were prepared with 3% skim milk powder in TBS-T. The membrane was incubated with secondary antibody for 1 h at RT with gentle shaking. The membrane was then washed twice with TBS-T for 5 min and once with TBS for 5 min. For detection of bound antibodies, 20X LumiGLO® chemiluminescent substrate (Cell Signaling Technology) was used according to manufacturer's instructions and the membrane was incubated with the luminol and hydrogen peroxide 1 min and chemiluminescent bands were detected by ChemiDocTM MP System (Biorad).

2.2.7 Cloning of 3'UTR of NFIB into pCR II_Blunt-TOPO vector

To monitor the effect of miRNAs predicted to bind the NFIB 3'UTR on NFIB expression, the 4541 bp relevant region of NFIB 3'UTR of was divided into four fragments (app. 1100 bp segments carrying putative binding sites of miRNAs). Those fragments were cloned into reporter vector (pmiRGLO Dual-Luciferase miRNA target expression vector). Reporter vector contains *Renilla* luciferase (RLuc)

and firefly luciferase (FLuc).

2.2.7.1 Primer design for the amplification of fragments of 3'UTR of NFIB for cloning

4.5 kb relevant region of NFIB 3'UTR of was divided into four fragments according to predicted miRNA binding sites for cloning into luciferase vector. Specific primers were designed considering the general rules of primer design using Integrated DNA Technologies (IDT) and Primer Blast. Finally, annealing and melting temperatures, GC content, hairpin and self-dimer formation were checked by IDT Scitools Oligo Analyzer. All primers are listed in Table 2.12.

2.2.7.2 Isolation of genomic DNA from SH-SY5Y cell line

Genomic DNA was isolated from the SH-SY5Y cell line with the DNA isolation kit for mammalian blood (Roche Life Sciences). For that purpose, $1x10^7$ cells were cultivated and harvested to isolate genomic DNA. Cells were pelleted by centrifugation at 300x*g* for 5 min and rinsed with PBS. The pellet was added 1 ml white cell lysis buffer and mixed thoroughly by vortexing to ensure the cells were completely lysed. 520 µl protein precipitation solution was added to sample and vortexed thoroughly; a brownish protein precipitate was seen clearly. Sample was centrifuged at 12000x*g* for 12 min. Supernatant, which contains the DNA, was poured carefully into a new sterile centrifuge tube. Two volumes of ethanol (15°C-25°C) was added to the supernatant to precipitate DNA and mixed gently. Then, sample was centrifuged at 12000x*g* for 10 min and the supernatant was discarded. 600 µl 70% cold ethanol was added to the DNA pellet and mixed carefully. Sample was centrifuged at 875x*g* for 5 min and the supernatant was discarded. Thereafter, DNA was dried overnight at RT until the ethanol was no longer visible. The DNA pellet was resuspended in 1 ml TE Buffer, pH 8.8. Finally, sample was incubated at 65°C for 30-60 min and vortexed periodically to aid in resuspension. Genomic DNA concentration and purity was quantified by measuring absorbance at 260 nm. Sample was stored at -20°C until use.

2.2.7.3 Polymerase chain reaction (PCR)

3'UTR fragments were amplified from genomic DNA of SH-SY5Y cells using the CloneAmp HiFi PCR premix (Clontech^{TM}) for 35 cycles (98°C, 10 sec; specified Tm

for primers, 15 sec; 72°C, 5 sec) by using T100^{TM} Thermal Cycler (BIORAD) with NFIB 3'UTR_1/10; NFIB 3'UTR_11/2; NFIB 3'UTR_9/8 and NFIB 3'UTR_11/2 forward and reverse primer sets. PCR components are shown in Table 2.30.

Table 2.30 : PCR components for amplification of NFIB 3'UTR by using CloneAmp HiFi PCR premix.

Reagent	Volume	Final Concentration
CloneAmp HiFi PCR premix	12.5 µl	1X
Primer (Forward) (10 µM)	2.5 µl	250 µM
Primer (Reverse) (10 µM)	2.5 µl	250 µM
Genomic DNA	x µl	1 ng
Sterilized distilled water	Up to 25 µl	

1% agarose gel electrophoresis was performed to analyse PCR products as desrcibed earlier.

2.2.7.4 Cloning of PCR products into pCR II_Blunt-TOPO vector

PCR products were not designed with sticky ends. For that reason, they were cloned into pCR II_Blunt-TOPO vector by using a Zero Blunt TOPO PCR cloning kit (Invitrogen) and transformed into NEB 5-alpha competent *E.coli* (high efficiency) cells for the expression of plasmids.

TOPO cloning reaction was set up using the reagents that are shown in Table 2.31.

Table 2.31 : Components of TOPO reaction.

Reagent	Volume
Fresh PCR product	4 µl
Salt solution	1 µl
pCR II_Blunt-TOPO	1 µl
Final volume	6 µl

The reaction was mixed gently and incubated for 5 min at RT. Then, it was placed on ice.

2.2.7.5 Transformation protocol for NEB 5-alpha competent *E.coli* cells

First, NEB 5-alpha competent *E.coli* cells were thawed on ice until the last crystals disappear and mixed gently. 4 µl TOPO cloning reaction were added into 50 µl competent cell mixture on ice and the tube was carefully flicked 4-5 times to mix.

Mixture was placed on ice for 30 min. Then, heat shock was performed at exactly 42°C for exactly 30 sec. The transformation reaction was cooled on ice for 5 min. 950 µl of RT SOC medium was added into the mixture and incubated at 37°C for 60 min with vigorous shaking at 250 rpm. Cells were mixed thoroughly by inverting the tube and diluted 1/5 in 100 µl Kan^+LB medium and the remainder of cells was centrifuged at 6000 rpm for 5 min and supernatant was discarded. Then, pellet was resuspended in 100 µl Kan^+LB medium again and each dilution were spread onto a kanamycin selection plate and incubated overnight at 37°C. In order to isolate pCR Blunt II_TOPO constructs, which contain segments of NFIB 3'UTR, NucleoSpin Plasmid DNA Purification Kit (Macherey-Negel) was used for a small-scale plasmid preparation (described in 2.2.7.9.1) and NucleoBond Xtra Midi/Maxi Kit (Macherey-Negel) was used for larger-scale plasmid preparation (described in 2.2.7.9.2).

2.2.7.6 Quantitation of DNA

The concentration and purity of DNA was checked by measuring absorbance at 260 nm.

2.2.7.7 Restriction enzyme digestion

To check the insertion of PCR products into TOPO vector, diagnostic restriction digests with XhoI (NEB) and SacI-HF (NEB) were performed. 1 µg plasmid vector was digested with 0.5 µl XhoI and 0.5 µl SacI-HF enzymes in 1X CutSmart buffer (supplied by the manufacturer) for 50 µl reaction at 37°C for 2 h. Then, enzymes were heat-inactivated at 65°C for 15 min. After digested samples were analysed by 1% agarose gel electrophoresis. The sizes of bands were compared with the estimated band sizes.

2.2.7.8 Sequencing of selected constructs

Mini-preps that were yielded correct diagnostic pattern were selected for sequencing using the specific sequencing primers listed in Table 2.15.

2.2.7.9 Plasmid preparation

2.2.7.9.1 Mini-prep preparation

NucleoSpin Plasmid DNA Purification Kit (Macherey-Negel) was used for small-scale plasmid isolation. First of all, single colonies were chosen with micropipette tips from selection agar plates. Tips were transferred into 4 ml LB with selected

antibiotics, incubated overnight at 37°C on shaker (250 rpm). Next day, plasmid DNA was isolated using NucleoSpin Plasmid DNA Purification Kit. 4 ml *E.coli* LB culture was pelleted by centrifugation at 11000x*g* for 30 sec. The supernatant was discarded. For cell lysis, 250 µl Buffer A1 was added and the cell pellet was completely resuspended by vortexing or pipetting. Then, 250 µl Buffer A2 was added and mixed gently by inverting the tube 6-8 times and incubated at RT for up to 5 min. Finally, 300 µl Buffer A3 was added for neutralization and mixed thoroughly by inverting the tube 6-8 times. The lysate was clarified by centrifugation at 11000x*g* for 5 min at RT. Plasmid DNA was allowed to bind the NucleoSpin Plasmid resin as follows: the spin column was placed in a collection tube and max. 750 µl supernatant from the clarified lysate was transferred into column, avoiding to disturb the white pellet. The spin column was centrifuged at 11000x*g* for 1 min and the flow-through was discarded. This step was repeated with the remaining lysate. 500 µl Buffer AW pre-heated to 50°C was added to column and column was centrifuged at 11000x*g* for 1 min as an additional washing step. Then, the column was added 600 µl Buffer A4 and centrifuged at 11000x*g* for 1 min. The flow through was discarded and the column was centrifuged again for 2 min at 11000x*g* to dry silica membrane; the collection tube was discarded. Column was placed in a 1.5 ml microcentrifuge tube and DNA was eluted in 50 µl Buffer AE. Column was incubated for 1 min at RT and centrifuged for 1 min at 11000x*g*. After the purification of plasmid DNA, concentration and purity was checked by measuring absorbance at 260 nm.

2.2.7.9.2 Maxiprep preparation

After selected clones were checked with restriction digestion and sequencing, maxipreps of these clones were prepared using NucleoBond Xtra Midi/Maxi Kit (Macherey-Negel) as follows: single colonies were chosen from restreaked agar plates and incubated in 100 ml overnight *E.coli* culture one day before. Then, 100 ml culture was divided into two 50 ml polypropylene tubes and harvested by centrifugation at 3000x*g* for 20 min at 4°C. Supernatant was discarded and 6 ml resuspension buffer (RES) was added into each tube to resuspend pellets completely. Resuspension from two 50 ml tubes were combined and added 12 ml lysis buffer (LYS). The tube was inverted 6-8 times to mix gently and incubated at RT for 5 min. During this incubation, NucleoBond Xtra column with the inserted column filter was equilibrated with 25 ml equilibrium buffer (EQU). 12 ml neutralization buffer (NEU)

was added to the suspension and mixed by inverting until sample color turn from blue to colorless. Then, lysate was inverted three times and applied to the filter/column. The column filter was washed with 15 ml EQU buffer and filter was removed. The column was then washed with 25 ml wash buffer (WASH). Plasmid DNA was eluted into 50 ml centrifuge tube in 15 ml elution buffer (ELU). 10.5 ml isopropanol was added into the eluate and vortexed well to precipate DNA. Mixture was incubated for 2 min. Then, mixture was loaded into 30 ml syringe and passed through filter (NucleoBond finalizer) drop by drop. Filter was then washed with 4 ml 70% ethanol and dried it via pressing air more than six times. Finally, 500 µl nuclease free water was pipetted into 1 ml syringe and passed through filter into a fresh eppendorf tube drop by drop and plasmid DNA was eluated. Concentration and purity was checked by measuring absorbance at 260 nm. Plasmids were checked by diagnostic restriction endonuclease digests as described before.

2.2.8 Clonining of NFIB 3'UTR fragments from pCR Blunt II_TOPO vector to pmiRGLO Dual-Luciferase miRNA target expression vector

2.2.8.1 First strategy for the cloning of PCR products

2.2.8.1.1 DNA restriction

Sequencing results showed that 3'UTR fragments were cloned in the in pCR Blunt II_TOPO vector MCS in two orientations. We performed ligations to subclone when the orientation of PCR products was the same as in pmiRGLO Dual-Luciferase miRNA target expression vector. Both vectors (TOPO and pmiRGLO) were digested with restriction endonucleases (SacI-HF and XhoI) as described before.

2.2.8.1.2 Alkaline phosphatase treatment

To prevent re-ligation of the linearized pmiRGLO vector, 5' ends of vector was dephosphorylated by Shrimp Alkaline Phosphatase (rSAP, NEB). For that purpose, restricted pmiRGLO was added 2 µl rSAP and incubated at 37°C for 30 min. Then, the reaction was stopped by heat inactivation at 65°C for 15 min.

2.2.8.1.3 DNA purification from agarose gel

Amplified 3'UTR inserts were digested out of the TOPO vectors and run on 1% agarose gel electrophoresis as described before. Bands corresponding to the correct size fragments were purified from agarose gel by using Nucleospin gel and PCR

clean-up kit (Macherey Nagel). DNA fragment was excised from an agarose gel by using a clean scalpel and the weight of the gel was determined. Then, for each 100 mg of agarose 200 µl Buffer NTI was added and incubated at 50°C for 5-10 min until the gel slice was completely dissolved. Then, sample was loaded into a NucleoSpin Gel and PCR Clean-up column and centrifuged for 30 s at 11000x*g*. Flow-through was discarded and remaining sample was loaded again if necessary and the centrifuge step was repeated. The column was washed with 700 µl Buffer NT3 and centrifuged again for 30 sec at 11000x*g*. The column was centrifuged for an additional 1 min at 11000x*g* to dry the silica membrane. NucleoSpin gel and PCR Clean-up column was placed into a new centrifuge tube and DNA was eluted in 30 µl Buffer NE for 1 min at RT. Finally, the eluate was collected by centrifugation at 11000x*g* for 1 min. The concentration and purity of DNA was checked by measuring absorbance at 260nm.

2.2.8.1.4 DNA ligation

Ligation reaction was performed with Quick ligation kit (NEB). 50 ng pmiRGLO vectors were combined with 150 ng insert and volume was adjusted to 10 µl. 10 µl 2X Quick Ligation Buffer was added into the reaction tube and 1 µl Quick T4 DNA Ligase was added, mixed and centrifuged briefly. The mixture was incubated at RT for 5 min and chilled on ice before transformation. Chemically competent XL1-Blue *E.coli* strain was used for the transformation of ligated product.

2.2.8.1.5 Transformation for XL1-Blue *E.coli* strain

4 µl ligation reaction mixture was added to 50 µl of competent cells in a sterile pre-chilled microcentrifuge tube. The tube was placed on ice bath for 30 min. Cells were heat shocked at 42°C for 45 sec in a water bath. Then, the mixture was cooled on ice for 2 min. Cells were added LB medium to a final volume of 500 µl and incubated at 37°C for 45 min. Finally, cells were diluted 1/5 in 100 µl Amp^+LB medium and the remainder of cells was centrifuged at 6000 rpm for 5 min and supernatant was discarded. Then, pellet was resuspended in 100 µl Amp^+LB medium again and each dilution were spread onto separate LB plates containing ampicillin. Plates were incubated overnight at 37°C.

2.2.8.2 Second strategy for the cloning of PCR products

For fragments cloned in reverse orientation (the orientation of amplified 3'UTR fragments in pCR Blunt II_TOPO vector was the opposite orientation to be cloned in pmiRGLO), subcloning was achieved with In-Fusion cloning since restriction sites within the pmiRGLO and TOPO vectors were not compatible.

2.2.8.2.1 In-Fusion HD cloning (Clontech)

First of all, PCR primers were designed to contain 15 bp 5'ends homologous to TOPO vector (Table 2.14). pmiRGLO vector was linearized with XhoI and SacI-HF restriction digestion that as described before and digested plasmid was isolated by gel electrophoresis followed by Nucleospin gel and PCR clean-up kit (Macherey Nagel). Then, the cloned 3'UTR fragment was amplified out of the TOPO construct with CloneAmp^{TM} DNA polymerase (the reaction is shown in Table 2.32). Thermal Cycler (BIORAD) was set for 35 cycles (98°C, 10 sec; specified Tm for primers (45°C), 15 sec; 72°C, 5 sec).

1% agarose gel electrophoresis was performed to analyse PCR products as desrcibed earlier. The amplified NFIB 3'UTR fragment was isolated using Nucleospin gel and PCR clean-up kit (Macherey Nagel). The concentration and purity of DNA was checked by measuring absorbance at 260 nm.and the concentration was checked again by agarose gel electrophoresis. Finally, In-Fusion reaction was set up as shown in Table 2.33. In-Fusion reaction mixture was mixed and centrifuged briefly. Then, it was incubated for 15 min at 50°C. Then, it was placed on ice before transformation.

Table 2.32 : PCR components by using CloneAmp Hi-Fi PCR Premix.

Reagent	Volume	Final Concentration
CloneAmp HiFi PCR Premix	12.5 µl	1X
Primer (Forward) (100 µM)	0.75 µl	0.3 µM
Primer (Reverse) (100 µM)	0.75 µl	0.3 µM
Plasmid DNA	x µl	1 ng
Sterilized distilled water	Up to 25 µl	

Table 2.33 : In-Fusion cloning reaction components.

Reagent	Volume	Final Concentration
5X In fusion HD Enzyme Premix	2 µl	1X
Linearized pmiRGLO vector	x µl	50 ng
Insert	x µl	100 ng
dH_2O	Up to 10 µl	
Total volume	10 µl	

2.2.8.2.2 Transformation for Stellar competent cells

Stellar competent cells were used for transformation for the In-Fusion reactions. 2,5 µl of In-Fusion sample was transferred into pre-chilled tubes with 50 µl of stellar competent cells and incubated 30 min on ice. Cells were heat shocked at 42°C for 45 sec. Later, tubes were placed on ice again for 2 min. 500 µl of SOC medium was added into the tubes. The tubes were incubated at 37°C for 1 h. 100 µl of these transformed cells were spread on the plates that include ampicillin as antibiotics. The rest of the transformed cells were centrifugated at 6000 rpm for 5 min. 300 µl of supernatant was discarded and the pellet was resuspended with the remaining supernatant. Then, these cells were spread on the Amp^+LB plates and incubated at 37°C overnight. Clones were selected from isolated colonies and plasmids were purified as before. Selected plasmids were digested with restriction endonucleases (SacI-HF and XhoI as described above. Then, 1% agarose gel electrophoresis was performed to analyse restriction digests as desrcibed earlier. Mini-preps that were yielded correct diagnostic pattern were selected for sequencing using the specific sequencing primers listed in Table 2.13.

2.2.9 QuikChange site-directed mutagenesis for the reporter constructs

2.2.9.1 Mutant strand synthesis

We performed site directed mutagenesis of the predicted miR-21, miR-124a and miR-153 binding sites on 3'UTR NFIB as follows: Primers were designed to mutate the putative binding sites of miR-21, miR-124a and miR-153 on NFIB 3'UTR with carrying four mismatches shown in Figure 2.4 and designed primers are listed in Table 2.35.

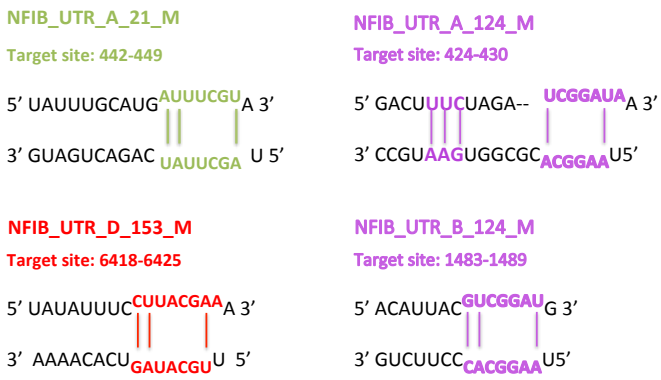


Figure 2.4 : Primers were designed to mutate putative miRNA binding sites on 3'UTR of NFIB. Primers for miR-21 (green), miR-153 (red) and miR124 (pink) binding sites on 3'UTR of NFIB carry four mismatches within seed regions for site directed mutagenesis.

For that purpose, two different kits (QuikChange II XL site-directed mutagenesis kit and QuikChange Multi site-directed kit) were used for mutagenesis reaction.

Table 2.34 : Reagents used for QuikChange multi site-directed mutagenesis kit of desired miRNAs binding sites in NFIB 3'UTR and respective control.

Reaction components	pmiRGLO with 3'UTR_A/B mutagenesis	Control mutagenesis
10X Quikchange Multi Buffer	2.5 µl	2.5 µl
dH_2O	up to 25 µl	up to 25 µl
QuikSolution	0.75 µl	-
ds-DNA template	100 ng	1 µl Quikchange Multi Control Template
Mutagenic primer	100 ng	1 µL Quikchange Multi Control Primer Mix
dNTP mix	1 µL	1 µL
QuikChange multi enzyme blend	1 µL	1 µL

Briefly, site directed mutagenesis reaction contains three steps: Mutant strand synthesis using designed mutagenic primers; DpnI digestion to degrade original plasmid and transformation of the mutated single stranded plasmid DNA into XL10-Gold ultracompetent cells or NEB-5 alpha ultracompetent cells.

Only first step of mutagenesis reaction differs between two kits. In the first step of QuikChange multi site-directed mutagenesis kit, pmiRGLO vector carrying the desired part of NFIB 3'UTR (NFIB 3'UTR_A; NFIB 3'UTR_B) was amplified with mutagenic primer (carrying four mismatches within the seed region, see in Table 2.35) using *PfuTurbo* DNA polymerase which is provided with the kit.

Table 2.35 : Primers to mutate binding sites of selected miRNAs on NFIB 3'UTR.

Primer name	Sequence
NFIB_UTR_A_124_M1_S	CAATATATTTTAACTGACTTTCTAGATCGGATAATATTTGCATGATAAG
NFIB_UTR_A_21_M1_S	GCCTTAATATTTGCATGATTTCGTAGTTTTATTGGTTTAGTATTCTTG
NFIB_UTR_B_124_M1_S	GATATAATGTCCACATTACGTCGGATGCCTTGAAATCTAAAAAAC
NFIB_UTR_D_153_M1_S	GAAGCGGATATATTTCCTTACGAAAAACTGTTTAAACAATAAAATGAGC
NFIB_UTR_A_124_M1_AS	CTTATCATGCAAATATTATCCGATCTAGAAAGTCAGTTAAAATATATTG
NFIB_UTR_A_21_M1_AS	CAAGAATACTAAACCAATAAAACTACGAAATCATGCAAATATTAAGGC
NFIB_UTR_B_124_M1_AS	GTTTTTTAGATTTCAAGGCATCCGACGTAATGTGGACATTATATC
NFIB_UTR_D_153_M1_AS	GCTCATTTTATTGTTTAAACAGTTTTTCGTAAGGAAATATATCCGCTTC

After the components were mixed which was shown in Table 2.34, mutant strand synthesis was carried out using the PCR parameters provided in Table 2.36.

Table 2.36 : Thermocycling parameters for mutant strand synthesis reaction for QuikChange multi site-directed kit.

Segment	Cycles	Temperature	Time
1	1	95°C	1 min
2	30	95°C	1 min
		55°C	1 min
		65°C	16 min

Alternatively, mutant strand synthesis was also attempted with QuikChange XL site-directed mutagenesis kit using *Pfu Ultra* DNA polymerase and mutagenic primers listed in Table 2.35. Reaction contents were mixed as indicated in Table 2.37 and carried out using the thermocycling parameters shown in Table 2.38.

Table 2.37 : Reagents used for QuikChange II XL site-directed mutagenesis kit of desired miRNAs binding sites in NFIB 3'UTR and respective control.

Reaction components	pmiRGLO with 3'UTR_A/D mutagenesis
10X Quikchange Multi Buffer	5 µl
dH_2O	up to 50 µl
QuikSolution	3 µl
ds-DNA template	10 ng
Mutagenic primer	125 ng
dNTP mix	1 µL
QuikChange multi enzyme blend	1 µL

Table 2.38 : Thermocycling parameters for mutant strand synthesis reaction for QuikChange II XL site-directed kit.

Segment	Cycles	Temperature	Time
1	1	95°C	1 min
		95°C	50 sec
2	18	50°C	50 sec
		68°C	8 1/2 min
3	1	68°C	7 min

The subsequent steps are the same in the two kits. Original plasmid was treated with 1 µl DNA endonuclease *DpnI* and incubated at 37°C for 1 h. DpnI specifically degrades dam methylated DNA. The newly synthesized mutated strand does not carry the parental methylation pattern and cannot be degraded by *DpnI*. Following DpnI treatment, mutated single stranded DNA was transformed into E.coli XL10-Gold ultracompetent cells, where the double strand synthesis and amplification was performed.

2.2.9.2 Transformation of ultracompetent XL10-Gold *E.coli* competents

Transformation was carried out according to the protocol defined within the kit. Firstly, *E.coli* strain XL10-Gold was thawed on ice. 45 µl of bacteria was transferred into prechilled 50 ml polypropylene tubes per each reaction, and added 2 µl of beta-mercaptoethanol. Mixture was incubated at 10 min on ice. Then, cells were added 1.5 µl DpnI treated plasmid from QuikChange multi site-directed mutagenesis reaction or 2 µl DpnI treated plasmid from QuikChange XL site-directed mutagenesis reaction (or 1 µl pUC18 plasmid for a transformation control) and incubated on ice for 30 min. After cells were heat shocked at 42°C for 30 sec, the cells were cooled on ice for 2 min. 500 µl NZY Broth was added into the bacteria and incubated at 37°C for 1 h at 250 rpm. All transformed bacteria were plated on ampicillin contained selection plates.

Colonies were selected for small-scale plasmid preparation and plasmids were purified with GeneJET Plasmid Miniprep Kit (Thermo Scientific). Clones were sequenced to verify successful mutagenesis reaction.

2.2.10 Dual luciferase assay

2.2.10.1 miRNA mimic and/or inhibitor and reporter construct tranfection using DharmaFECT 1 transfection reagent

The miRNA reporter plasmids were generated by cloning NFIB 3'UTR segments corresponding to the matched target sites for miR-21, miR-153, miR-124a and miR30a. To perform the Dual-luciferase reporter assay (Promega), HEK293T cells were plated into 96-well plates, at 20,000 cells/well. After 24h of incubation, 150 ng/well reporter plasmids and 20 nM miRNa mimics (Ambion) and/or 100 nM miRNA inhibitors (Ambion) were co-transfected into the cells in triplicate in 100 µl/well Opti-MEM using DharmaFECT-1 Transfection Reagent (Dharmacon) according to the manufacturer's instructions

For that purpose, 10 µl serum free medium was prepared by diluting 20 nM miRNa mimics and/or 100 nM inhibitors as well as 150 ng reporter vector in OptiMEM (Tube 1). At the same time, 0.2 µl DharmaFECT transfection reagent was diluted in 10 µl serum free medium in another tube (Tube 2). Then, each tube was gently mixed and incubated for 5 min at RT. The contents of tube 1 was transferred into tube 2 (total volume was 20 µl) and mixed again carefully and incubated for 20 min at RT. Finally, 80 µl complete medium was added into the mixture to make 100 µl. Medium was removed from the wells of the 96 well plates and transfection mixture was transferred into well. Cells were incubated at 37°C in 5% CO_2 for 48 h.

2.2.10.2 Luciferase assay

48 h after transfection, cells were washed once with PBS and lysed by adding 50 µl 1X Passive Lysis Buffer. Homogenous lysates were prepared by shaking the culture plate for 15 min at RT. Then, the lysate was transferred into microcentrifuge tube and centrifuged for 30 sec at max. speed. First of all, firefly luciferase *(Photinus pyralis)* reporter signal was measured by adding 100 µl Luciferase Assay Reagent II (LAR II) onto 20 µl of the cell lysate (from the supernatant). Then, for *Renilla (Renilla reniformis)* luciferase signal measurement, 100 µl Stop & Glo Reagent was added into the same well to quench firefly luciferase reaction and initiate *Renilla* luciferase reaction. Chemiluminescence was measured using Fluoroskan Ascent FL luminometre (Thermo Electron Corporation) and default settings were used for the PMT voltage (845) and the integration time was choosen as 10000. Relative firefly luciferase signals were normalized against *Renilla* luciferase signals to minimize

experimental variability caused by differences in transfection efficiency and cell viability. Results are expressed as relative FLuc/RLuc ratios to that of pmiRGLO-treated cells. Each experiment was performed at least three times.

2.2.11 Statistical analyses

p values were calculated using Graphpad Prism 6.0 Software. Statistical significance was determined by Student t-test (qRT-PCR expression analysis, luciferase experiments) or one way ANOVA analysis (qRT-PCR time-dependent expression analysis). In all analyses, p value of less than 0.05 was considered statistically significant and determined p values were indicated in column bar graphs with the symbols ***$p<0.0001$; **$p<0.001$; *$p<0.05$.

3. RESULTS

In order to study regulation of the downstream targets of NFIB and miRNAs that regulate NFIB, we characterized H9 derived human neural stem cells (hNSCs, Gibco) during differentiation. Expression profiles of NFIs and potential target genes of NFIB (*CDO, FGF19* and *COL2A1*) were examined in differentiating hNSCs. We also looked for changes in the expression of miRNAs that potentially target NFIB in differentiating hNSCs and analysed their binding to 3'UTR of NFIB.

3.1 hNSCs Differentiate into Neurons in Cell Culture

3.1.1 Expression of Nestin and neural differentiation marker, TUJ1

In order to study the role of NFIs in neural differentiation *in vitro*, we chose the commercially available human neural stem cell line (hNSCs, Gibco), which can differentiate into different neural subtypes (multiple neuronal phenotypes such as dopaminergic neurons, cholinergic motoneurons as well as astrocytes and glia) (Shin et al., 2005, 2006, 2010). hNSCs were subjected to growth factor withdrawal for seven days in culture in the presence of neurotrophins, BDNF and NT-3 to increase cell survival upon growth factor withdrawal.

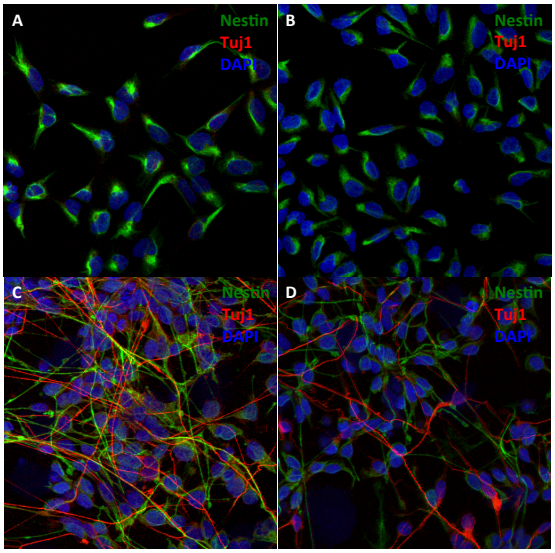


Figure 3.1 : Expression of neural stem cell and differentiation markers in progenitor and differentiated human Neural Stem Cells (hNSCs).

Figure 3.1 (cont'd) : Expression of neural stem cell and differentiation markers in progenitor and differentiated human Neural Stem Cells (hNSCs). β-Tubulin III (Tuj1) (red) and Nestin (green) expressed in the cells were immunocytochemicallys stained and imaged with a confocal microscope. Cell nuclei were counterstained with DAPI (blue) **A-B:** Progenitor hNSCs **C-D:** hNSCs cultured under differentiation conditions for seven days. Magnification: 100x.

To validate our differentiation protocol and confirm differentiation capacity of hNSCs, cell marker expression was characterized. hNSCs were first assayed for expression of Nestin (multipotent neural stem cell marker) and β-Tubulin III (Tuj1) (neuron specific marker) by immunofluorescence and nearly all the hNSCs were Nestin$^+$ (Fig.3.1A, B) while there were no β-III tubulin$^+$ neurons contaminating the culture. Upon differentiation, we observed cells with elongated processes (neurites) which were β-III tubulin$^+$ (Fig.3.1A, B). Decrease in nestin expression was also observed (Figure 3.1).

3.1.2 Flow cytometry analyses of hNSCs progenitors and differentiated hNSCs

In order to quantify cell marker expression in hNSCs, we performed flow cytometry analysis (Figure 3.2).

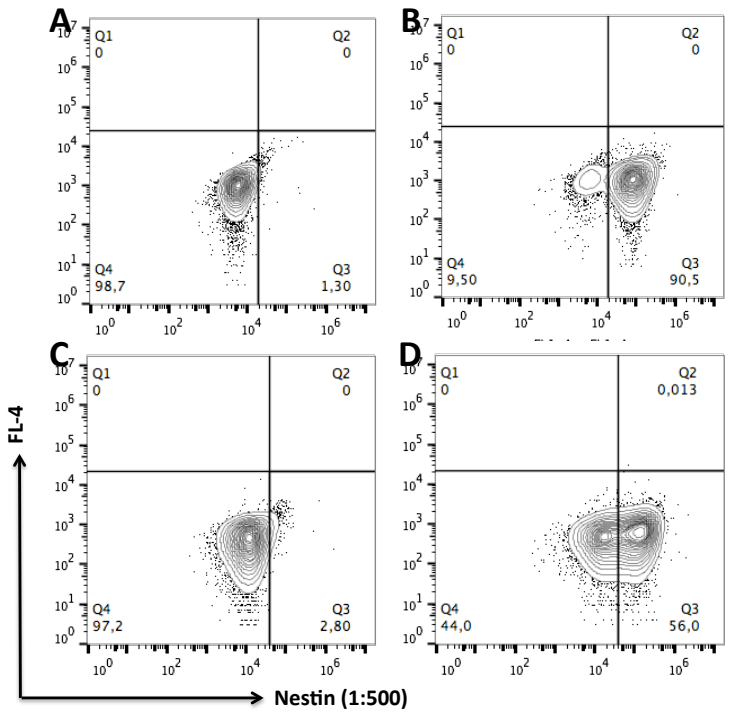


Figure 3.2 : The ratio of Nestin$^+$ hNSCs decreases upon differentiation.

Figure 3.2 (cont'd) : The ratio of Nestin$^+$ hNSCs decreases upon differentiation. Flow cytometry plot of progenitor and differentiated hNSCs compared to secondary antibody control to determine the percentage of cells expressing cytoplasmic progenitor cell marker, Nestin **A:** IgG control of proliferative hNSCs **B:** Nestin staining of proliferative hNSCs (1:500) **C:** IgG control of differentiated hNSCs **D:** Nestin staining of differentiated hNSCs (1:500 dilution). Values in quadrants indicate percentages of cells. Results are representative of two independent experiments. Proliferative hNSCs were 90.5% Nestin$^+$, while differentiated hNSCs were 56% Nestin$^+$.

Proliferative neural stem cells were 90% Nestin$^+$, this ratio decreased by 34.5 % upon differentiation (Figure 3.2). This result is consistent with reports on differentiation of neural stem cells in culture, where differentiation takes place over time, with generation of neurons followed by astrocytes and glia (Temple 2001, Gaspard 2008). In order to quantify cells that have differentiated into neurons, we also examined expression of β-III tubulin by flow cytometry. However, β-III tubulin expression seen in neurites by immunoflurescence could not be observed in the fluorescence signals obtained in flow cytometry experiments (data not shown). Technical problems associated with this experiment are explained in the Discussion part of the thesis.

3.2 Characterization of *NFI* Expression during Differentiation

In order to study NFI function in the hNSC cell line, we first wanted to characterize NFI expression. hNSCs were subjected to differentiation conditions for seven days in cell culture and NFI mRNA expression was determined in proliferative and differentiated hNSCs, in three independent experiments.

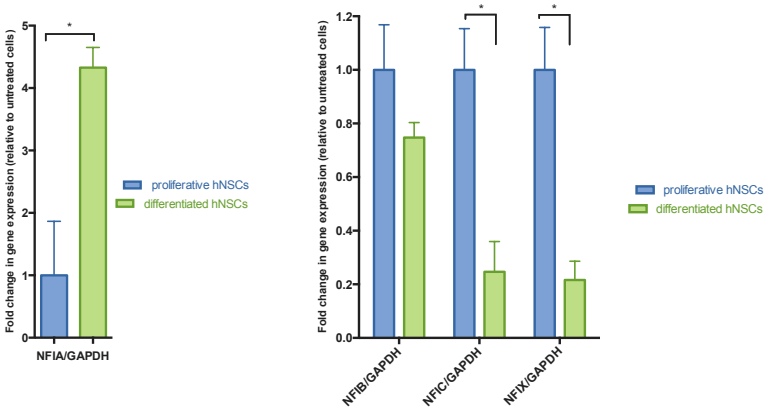


Figure 3.3 : Upon differentiation of hNSCs *NFIB, NFIC* and *NFIX* are downregulated while *NFIA* is upregulated (I).

Figure 3.3 (cont'd) : Upon differentiation of hNSCs *NFIB, NFIC* and *NFIX* are downregulated while *NFIA* is upregulated (I). Expression levels of *NFI* transcripts were measured by qRT-PCR in proliferative hNSCs (blue bars) and differentiated hNSCs (green bars). Gene expression levels were normalized to *GAPDH* expression. Data show the mean±S.D from 2 replicates. Statistical significance was determined according to Student's t-test (***p<0.0001; **p<0.001; *p<0.05). The result of the first independent experiment is shown. *NFIB*, *NFIC* and *NFIX* expression levels decreased to 75%, 25% and 22% of those in proliferative cells respectively and *NFIA* expression increased 4.3 fold upon differentiation.

In the first experiment, *NFIB* levels decreased only by 25%, however decrease in *NFIC* and *NFIX* expression was remarkable (by 75% and 78% respectively) upon differentiation while *NFIA* expression increased 4.3 fold.

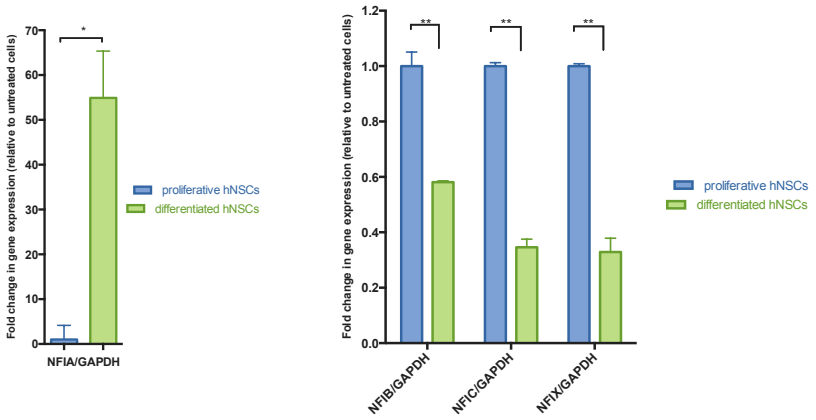


Figure 3.4 : Upon differentiation of hNSCs *NFIB, NFIC* and *NFIX* are downregulated while *NFIA* is upregulated (II). Expression levels of *NFI* transcripts were measured by qRT-PCR in proliferative hNSCs (blue bars) and differentiated hNSCs (green bars). Gene expression levels were normalized to *GAPDH* expression. Data show the mean mean±S.D from 2 replicates. Statistical significance was determined according to Student's t-test (***p<0.0001; **p<0.001; *p<0.05). The result of the second independent experiment is shown. *NFIB*, *NFIC* and *NFIX* expression levels decreased to 58%, 35% and 33% of those in proliferative cells and *NFIA* expression increased 55 fold upon differentiation.

In the second assay, *NFIB, NFIC* and *NFIX* expression was significantly reduced by 42%, 65% and 67% upon differentiation. However, upregulation of *NFIA* expression (55 fold) was higher than the increase observed in the first experiment. This discrepancy may be due to our inability to accurately determine NFIA expression levels once they fall below detection range.

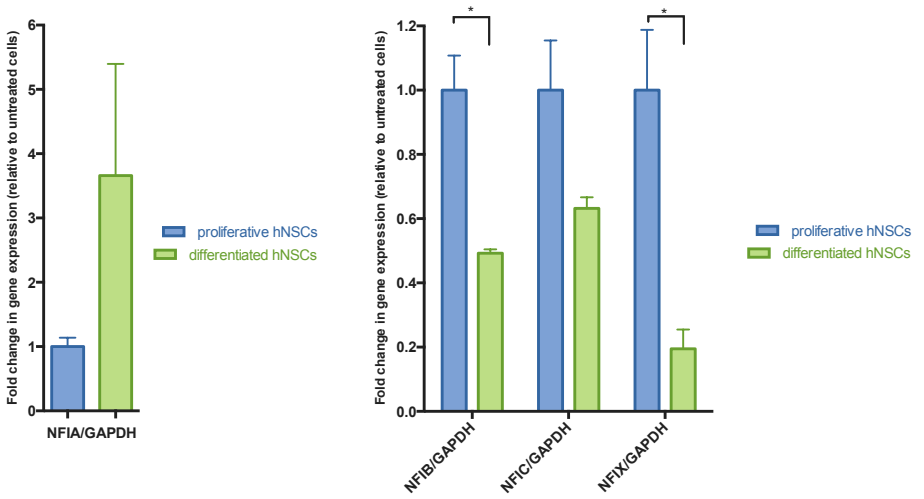


Figure 3.5 : Upon differentiation of hNSCs *NFIB, NFIC* and *NFIX* are downregulated while *NFIA* is upregulated (III). Expression levels of *NFI* transcripts were measured by qRT-PCR in proliferative hNSCs (blue bars) and differentiated hNSCs (green bars). Expression levels of *NFI* transcripts were measured by qRT-PCR in proliferative hNSCs (blue bars) and differentiated hNSCs (green bars). Gene expression levels were normalized to *GAPDH* expression. Data show the mean±S.D from 2 replicates. Statistical significance was determined according to Student's t-test (***p<0.0001; **p<0.001; *p<0.05). The result of the third independent experiment is shown. Expression levels of *NFIB*, *NFIC* and *NFIX* decreased to 49%, 63% and 19% of those in proliferative cells and *NFIA* expression increased 3.7 fold upon differentiation.

In the third experiment, *NFIB, NFIC* and *NFIX* levels decreased (by 51%, 37% and 81% respectively) upon differentiation, while *NFIA* was upregulated 3.7 fold.

Results from three independent experiments show that *NFIA* levels consistently increase whereas *NFIB*, *NFIX* and *NFIC* levels decrease upon differentiation (Figure 3.3, Figure 3.4 and Figure 3.5). However, fold changes in *NFI* expression levels are different in three independent assays (Table 3.1). Since differentiation of hNSCs in culture produced a heterogeneous population of proliferative and differentiated cells, which presumably varied in each experiment, we may have measured different ratios of gene expression change in each experiment. However, we reliably observed NFIB, NFIC and NFIX expression levels to be reduced (at least 1.3, 2.9 and 3 fold respectively) while NFIA expression increased at least 3.7 fold (Table 3.1).

Table 3.1 : Fold changes of *NFIA, NFIB, NFIC* and *NFIX* expression levels between proliferative and differentiating hNSCs in three independent assays. Negative fold change values indicate lower expression in differentiating hNSCs.

	Fold change in mRNA expression level upon differentiation			
	NFIA	***NFIB***	***NFIC***	***NFIX***
Assay-I	4.3	-1.33	-4	-4.6
Assay-II	55	-1.72	-2.9	-3
Assay-III	3.7	-2	-3	-5.3

In order to examine regulation of NFI expression further, we carried out a time course experiment and measured NFI mRNA expression over day 0, 3, 5 and 7 during differentiation of hNSCs.

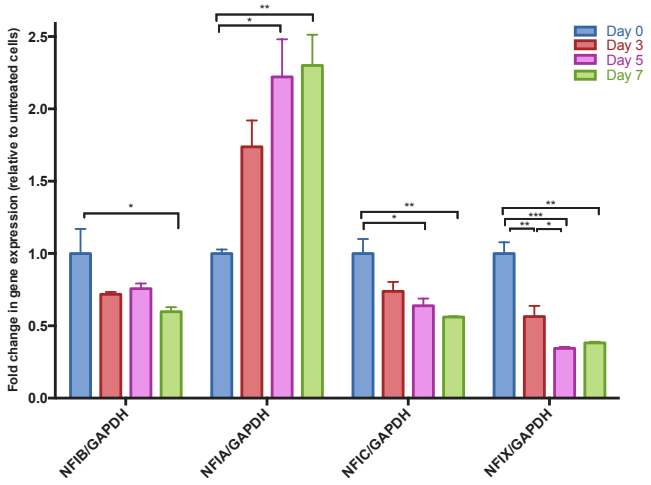


Figure 3.6 : *NFIA* is upregulated while *NFIB, NFIC* and *NFIX* are downregulated in differentiating hNSCs in a time-dependent manner. Expression levels of *NFI* transcripts in hNSCs were measured by qRT-PCR during various time points of differentiation (Day 0 (blue bars), day 3 (red bars), day 5 (pink bars), day 7 (green bars)). Gene expression levels were normalized to *GAPDH* expression. Data show the mean±S.D from 2 replicates. Statistical significance was determined according to one-way ANOVA analysis (***p<0.0001; **p<0.001; *p<0.05). Results are representative of 4 independent time-course experiments. NFIB decreased by 28% at day 3; by 24% at day 5 and by 40% at day 7. NFIC decreased by 27% at day 3; by 36% at day 5 and by 44% at day 7. NFIX decreased by 44% at day 3; by 66% at day 5 and by 62% at day 7, as NFIA increased 1.7 fold at day 3; 2.2 fold at day 5 and 2.3 fold at day 7.

Data indicate that decrease in expression of *NFIB* (by 28%), *NFIC* (by 27%) and *NFIX* (by 44%) was seen as early as day 3, as the increase in NFIA (1.7 fold) (Figure

3.6). While changes of NFI expressions in differentiating hNSCs from day 0 to day 7 correlate with results of endpoint experiments, we could not detect an upregulation of NFIB that would support its role in neurogenesis. While expression of NFIs was also characterized at earlier time points (day 1 and 2), the trend in expression changes is the same (see Appendix E). The fact that only a portion of stem cells differentiate and that the culture contains a heterogenous population of cells renders the differentiation assay as not very rigorous nor reproducible, making it difficult to determine subtle changes in gene expression. It may be necessary to purify different cell populations or assay expression by immunofluorescence or flow cytometry to circumvent this problem.

3.3 NFIB Protein Levels Decrease during hNSC Differentiation

We next wanted analyse NFI protein expression in hNSCs. Ct values obtained from qRT-PCR analysis for the different NFI transcripts indicated that *NFIA*, *NFIC* and *NFIX* expression levels were significantly lower than that of *NFIB* (Ct values of *NFIA, NFIC* and *NFIX* were at least 11, 4 and 6 cycles higher than that of *NFIB* respectively). Therefore, we analysed NFIB protein expression only. In order to enrich for transcription factors, we obtained nuclear protein extracts from hNSCs and subjected these to Western blot analysis. However, as four different alternative splicing forms of NFIB have been reported in the literature, we first wanted to determine the NFIB isoforms expressed in hNSCs. To that end, primers were designed specifically for alternatively spliced NFIB transcripts and expression was determined by RT-PCR.

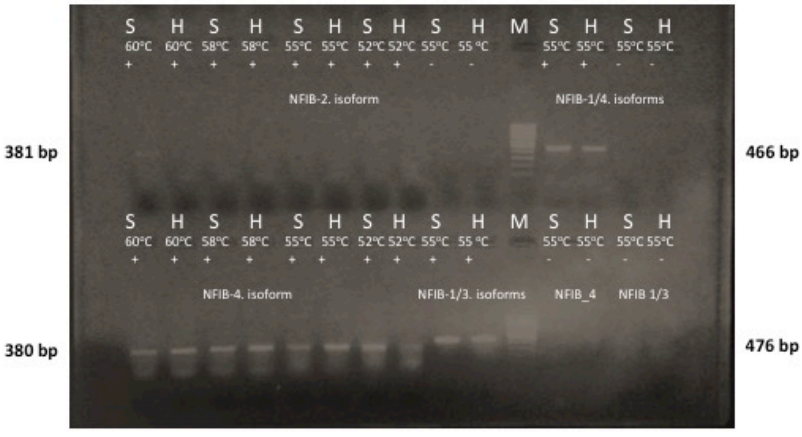
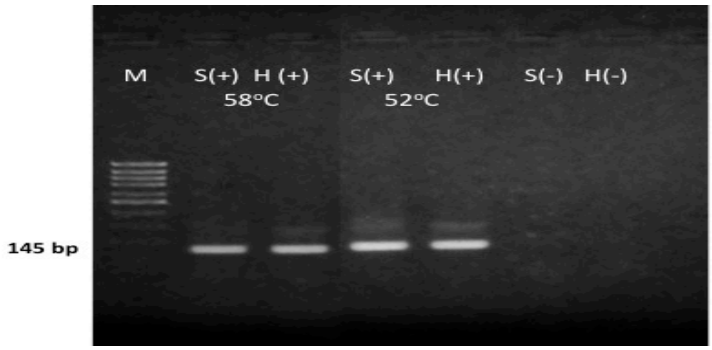


Figure 3.7 : NFIB-1 and/or NFIB-3 and NFIB-4 isoforms are expressed in progenitor hNSCs.

Figure 3.7 (cont'd) : NFIB-1 and/or NFIB-3 and NFIB-4 isoforms are expressed in progenitor hNSCs. RNAs from proliferative hNSCs and SH-SY5Y cells were reverse transcribed and gradient PCR was performed with the various NFIB isoform specific primers. SH-SY5Y human cell line, which expresses significant levels of NFIB, was used as positive control. (**H:** proliferative hNSCs; **S:** SH-SY5Y; **M:** Marker; **+:** cDNA samples; **-:** Negative control of cDNA reaction).

PCR primer sets detected either NFIB-2, or NFIB-4, or NFIB-1 and -3 *(NFIB-1/3),* or NFIB-1 and -4 (NFIB-1/4). We could not detect transcripts of NFIB-2, but obtained positive results for NFIB-4, NFIB-1/3 and NFIB-1/4 indicating these three isoforms could be expressed.



F**igure 3.8 : NFIB-3 is expressed by hNSCs (I).** RNAs from proliferative hNSCs and SH-SY5Y cells were reverse transcribed and gradient PCR was performed with the universal primers to amplify all NFIB isoforms. Amplicon sizes differs isoforms to each other (amplicon sizes: NFIB-1: 367 bp; NFIB-2 and NFIB-3: 145 bp; NFIB-4: 483 bp). SH-SY5Y human cell line, which expresses significant levels of NFIB, was used as positive control. (**H:** proliferative hNSCs; **S:** SH-SY5Y; **M:** Marker; **+:** cDNA samples; **-:** Negative control of cDNA reaction).

We then designed universal primers that will amplify all isoforms, but result in different sized amplicons (amplicon sizes: NFIB-1: 367 bp; NFIB-2 and NFIB-3: 145 bp; NFIB-4: 483 bp). A second PCR was performed with these universal primers, and a 145 bp PCR product, which shows the expression of NFIB-2 and/or NFIB-3, was detected. However, we could not amplify the PCR product for NFIB-4 (483 bp) whose expression was determined in the previous experiment. Therefore, it is also possible that NFIB-1 was not amplified even though it was expressed (Figure 3.8). Together with previous data, this result indicated the presence of NFIB-3 in hNSCs.

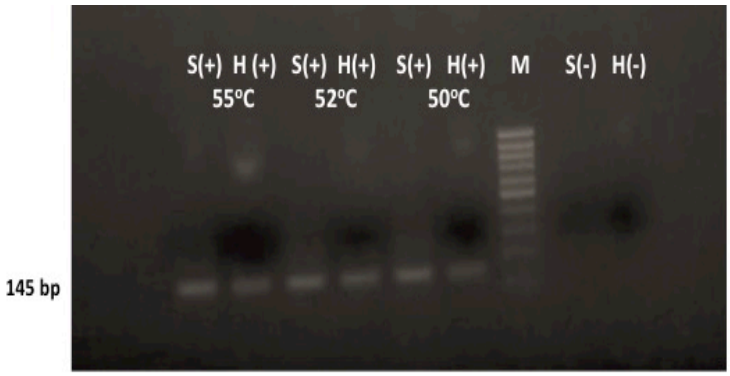


Figure 3.9 : NFIB-3 is expressed by hNSCs (II). RNAs from proliferative hNSCs and SH-SY5Y cells were reverse transcribed and gradient PCR was performed with the universal primers to amplify all NFIB isoforms. Amplicon sizes differs isoforms to each other (amplicon sizes: NFIB-1: 367 bp; NFIB-2 and NFIB-3: 145 bp; NFIB-4: 483 bp). SH-SY5Y human cell line, which expresses significant levels of NFIB, was used as positive control. (**H:** proliferative hNSCs; **S:** SH-SY5Y; **M:** Marker; **+:** cDNA samples; **-:** Negative control of cDNA reaction).

As we could amplify the 483 bp PCR product for NFIB-4, which was clearly expressed according the first experiment, amplification of longer amplicons may be less efficient. We repeated the experiments with different polymerases (*One Taq* Polymerase, Figure 3.9.) and obtained similar results. In short, PCR analysis showed that hNSCs have expression of NFIB-3 and NFIB-4 isoforms, but not NFIB-2. Since specific primer set for NFIB-1 could not be designed because of high degree of sequence homology between isoforms, we could not determine if hNSCs express NFIB-1 (see also Fig. 2.3). Therefore, we went on to analyse bands corresponding to NFIB-3 (44 kDa) and also NFIB-1 (56 kDa) by Western blot analysis.

NFIB expression from nuclear extracts of hNSCs (described in Ravichandran, 2006) was determined in three independent assays and results are shown below (Figure 3.10, Figure 3.11, Figure 3.12, Figure 3.13).

For the first experiment, different loading controls were used to control for preparation of nuclear extracts and check for correct cellular fractionation. Antibodies recognizing whole cell proteins (GAPDH, Vinculin) and nuclear protein (TBP) were used to identify correct partitioning of these proteins in various samples (whole cell extract, cytosolic, nuclear extracts). Presence of TBP in nuclear extracts shows that our cellular fractionation protocol is successful. Also, specificity of NFIB antibody (Aviva Systems Biology) was checked using NFI transfected whole cell extracts (data not shown).

The first Western blot experiment shows that NFIB protein levels were decreased by 32% in differentiated hNCSs (Figure 3.10). We found that TBP antibody does not have re-blotting activity. Therefore, we changed our nuclear loading control to Lamin B1, which is a nuclear envelope protein. We also increased amount of nuclear extract resolved on SDS-PAGE to increase the NFIB signal (70 µg instead of 50 µg). Since we observed non-specific bands with rabbit polyclonal anti-NFIB antibody (Aviva Systems Biology), we switched to rabbit polyclonal anti-NFIB antibody (Sigma) after the first differentiation experiment, because it has lower background. Specificity of this antibody was also validated by blotting NFI transfected whole cell extracts (data not shown).

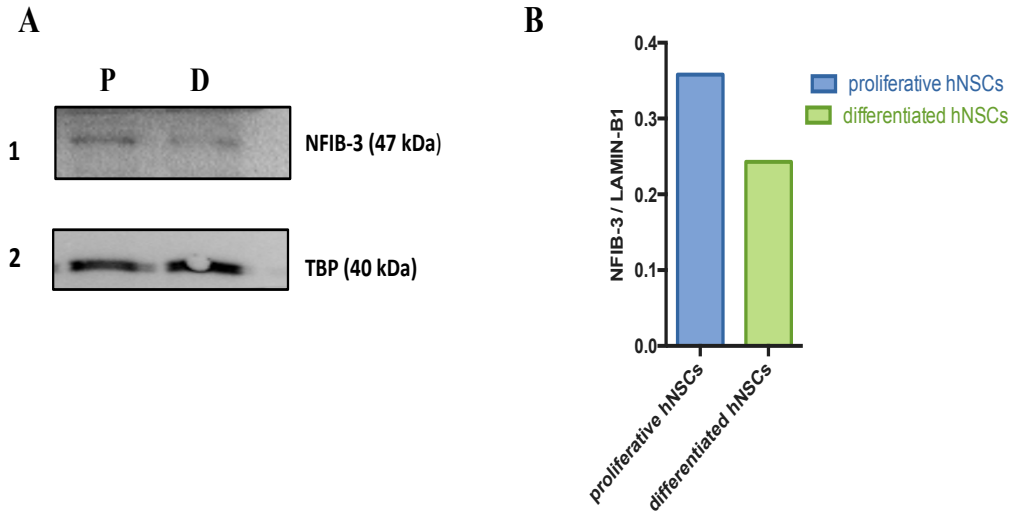


Figure 3.10 : Characterization of NFIB expression in hNSCs upon differentiation (I). Nuclear protein extractions from proliferative (P) and differentiated hNSCs (D) were analysed by Western blot analysis for NFIB expression. 50 µg nuclear extract was resolved by 7.5 % SDS-PAGE and immunoblotted with rabbit polyclonal anti-NFIB antibody (Aviva Systems Biology). TBP was used as loading control **A:** Western blotting data from one of the three independent experiments (first differentiation experiment). Western blotting data **B:** Densitometric analysis of the NFIB bands in proliferative (blue bars) and differentiated (green bars) hNSCs is shown.

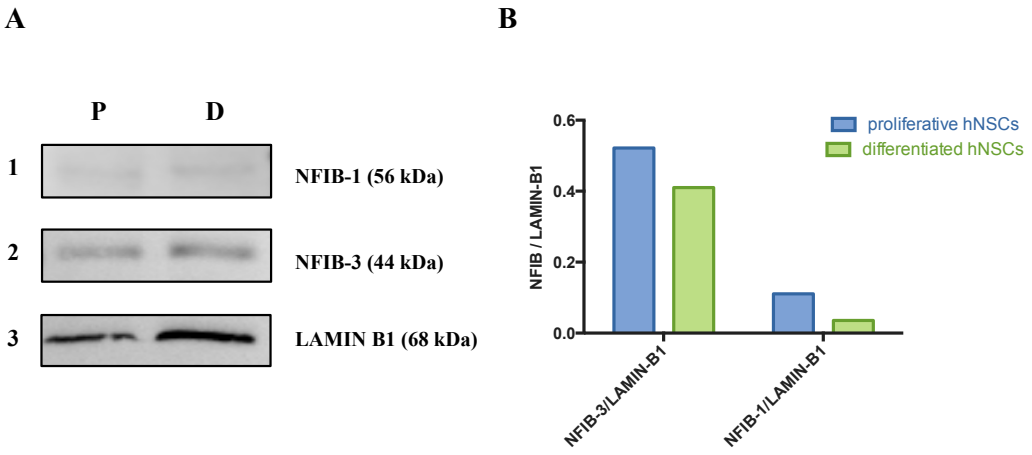


Figure 3.11 : Expression of two alternative splicing forms of NFIB decrease during differentiation of hNSCs (II). Nuclear protein extracts from proliferative (P) and differentiated hNSCs (D) were analysed for NFIB expression. 70 µg nuclear extract was resolved on 7.5 % SDS-PAGE and immunoblotted by rabbit polyclonal anti-NFIB antibody (Sigma). Lamin-B1 was used as loading control. **A:** Western blotting data from the second differentiation experiment. **B:** Densitometric analysis of the NFIB bands in proliferative (blue bars) and differentiated (green bars) hNSCs is shown.

Signal from anti-NFIB blot was normalized to that obtained from Lamin-B1. As a result, two different alternative splice forms of NFIB (NFIB-1 (56 kDa) and NFIB-3 (44 kDa)) were seen on the membrane. NFIB-1 expression was significantly lower than NFIB-3 expression. Densitometric analysis of Western blotting of hNSCs nuclear extracts show that NFIB-1 and NFIB-3 protein levels were decreased by 68% and 21% in differentiated hNCSs (Figure 3.11).

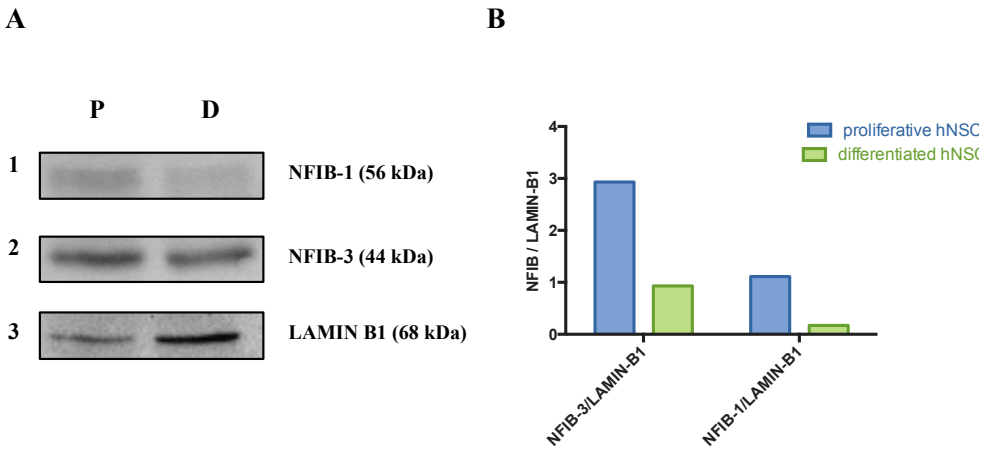


Figure 3.12 : Expression of two alternative splicing forms of NFIB decrease during differentiation of hNSCs (III).

Figure 3.12 (cont'd) : Expression of two alternative splicing forms of NFIB decrease during differentiation of hNSCs (III). Nuclear protein extracts from proliferative (P) and differentiated hNSCs (D) were analysed for NFIB expression. 100 µg nuclear extracts were resolved on SDS-PAGE and immunoblotted with rabbit polyclonal anti-NFIB antibody (Sigma). Lamin-B1 was used as loading control. **A:** Western blotting data from the third differentiation experiment. **B:** Densitometric analysis of the NFIB bands in proliferative (blue bars) and differentiated (green bars) hNSCs is shown.

Amount of nuclear extract analysed was increased further (70 µg to 100 µg) in the third Western blot experiment to increase the NFIB-1 isoform signal. Finally, two different alternative splice forms of NFIB (NFIB-1 and NFIB-3) were both detected. As a result of densitometric analysis of Western blotting of hNSCs nuclear extracts show that NFIB-1 and NFIB-3 protein levels were decreased by 68% and 84% in differentiated hNCSs (Figure 3.12).

In order to confirm that the 56 kDa band identified as NFIB-1 isoform is indeed NFIB, experiment was repeated with PAN-NFI antibody (Santa Cruz Biotechnology). Normalization was perfomed as before. Similar sized bands were seen with PAN-NFI antibody as with the anti-NFIB (Sigma). Also, bands corresponding to NFIB-1 and NFIB-3 were also detected with this antibody. Densitometric analysis of western blotting of hNSC nuclear extracts indicated that NFIB-1 and NFIB-3 protein levels decreased by 80% and 83% in differentiated hNCSs (Figure 3.13).

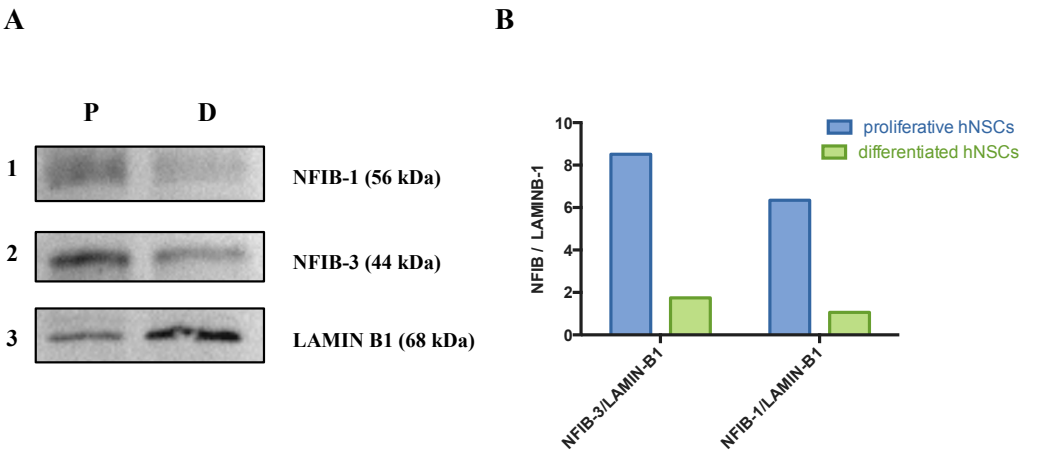


Figure 3.13 : Expression of two alternative splicing forms of NFIB decrease during differentiation of hNSCs (III).

Figure 3.13 (cont'd) : Expression of two alternative splicing forms of NFIB decrease during differentiation of hNSCs (III). Nuclear protein extracts from proliferative (P) and differentiated hNSCs (D) were analysed for NFIB expression. 100 µg nuclear extracts were resolved by SDS-PAGE and immunoblotted with rabbit polyclonal NFI antibody (Santa Cruz Biotechnology). Lamin-B1 (Abcam) was used as loading control. **A:** Western blotting data from third differentiation experiment. **B:** Densitometric analysis of the NFIB bands in proliferative (blue bars) and differentiated (green bars) hNSCs is shown.

Western blotting and densitometric analyses of the NFIB bands indicate that NFIB protein levels decreased in differentiating hNSCs. The decrease in expression levels was measured to be from 20-79% for NFIB-1 and 16-68% for NFIB-3 (Table 3.2).

Table 3.2 : Normalized expression of NFIB-1 and NFIB-3 in three independent differentiation assays. Expression is expressed as percentage of proliferative hNSCs.

Normalized NFIB expression in differentiated hNSCs						
Assay-I (NFIB antibody (Aviva))	Assay-II (NFIB antibody (Sigma))		Assay-III (NFIB antibody (Sigma))		Assay-III (PAN_NFI antibody)	
NFIB-3/TBP	NFIB-3/LAMIN B1	NFIB-1/LAMIN B1	NFIB-3/LAMIN B1	NFIB-1/LAMIN B1	NFIB-3/LAMIN B1	NFIB-1/LAMIN B1
0.32	0.68	0.21	0.84	0.68	0.83	0.80

Decrease in mRNA expression levels of NFIB correlated with the reduction of NFIB protein levels. However, fold changes in mRNA levels did not correspond to the same fold change in protein levels in any of the three independent differentiation assays.

3.4 Expression of Putative Downstream Targets of NFIB (*CDO, COL2A1, FGF19*) are Regulated during hNSC Differentiation

Previously we found that NFIB regulates neurogenesis of precerebellar neurons of the hindbrain (Kumbasar et al., 2009) and that *CDO*, *COL2A1* and *FGF19* are upregulated in *NFIB*$^{-/-}$ precerebellar progenitor cells (Kumbasar, unpublished data). We hypothesized that these genes could also be downstream targets of NFIB in hNSCs and examined expression pattern of these genes during hNSC differentiation.

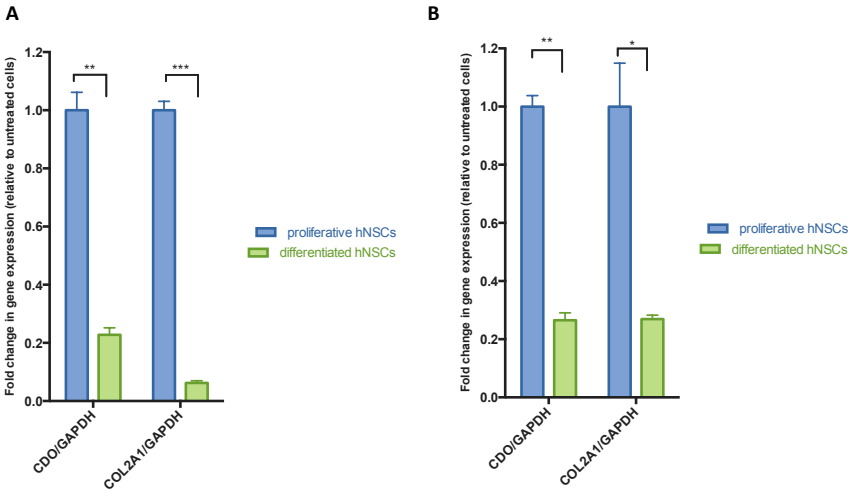


Figure 3.14 : Characterization of expression of putative NFIB downstream targets (*CDO*, *COL2A1*) in hNSC during differentiation. Expression levels of NFI targeted genes (*CDO* and *COL2A1*) were measured by qRT-PCR in proliferative hNSCs (blue bars) and differentiated hNSCs (green bars). Gene expression levels were normalized to *GAPDH* expression. Data show the mean±S.D from 2 replicates. Statistical significance was determined according to Student's t-test (***p<0.0001; **p<0.001; *p<0.05). Data shown are first **(A)** and second **(B)** independent experiments. *CDO* and *COL2A1* expression decreased by 77% and 94% in first differentiation assay and by 73% and 73% in second differentiation assay respectively.

qRT-PCR analyses show that, *CDO* expression was downregulated (by 77%, 73% and 65%), and *COL2A1* expression decreased (by 94%, 73%, 84%) in hNSCs upon differentiation (Figure 3.14., Figure 3.15).

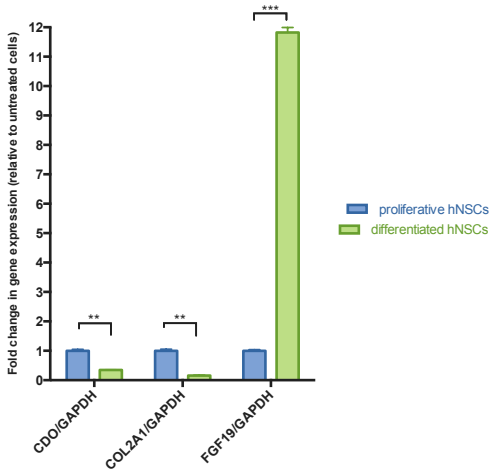


Figure 3.15 : Characterization of expression of putative NFIB downstream targets (*CDO*, *COL2A1*, *FGF19*) in hNSC during differentiation.

Figure 3.15 (cont'd) : Characterization of expression of putative NFIB downstream targets (*CDO*, *COL2A1*, *FGF19*) in hNSC during differentiation. Expression levels of NFI targeted genes (*CDO, COL2A1* and *FGF19*) were measured by qRT-PCR in proliferative hNSCs (blue bars) and differentiated hNSCs (green bars). Gene expression levels were normalized to *GAPDH* expression. Data show the mean±S.D from 2 replicates. Statistical significance was determined according to Student's t-test (***p<0.0001; **p<0.001; *p<0.05). Data shown is third differentiation assay. *CDO* and *COL2A1* expression was downregulated (by 65%; 84% respectively) while FGF19 expression increased 11.8 fold upon differentiation.

FGF19, on the other hand, was upregulated (11.8 fold) (Figure 3.15). While we did not repeat the FGF19 experiment multiple times, we observed similar results in time course experiments (Figure 3.16 and Appendix F). These data show a correlation between downregulation of NFIB with upregulation of FGF19. This pattern of expression would be expected if NFIB repressed FGF19 expression in hNSCs as it does in precerebellar progenitors.

Next, we asked whether NFIB target genes are regulated earlier during hNSC differentiation. Expression of target genes was measured by qRT-PCR in a time-course experiment over day 0, 3, 5 and 7.

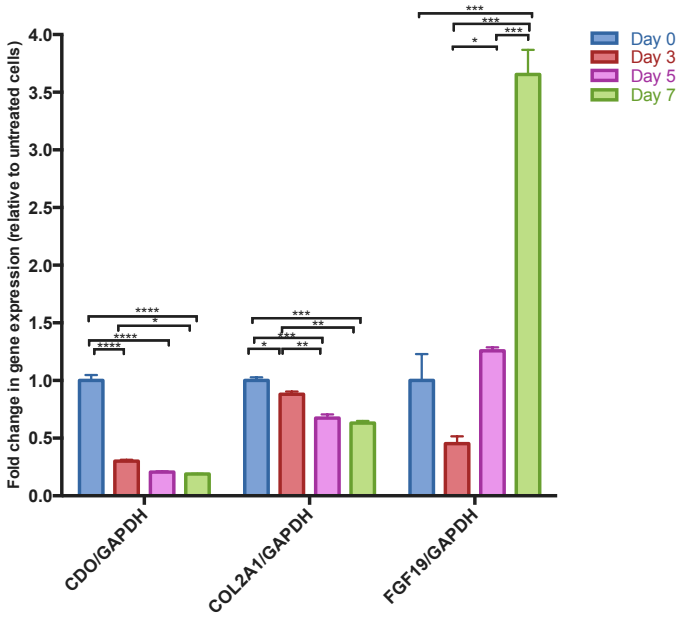


Figure 3.16 : Characterization of expression of putative NFIB downstream targets (*CDO*, *COL2A1*, *FGF19*) in hNSC during differentiation in a time-dependent manner.

Figure 3.16 (cont'd) : Characterization of expression of putative NFIB downstream targets (*CDO*, *COL2A1, FGF19*) in hNSC during differentiation in a time-dependent manner. Expression levels of NFIB targeted genes (*CDO, COL2A1* and *FGF19*) were measured by qRT-PCR during time points of differentiation of hNSCs (day 0 (blue bars), day 3 (red bars), day 5 (purple bars), day 7 (green bars)). Gene expression levels were normalized to *GAPDH* expression. Data show the mean±S.D from 2 replicates. Statistical significance was determined according to one-way ANOVA analysis (***$p<0.0001$; **$p<0.001$; *$p<0.05$). Results are representative of 4 independent time-course experiments.

CDO and *COL2A1* expression decreased as early as day3, (70%; 80% and 81%); (12%; 33% and 37%) during the differentiation process. *FGF19* expression decreased (by 55%) at day 3 without statistical significance, and then increased progressively (1.2 fold and 3.6 fold) (Figure 3.16). The decrease at day 3 was also not observed when the experiment was repeated (see Appendix F). These findings are consistent with endpoint experiments (Figure 3.14 and 3.15).

3.5 Several miRNAs that can Bind NFIB 3'UTR are Upregulated during hNSC Differentiation

We also wanted to investigate molecular events that act upstream from NFIB. One of the ways NFIB function may be affected is post-transcriptional regulation by miRNAs. Previous data indicated that several miRNAs that potentially target NFIB are highly expressed in hNSCs (Kumbasar, unpublished data). We selected 7 miRNAs (miR-21, miR-153, miR-124a, miR-92b, miR-30a, miR-130a and miR-363), one of which was already shown to target NFIB in HL60 cells (Fujita et al., 2008) for further study.

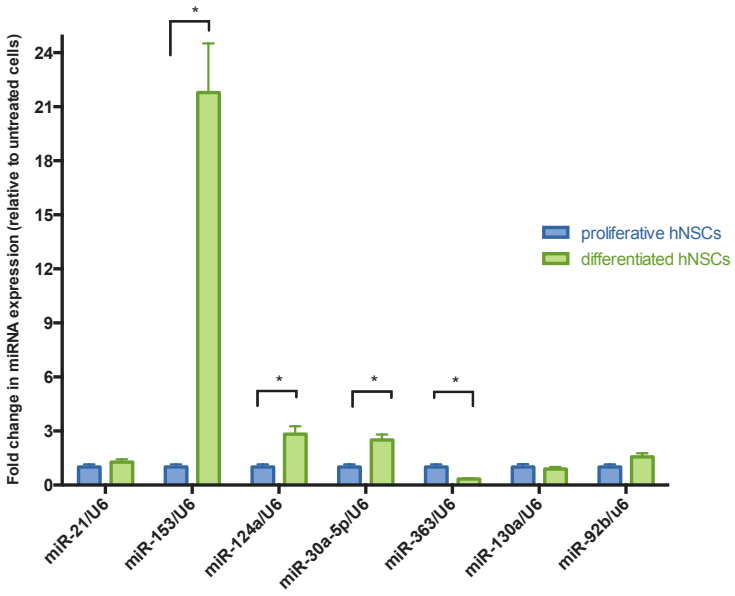


Figure 3.17 : Characterization of NFIB targeting miRNAs on mRNA level. Taqman assays were performed to determine expression levels of miRNAs predicted NFIB targeting miRNAs (miR-21, miR-153, miR-124a, miR-30a, miR-363, miR-130a, miR-92b) in proliferative (blue bars) and differentiated (green bars) hNSCs. Expression of miRNAs were normalized to U6 snRNA expression. The significance of differences was determined using Student's t-test analysis (***$p<0.0001$; **$p<0.001$; *$p<0.05$). Results are representative of two independent experiments. miR-153, miR-124a and miR-30a expression increase (21.8 fold; 2.8 fold and 2.5 fold) while miR-363 expression decreases 67%.

First we confirmed their expression in hNSCs and then tested if expression changed upon differentiation. miRNA expression was measured by qRT-PCR and the expression of all 7 miRNAs was detected in proliferating hNSCs. miR-21, miR-130a, miR-30a and miR-92b were expressed at high levels as indicated by Cts and microarray data (data not shown) while miR-124a and miR-363 expression levels were lower (2^5 fold) than in proliferative hNSCs. Exact measurement of miR-153 expression levels is difficult because of its low-level expression (2^{12} fold lower than miR-21 expression) in proliferative hNSCs. miR-153 expression highly increased as a result of differentiation (21.8 fold). miR-30a and miR-124a were also significantly up-regulated (2.5 fold and 2.8 fold) while only miR-363 expression was down-regulated (67%) in hNSCs upon differentiation. miR-21, miR-92b and miR-130a expression were not regulated significantly. Thus, as expression pattern of miR-153, miR-30a and miR-124a correlates with downregulation of NFIB, these miRNAs could potentially target NFIB during differentiation and were selected for further

study (Figure 3.17). We confirmed upregulation of miR-153, miR-124a and miR-30a and downregulation of miR-363 by repeating this experiment (n=2 for miR124a, n=3 miR-153, miR-363 and miR-30a); however, miR-130a was seen to be upregulated in one experiment (see Appendix G).

We also performed time course expression analysis of *NFIB* targeting miRNAs during differentiation of hNSCs, expression was measured by qRT-PCR over day 0, 3, 5 and 7.

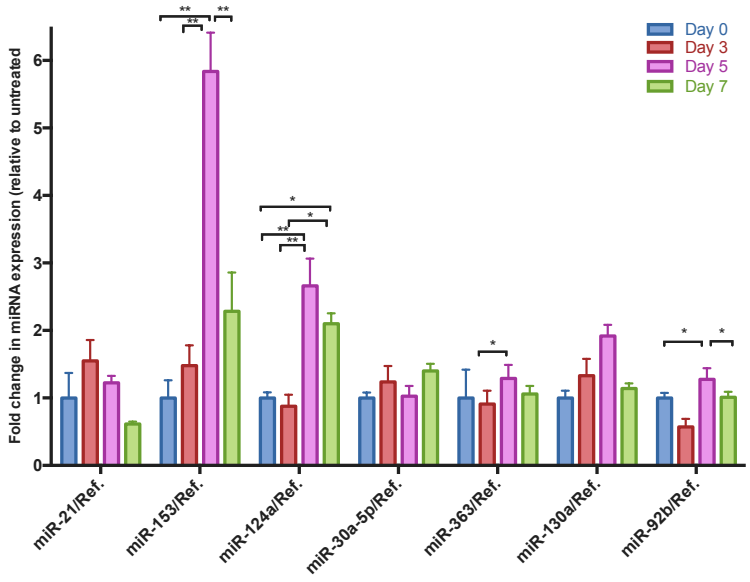


Figure 3.18 : Characterization of NFIB targeting miRNAs on mRNA level during differentiation of hNSCs in a time-dependent manner. Taqman assays were performed to determine expression levels of miRNAs predicted NFIB targeting miRNAs (miR-21, miR-153, miR-124a, miR-30a, miR-363, miR-130a, miR-92b) during differentiation (day 0 (blue bars), day 3 (red bars), day 5 (pink bars), day 7 (green bars)). Expression of miRNAs were normalized to geometric means of U6 snRNA, miR-140 and miR-103 expression. Statistical significance was determined according to one-way ANOVA analysis (***p<0.0001; **p<0.001; *p<0.05). The result of the first independent time-course experiment is shown.

In this experiment, miR-21 levels seem fluctuate but the change in gene expression was not significant. miR-153 showed enhanced upregulation at day 5, however, this upregulation was not replicated in other independent experiments (Figure 3.18). Upregulation of miR-124a can also be seen as early as day 5, also seen in subsequent independent experiments (see Appendix H). miR-124a expression is generally low in progenitors and is upregulated during neurogenesis, validating differentiation of hNSCs into neurons. We see some fluctuations in expression of miR-363, miR-130a

and miR-92b, these changes are not significant and are not seen in other independent experiments. For miR-30a we actually see no regulation of expression while enpoint experiments reliably show this miRNA to be upregulated.

3.6 Identification of miRNA Binding Sites on NFIB 3'UTR *in Silico*

In order to find out if any of these miRNAs directly target NFIB, we first utilized bioinformatic tools (Targetscan, http://www.targetscan.org; PicTar, http://pictar.mdc-berlin.de/ and Mfold, http://mfold.rna.albany.edu) to perform an *in silico* analysis NFIB 3'UTR. We also included miR-21 in the analysis as a positive control.

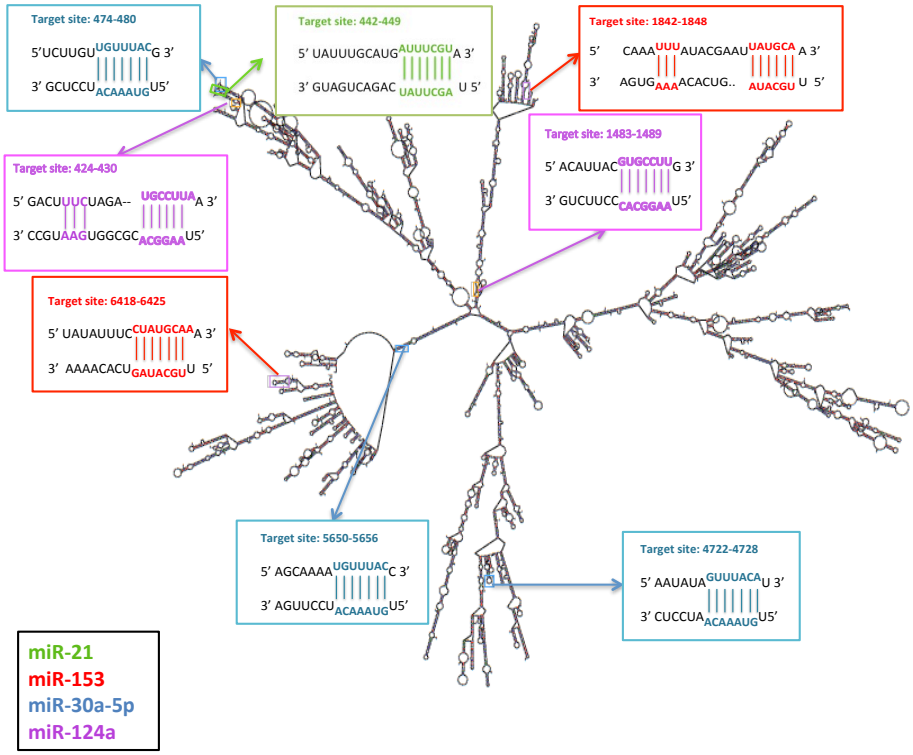


Figure 3.19: Predicted binding sites of potential NFIB targeting miRNAs on 3'UTR of NFIB. *In silico* analysis of the secondary structure confirmation of 3'UTR of NFIB (Mfold, http://mfold.rna.albany.edu). Predicted binding sites of miRNAs were identified using TargetScan. miR-21 binding sequence is shown in green, miR-153 binding sequences are shown in red, miR-30a predicted binding sites are shown blue whereas miR-124a binding sequences shown in purple. Target 442-449, Target 474-480, Target 1483-1489, Target 5650-5646, Target 6418-6425 are located in linear portions whereas Target 424-430, Target 4722-4728, Target 1842-1848 are located in complex stem-loop structures.

Targetscan was used to identify putative binding sites on 3'UTR. miR-124a and miR-153 have two miR-30a has three and miR-21 has only one putative binding sites

on NFIB 3'UTR. *In silico* analysis (Mfold, http://mfold.rna.albany.edu) of the folding of the NFIB 3'UTR indicates several miRNA binding sites are located in a linear portion (miR-21 (442-449), miR-30a (474-480), miR-124a (1483-1489), miR-30a (5650-5656), miR-153 (6418-6425)) while other regulatory sites are located in complex of branched stem-loop structures (miR-124a (424-430), miR-30a (4722-4728), miR-153 (1842-1848)) (Figure 3.19). This analysis shows that binding sites of putative NFIB targeting miRNAs mostly localize to the linear portions of the 3'UTR. Also, one of the predicted sites for miR-124a (424-430) and miR-30a (474-480) are quite proximal to the known binding site for miR-21.

3.7 NFIB 3'UTR-Reporter Constructs

In order to find out if NFIB mRNA is a possible target of these miRNAs, we wanted to set up an assay in which the 3'UTR of NFIB gene, including the putative miRNA target site, was inserted downstream of a luciferase open reading frame. To that end, the NFIB 3'UTR including the predicted microRNA binding sites, was divided into four regions of approximately 1 kb long, (NFIB 3'UTR_A; NFIB 3'UTR_B; NFIB 3'UTR_C; NFIB 3'UTR_D; Figure 3.20). It is shown above that binding sites of predicted miRNAs on NFIB 3'UTR_A-B, and NFIB 3'UTR_D are conserved regions in rat, mouse and human 3'UTRs. Only human NFIB 3'UTR has predicted miR-30a binding site on NFIB 3'UTR_C (see in Appendix T).

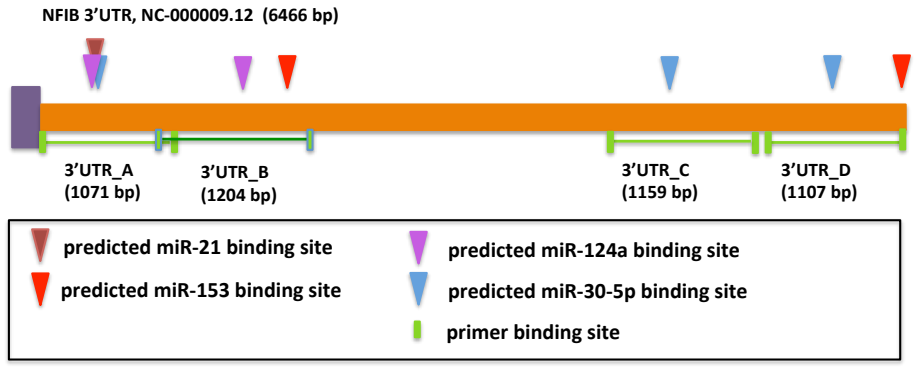


Figure 3.20 : Fragments of 3'UTR of NFIB was cloned into luciferase reporter vector according to predicted miRNA binding sites. Schematic representation of the NFIB 3'UTR depicting the location of the four NFIB 3'UTR fragments (NFIB 3'UTR_A; NFIB 3'UTR_B; NFIB 3UTR_C; NFIB 3'UTR_D) that were cloned downstream from luciferase gene (pmiRGLO).

Primers shown in Table 2.11 were designed to specifically amplify these 3'UTR fragments from SH-SY5Y genomic DNA.

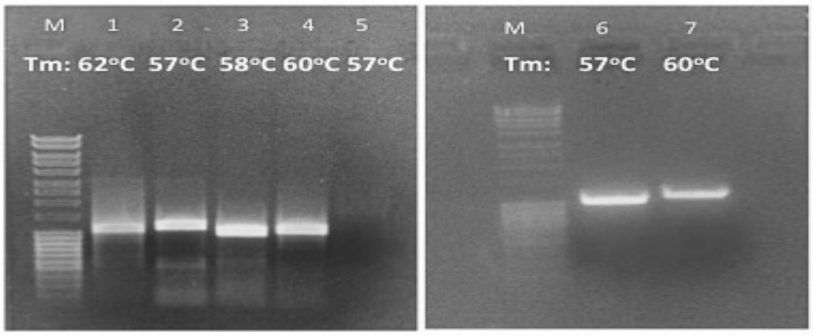


Figure 3.21 : NFIB 3'UTR fragments amplified from SH-SY5Y gDNA. NFIB 3'UTR Fragments shown in Fig 3.18 were amplified from SH-SY5Y gDNA and analyzed by agarose gel electrophoresis (1% agarose gel). In order to amplify NFIB 3'UTR_B, two different annealing temperatures were used (60°C and 57°C) and nonspecific bands were not observed at the higher annealing temperature. (M: Fermentas MassRuler DNA Ladder Mix, 1kb; **1:** NFIB 3'UTR_9/6 primer set PCR products (1163 bp); **2**: NFIB 3'UTR_B (9/8 primer set) PCR product (1204 bp); **3:** NFIB 3'UTR_A (10/1 primer set) PCR product (1071 bp); **4:** NFIB 3'UTR_D (11/2 primer set) PCR product (1107 bp); **5-6:** NFIB 3'UTR_C (12/7 primer set) PCR product (1159 bp); **7:** NFIB 3'UTR_B (9/8 primer set) PCR product (1204 bp)).

In order to amplify NFIB 3'UTR_B, two different annealing temperatures were used (60°C and 57°C) and nonspecific bands were not observed at the higher temperature (60°C). Amplified PCR products corresponding to 3'UTR_A (1071 bp); 3'UTR_B (1204 bp); 3'UTR_C (1159 bp) and 3'UTR_D (1107 bp) are shown in Figure 3.21. PCR fragments were then subcloned into pCR-Blunt-II TOPO vector. Isolated plasmids were checked for presence of PCR products by HindIII/XmaI and XhoI/SacI restriction digests and further confirmed by sequencing.

Sequencing results showed that we obtained three clones of NFIB 3'UTR_A (E2_1, E3_1 and E5_1); three clones of NFIB 3'UTR_B (D6_1; D7_1 and D8_1) in the 5'-3' orientation. One clone each of NFIB 3'UTR_C PCR (G1_1) and NFIB 3'UTR_D (F2_1) were located in the 3'-5' (reverse) orientation within the MCS of the TOPO vector (see Appendix I).

The forward and reverse orientation of the cloned 3'UTR fragments within the MCS of the TOPO vector lead us to use two different cloning strategies to transfer these fragments into the pmirGLO Dual-luciferase miRNA target expression vector. Products with the 5'-3' orientation (NFIB 3'UTR_A and NFIB 3'UTR_B) were inserted into pmiRGLO reporter vector by directional cloning using the XhoI/SacI

restriction enzymes. Plasmid isolated after the ligation reaction were checked by (XhoI/SacI) restriction digestion (Figure 3.22).

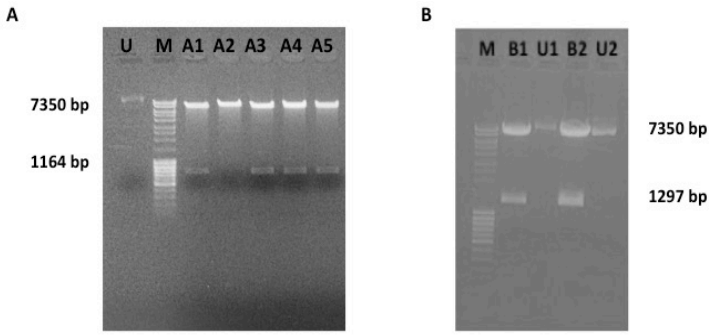


Figure 3.22 : NFIB 3'UTR_A and NFIB 3'UTR_B fragments were cloned into luciferase reporter vector (pmiRGLO). Luc-NFIB 3'UTR_A and Luc-NFIB 3'UTR_B plasmids were restricted with XhoI/SacI enzymes and analysed by agarose gel electrophoresis (1% agarose gel). (Lanes: **M**: Fermentas MassRuler DNA Ladder Mix, 1kb; **A1, A2, A3, A4, A5:** Luc-NFIB 3'UTR_A vectors restricted with XhoI/SacI; **B1, B2:** Luc-NFIB 3'UTR_B restricted with XhoI/SacI; **U:** Uncut Luc-NFIB 3'UTR_A **U1, U2:** Luc-NFIB 3'UTR_B reporter vectors).

NFIB 3'UTR_C and NFIB 3'UTR_D fragments, which were in the reverse orientation, were cloned into pmiRGLO reporter vector by homologous recombination (InFusion HD Cloning Kit, Clontech). Fragments were reamplified using primers (Table 2.12) that created PCR products with end regions homologous to the vector. Plasmids obtained from the In-Fusion reaction were checked for the presence of the UTR fragment by XhoI/HindIII restriction digests (Figure 3.23).

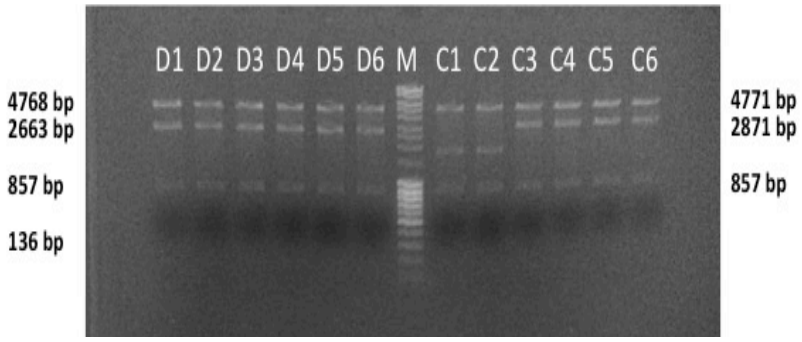


Figure 3.23 : NFIB 3'UTR_C and NFIB 3'UTR_D fragments were cloned into luciferase reporter vector (pmiRGLO). Luc-NFIB 3'UTR_C and Luc-NFIB 3'UTR_D plasmids, which were cloned by In-Fusion cloning, were restricted with XhoI/HindIII enzymes and analysed by agarose gel electrophoresis (1% agarose gel). (Lanes: **M:** Fermentas MassRuler DNA Ladder Mix, 1kb; **D1-D6:** Luc-NFIB 3'UTR_D vectors; **C1-C6:** Luc-NFIB 3'UTR_C vectors).

Plasmids with correct restriction pattern were then checked by sequencing. One clone each for Luc-NFIB 3'UTR_C (C4) and Luc-NFIB 3'UTR_D (D1) were confirmed to have the correct sequence (see Appendix J).

Mutations in predicted miR-21, miR-124a and miR-153 binding sites of Luc-NFIB 3'UTR_A (Target 442-449 and Target 424-430), Luc-NFIB 3'UTR_B (Target 1483-1489), and Luc-NFIB 3'UTR_D (Target 6418-6425) were created by site directed mutagenesis. Clones obtained after mutagenesis reactions were checked by (SacI) restriction digestion (Luc-NFIB 3'UTR_B-124M and Luc-NFIB 3'UTR_A-21M mutant vectors shown in Figure 3.24).

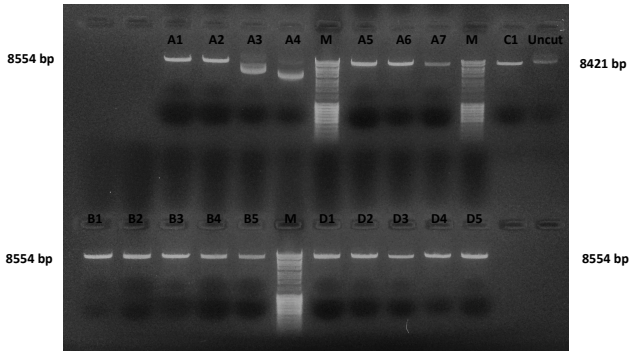


Figure 3.24 : Luc-NFIB 3'UTR_B-124M mutant reporter vectors were generated by site-directed mutagenesis. Luc-NFIB 3'UTR_B-124M mutant vectors and Luc-NFIB 3'UTR_A-21M mutant plasmids, which were cloned by using two different QuikChange site-directed mutagenesis kits, were restricted with SacI and analysed by agarose gel electrophoresis (1% agarose gel). (Lanes: **A1-A7:** Luc-NFIB 3'UTR_B-124M vectors generated with QuikChange II XL site-directed mutagenesis kit and cloned into XL-10 Gold competent cells; **B1-B5:** Luc-NFIB 3'UTR_B-124M vectors generated with QuikChange II XL site-directed mutagenesis kit and cloned into NEB-5 alpha ultracompetent cells; **C1:** Luc-NFIB 3'UTR_A-21M mutant vectors generated with QuikChange multi site-directed mutagenesis kit and cloned into NEB-5 alpha ultracompetent cells; **D1-D5:** Luc-NFIB 3'UTR_B-124M mutant vectors generated with QuikChange multi site-directed mutagenesis kit and cloned into NEB-5 alpha ultracompetent cells).

Plasmids with correct restriction patterns were checked by sequencing. Seven clones of Luc-NFIB 3'UTR_B-124M (A1, A2, B1-B5) were confirmed to have the correct sequence (see Appendix K). Interestingly, only plasmids generated with Quikchange II XL site-directed mutagenesis kit carried the correct mutated sequences. Therefore, we chose to use QuikChange II XL site-directed mutagenesis kit for subsequent

mutagenesis reactions. This kit has some advantages for cloning. PCR reaction that generates the necessary reporter constructs takes approximately 3 1/2 hours with QuikChange II XL site-directed mutagenesis kit instead of the 9 2/3 hours required for the QuikChange multi site-directed mutagenesis kit. Thus, enzyme efficiency appears to be higher for this kit. Also, this kit requires lower amounts of template to amplify and reduces the chance to transform wild-type strand.

We attempted to generate Luc-NFIB 3'UTR_D-153M, Luc-NFIB 3'UTR_A-21M and Luc-NFIB 3'UTR_A-124M constructs carrying the appropriate mutations with the QuikChange II site-directed mutagenesis kit. These reactions were checked by (SacI) restriction digestion (Figure 3.25).

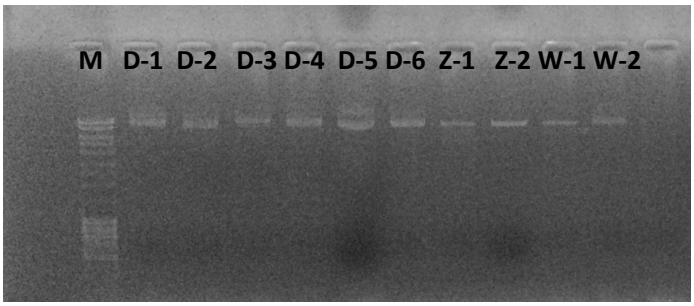


Figure 3.25 : Luc-NFIB 3'UTR_D-153M mutant vectors were generated by site-directed mutagenesis. Luc-NFIB 3'UTR_D-153M, Luc-NFIB 3'UTR_A-21M and Luc-NFIB 3'UTR_A-124M mutant plasmids, which cloned by using QuikChange II XL site-directed mutagenesis kit, were restricted with SacI and analysed by agarose gel electrophoresis (1% agarose gel). (Lanes: M: Fermentas Massruler DNA Ladder (1 kb); **D1-D5:** Luc-NFIB 3'UTR_D-153M mutant vectors cloned into XL-10 Gold competent cells; **D6:** Luc-NFIB 3'UTR_D-153M mutant vectors cloned into NEB-5 alpha ultracompetent cells; **Z1-Z2:** Luc-NFIB 3'UTR_A-21M mutant vectors cloned into NEB-5 alpha ultracompetent cells; **W1:** Luc-NFIB 3'UTR_A-124M mutant vectors cloned into XL-10 Gold competent cells; **W2:** Luc-NFIB 3'UTR_A-124M mutant vectors cloned into NEB-5 alpha ultracompetent cells).

Plasmids with the correct restriction pattern were then checked by sequencing. Two clones for Luc-NFIB 3'UTR_D-153M (D4, D5) were confirmed to have the correct mutated sequence (see Appendix K). However, the rest of the samples were wild type sequences. As an alternative, we carried out the mutagenesis reactions using the Q5 High Fidelity DNA polymerase (NEB) for the mutagenesis for Luc-NFIB 3'UTR_A-21M and Luc-NFIB 3'UTR_A-124M, clones were checked by (SacI) restriction digests (Figure 3.26).

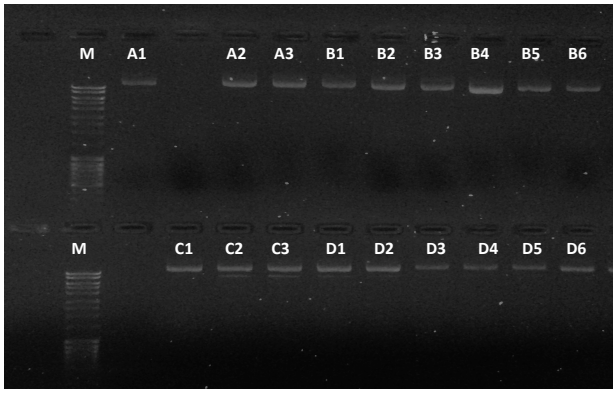


Figure 3.26 : Luc-NFIB 3'UTR_A-124M and Luc-NFIB 3'UTR_A-21 M mutant vectors were generated by site-directed mutagenesis. Luc-NFIB 3'UTR_A-124M and Luc-NFIB 3'UTR_A-21M mutant plasmids, which cloned Q5 High fidelity DNA polymerase and by using QuikChange II XL site-directed mutagenesis kit, were restricted with SacI and analysed by agarose gel electrophoresis (1% agarose gel). (Lanes **M:** Fermentas Massruler DNA Ladder (1 kb); **Upper lanes:** generated by Q5 High fidelity DNA polymerase enzyme **A1-A3:** Luc-NFIB 3'UTR_A-124M mutant vectors cloned into XL-10 Gold competent cells. **B1-B6:** Luc-NFIB 3'UTR_A-21M mutant vectors cloned into XL-10 Gold competent cells. Lower lanes: gererated by QuikChange II XL site-directed mutagenesis kit. **C1-C3**: Luc-NFIB 3'UTR_A-124M mutant vectors cloned into NEB-5 alpha ultracompetent cells; **D1-D6:** Luc-NFIB 3'UTR_A-21M mutant vectors cloned into NEB-5 alpha ultracompetent cells).

Site-directed mutagenesis of Luc-NFIB 3'UTR_A-21M and Luc-NFIB 3'UTR_ A-124M is ongoing.

Mutagenized constructs were used in parallel with Luc-NFIB 3'UTR_A, Luc-NFIB 3'UTR_B, and Luc-NFIB 3'UTR_D in Dual luciferase assays.

3.8 Activity of Luc-NFIB 3'UTR Constructs in HEK293T Cells

Once the NFIB 3'UTR fragments that contain the putative miRNA target sites were cloned downstream of a luciferase reporter gene (Luc-NFIB 3'UTR_A-D), we carried out luciferase assays to test if these miRNAs target NFIB. The different luciferase constructs were transfected into HEK293T cells, with miRNA mimic or control and assayed for luciferase activity after 48 h.

3.8.1 Activity of Luc-NFIB 3'UTR_A and Luc-NFIB 3'UTR_B is repressed by endogenous miRNAs in HEK293T cells

We expected some of the miRNAs to be expressed in HEK293T cells, thus initially we wanted to assay for the effect of endogenous miRNAs on the reporter gene

expression carrying the different NFIB 3'UTR fragments. Expression levels of miRNAs in HEK293T cells were identified by qRT-PCR and microarray analysis previously (see section 3.5). High expression levels of miR-130a, miR-92b were detected while miR-21, miR-124a, miR-30a and miR-363 expressions were present at lower levels. In addition, an endogeneous expression level of miR-153 was below detection levels.

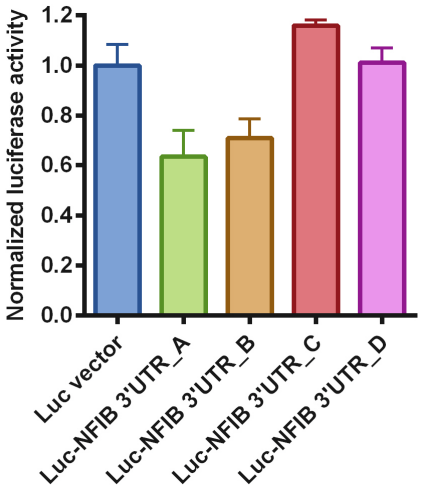


Figure 3.27 : Endogenously expressed miRNAs in HEK293T cells repress (translation of) Luc-NFIB 3'UTR_A and Luc-NFIB 3'UTR_B. We assayed firefly luciferase activity relative to *Renilla* luciferase activity in HEK293T cells ($2x10^4$ number of cells/well) 48 h after transfection with reporter constructs. Bars represent luciferase activity normalized to the mean activity of samples transfected with the luciferase vector (pmiRGLO). Data show the mean±S.D. from 3 replicates. Statistical significance was determined according to Student's t test (*$p<0.05$). Results are representative of at least three independent experiments.

Endogenous expression of miRNAs affect the translation of Luc-NFIB 3'UTR_A and Luc-NFIB 3'UTR_B, however the change in luciferase activity is not significant (Figure 3.27). We consistently saw that Luc-NFIB 3'UTR_A and Luc-NFIB 3'UTR_B exhibited decreased expression levels when compared to Luc (pmiRGLO), Luc-NFIB 3'UTR_C and Luc-NFIB 3'UTR_D expression. Luc-NFIB 3'UTR_A contains miR-124a, miR-21 and miR-30a putative binding sites while Luc-NFIB 3'UTR_B includes miR-aa, miR-363, miR-153 and miR-30a putative binding sites.

3.8.2 Identification of miRNAs that regulate post-transcriptional expression of NFIB

Next we transfected HEK293T cells with the luciferase constructs carrying defined miRNA binding sites in the presence of miRNA mimics, in order to find out if these NFIB 3'UTR fragments are regulated by specific miRNAs. First we tested whether Luc-NFIB 3'UTR_A was repressed by miR-21.

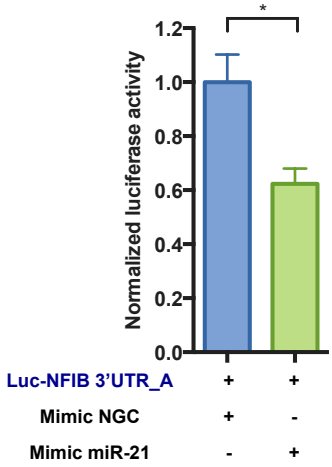


Figure 3.28 : miR-21 represses Luc-NFIB 3'UTR_A. We assayed firefly luciferase activity relative to *Renilla* luciferase activity in HEK293T cells ($2x10^4$ number of cells/well) 48 h after transfected with reporter construct in the presence of 20 nM miR-21 mimic (pre-miR-21) or mimic negative control (NGC). Bars represent luciferase activity normalized to the mean activity of samples transfected with the mimic negative control. x-axis depicts treatment conditions. Data are expressed as mean±s.e.m from 3 independent experiments (n=3). Statistical significance was determined according to Student's t test (*$p<0.05$).

The data indicates that translation of Luc-NFIB 3'UTR_A was repressed by miR-21 mimic by 38 % when compared to negative control mimic (Figure 3.28). As miR-21 has been shown to target NFIB (Fujita et al., 2008; Hannafin et al. 2011), this result was consistent with previous findings and in fact we designed the experiment as a positive control.

In order to test the specificity of repression of the Luc-NFIB 3'UTR_A by miR-21, we co-transfected with miR-21 inhibitors (anti-miR-21, Ambion) rescue the repressive effect of miR-21. Transfection with anti-miR-21 alone had no effect on translation of Luc-NFIB 3'UTR_A suggesting that endogenous miR-21 expression was not suppressed by anti-miR-21 (data not shown). In order to rescue the

repressive effect of miR-21 mimic, we repeated miR-21 mimic experiments in the presence of anti-miR-21.

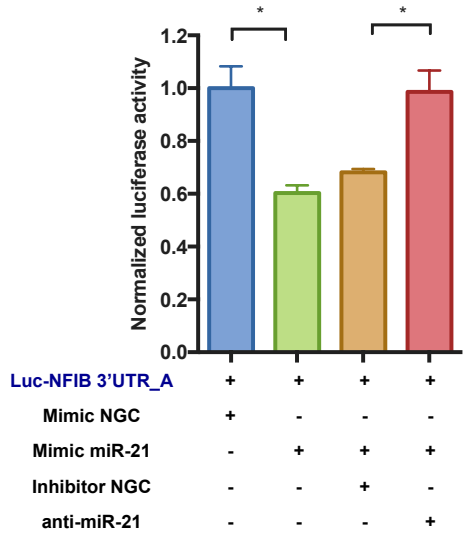


Figure 3.29 : Repression of NFIB 3'UTR_A by miR-21 is rescued by anti-miR-21. HEK293T cells ($2x10^4$ number of cells/well) were transfected with reporter constructs (Luc-NFIB 3'UTR_A; 150 ng) in the presence of 20 nM miR-21 mimic (pre-miR-21-5p), or mimic negative control (NGC) with 100 nM anti-miR-21 or 100 nM inhibitor negative control and assayed for firefly luciferase activity relative to renilla luciferase activity after 48 h. Bars represent luciferase activity normalized to the mean activity of samples transfected with the mimic negative control (NGC). x-axis depicts treatment conditions. Data are expressed as mean±s.e.m from three independent experiments (n=3). Statistical significance was determined according to Student's t-test (*$p<0.05$).

The repressive effect of miR-21 mimic on translation of Luc-NFIB-3'UTR-A could be rescued by anti-miR-21 (Figure 3.29) indicating that Luc-NFIB 3'UTR_A, therefore NFIB 3'UTR can be a direct target of miR-21.

There are two miR-124a binding sites on NFIB 3'UTR (on Luc-NFIB 3'UTR_A and Luc-NFIB 3'UTR_B). Next we tested if mir-124a could repress expression of luciferase gene fused to either of these NFIB 3'UTR fragments. As can be seen in Figure 3.27, mir-124a could repress activity from Luc-NFIB 3'UTR_B construct (by 43% compared to mimic negative control), but not from the Luc-NFIB 3'UTR_A construct (Figure 3.30).

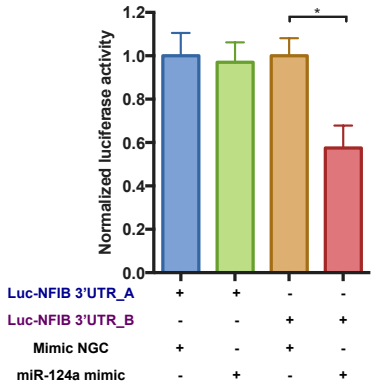


Figure 3.30 : miR-124a represses Luc-NFIB 3'UTR_B, but not Luc-NFIB 3'UTR_A. We assayed firefly luciferase activity relative to *Renilla* luciferase activity in HEK293T cells ($2x10^4$ number of cells/well) 48 h after transfected with reporter construct in the presence of 20 nM miR-124a mimic, or mimic negative control (NGC). Bars represent luciferase activity normalized to the mean activity of samples transfected with the mimic negative control. x-axis depicts treatment conditions. Data are expressed as mean±s.e.m from 4 replicates (n=4). Statistical significance was determined according to Student's t-test (*$p<0.05$).

To explore the specificity of regulation of translation of the Luc-NFIB 3'UTR_B by miR-124a, we transfected Luc-NFIB 3'UTR_B-124M with miR-124a mimics to see they would rescue the repressive effect of miR-124a.

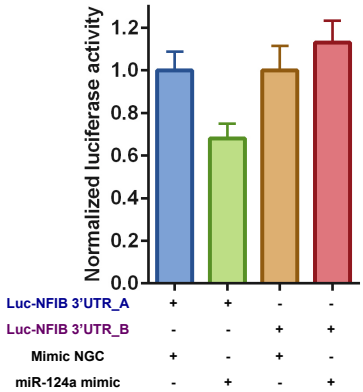


Figure 3.31 : Binding of miR-124a does not repress Luc-NFIB 3'UTR-B_124M. The average calculated signal ratios of *Renilla* and firefly luciferase from three different experiments 48h after co-transfection of vector constructs (Luc-NFIB 3'UTR_B and Luc-NFIB 3'UTR_B-124M; 150 ng) and 20 nM miR-124a mimics to HEK293T cells ($2x10^4$ number of cells/well). Bars represent luciferase activity normalized to the mean activity of samples transfected with the mimic negative control (NGC). x-axis depicts treatment conditions. Data are expressed as mean±s.e.m from 3 replicates (n=3). Statistical significance was determined according to Student's t-test (*$p<0.05$).

Preliminary results indicate that mutating the mir-124a binding site may rescue of the repression of Luc-NFIB 3'UTR_B by miR-124a (Figure 3.31). However in these experiments repression by miR-124a mimic alone was not significant (by 32%, compare Figure 3.30 with Figure 3.31) even though previously the repressive effect was reproducibly significant (Figure 3.30). Therefore, in the first set of independent experiments (n=3) we couldn't show a rescue of translational repression. However, once we were able to obtain a rigorous effect by miR-124a mimic, we also saw recovery of expression by Luc-NFIB 3'UTR_B-124M at significant levels (see Appendix N). We believe that repeating these experiments will resolve this issue.

miR-30a is one of the microRNAs that were upregulated in differentiated hNSCs. There are three miR-30a binding sites on NFIB 3'UTR (on Luc-NFIB 3'UTR_A, Luc-NFIB 3'UTR_C and Luc-NFIB 3'UTR_D). We carried out transfection experiments as before with these reporter constructs in the presence of miR-30a mimic or mimic negative control.

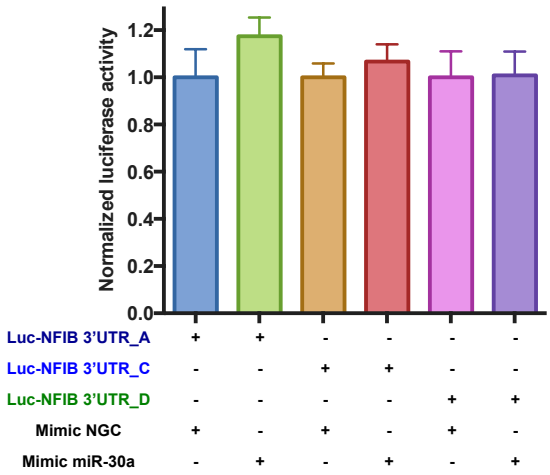


Figure 3.32 : miR-30a cannot repress translation from Luc-NFIB 3'UTR_A, Luc-NFIB 3'UTR_C or Luc-NFIB 3'UTR_D. HEK293T cells ($2x10^4$ number of cells/well) were transfected with reporter constructs (Luc-NFIB 3'UTR_A, Luc-NFIB 3'UTR_C and Luc-NFIB 3'UTR_D) in the presence of 20 nM miR-30a mimics, or mimic negative controls (NGC). Bars represent luciferase activity normalized to the mean activity of samples transfected with the mimic negative control. x-axis depicts treatment conditions. Data were expressed as mean±s.e.m from three independent experiments. Statistical significance was determined according to Student's t-test (*$p<0.05$).

Translation of Luc-NFIB 3'UTR_A, Luc-NFIB 3'UTR_C or Luc-NFIB 3'UTR_D was not affected by miR-30a mimic, when compared with negative mimic control

indicating that miR-30a does not target NFIB 3'UTR (Figure 3.32). However, we have not tried to transfect higher concentrations of miR-30a mimic in these experiments, in case this miRNA has lower binding affinity for NFIB 3'UTR and higher amounts are required to see an effect. Moreover, we do not have a positive control reporter construct to control for activity of miR-30a mimic.

Finally, miR-153 was also upregulated during differentiation and selected for further analysis. There are two miR-153 binding sites on NFIB 3'UTR that are located in 3'UTR_B and 3'UTR_D reporter constructs.

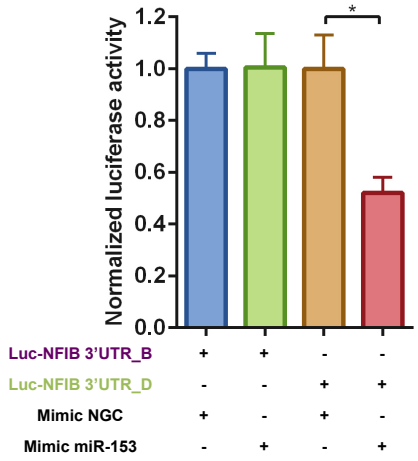


Figure 3.33 : miR-153 repressed Luc-NFIB 3'UTR_D but not Luc-NFIB 3'UTR_B. We assayed firefly luciferase activity relative to *Renilla* luciferase activity in HEK293T cells ($2x10^4$ number of cells/well) 48 h after transfected with reporter construct in the presence of 20 nM miR-153 mimics, or mimic negative control (NGC). Bars represent luciferase activity normalized to the mean activity of samples transfected with the mimic negative control. x-axis depicts treatment conditions. Data were expressed as mean±s.e.m from three independent experiments. Statistical significance was determined according to Student's t-test (*$p<0.05$).

Transfection with miR-153 mimic did not repress luciferase activity from Luc-NFIB 3'UTR_B construct compared with mimic negative control, while repressing luciferase activity from Luc-NFIB 3'UTR_D by 48% (Figure 3.33). These results indicate that 3'UTR_D may be a target of miR-153 and are consistent with recently published reports (Tsai et al., 2014).

To explore the specificity of post-transcriptional regulation of the Luc-NFIB 3'UTR_D by miR-153, we transfected Luc-NFIB 3'UTR_D-153M with miR-153 mimics to see they would rescue the repressive effect of miR-153.

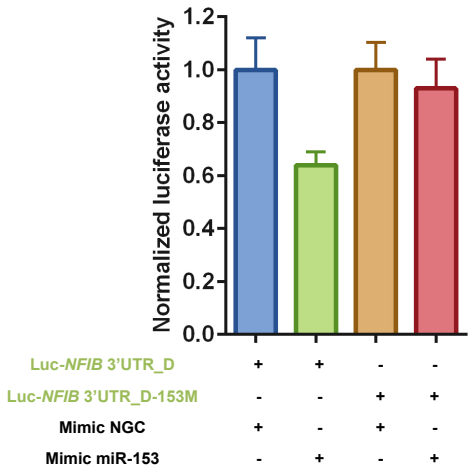


Figure 3.34 : Binding of miR-153 does not repress Luc-NFIB 3'UTR_D-153M. The average calculated signal ratios of *Renilla* and firefly luciferase from three different experiments 48h after co-transfection of vector constructs (Luc-NFIB 3'UTR_D and Luc-NFIB 3'UTR_D-153M; 150 ng) and 20 nM miR-153 mimics to HEK293T cells ($2x10^4$ number of cells/well). Bars represent luciferase activity normalized to the mean activity of samples transfected with the mimic negative control (NGC). x-axis depicts treatment conditions. Data are expressed as mean±s.e.m from 3 replicates. Statistical significance was determined according to Student's t-test (*$p<0.05$).

Results indicate that mutated miR-153 binding site on 3'UTR_D vector rescues the effect of miR-153 on post-transcriptional regulation (Figure 3.34). However, since the repression of miR-153 mimic was not significant, mutating the miR-153 binding does not significantly rescue this inhibition (compare Figure 3.33 and Figure 3.34). Results from two of three independent experiments show miR-153 represses 3'UTR_D expression significantly and while it has not effect on expression from Luc-NFIB 3'UTR_D-153M (see in Appendix S).

We are still conducting site direct mutagenesis experiments on the miR-21 and miR-124a binding sites on Luc-NFIB 3'UTR_A to confirm the specificity of inhibition by these miRNAs. The complete sets of independent experiments refrerred to here are shown in Appendix L, Appendix M, Appendix N, Appendix O and Appendix P, Appendix R and Appendix S.

4. DISCUSSION AND CONCLUSION

In order to study the role and regulation of NFIB in hNSCs during neural differentiation, we first characterized expression of *NFIB* and other NFI family members, putative NFIB target genes downstream from *NFIB* as well as miRNAs. We investigated miRNAs that were upregulated in differentiating hNSCs as potential upstream regulators of NFIB.

First we characterized the hNSCs in our culture conditions: proliferating hNSCs were 90.5% Nestin$^+$ and withdrawal of growth factors for one week in culture lead to 34-36% decrease in Nestin$^+$ cell population. This decrease in Nestin$^+$ cells correlated with appearance of β-III tubulin$^+$ cells bearing neurites, indicating differentiation into neurons. However, number of β-III tubulin$^+$ cells could not be quantitated by flow cytometry.

We also wanted to correlate changes in NFI gene expression with putative NFIB target genes as well as miRNAs that can bind NFIB 3'UTR. We found that, expression of NFIB mRNA is downregulated in hNSCs upon differentiation. Expression levels of other NFI transcripts are considerably lower than NFIB, however, NFIC and NFIX mRNA expression levels also decrease while NFIA expression increases after growth factor withdrawal. As transcript levels are low, we only examined NFIB protein expression and found that NFIB protein levels are also downregulated in differentiated hNSCs. Expression levels of two putative NFIB target genes; *CDO* and *COL2A1* decrease whereas *FGF19* increases in differentiated hNSCs. This result makes *FGF19* a good candidate NFIB target to study in neurogenesis. However, changes in expression of NFI transcripts do not recapitulate the hindbrain expression profiles. If NFIB acts as a repressor of these genes in hNSCs as it does in the hindbrain, only FGF19 could be regulated by NFIB during neuronal differentiation in hNSCs. Experiments that will definitively address this question are discussed below.

Several miRNAs (miR-124a, miR-30a, miR-153, miR-130a, miR-92b, miR-363) that are predicted to bind NFIB 3'UTR are upregulated in differentiating hNSCs. Among these, preliminary data indicate that miR-153 and miR-124a can regulate NFIB translation directly.

miRNAs play an important role in differentiation of hNSCs and several miRNAs are found to regulate expression of NFIB. At the beginning of this study, two miRNAs, miR-21 ve miR-372/373, had been shown to target NFIB inside the CNS (Guo et al., 2011). We set out to find new upstream regulators of NFIB in neural cells and picked hNSC culture system to do so. We found that miR-124a, miR-153 and miR-30a are upregulated in hNSCs while mir-363 is downregulated upon differentiation. Additionally, we observed that translation of NFIB could be regulated by miR-124a and miR-153. The regulatory sites of these miRNAs are located on NFIB 3' UTR sequences that are identical in the human and mouse. Analysis of NFIB 3'UTR folding shows that detected miRNA-binding sites are located within a more linear structure (see Figure 3.16).

Previous studies show that miR-124a is most abundant miRNA (25-48% of all brain miRNAs) in the brain (Lagos-Quintana et al., 2002) and its expression increases during the development of the CNS (Lim et al., 2005). It is mostly expressed in post-mitotic neurons, although also found in neural precursors located in the VZ. Overexpression of miR-124a in HeLa cells lead to supression of non-neuronal genes and induction of neuronal genes and promoted neurogenesis (Lewis et al., 2005). General mechanisms of miR-124a during neurogenesis in adult and embyonic brain are presented in Figure 4.1.

miR-124a can regulate neurogenesis through several pathways (Figure 4.1). First, overexpression of miR-124a during spinal cord development results in basal lamina defects and miR-124a downregulates integrin β1 and laminin γ1expression (Cao et al., 2007). Additionally, REST and miR-124a function as two global negative regulators of cell fate decisions. REST/SCP1 pathway inhibits neuronal differentiation by repressing expression of neuronal genes and miR-124a in non-neuronal cells and miR-124a acts as a negative regulator of non-neuronal gene expression in neuronal cells (Conaco et al., 2006). Also, miR-124a regulates the SCP1 expression (Visvanathan et al., 2007). Therefore, negative feedback loop between the anti-neural REST/SCP1 pathway and proneural miR-124a pathways

maintains the balance of gene expression between neurogenesis and stem cell maintanence. In a third mechanism, repression of BAF53a expression, which is a component of ATP-dependent chromatin remodeling complex, is maintained by regulation of miR-124a during neural development (Yoo et al., 2009). In addition to miRNAs, REST has an antagonistic effect on BAF53a expression in differentiated neurons. Fourth, miR-124a expression downregulates polypyrimidine tract-binding protein (PTBP1) in neuronal cells, leading to neuronal specific alternative splicing of PTBP2 (Makeyev et al., 2007). Cell surface proteins (Ephrin B1) could also be targeted by miR-124a during neuronal differentiation (Arvanitis et al., 2010). In addition, in the olfactory bulb (OB) miR-124a regulates the timing of the transition of SVZ transit amplifying cells to neuroblasts through repression of SOX9, which is required for neurogenesis (Cheng et al., 2009). Also, neurogenic effect of miR-124a has been employed for spontaneous differentiation of induced pluripotent stem cells (iPSCs). Zare et al. (2014) showed that transducing iPSCs with miR-124a and miR-128 caused these cells to differentiate into mature neurons in the absence of any extrinsic factors. In addition to neurogenic function of miR-124a, it controls the timing of neurogenesis and astrocytogenesis in mouse neural stem cells by regulating EZH2 expression (Neo et al., 2013). On the other hand, not only miR-124a promotes neurogenesis, but also its inhibitory role was detected in early eye development (Liu et al., 2010) NEURO-D1, which is a well-known neurogenic basic helix-loop-helix transcription factor, is downregulated by miR-124a during the optic vesicle development and inhibits neurogenesis.

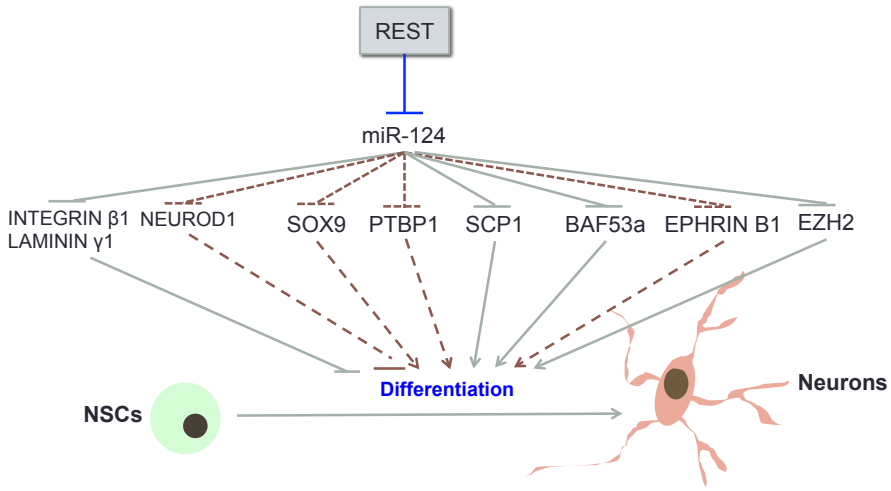


Figure 4.1 : miR-124a is a key regulator during neurogenesis in embryo and adult brains.

Figure 4.1 (cont'd) : miR-124a is a key regulator during neurogenesis in embryo and adult brains. miR-124a expression is downregulated by REST and miR-124a itself generally promotes by interacting with several mRNAs to regulate their translation, but can also inhibits neurogenesis thorugh repression of NEUROD1 (adapted from Lang and Shi et al., 2012) (dashed and brown lines represent in adult brain; green lines represent in embryo brain).

After we started this study, miR-124a was reported to directly target NFIB during maturation of fetal rat lung epithelial cells (Wang et al., 2015), consistent with our findings. Here, miR-124a binds sites (positions 214-418 and 1481-1487) 3'UTR of NFIB. We found that two binding sites are conserved in human, rat and mouse (see in Appendix P). In this study, we only see regulation by the site (1481-1487) on 3'UTR_B of NFIB. We have yet to perform of mutation analysis of the NFIB 3'UTR_A site, these experiments will show if there is a discrepancy between results obtained in this thesis and that of Wang et al (2015). They observed that translation of NFIB is decreased by 50% when two binding sites are targeted by miR-124a while expression of NFIB is decreased 25% if one of the binding sites is mutated. Our experiments showed that translation of 3'UTR_B is downregulated by miR-124a (32%) and its effect is rescued when binding site of miR-124a is mutated (in Figure 3.31). However, in these experiments miR-124a could not significantly repress NFIB 3'UTR_B expression compared to previous experiments (43%, see Figure 3.30 and Figure 3.31). Only one of three independent experiments shows the repressive effect of miR-124a at significant levels (see Appendix N). These experiments will be repeated to obtain statistical significance.

We found that miR-153 can also regulate NFIB expression and is upregulated in differentiating hNSCs. Coincidentally, during this project, miR-153 was also discovered to target NFIA and NFIB, initially in the fetal mouse brain. Tsai et al. (2014) found that NFIA/NFIB expression in mouse fetal neural stem cells is regulated by miR-153, which is required for neuronal maturation. They showed that miR-153 binds one of two predicted binding sites (NFIB 3'UTR (6559-6566)) and regulates NFIB translation. Consistent with this result, we observed that miR-153 binds on human NFIB 3'UTR (6418-6425), which is similar to mouse NFIB 3'UTR (6559-6566) and downregulates NFIB expression. Specificity of the regulation of miR-153 on translation of NFIB 3'UTR_D was determined by mutational analysis.

While translation of 3'UTR_D is downregulated by miR-153 (37%), translation of 3'UTR_D-153M is not regulated by miR-153 (Figure 3.34). However, in these experiments miR-153 could not significantly repress NFIB 3'UTR_D expression compared to previous experiments (48%, see Figure 3.33 and Figure 3.34). Two of three independent experiments show the repressive effect of miR-124a at significant levels (see Appendix S). These experiments will be repeated to obtain statistical significance.

In a more recent study, Tsuyama et al. (2015) showed that intrinsic factors (LIF, BMP2 as gliogenic factors) inhibit NFIB expression by upregulating miR-153 in the earlier neurogenesis. When these factors are downregulated in the later stages of neurogenesis, miR-153 expression decreases and allows NFIB expression to upregulate gliogenesis genes (*GFAP*). We showed that NFIB expression is downregulated while miR-153 expression increases in differentiating hNSCs. This result may be consistent with the previous observation (Tsuyama et al., 2015) and shows that miR-153 overexpression inhibits the role of NFIB in gliogenesis in the early neurogenic stage of hNSCs. However, gain and loss of function studies will yet determine the function of NFIB during differentiation of hNSCs.

In addition, miR-153 function has been examined in neuro-pathological conditions. miR-153 was found to regulate of alfa-synuclein (SNCA), which is involved in the pathogenesis of Parkinsons disease, amyloid precursor protein (APP) and amyloid precursor-like protein 2 (APLP2), which are involved in the pathogenesis of Alzheimer disease, and miR-153 plays important roles to control the accumulation of those proteins (Doxakis, 2010; Liang et al., 2012). miR-153 also controls SNAP-25 (core component of SNARE complex) translation to induce motor neuron development (Wei et al., 2013).

Finally, miR-30a was also upregulated in differentiating hNSCs. miR-30a belongs to the miR-30 family. This family of miRNAs were defined as tumor suppressors (Zhao et al., 2014). However, miR-30 function in central nervous system has not been reported to date. However, miR-30 is implicated in the pathophysiology of schizophrenia: several schizophrenia related genes (*MAP6* (Shimizu et al., 2006), *NR4A2* (Nojas et al., 2007), *GRM3* (Egan et al., 2004), *GRM5* (Devon et al., 2001), *CNR1* (Ujike et al., 2002), *NCAM1* (Sullivan et al., 2007) and *NEUROG1* (Fanous et

al., 2007) are targets of miR-30a. We found no evidence for the role of miR-30a in regulating NFIB expression in differentiating hNSCs.

One of the technical problems we experienced during this project was quantification of the changes of β-III tubulin$^+$ cells by flow cytometry in differentiating hNSCs. To solve this problem, changes in several steps of flow cytometry protocol (fixation time (30 min instead of 15 min); detergent for permeabilization buffer (Tween-20 to saponin); blocking solution (10% goat serum to 3% goat serum); different antibodies (Mouse monoclonal anti-tubulin beta III isoform antibody (Millipore) to mouse monoclonal neuronal class III beta-tubulin isoform, Alexa Fluor® 488 labeled antibody (Covance)); different enzymatic diassociation reagents (trypsin instead of accutase)) were performed (data not shown) and similar results were obtained: Number of β-III tubulin$^+$ cells did not increase but in fact decreased during differentiation of hNSCs. This result could be caused by our failure to obtain intact cells for flow cytometry. Long processes such as neurites could be damaged or lost which would then lead to decrease in of the number of β-III tubulin$^+$ cells after differentiation. However, flow cytometry has been successfully used to examine expression levels of β-III tubulin in different cell types (brain progenitor cells, parkin knockout embryonic stem cells and SH-SY5Y neuroblastoma cell (Hwant et al., 2013, Iwata et al., 2007 and Turac et al., 2013).

As mentioned above, in hNSCs, *FGF19* is upregulated while NFIB is downregulated, similar to the expressional regulation seen in precrebellar progenitors. In order to investigate whether *FGF19* is direct target of NFIB in hNSCs, functional experiments can be performed. In addition to functional experiments, regulatory regions of target genes could be examined for potential NFIB binding sites by *in silico* analysis. Then, NFI binding to putative sites could be analyzed by *in vitro* (Electrophoretic mobility shift assay, EMSA) and *in vivo* (Chromatin immunoprecipitation, ChIP) determination methods. Finally, functionality of NFI binding should be tested by reporter gene expression contructs to demonstrate NFIB binding to these regulatory regions activate or repress transcription.

We found that miR-124a, miR-153 and miR-30a were regulated in hNSCs upon differentiation and miR-124a and miR-153 could regulate NFIB expression. However, binding of miR-30a to NFIB 3'UTR has no effect on its translation. miR-

30a function could be further investigated by studying the effect of miR-30a overexpression on fate and proliferation of hNSCs. If miR-30a is found to influence hNSC differentiation, downstream targets of miR-30a can be explored further.

There are other predicted miRNA binding sites on NFIB 3'UTR; regulation of these miRNAs has not been observed in differentiating hNSCs. However, these miRNAs could still repress translation of NFIB specifically elsewhere. In this study, we screened for hNSC miRNAs that were upregulated upon differentiation to identify those miRNAs that regulate translation of NFIB during neurogenesis: miR-124a and miR-153 have the ability to do so. To explore the role of miR-124a and other miRNAs in regulation of neuronal differentiation, functional analysis experiments, based on overexpression and knockdown of miRNAs in hNSCs, are required. These *in vitro* experiments need to be supplemented by *in vivo* functional studies on neurogenesis during brain development. In order to determine if some of their effects on neurogenesis are through regulation of NFIB, *in vitro* and *in vivo* functional studies are needed.

REFERENCES

das Neves, L., Duchala, C. S., Tolentino-Silva, F., Haxhiu, M. A., Colmenares, C., Macklin, W. B., ... Gronostajski, R. M. (1999). Disruption of the murine nuclear factor I-A gene (Nfia) results in perinatal lethality, hydrocephalus, and agenesis of the corpus callosum. *Proc Natl Acad Sci USA, 96*(21), 11946-11951.

Alevizopoulos, A., Dusserre, Y., Tsai-Pflugfelder, M., von der Weid, T., Wahli, W., & Mermod, N. (1995). A proline-rich TGF-beta-responsive transcriptional activator interacts with histone H3. *Genes Dev, 9*(24), 3051-3066.

Apt, D., Chong, T., Liu, Y., & Bernard, H. U. (1993). Nuclear factor I and epithelial cell-specific transcription of human papillomavirus type 16. *J Virol, 67*(8), 4455-4463.

Apt, D., Liu, Y., & Bernard, H. U. (1994). Cloning and functional analysis of spliced isoforms of human nuclear factor I-X: interference with transcriptional activation by NFI/CTF in a cell-type specific manner. *Nucleic Acids Res, 22*(19), 3825-3833.

Arvanitis, D. N., Jungas, T., Behar, A., & Davy, A. (2010). Ephrin-B1 reverse signaling controls a posttranscriptional feedback mechanism via miR-124. *Mol Cell Biol, 30*(10), 2508-2517. doi: 10.1128/mcb.01620-09.

Bandyopadhyay, S., & Gronostajski, R. M. (1994). Identification of a conserved oxidation-sensitive cysteine residue in the NFI family of DNA-binding proteins. *J Biol Chem, 269*(47), 29949-29955.

Bandyopadhyay, S., Starke, D. W., Mieyal, J. J., & Gronostajski, R. M. (1998). Thioltransferase (glutaredoxin) reactivates the DNA-binding activity of oxidation-inactivated nuclear factor I. *J Biol Chem, 273*(1), 392-397.

Bartel, D. P. (2004). MicroRNAs: genomics, biogenesis, mechanism, and function. *Cell, 116*(2), 281-297.

Betancourt, J., Katzman, S., & Chen, B. (2014). Nuclear factor one B regulates neural stem cell differentiation and axonal projection of corticofugal neurons. *J Comp Neurol, 522*(1), 6-35. doi: 10.1002/cne.23373.

Bisgrove, D. A., Monckton, E. A., Packer, M., & Godbout, R. (2000). Regulation of brain fatty acid-binding protein expression by differential phosphorylation of nuclear factor I in malignant glioma cell lines. *J Biol Chem, 275*(39), 30668-30676. doi: 10.1074/jbc.M003828200.

Borello, U., Cobos, I., Long, J. E., McWhirter, J. R., Murre, C., & Rubenstein, J. L. (2008). FGF15 promotes neurogenesis and opposes FGF8 function during neocortical development. *Neural Dev, 3*, 17. doi: 10.1186/1749-8104-3-17.

Borgmeyer, U., Nowock, J., & Sippel, A. E. (1984). The TGGCA-binding protein: a eukaryotic nuclear protein recognizing a symmetrical sequence on double-stranded linear DNA. *Nucleic Acids Res, 12*(10), 4295-4311.

Brun, M., Glubrecht, D. D., Baksh, S., & Godbout, R. (2013). Calcineurin regulates nuclear factor I dephosphorylation and activity in malignant glioma cell lines. *J Biol Chem, 288*(33), 24104-24115. doi: 10.1074/jbc.M113.455 832.

Campbell, C. E., Piper, M., Plachez, C., Yeh, Y. T., Baizer, J. S., Osinski, J. M., ... Gronostajski, R. M. (2008). The transcription factor Nfix is essential for normal brain development. *BMC Dev Biol, 8*, 52. doi: 10.1186/1471-213x-8-52.

Conaco, C., Otto, S., Han, J.-J., & Mandel, G. (2006). Reciprocal actions of REST and a microRNA promote neuronal identity. *Proceedings of the National Academy of Sciences of the United States of America*, *103*(7), 2422–2427. doi:10.1073/pnas. 0511041103.

Cao, X., Pfaff, S. L., & Gage, F. H. (2007). A functional study of miR-124 in the developing neural tube. *Genes Dev, 21*(5), 531-536. doi: 10.1101/gad. 15 1920.

Cebolla, B., & Vallejo, M. (2006). Nuclear factor-I regulates glial fibrillary acidic protein gene expression in astrocytes differentiated from cortical precursor cells. *J Neurochem, 97*(4), 1057-1070. doi: 10.1111/j.1471-4159.2006.03804 .x.

Chang, C. Y., Pasolli, H. A., Giannopoulou, E. G., Guasch, G., Gronostajski, R. M., Elemento, O., & Fuchs, E. (2013). NFIB is a governor of epithelial-melanocyte stem cell behaviour in a shared niche. *Nature, 495*(7439), 98-102. doi: 10.1038/nature11847.

Chaudhry, A. Z., Lyons, G. E., & Gronostajski, R. M. (1997). Expression patterns of the four nuclear factor I genes during mouse embryogenesis indicate a potential role in development. *Dev Dyn, 208*(3), 313-325. doi: 10.1002/.

Chaudhry, A. Z., Vitullo, A. D., & Gronostajski, R. M. (1998). Nuclear factor I (NFI) isoforms differentially activate simple versus complex NFI-responsive promoters. *J Biol Chem, 273*(29), 18538-18546.

Chaudhry, A. Z., Vitullo, A. D., & Gronostajski, R. M. (1999). Nuclear factor I-mediated repression of the mouse mammary tumor virus promoter is abrogated by the coactivators p300/CBP and SRC-1. *J Biol Chem, 274*(11), 7072-7081.

Cheah, K. S., Au, P. K., Lau, E. T., Little, P. F. and Stubbs, L. (1991) The mouse Col2a-1 gene is highly conserved and is linked to Int-1 on chromosome 15. Mamm. Genome 1, 171 – 183.

Chen, L., Kostadima, M., Martens, J. H. A., Canu, G., Garcia, S. P., Turro, E., ... Rendon, A. (2014). Transcriptional diversity during lineage commitment of human blood progenitors. *Science, 345*(6204). doi: 10.1126/science.1251033.

Chendrimada, T. P., Finn, K. J., Ji, X., Baillat, D., Gregory, R. I., Liebhaber, S. A., ... Shiekhattar, R. (2007). MicroRNA silencing through RISC recruitment of eIF6. *Nature, 447*(7146), 823-828. doi: 10.1038/nature058 41.

Cheng, L. C., Pastrana, E., Tavazoie, M., & Doetsch, F. (2009). miR-124 regulates adult neurogenesis in the subventricular zone stem cell niche. *Nat Neurosci, 12*(4), 399-408. doi: 10.1038/nn.2294.

Cheng, P., Andersen, P., Hassel, D., Kaynak, B. L., Limphong, P., Juergensen, L., ... Srivastava, D. (2013). Fibronectin mediates mesendodermal

cell fate decisions. *Development, 140*(12), 2587-2596. doi: 10.1242/dev.089052.

Chiang, C. M., & Roeder, R. G. (1995). Cloning of an intrinsic human TFIID subunit that interacts with multiple transcriptional activators. *Science, 267*(5197), 531-536.

Conaco, C., Otto, S., Han, J. J., & Mandel, G. (2006). Reciprocal actions of REST and a microRNA promote neuronal identity. *Proc Natl Acad Sci U S A, 103*(7), 2422-2427. doi: 10.1073/pnas.0511041103.

Deneen, B., Ho, R., Lukaszewicz, A., Hochstim, C. J., Gronostajski, R. M., & Anderson, D. J. (2006). The transcription factor NFIA controls the onset of gliogenesis in the developing spinal cord. *Neuron, 52*(6), 953-968. doi: 10.1016/j.neuron.2006.11.019.

Devon, R. S., Anderson, S., Teague, P. W., Muir, W. J., Murray, V., Pelosi, A. J., ... Porteous, D. J. (2001). The genomic organisation of the metabotropic glutamate receptor subtype 5 gene, and its association with schizophrenia. *Mol Psychiatry,* 6(3), 311-314. doi: 10.1038/sj.mp.40008 48.

Doxakis, E. (2010). Post-transcriptional Regulation of α-Synuclein Expression by mir-7 and mir-153. *J Biol Chem*, 285(17), 12726-12734. doi: 10.1074/jbc.M109.086827.

Egan, M. F., Straub, R. E., Goldberg, T. E., Yakub, I., Callicott, J. H., Hariri, A. R., ... Weinberger, D. R. (2004). Variation in GRM3 affects cognition, prefrontal glutamate, and risk for schizophrenia. *Proc Natl Acad Sci U S A*, 101(34), 12604-12609. doi: 10.1073/pnas.0405077101.

Fanous, A. H., Chen, X., Wang, X., Amdur, R. L., O'Neill, F. A., Walsh, D., & Kendler, K. S. (2007). Association between the 5q31.1 gene neurogenin1 and schizophrenia. Am J *Med Genet B Neuropsychiatr Genet*, 144b(2), 207-214. doi: 10.1002/ajmg.b.30423.

Fazi, F., Rosa, A., Fatica, A., Gelmetti, V., De Marchis, M. L., Nervi, C., & Bozzoni, I. (2005). A minicircuitry comprised of microRNA-223 and transcription factors NFI-A and C/EBPalpha regulates human granulopoiesis. *Cell, 123*(5), 819-831. doi: 10.1016/j.cell.2005.09.023

Fischer, S., Filipek-Gorniok, B., & Ledin, J. (2011). Zebrafish Ext2 is necessary for Fgf and Wnt signaling, but not for Hh signaling. *BMC Dev Biol, 11*, 53. doi: 10.1186/1471-213x-11-53.

Fletcher, C. F., Jenkins, N. A., Copeland, N. G., Chaudhry, A. Z., & Gronostajski, R. M. (1999). Exon structure of the nuclear factor I DNA-binding domain from C. elegans to mammals. *Mamm Genome, 10*(4), 390-396.

Fujita, S., Ito, T., Mizutani, T., Minoguchi, S., Yamamichi, N., Sakurai, K., & Iba, H. (2008). miR-21 Gene expression triggered by AP-1 is sustained through a double-negative feedback mechanism. *J Mol Biol, 378*(3), 492-504. doi: 10.1016/j.jmb.2008.03.015.

Gao, B., Jaffe, H., & Kunos, G. (1998). Histone H1 isoforms purified from rat liver bind nonspecifically to the nuclear factor 1 recognition sequence and serve as generalized transcriptional repressors. *Mol Cell Biochem, 178*(1-2), 187-196.

Garzon, R., Pichiorri, F., Palumbo, T., Visentini, M., Aqeilan, R., Cimmino, A., . . . Croce, C. M. (2007). MicroRNA gene expression during retinoic

acid-induced differentiation of human acute promyelocytic leukemia. *Oncogene, 26*(28), 4148-4157. doi: 10.1038/sj.onc.1210186.

Gimeno, L., & Martinez, S. (2007). Expression of chick Fgf19 and mouse Fgf15 orthologs is regulated in the developing brain by Fgf8 and Shh. *Dev Dyn, 236*(8), 2285-2297. doi: 10.1002/dvdy.21237.

Glasgow, S. M., Zhu, W., Stolt, C. C., Huang, T. W., Chen, F., LoTurco, J. J., . . . Deneen, B. (2014). Mutual antagonism between Sox10 and NFIA regulates diversification of glial lineages and glioma subtypes. *Nat Neurosci, 17*(10), 1322-1329. doi: 10.1038/nn.3790.

Glasgow, S. M., Laug, D., Brawley, V. S., Zhang, Z., Corder, A., Yin, Z., . . . Deneen, B. (2013). The miR-223/nuclear factor I-A axis regulates glial precursor proliferation and tumorigenesis in the CNS. *J Neurosci, 33*(33), 13560-13568. doi: 10.1523/jneurosci.0321-13.2013

Goetz, R., Beenken, A., Ibrahimi, O. A., Kalinina, J., Olsen, S. K., Eliseenkova, A. V., … Mohammadi, M. (2007). Molecular insights into the klotho-dependent, endocrine mode of action of fibroblast growth factor 19 subfamily members. *Mol Cell Biol, 27*(9), 3417-3428. doi: 10.1128/mcb. 02249-06.

Gounari, F., De Francesco, R., Schmitt, J., van der Vliet, P., Cortese, R., & Stunnenberg, H. (1990). Amino-terminal domain of NF1 binds to DNA as a dimer and activates adenovirus DNA replication. *EMBO J, 9*(2), 559-566.

Gronostajski, R. M., Nagata, K., & Hurwitz, J. (1984). Isolation of human DNA sequences that bind to nuclear factor I, a host protein involved in adenovirus DNA replication. *Proc Natl Acad Sci U S A, 81*(13), 4013-40 17.

Gronostajski, R. M., Adhya, S., Nagata, K., Guggenheimer, R. A., & Hurwitz, J. (1985). Site-specific DNA binding of nuclear factor I: analyses of cellular binding sites. *Mol Cell Biol, 5*(5), 964-971.

Gronostajski, R. M. (1986). Analysis of nuclear factor I binding to DNA using degenerate oligonucleotides. *Nucleic Acids Res, 14*(22), 9117-9132.

Gronostajski, R. M. (1987). Site-specific DNA binding of nuclear factor I: effect of the spacer region. *Nucleic Acids Res, 15*(14), 5545-5559.

Gronostajski, R. M. (2000). Roles of the NFI/CTF gene family in transcription and development. *Gene, 249*(1-2), 31-45.

Grunder, A., Ebel, T. T., Mallo, M., Schwarzkopf, G., Shimizu, T., Sippel, A. E., & Schrewe, H. (2002). Nuclear factor I-B (Nfib) deficient mice have severe lung hypoplasia. *Mech Dev, 112*(1-2), 69-77.

Guo, H., Liu, H., Mitchelson, K., Rao, H., Luo, M., Xie, L., ... Cheng, J. (2011). MicroRNAs-372/373 promote the expression of hepatitis B virus through the targeting of nuclear factor I/B. *Hepatology, 54*(3), 808-819. doi: 10.1002/hep.24441.

Guasconi, V., & Puri, P. L. (2009). Chromatin: the interface between extrinsic cues and the epigenetic regulation of muscle regeneration. *Trends Cell Biol, 19*(6), 286-294. doi: 10.1016/j.tcb.2009.03.002.

Hannafon, B. N., Sebastiani, P., de las Morenas, A., Lu, J., & Rosenberg, C. L. (2011). Expression of microRNA and their gene targets are dysregulated in preinvasive breast cancer. *Breast Cancer Res, 13*(2), R24. doi: 10.1186/bcr2839.

Ha, M., & Kim, V. N. (2014). Regulation of microRNA biogenesis. *Nat Rev Mol*

Cell Biol, 15(8), 509-524. doi: 10.1038/nrm3838.

Hayashi, Y., Furue, M. K., Okamoto, T., Ohnuma, K., Myoishi, Y., Fukuhara, Y., ... Asashima, M. (2007). Integrins Regulate Mouse Embryonic Stem Cell Self-Renewal. *Stem Cells, 25*(12), 3005-3015. doi: 10.1634/stemcells.2007-0103.

Heng, Y.H., Barry, G., Richards, L.J., Piper M. (2012). Nuclear factor I genes regulate neuronal migration. *Neurosignals,* 20(3), 159-67.

Hennighausen, L., Siebenlist, U., Danner, D., Leder, P., Rawlins, D., Rosenfeld, P., & Kelly, T., Jr. (1985). High-affinity binding site for a specific nuclear protein in the human IgM gene. *Nature, 314*(6008), 289-292.

Holmfeldt, P., Pardieck, J., Saulsberry, A. C., Nandakumar, S. K., Finkelstein, D., Gray, J. T., ... McKinney-Freeman, S. (2013). Nfix is a novel regulator of murine hematopoietic stem and progenitor cell survival. *Blood, 122*(17), 2987-2996. doi: 10.1182/blood-2013-04-493973.

Huntzinger, E., & Izaurralde, E. (2011). Gene silencing by microRNAs: contributions of translational repression and mRNA decay. *Nat Rev Genet, 12*(2), 99-110. doi: 10.1038/nrg2936.

Hwang, M., Lee, J. M., Kim, Y., & Geum, D. (2014). Functional Role of Parkin against Oxidative Stress in Neural Cells. *Endocrinol Metab (Seoul), 29*(1), 62-69. doi: 10.3803/EnM.2014.29.1.62.

Itoh, N., & Ornitz, D. M. (2004). Evolution of the Fgf and Fgfr gene families. *Trends Genet, 20*(11), 563-569. doi: 10.1016/j.tig.2004.08.007.

Iwata, N., Yoshida, H., Tobiume, M., Ono, F., Shimazaki, T., Sata, T., & Nakajima, N. (2007). Simian fetal brain progenitor cells for studying viral neuropathogenesis. *J Neurovirol, 13*(1), 11-22. doi: 10.1080/13550280601086064.

Izzi, L., Levesque, M., Morin, S., Laniel, D., Wilkes, B. C., Mille, F., ... Charron, F. (2011). Boc and Gas1 each form distinct Shh receptor complexes with Ptch1 and are required for Shh-mediated cell proliferation. *Dev Cell, 20*(6), 788-801. doi: 10.1016/j.devcel.2011. 04.017.

Jeong, M. H., Ho, S. M., Vuong, T. A., Jo, S. B., Liu, G., Aaronson, S. A., . . . Kang, J. S. (2014). Cdo suppresses canonical Wnt signalling via interaction with Lrp6 thereby promoting neuronal differentiation. *Nat Commun, 5*, 5455. doi: 10.1038/ncomms6455.

Jones, K. A., Kadonaga, J. T., Rosenfeld, P. J., Kelly, T. J., & Tjian, R. (1987). A cellular DNA-binding protein that activates eukaryotic transcription and DNA replication. *Cell, 48*(1), 79-89.

Kane, R., Murtagh, J., Finlay, D., Marti, A., Jaggi, R., Blatchford, D., ... Martin, F. (2002). Transcription factor NFIC undergoes N-glycosylation during early mammary gland involution. *J Biol Chem, 277*(29), 25893-25903. doi: 10.1074/jbc.M202469200.

Kang, J. S., Gao, M., Feinleib, J. L., Cotter, P. D., Guadagno, S. N., & Krauss, R. S. (1997). CDO: an oncogene-, serum-, and anchorage-regulated member of the Ig/fibronectin type III repeat family. *J Cell Biol, 138*(1), 203-213.

Kang, J. S., Mulieri, P. J., Miller, C., Sassoon, D. A., & Krauss, R. S. (1998). CDO, a robo-related cell surface protein that mediates myogenic differentiation. *J Cell Biol, 143*(2), 403-413.

Kang, J. S., Feinleib, J. L., Knox, S., Ketteringham, M. A., & Krauss, R. S. (2003). Promyogenic members of the Ig and cadherin families

associate to positively regulate differentiation. *Proc Natl Acad Sci U S A, 100*(7), 3989-3994. doi: 10.1073/pnas.0736565100.

Kang, J. S., Bae, G. U., Yi, M. J., Yang, Y. J., Oh, J. E., Takaesu, G., . . . Krauss, R. S. (2008). A Cdo-Bnip-2-Cdc42 signaling pathway regulates p38alpha/beta MAPK activity and myogenic differentiation. *J Cell Biol, 182*(3), 497-507. doi: 10.1083/jcb.200801119.

Kang, P., Lee, H. K., Glasgow, S. M., Finley, M., Donti, T., Gaber, Z. B., . . . Deneen, B. (2012). Sox9 and NFIA coordinate a transcriptional regulatory cascade during the initiation of gliogenesis. *Neuron, 74*(1), 79-94. doi: 10.1016/j.neuron.2012.01.024.

Kawamura, H., Nagata, K., Masamune, Y., & Nakanishi, Y. (1993). Phosphorylation of NF-I in vitro by cdc2 kinase. *Biochem Biophys Res Commun, 192*(3), 1424-1431. doi: 10.1006/bbrc.1993.1575.

Kawamata, T., & Tomari, Y. (2010). Making RISC. *Trends Biochem Sci, 35*(7), 368-376. doi: 10.1016/j.tibs.2010.03.009.

Kilpatrick, D. L., Wang, W., Gronostajski, R., & Litwack, E. D. (2012). Nuclear factor I and cerebellar granule neuron development: an intrinsic-extrinsic interplay. *Cerebellum, 11*(1), 41-49. doi: 10.1007/s12311-010-0227-0.

Kim, J., Krichevsky, A., Grad, Y., Hayes, G. D., Kosik, K. S., Church, G. M., & Ruvkun, G. (2004). Identification of many microRNAs that copurify with polyribosomes in mammalian neurons. *Proc Natl Acad Sci U S A, 101*(1), 360-365. doi: 10.1073/pnas.2333854100.

Kim, T. K., & Roeder, R. G. (1994). CTD-like sequences are important for transcriptional activation by the proline-rich activation domain of CTF1. *Nucleic Acids Res, 22*(2), 251.

Kiriakidou, M., Tan, G. S., Lamprinaki, S., De Planell-Saguer, M., Nelson, P. T., & Mourelatos, Z. (2007). An mRNA m7G cap binding-like motif within human Ago2 represses translation. *Cell, 129*(6), 1141-1151. doi: 10.1016/j.cell.2007.05.016.

Kumbasar, A., Plachez, C., Gronostajski, R. M., Richards, L. J., & Litwack, E. D. (2009). Absence of the transcription factor Nfib delays the formation of the basilar pontine and other mossy fiber nuclei. *J Comp Neurol, 513*(1), 98-112. doi: 10.1002/cne.21943.

Lagos-Quintana, M., Rauhut, R., Lendeckel, W., & Tuschl, T. (2001). Identification of novel genes coding for small expressed RNAs. *Science, 294*(5543), 853-858. doi: 10.1126/science.1064921.

Lagos-Quintana, M., Rauhut, R., Yalcin, A., Meyer, J., Lendeckel, W., & Tuschl, T. (2002). Identification of tissue-specific microRNAs from mouse. *Curr Biol, 12*(9), 735-739.

Lang, M. F., & Shi, Y. (2012). Dynamic Roles of microRNAs in Neurogenesis. *Front Neurosci, 6*, 71. doi: 10.3389/fnins.2012.00071.

Lau, N. C., Lim, L. P., Weinstein, E. G., & Bartel, D. P. (2001). An abundant class of tiny RNAs with probable regulatory roles in Caenorhabditis elegans. *Science, 294*(5543), 858-862. doi: 10.1126/science.1065062.

Lee, R. C., Feinbaum, R. L., & Ambros, V. (1993). The C. elegans heterochronic gene lin-4 encodes small RNAs with antisense complementarity to lin-14. *Cell, 75*(5), 843-854.

Lee, R. C., & Ambros, V. (2001). An extensive class of small RNAs in Caenorhabditis elegans. *Science, 294*(5543), 862-864. doi: 10.1126/

science.1065329.

Lee, Y., Kim, M., Han, J., Yeom, K. H., Lee, S., Baek, S. H., & Kim, V. N. (2004). MicroRNA genes are transcribed by RNA polymerase II. *EMBO J, 23*(20), 4051-4060. doi: 10.1038/sj.emboj.7600385.

Leegwater, P. A., van Driel, W., & van der Vliet, P. C. (1985). Recognition site of nuclear factor I, a sequence-specific DNA-binding protein from HeLa cells that stimulates adenovirus DNA replication. *EMBO J, 4*(6), 1515-1521.

Leegwater, P. A., van der Vliet, P. C., Rupp, R. A., Nowock, J., & Sippel, A. E. (1986). Functional homology between the sequence-specific DNA-binding proteins nuclear factor I from HeLa cells and the TGGCA protein from chicken liver. *EMBO J, 5*(2), 381-386.

Leung, K. K., Ng, L. J., Ho, K. K., Tam, P. P. and Cheah, K. S. (1998) Different cis-regulatory DNA elements mediate developmental stage- and tissue-specific expression of the human COL2A1 gene in transgenic mice. *J. Cell. Biol.* 141, 1291 – 300.

Lewis, B. P., Burge, C. B., & Bartel, D. P. (2005). Conserved seed pairing, often flanked by adenosines, indicates that thousands of human genes are microRNA targets. *Cell, 120*(1), 15-20. doi: 10.1016/j.cell.2004. 12.035.

Liang, C., Zhu, H., Xu, Y., Huang, L., Ma, C., Deng, W., ... Qin, C. (2012). MicroRNA-153 negatively regulates the expression of amyloid precursor protein and amyloid precursor-like protein 2. *Brain Res*, 1455, 103-113. doi: http://dx.doi.org/10.1016/j.brainres.2011.10.051.

Lim, L. P., Lau, N. C., Garrett-Engele, P., Grimson, A., Schelter, J. M., Castle, J., . . . Johnson, J. M. (2005). Microarray analysis shows that some microRNAs downregulate large numbers of target mRNAs. *Nature, 433* (7027), 769-773. doi: 10.1038/nature03315

Liu, K., Liu, Y., Mo, W., Qiu, R., Wang, X., Wu, J. Y., & He, R. (2011). MiR-124 regulates early neurogenesis in the optic vesicle and forebrain, targeting NeuroD1. *Nucleic Acids Res, 39*(7), 2869-2879. doi: 10.1093/nar/gkq904.

Llave, C., Xie, Z., Kasschau, K. D., & Carrington, J. C. (2002). Cleavage of Scarecrow-like mRNA targets directed by a class of Arabidopsis miRNA. *Science, 297*(5589), 2053-2056. doi: 10.1126/science.1076 311.

Lu, M., & Krauss, R. S. (2010). N-cadherin ligation, but not Sonic hedgehog binding, initiates Cdo-dependent p38alpha/beta MAPK signaling in skeletal myoblasts. *Proc Natl Acad Sci U S A, 107*(9), 4212-4217. doi: 10.1073/pnas.0908883107.

Lui, V. C., Ng, L. J., Nicholls, J., Tam, P. P. and Cheah, K. S. (1995) Tissue-specific and differential expression of alternatively spliced alpha 1(II) collagen mRNAs in early human embryos. *Dev. Dyn*. 203, 198 – 211.

Lytle, J. R., Yario, T. A., & Steitz, J. A. (2007). Target mRNAs are repressed as efficiently by microRNA-binding sites in the 5' UTR as in the 3' UTR. *Proc Natl Acad Sci U S A, 104*(23), 9667-9672. doi: 10.1073/pnas. 070382010.

Maiorano, N. A., & Mallamaci, A. (2009). Promotion of embryonic cortico-cerebral neuronogenesis by miR-124. *Neural Dev, 4*, 40. doi: 10.1186/1749-8104-4-40.

Makeyev, E. V., Zhang, J., Carrasco, M. A., & Maniatis, T. (2007). The MicroRNA miR-124 promotes neuronal differentiation by triggering brain-specific alternative pre-mRNA splicing. *Mol Cell, 27*(3), 435-448. doi: 10.1016/j. molcel.2007.07.015.

Martynoga, B., Mateo, J. L., Zhou, B., Andersen, J., Achimastou, A., Urban, N., ... Guillemot, F. (2013). Epigenomic enhancer annotation reveals a key role for NFIX in neural stem cell quiescence. *Genes Dev, 27*(16), 1769-1786. doi: 10.1101/gad.216804.113.

Mason, I. (2007). Initiation to end point: the multiple roles of fibroblast growth factors in neural development. *Nat Rev Neurosci, 8*(8), 583-596. doi: 10.1038 /nrn2189.

McWhirter, J. R., Goulding, M., Weiner, J. A., Chun, J., & Murre, C. (1997). A novel fibroblast growth factor gene expressed in the developing nervous system is a downstream target of the chimeric homeodomain oncoprotein E2A-Pbx1. *Development, 124*(17), 3221-3232.

Meisterernst, M., Gander, I., Rogge, L., & Winnacker, E. L. (1988). A quantitative analysis of nuclear factor I/DNA interactions. *Nucleic Acids Res, 16*(10), 4419-4435.

Mellios, N., Huang, H.-S., Grigorenko, A., Rogaev, E., & Akbarian, S. (2008). A set of differentially expressed miRNAs, including miR-30a-5p, act as post-transcriptional inhibitors of BDNF in prefrontal cortex. *Human Molecular Genetics*, 17(19), 3030-3042. doi: 10.1093/hmg/ddn201.

Mermod, N., O'Neill, E. A., Kelly, T. J., & Tjian, R. (1989). The proline-rich transcriptional activator of CTF/NF-I is distinct from the replication and DNA binding domain. *Cell, 58*(4), 741-753.

Messina, G., Biressi, S., Monteverde, S., Magli, A., Cassano, M., Perani, L., . . . Cossu, G. (2010). Nfix regulates fetal-specific transcription in developing skeletal muscle. *Cell, 140*(4), 554-566. doi: 10.1016/j.cell.2010.01.027.

Miyake, A., Nakayama, Y., Konishi, M., & Itoh, N. (2005). Fgf19 regulated by Hh signaling is required for zebrafish forebrain development. *Dev Biol, 288*(1), 259-275. doi: 10.1016/j.ydbio.2005.09.042.

Muguruma, K., Nishiyama, A., Kawakami, H., Hashimoto, K., & Sasai, Y. (2015). Self-organization of polarized cerebellar tissue in 3D culture of human pluripotent stem cells. *Cell Rep, 10*(4), 537-550. doi: 10.1016/j.celrep. 2014.12.051.

Mukhopadhyay, S. S., & Rosen, J. M. (2007). The C-terminal domain of the nuclear factor I-B2 isoform is glycosylated and transactivates the WAP gene in the JEG-3 cells. *Biochem Biophys Res Commun, 358*(3), 770-776. doi: 10. 1016/j.bbrc.2007.04.185.

Mulieri, P. J., Okada, A., Sassoon, D. A., McConnell, S. K., & Krauss, R. S. (2000). Developmental expression pattern of the cdo gene. *Dev Dyn, 219*(1), 40-49. doi: 10.1002/1097-0177(2000)9999:9999<::aid-dvdy1032>3.0.co;2-m.

Nagata, K., Guggenheimer, R. A., Enomoto, T., Lichy, J. H., & Hurwitz, J. (1982). Adenovirus DNA replication in vitro: identification of a host factor that stimulates synthesis of the preterminal protein-dCMP complex. *Proc Natl Acad Sci U S A, 79*(21), 6438-6442.

Namihira, M., Kohyama, J., Semi, K., Sanosaka, T., Deneen, B., Taga, T., & Nakashima, K. (2009). Committed neuronal precursors confer

astrocytic potential on residual neural precursor cells. *Dev Cell, 16*(2), 245-255. doi: 10.1016/j.devcel.2008.12.014.

Nelson, P. T., Hatzigeorgiou, A. G., & Mourelatos, Z. (2004). miRNP:mRNA association in polyribosomes in a human neuronal cell line. *Rna, 10*(3), 387-394.

Neo, W. H., Yap, K., Lee, S. H., Looi, L. S., Khandelia, P., Neo, S. X., ... Su, I. H. (2014). MicroRNA miR-124 controls the choice between neuronal and astrocyte differentiation by fine-tuning Ezh2 expression. *J Biol Chem, 289*(30), 20788-20801. doi: 10.1074/jbc.M113.525493.

Nilsson, J., Bjursell, G., & Kannius-Janson, M. (2006). Nuclear Jak2 and transcription factor NF1-C2: a novel mechanism of prolactin signaling in mammary epithelial cells. *Mol Cell Biol, 26*(15), 5663-5674. doi: 10. 1128/mcb.02095-05.

Nishimura, T., Utsunomiya, Y., Hoshikawa, M., Ohuchi, H., & Itoh, N. (1999). Structure and expression of a novel human FGF, FGF-19, expressed in the fetal brain. *Biochim Biophys Acta, 1444*(1), 148-151.

Nottrott, S., Simard, M. J., & Richter, J. D. (2006). Human let-7a miRNA blocks protein production on actively translating polyribosomes. *Nat Struct Mol Biol, 13*(12), 1108-1114. doi: 10.1038/nsmb1173.

Nowock, J., Borgmeyer, U., Puschel, A. W., Rupp, R. A., & Sippel, A. E. (1985). The TGGCA protein binds to the MMTV-LTR, the adenovirus origin of replication, and the BK virus enhancer. *Nucleic Acids Res, 13*(6), 2045-2061.

Oh, J. E., Bae, G. U., Yang, Y. J., Yi, M. J., Lee, H. J., Kim, B. G., ... Kang, J. S. (2009). Cdo promotes neuronal differentiation via activation of the p38 mitogen-activated protein kinase pathway. *Faseb j, 23*(7), 2088-2099. doi: 10.1096/fj.08-119255.

Okada, C., Yamashita, E., Lee, S. J., Shibata, S., Katahira, J., Nakagawa, A., ... Tsukihara, T. (2009). A high-resolution structure of the pre-microRNA nuclear export machinery. *Science, 326*(5957), 1275-1279. doi: 10.1126/ science.1178705.

Okazawa, M., Abe, H., Katsukawa, M., Iijima, K., Kiwada, T., & Nakanishi, S. (2009). Role of calcineurin signaling in membrane potential-regulated maturation of cerebellar granule cells. *J Neurosci, 29*(9), 2938-2947. doi: 10.1523/jneurosci.5932-08.2009.

Petersen, C. P., Bordeleau, M. E., Pelletier, J., & Sharp, P. A. (2006). Short RNAs repress translation after initiation in mammalian cells. *Mol Cell, 21*(4), 533-542. doi: 10.1016/j.molcel.2006.01.031.

Pillai, R. S., Bhattacharyya, S. N., Artus, C. G., Zoller, T., Cougot, N., Basyuk, E., ... Filipowicz, W. (2005). Inhibition of translational initiation by Let-7 MicroRNA in human cells. *Science, 309*(5740), 1573-1576. doi: 10.1126 /science.1115079.

Piper, M., Barry, G., Hawkins, J., Mason, S., Lindwall, C., Little, E., . . . Richards, L. J. (2010). NFIA controls telencephalic progenitor cell differentiation through repression of the Notch effector Hes1. *J Neurosci, 30*(27), 9127-9139. doi: 10.1523/jneurosci.6167-09.2010.

Piper, M., Harris, L., Barry, G., Heng, Y. H., Plachez, C., Gronostajski, R. M., & Richards, L. J. (2011). Nuclear factor one X regulates the development of multiple cellular populations in the postnatal cerebellum. *J Comp Neurol, 519*(17), 3532-3548. doi:

10.1002/cne.22721.

Piper, M., Barry, G., Harvey, T. J., McLeay, R., Smith, A. G., Harris, L., . . . Richards, L. J. (2014). NFIB-mediated repression of the epigenetic factor Ezh2 regulates cortical development. *J Neurosci, 34*(8), 2921-2930. doi: 10.1523/jneurosci.2319-13.2014.

Plachez, C., Lindwall, C., Sunn, N., Piper, M., Moldrich, R. X., Campbell, C. E., ... Richards, L. J. (2008). Nuclear factor I gene expression in the developing forebrain. *J Comp Neurol, 508*(3), 385-401. doi: 10.1002/cne.21645.

Plachez, C., Cato, K., McLeay, R. C., Heng, Y. H. E., Bailey, T. L., Gronostasjki, R. M., ... Piper, M. (2012). Expression of nuclear factor one A and -B in the olfactory bulb. *J Comp Neurol, 520*(14), 3135-3149. doi: 10.1002/cne.23081.

Puklin-Faucher, E., & Sheetz, M. P. (2009). The mechanical integrin cycle. *J Cell Sci, 122*(2), 179-186. doi: 10.1242/jcs.042127.

Reinhart, B. J., Slack, F. J., Basson, M., Pasquinelli, A. E., Bettinger, J. C., Rougvie, A. E., ... Ruvkun, G. (2000). The 21-nucleotide let-7 RNA regulates developmental timing in Caenorhabditis elegans. *Nature, 403*(6772), 901-906. doi: 10.1038/35002607.

Rhoades, M. W., Reinhart, B. J., Lim, L. P., Burge, C. B., Bartel, B., & Bartel, D. P. (2002). Prediction of plant microRNA targets. *Cell, 110*(4), 513-520.

Rojas, P., Joodmardi, E., Hong, Y., Perlmann, T., & Ogren, S. O. (2007). Adult mice with reduced Nurr1 expression: an animal model for schizophrenia. *Mol Psychiatry*, 12(8), 756-766. doi: 10.1038/sj.mp.4001993.

Ruby, J. G., Jan, C. H., & Bartel, D. P. (2007). Intronic microRNA precursors that bypass Drosha processing. *Nature, 448*(7149), 83-86. doi: 10.1038/nature05983.

Rupp, R. A., Kruse, U., Multhaup, G., Gobel, U., Beyreuther, K., & Sippel, A. E. (1990). Chicken NFI/TGGCA proteins are encoded by at least three independent genes: NFI-A, NFI-B and NFI-C with homologues in mammalian genomes. *Nucleic Acids Res, 18*(9), 2607-2616.

Saitsu, H., Komada, M., Suzuki, M., Nakayama, R., Motoyama, J., Shiota, K., & Ishibashi, M. (2005). Expression of the mouse Fgf15 gene is directly initiated by Sonic hedgehog signaling in the diencephalon and midbrain. *Dev Dyn, 232*(2), 282-292. doi: 10.1002/dvdy.20236.

Santoro, C., Mermod, N., Andrews, P. C., & Tjian, R. (1988). A family of human CCAAT-box-binding proteins active in transcription and DNA replication: cloning and expression of multiple cDNAs. *Nature, 334*(6179), 218-224. doi: 10.1038/334218a0.

Scott, C. E., Wynn, S. L., Sesay, A., Cruz, C., Cheung, M., Gomez Gaviro, M. V., ... Briscoe, J. (2010). SOX9 induces and maintains neural stem cells. *Nat Neurosci, 13*(10), 1181-1189. doi: 10.1038/nn.2646.

Shi, Y., Zhao, X., Hsieh, J., Wichterle, H., Impey, S., Banerjee, S., … Kosik, K. S. (2010). microRNA regulation of neural stem cells and neurogenesis. *The Journal of Neuroscience : The Official Journal of the Society for Neuroscience*,*30*(45), 14931–14936. doi:10.1523/JNEUROSCI.4280-10.2010.

Shimizu, H., Iwayama, Y., Yamada, K., Toyota, T., Minabe, Y., Nakamura, K., ... Yoshikawa, T. (2006) Genetic and expression analyses of the STOP (MAP6) gene in schizophrenia. Schizophr Res, 84(2), 244-252. doi: 10.1016/j.schres.2006.03.017.

Shimojo, H., Ohtsuka, T., & Kageyama, R. (2008). Oscillations in notch signaling regulate maintenance of neural progenitors. *Neuron, 58*(1), 52-64. doi: 10.1016/j.neuron.2008.02.014.

Shin, S., & Vemuri, M. (2010). Culture and Differentiation of Human Neural Stem Cells. In L. C. Doering (Ed.), *Protocols for Neural Cell Culture* (pp. 51-73): Humana Press.

Shin, S., Sun, Y., Liu, Y., Khaner, H., Svant, S., Cai, J., ... Chesnut, J. D. (2007). Whole genome analysis of human neural stem cells derived from embryonic stem cells and stem and progenitor cells isolated from fetal tissue. *Stem Cells, 25*(5), 1298-1306. doi: 10.1634/stemcells.2006-0660.

Shin, S., Mitalipova, M., Noggle, S., Tibbitts, D., Venable, A., Rao, R., & Stice, S. L. (2006). Long-term proliferation of human embryonic stem cell-derived neuroepithelial cells using defined adherent culture conditions. *Stem Cells, 24*(1), 125-138. doi: 10.1634/stemcells.2004-0150.

Singh, S. K., Wilczynska, K. M., Grzybowski, A., Yester, J., Osrah, B., Bryan, L., ... Kordula, T. (2011). The unique transcriptional activation domain of nuclear factor-I-X3 is critical to specifically induce marker gene expression in astrocytes. *J Biol Chem, 286*(9), 7315-7326. doi: 10.1074 /jbc.M110.152421.

Shu, T., & Richards, L. J. (2001). Cortical axon guidance by the glial wedge during the development of the corpus callosum. *J Neurosci, 21*(8), 2749-2758.

Shu, T., Butz, K. G., Plachez, C., Gronostajski, R. M., & Richards, L. J. (2003). Abnormal development of forebrain midline glia and commissural projections in Nfia knock-out mice. *J Neurosci, 23*(1), 203-212.

Silver, J., Lorenz, S. E., Wahlsten, D., & Coughlin, J. (1982). Axonal guidance during development of the great cerebral commissures: Descriptive and experimental studies, in vivo, on the role of preformed glial pathways. *J Comp Neurol, 210*(1), 10-29.doi: 10.1002/cne.902100103.

Silver, J., & Ogawa, M. Y. (1983). Postnatally induced formation of the corpus callosum in acallosal mice on glia-coated cellulose bridges. *Science, 220*(4601), 1067-1069.

Steele-Perkins, G., Butz, K. G., Lyons, G. E., Zeichner-David, M., Kim, H. J., Cho, M. I., & Gronostajski, R. M. (2003). Essential role for NFI-C/CTF transcription-replication factor in tooth root development. *Mol Cell Biol, 23*(3), 1075-1084.

Steele-Perkins, G., Plachez, C., Butz, K. G., Yang, G., Bachurski, C. J., Kinsman, S. L., ... Gronostajski, R. M. (2005). The transcription factor gene Nfib is essential for both lung maturation and brain development. *Mol Cell Biol, 25*(2), 685-698. doi: 10.1128/mcb.25.2.685-698.2005.

Steele-Perkins, G., Butz, K. G., Lyons, G. E., Zeichner-David, M., Kim, H. J., Cho, M. I., & Gronostajski, R. M. (2003). Essential role for NFI-

C/CTF transcription-replication factor in tooth root development. *Mol Cell Biol, 23*(3), 1075-1084.

Sullivan, P. F., Keefe, R. S., Lange, L. A., Lange, E. M., Stroup, T. S., Lieberman, J., & Maness, P. F. (2007). NCAM1 and neurocognition in schizophrenia. *Biol Psychiatry*, 61(7), 902-910. doi: 10.1016/j.biopsych.2006.07.036.

Takizawa, T., Nakashima, K., Namihira, M., Ochiai, W., Uemura, A., Yanagisawa, M., . . . Taga, T. (2001). DNA methylation is a critical cell-intrinsic determinant of astrocyte differentiation in the fetal brain. *Dev Cell, 1*(6), 749-758.

Tapscott, S. J. (2005). The circuitry of a master switch: Myod and the regulation of skeletal muscle gene transcription. *Development, 132*(12), 2685-2695. doi: 10.1242/dev.01874.

Tenzen, T., Allen, B. L., Cole, F., Kang, J. S., Krauss, R. S., & McMahon, A. P. (2006). The cell surface membrane proteins Cdo and Boc are components and targets of the Hedgehog signaling pathway and feedback network in mice. *Dev Cell, 10*(5), 647-656. doi: 10.1016/j.devcel.2006.04.004.

Tsai, P. C., Bake, S., Balaraman, S., Rawlings, J., Holgate, R. R., Dubois, D., & Miranda, R. C. (2014). MiR-153 targets the nuclear factor-1 family and protects against teratogenic effects of ethanol exposure in fetal neural stem cells. *Biol Open, 3*(8), 741-758. doi: 10.1242/bio.20147765.

Tsuyama, J., Bunt, J., Richards, L. J., Iwanari, H., Mochizuki, Y., Hamakubo, T., ... Okano, H. (2015). MicroRNA-153 Regulates the Acquisition of Gliogenic Competence by Neural Stem Cells. Stem Cell Reports. doi: 10.1016/j.stemcr.2015.06.006.

Turac, G., Hindley, C. J., Thomas, R., Davis, J. A., Deleidi, M., Gasser, T., ... Pruszak, J. (2013). Combined flow cytometric analysis of surface and intracellular antigens reveals surface molecule markers of human neuropoiesis. *PLoS One, 8*(6), e68519. doi: 10.1371/journal. pone.0068519.

Uchihashi, T., Kimata, M., Tachikawa, K., Koshimizu, T., Okada, T., Ihara-Watanabe, M., ... Michigami, T. (2007). Involvement of nuclear factor I transcription/replication factor in the early stage of chondrocytic differentiation. *Bone, 41*(6), 1025-1035. doi: 10.1016/j.bone.2007.08.028.

Ujike, H., Takaki, M., Nakata, K., Tanaka, Y., Takeda, T., Kodama, M., ... Kuroda, S. (2002). CNR1, central cannabinoid receptor gene, associated with susceptibility to hebephrenic schizophrenia. *Mol Psychiatry*, 7(5), 515-518. doi: 10.1038/sj.mp.4001029.

Valinezhad Orang, A., Safaralizadeh, R., & Kazemzadeh-Bavili, M. (2014). Mechanisms of miRNA-Mediated Gene Regulation from Common Downregulation to mRNA-Specific Upregulation. *International Journal of Genomics, 2014*, 15. doi: 10.1155/2014/970607.

Visvanathan, J., Lee, S., Lee, B., Lee, J. W., & Lee, S. K. (2007). The microRNA miR-124 antagonizes the anti-neural REST/SCP1 pathway during embryonic CNS development. *Genes Dev, 21*(7), 744-749. doi: 10.1101 /gad.1519107.

Wang, W., Stock, R. E., Gronostajski, R. M., Wong, Y. W., Schachner, M., &

Kilpatrick, D. L. (2004). A role for nuclear factor I in the intrinsic control of cerebellar granule neuron gene expression. *J Biol Chem, 279*(51), 53491-53497. doi: 10.1074/jbc.M410370200.

Wang, W., Mullikin-Kilpatrick, D., Crandall, J. E., Gronostajski, R. M., Litwack, E. D., & Kilpatrick, D. L. (2007). Nuclear factor I coordinates multiple phases of cerebellar granule cell development via regulation of cell adhesion molecules. *J Neurosci, 27*(23), 6115-6127. doi: 10.1523 /jneurosci.0180-07.2007.

Wang, W., Crandall, J. E., Litwack, E. D., Gronostajski, R. M., & Kilpatrick, D. L. (2010). Targets of the nuclear factor I regulon involved in early and late development of postmitotic cerebellar granule neurons. *J Neurosci Res, 88*(2), 258-265. doi: 10.1002/jnr.22199.

Wang, X. (2014). Composition of seed sequence is a major determinant of microRNA targeting patterns. *Bioinformatics, 30*(10), 1377-1383. doi: 10.1093 /bioinformatics/btu045.

Wang, Y., Sheng, G., Juranek, S., Tuschl, T., & Patel, D. J. (2008). Structure of the guide-strand-containing argonaute silencing complex. *Nature, 456*(7219), 209-213. doi: 10.1038/nature07315.

Wang, Y., Huang, C., Chintagari, N. R., Xi, D., Weng, T., & Liu, L. (2015). miR-124 regulates fetal pulmonary epithelial cell maturation. *American Journal of Physiology - Lung Cellular and Molecular Physiology*.

Watt, F. M., & Huck, W. T. S. (2013). Role of the extracellular matrix in regulating stem cell fate. *Nat Rev Mol Cell Biol, 14*(8), 467-473. doi: 10.1038/nrm3620.

Wei, C., Thatcher, E. J., Olena, A. F., Cha, D. J., Perdigoto, A. L., Marshall, A. F., ... Patton, J. G. (2013). miR-153 Regulates SNAP-25, Synaptic Transmission, and Neuronal Development. *PLoS One,* 8(2), e57080. doi: 10.1371/journal.pone.0057080.

Wilczynska, K. M., Singh, S. K., Adams, B., Bryan, L., Rao, R. R., Valerie, K., ... Kordula, T. (2009). Nuclear factor I isoforms regulate gene expression during the differentiation of human neural progenitors to astrocytes. *Stem Cells, 27*(5), 1173-1181. doi: 10.1002/stem.35.

Wright, T. J., Ladher, R., McWhirter, J., Murre, C., Schoenwolf, G. C., & Mansour, S. L. (2004). Mouse FGF15 is the ortholog of human and chick FGF19, but is not uniquely required for otic induction. *Dev Biol, 269*(1), 264-275. doi: 10.1016/j.ydbio.2004.02.003.

Xiao, H., Lis, J. T., Xiao, H., Greenblatt, J., & Friesen, J. D. (1994). The upstream activator CTF/NF1 and RNA polymerase II share a common element involved in transcriptional activation. *Nucleic Acids Res, 22*(11), 1966-1973.

Yao, S., Lum, L., & Beachy, P. (2006). The ihog cell-surface proteins bind Hedgehog and mediate pathway activation. *Cell, 125*(2), 343-357. doi: 10.1016 /j.cell.2006.02.040.

Yoo, A. S., Staahl, B. T., Chen, L., & Crabtree, G. R. (2009). MicroRNA-mediated switching of chromatin-remodelling complexes in neural development. *Nature, 460*(7255), 642-646. doi: 10.1038/nature08139.

Zare, M., Soleimani, M., Akbarzadeh, A., Bakhshandeh, B., Aghaee-Bakhtiari, S. H., & Zarghami, N. (2014). A Novel Protocol to Differentiate Induced Pluripotent Stem Cells by Neuronal microRNAs to Provide a Suitable Cellular Model. *Chem Biol Drug Des*. doi: 10.1111/cbdd.

12485.

Zhang, H., Kolb, F. A., Jaskiewicz, L., Westhof, E., & Filipowicz, W. (2004). Single processing center models for human Dicer and bacterial RNase III. *Cell, 118*(1), 57-68. doi: 10.1016/j.cell.2004.06.017.

Zhang, W., Yi, M. J., Chen, X., Cole, F., Krauss, R. S., & Kang, J. S. (2006). Cortical thinning and hydrocephalus in mice lacking the immunoglobulin superfamily member CDO. *Mol Cell Biol, 26*(10), 3764-3772. doi: 10. 1128/mcb.26.10.3764-3772.2006.

Zhao, J. J., Lin, J., Zhu, D., Wang, X., Brooks, D., Chen, M., ... Carrasco, R. (2014). miR-30-5p functions as a tumor suppressor and novel therapeutic tool by targeting the oncogenic Wnt/beta-catenin/BCL9 pathway. *Cancer Res, 74*(6), 1801-1813. doi: 10.1158/0008-5472.can-13-3311-t.

APPENDICES

APPENDIX A: Laboratory equipments.
APPENDIX B: Commercial kits.
APPENDIX C: Chemicals.
APPENDIX D: Reagents, chemicals, small molecules and buffers.
APPENDIX E: Characterization of expression of NFI transcripts in a time-dependent manner.
APPENDIX F: Characterization of expression of putative NFIB downstream targets.
APPENDIX G: Characterization of expression of NFIB targeting miRNAs.
APPENDIX H: Characterization of expression of NFIB targeting miRNAs in a time-dependent manner.
APPENDIX I: Sequencing results for TOPO_NFIB 3'UTR constructs.
APPENDIX J: Sequencing results of Luc-NFIB 3'UTR vectors
APPENDIX K: Sequencing results for Luc-NFIB 3'UTR_B-124M and Luc-NFIB 3'UTR_D-153M.
APPENDIX L: miR-21 represses Luc-NFIB 3'UTR_A.
APPENDIX M: Binding of miR-21 on Luc-NFIB 3'UTR_A is reversed by anti-pre-miR-21.
APPENDIX N: miR-124a represses Luc-NFIB 3'UTR_B, but not Luc-NFIB 3'UTR_A.
APPENDIX O: Binding of miR-124a does not repress Luc-NFIB 3'UTR_B-124M.
APPENDIX P: miR-30a cannot repress translation from Luc-NFIB 3'UTR_A, Luc-NFIB 3'UTR_C or Luc-NFIB 3'UTR_D
APPENDIX R: miR-153 repressed Luc-NFIB 3'UTR_D but not Luc-NFIB 3'UTR_B.
APPENDIX S: Binding of miR-153 does not repress Luc-NFIB 3'UTR_D-153M.
APPENDIX T: Sequence alignment of mouse, rat and human NFIB 3'UTR sequences (by CLUSTAL-W2).

APPENDIX A:

Table A.1 : Laboratory equipment used in this study.

Equipment	Supplier Companies
Cell culture plates	Corning
Cell culture flasks	Corning
Centrifuges	ScanSpeed mini centrifuge, Labogene; Beckman Coulter Allegra TM 25 R Centrifuge; ScanSpeed 1730 R
Centrifuge tubes	Axygen
Chemidoc	ChemiDoc ^{TM} MP System (BIORAD)
Confocal Microscope	Leica TCS SP2MOD
Electrophoresis Gel System	Sub-Cell GT Agarose Gel Electrophoresis Systems, BIORAD
Electronic Pipettes	CappAid
Flow Cytometry	BD Accuri C6
Freezers	Panasonic Ultra Low Temperature Freezer MDF-U76V; Bosch 00046372 GSD30N12NE; Bosch K6N57VW20NNE
Hemacytometer	Isolab
Ice Machine	Scotsman AF10
Incubator with CO_2	BINDER &Thermo Scientific, 381
Laminar Air Flow Cabinets	Faster BH-EN 2003
Light Microscope	Olympus CH30
Magnetic stirrer	WiseStir MSH-20A, Wisd Lab Equipments
MicroAmp® Fast Optical 96-Well Plate	Applied Biosystems®
MicroAmp® Optical Adhesive Film	Applied Biosystems®
Microcentrifuge	ScanSpeed
Microplate luminometer plates	LUMITRAC™200, 96 well Greiner Bio-one
Microplate Spectrophotometer	Benchmark Plus, BIORAD
Microwave	Micro-Magic
Nitrogen Tank	Air liquid
Nucleic Acid Spectrophotometer	NanoDrop/Thermo Fisher Scientific Inc, USA
pH Meter	Mettler Toledo, MP220
Pipettes	Gilson 10 µl, 100 µl, 200 µl, 1000 µl and Socorex 10 µl, 200 µl, 1000 µl
Power Supply	BIORAD
Quick Spin	Harmony, LMS Group
SDS-PAGE Gel Electrophoresis System	BIO-RAD Mini-Protean Tetra Cell
Shakers	Thermo Scientific, 866-9 Orbital Shaker; Heidolp Duomax 1030
StepOnePlus™ Real-Time PCR System	Applied Biosystems®
Thermo Cycler	T100^{TM} Thermal Cycler (BIORAD)
Transfer system for Western blotting	Mini Trans-Blot Electrophoretic Transfer Cell, BIORAD
UV trans-illuminator	UVStar 321nm, Biometra
Vortex	Harmony, LMS Group (U2US10 VTX-3000L)

APPENDIX B:

Table B.1 : Commercial kits that are used in this thesis are listed.

Kit	Supplier Company
DharmaFECT 1 Transfection Reagent	Dharmacon, T2001-02
DNA isolation kit for mammalian blood	Roche Life Sciences, 11667327001
FuGENE® 6 Transfection Reagent	Promega, E2691
GeneJET Plasmid Miniprep Kit	Thermo Scientific, K0503
High Capacity cDNA Reverse Transcription Kit with RNase Inhibitor	Applied Biosystems®, 4374966
In-Fusion® HD Cloning Kit	ClontechTM, 639636
20X LumiGLO® Reagent and 20X Peroxide	Cell Signaling Technology, 7003
miRNeasy Mini Kit	Qiagen, 217004
mirVana™ miRNA Isolation Kit, with phenol	Ambion®, AM1560
NucleoSpin® Gel and PCR Clean-up Kit	Macherey-Nagel, 740609
NucleoSpin Plasmid DNA Purification Kit	Macherey-Nagel, 740588.50
NucleoBond® Xtra Midi/Maxi Kit	Macherey-Nagel, 740414.50
Pierce™ BCA Protein Assay Kit	Thermo Scientific, 23225
Power SYBR® Green PCR Master Mix	Applied Biosystems®, 4367659
Q5® High-Fidelity DNA Polymerase	NEB, M0491
Quickchange Multi Site Directed Mutagenesis Kit	Agilent Technologies200515
Quick ligation kit	NEB, M2200
RNase free DNase kit	Qiagen, 79254
TaqMan® MicroRNA Reverse Transcription Kit	Applied Biosystems®, 4366596
TaqMan® MicroRNA Assays	Applied Biosystems®, 4427975
The Dual-Luciferase® Reporter (DLR™) Assay System	Promega, E1910
The PureLink® RNA Mini Kit	Ambion®, 12183018A
Zero Blunt® TOPO® PCR Cloning Kit	Invitrogen, 450245

APPENDIX C:

Table C.1 : Chemicals that are used in this study are listed.

Chemical	Supplier Company
Acetic acid	J. T. Baker, 6052
Agar, Bacteriological	LabM, MC006
Agarose	SaeKem LE, 50004
APS	Fischer Scientific, BP179-100
Beta-mercaptoethanol	Sigma Aldrich, Mb250
Buffer solutions pH 4.0, 7.0, 10.0	Fluka, 33665; 33666; 33668
Bromophenol Blue	Fisher Scientific, BP115
DMSO	Fisher Scientific, BP-231
EDTA	Biochemica, A1103, 0250
EGTA	Sigma Aldrich, E3889
Ethanol, absolute	Carlo Erba Reagents, 4146082
Glycerol solution	Sigma Aldrich, 11524
Glycine	Fisher Scientific, BP381
HCl (37%)	Carlo Erba Reagents, 403872
HEPES	Fisher Scientific, BP310
Isopropyl Alcohol	J. T. Baker, 9080-03
KH_2PO_4	Merck, 1.04873.100
Methanol, analytical grade	Fisher Scientific, M4000
NaCl	Merck, 1.06404.1000
NaOH	Sigma Aldrich, 221465
Paraformaldehyde	Sigma Aldrich, P6148-
Ponceau-S	Fisher Scientific, BP103
Pronasafe Nucleic acid staining dye (20,000X)	Conda Lab., CK130
SDS	Millipore, 194831
Skim milk powder	Cell signaling, 9999
Sucrose	Merck, K26042553.903
Tris Base for molecular biology grade	Fisher Scientific, BP152
Triton X-100	Fisher Scientific, BP151
Tryptone	LabM, MC005
Tween-20	Fisher Scientific, BP337
Yeast Extract	LabM, MC001

APPENDIX D:

Table D.1 : List of reagents, chemicals, small molecules and buffers used for cell culture.

Product	Supplier
Dulbecco's Modified Eagle Medium (DMEM)	Lonza, BE12-614F
Dulbecco's Phosphate Buffered Saline (D-PBS), containing no calcium, magnesium, or phenol red	Invitrogen, 14190-144
EGF Recombinant Human	Invitrogen, PHG0314
EmbryoMax® Penicillin-Streptomycin Solution, 100X	Miilipore
GlutaMAX Supplement (100X)	Invitrogen, 35050038
KnockOut™ DMEM/F-12	Invitrogen, 12660-012
Laminin from Engelbreth-Holm-Swarm murine sarcoma basement membrane,	Sigma, L2020
L-Glutamine-200 mM (100X)	Invitrogen, 25030081
Opti-MEM® I Reduced Serum Medium	Invitrogen, 31985-062
Penicilin/Streptomycin Liquid, 100X	Invitrogen, 15140-122
Phosphatase Buffered Saline (PBS)	Invitrogen,
Poly-D-Lysine	Sigma Aldrich, P6407-5MG
Poly-L-ornithine	Sigma, P4957
Recombinant Human BDNF	Peprotech, 450-02
Recombinant Human NT-3	Peprotech, 450-03
StemPro® Accutase® Cell Dissociation Reagent	Invitrogen, A11105-01
StemPro® Neural Supplement	Invitrogen, A10508-01
StemPro® NSC SFM (contains KnockOutTM DMEM/F-12, FGF Basic Recombinant Human, EGF Recombinant Human, and StemPro® Neural Supplement)	Invitrogen, A1050901
Trypan Blue Stain	Invitrogen, 15250-061
Fetal Bovine Serum, qualified, E.U.-approved, S.America	Invitrogen, 10270106

APPENDIX E:

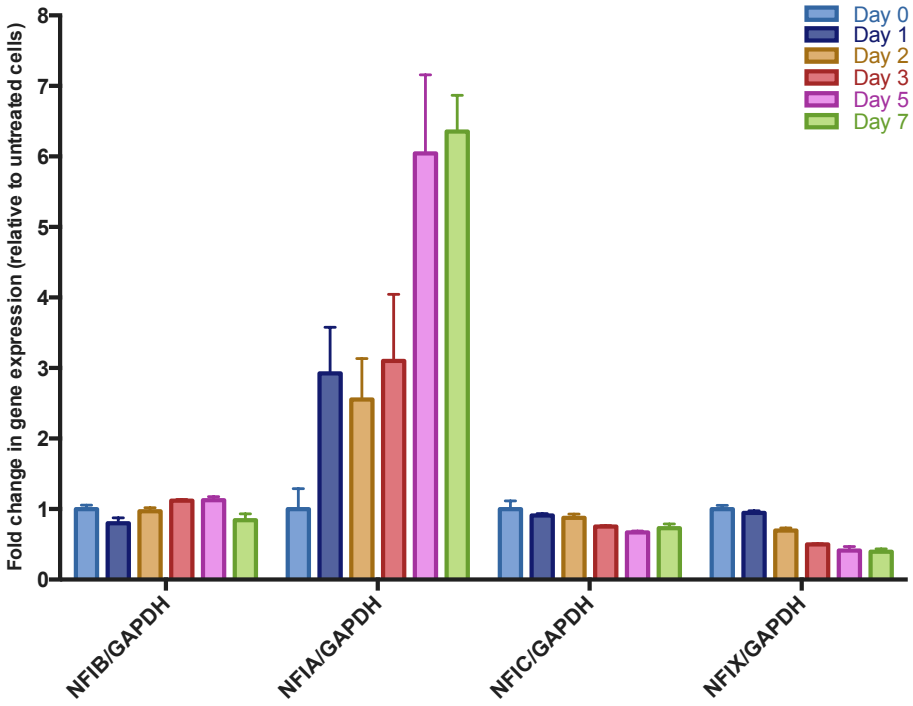


Figure E.1 : *NFIA* is upregulated while *NFIC* and *NFIX* are downregulated upon differentiation of hNSCs in a time-dependent manner. Levels of NFI transcripts were measured by qRT-PCR during time points of differentiation of hNSCs (day 0 (blue bars), day 1 (dark blue), day 2 (orange), day 3 (red bars), day 5 (pink bars), day 7 (green bars)). Gene expression levels were normalized to *GAPDH* gene expression. Data show the mean±S.D. from 2 replicates. Result shows the second independent time-course experiment.

APPENDIX F:

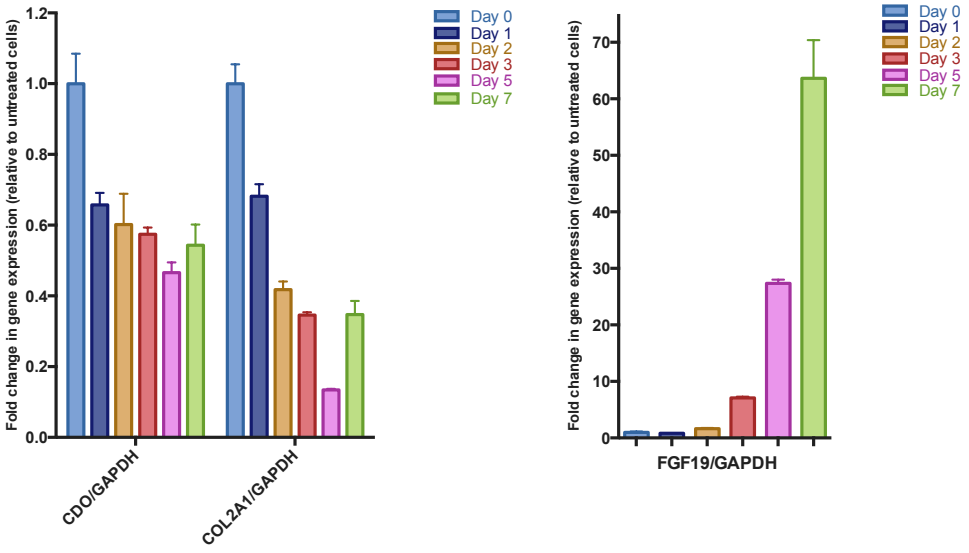


Figure F.1 : Characterization of expression of putative NFIB downstream targets (*CDO*, *COL2A1*, *FGF19*) in hNSC during differentiation in a time-dependent manner. Expression levels of NFI targeted genes (*CDO, COL2A1 and FGF19*) were measured by qRT-PCR during time points of differentiation of hNSCs (day 0 (blue bars), day 1 (dark blue), day 2 (orange), day 3 (red bars), day 5 (purple bars), day 7 (green bars)). Gene expression levels were normalized to *GAPDH* gene expression. Data show the mean±S.D. from 2 replicates. Result shows the second independent time-course experiment.

APPENDIX G:

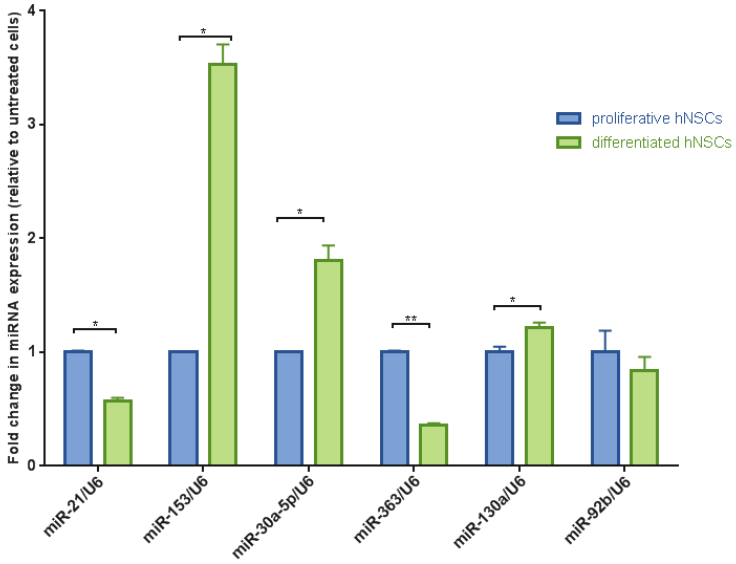


Figure G.1 : Characterization of NFIB targeting miRNAs on mRNA level. Taqman assays were run to determine expression levels of miRNAs predicted NFIB targeting miRNAs (miR-21, miR-153, miR-30a, miR-363, miR-130a, miR-92b) in proliferative (blue bars) and differentiated (green bars) hNSCs. Expressions of miRNAs were normalized to U6 snRNA expression. Data show the mean±S.D. from 2 replicates. The significance of differences was determined using Student's t-test analysis (***$p<0.0001$; **$p<0.001$; *$p<0.05$). Result shows one of two independent experiments.

APPENDIX H:

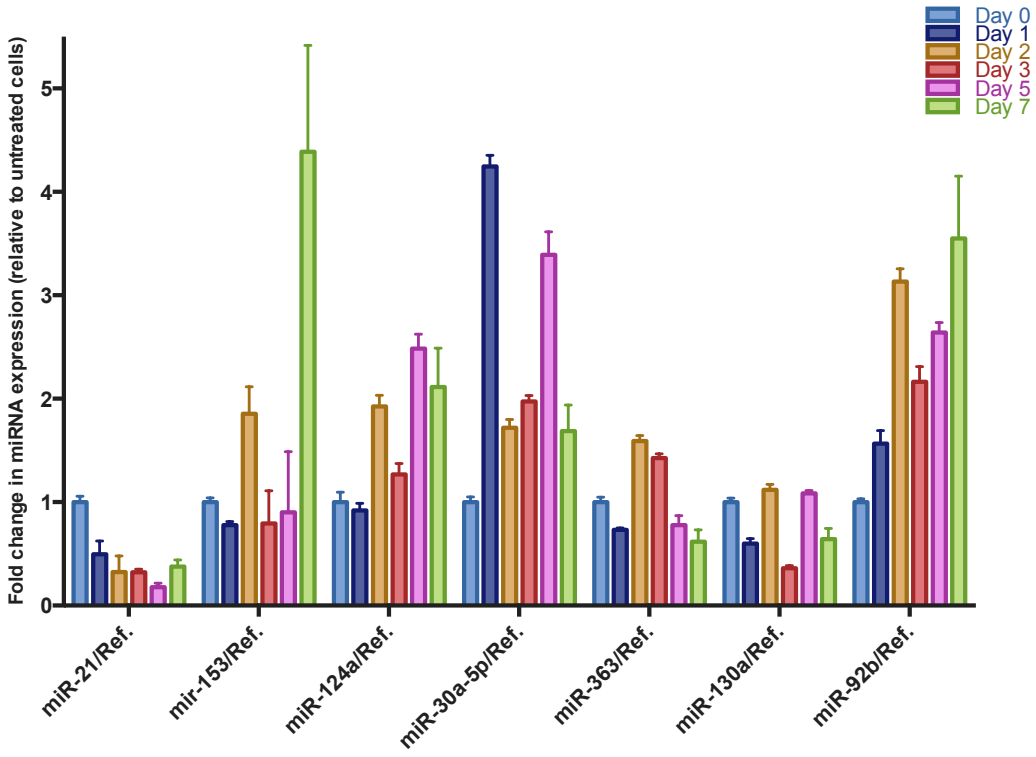


Figure H.1 : Characterization of NFIB targeting miRNAs on mRNA level during differentiation of hNSCs in a time-dependent manner. Taqman assays were run to determine expression levels of miRNAs predicted NFIB targeting miRNAs (miR-21, miR-153, miR-124a, miR-30a, miR-363, miR-130a, miR-92b) during differentiation (day 0 (blue bars), day 1 (dark blue), day 2 (orange), day 3 (red bars), day 5 (pink bars), day 7 (green bars)). Expressions of miRNAs were normalized to geometric means of U6 snRNA, miR-140 and miR-103 expression. Data show the mean±S.D. from 2 replicates. Result shows the second independent time-course experiment.

APPENDIX I:

Alignment data for TOPO_NFIB 3'UTR constructs with sequencing results.

Sequencing result of **TOPO-NFIB 3'UTR_A** (sample name: E2_1)

```
Seq_1  85    -------------------------AGGCTGCAGCTAAACCAACATAAGTGCTGTGTTTT  119
                                      ||||||||||||||||||||||||||||||||||
Seq_2  1126  aaataaataaattctacctccaaggaggctgcagctaaaccaacataagtgctgtgtttt  1067

Seq_1  120   CATTAATTTTATTTTTCTCAAGCACATGATTTGTCTTGATTTAATGCCTTTTTAATGCCC  179
             ||||||||||||||||||||||||||||||||||||||||||||||||||||||||||||
Seq_2  1066  cattaattttatttttctcaagcacatgatttgtcttgatttaatgccttttttaatgccc  1007

Seq_1  180   TCAAAAACTGAGGGGAAAATAAATTCGTTCAAAATTATTTTAAATTCTTTTTAATCCCCT  239
             ||||||||||||||||||||||||||||||||||||||||||||||||||||||||||||
Seq_2  1006  tcaaaaactgaggggaaaataaattcgttcaaaattattttaaattctttttaatccccct  947

Seq_1  240   CAATTTAGAGTCCAAGGGCTGAAGGACTTATAATCATGATTCCCCTTTAGATATAAATTT  299
             ||||||||||||||||||||||||||||||||||||||||||||||||||||||||||||
Seq_2  946   caatttagagtccaagggctgaaggacttataatcatgattccccttagatataaattt  887

Seq_1  300   ATAAATTGCACTTGCCTCTGTTAAGTGTTTCTTTTGTGGGGAAAATATTATATTAATTTT  359
             ||||||||||||||||||||||||||||||||||||||||||||||||||||||||||||
Seq_2  886   ataaattgcacttgcctctgttaagtgtttcttttgtggggaaaatattatattaatttt  827

Seq_1  360   TACTGTTGCATGCAGAGAGAACACTTCACCTACATAGAGGCATTTCTTCCATAGAGCCTT  419
             ||||||||||||||||||||||||||||||||||||||||||||||||||||||||||||
Seq_2  826   tactgttgcatgcagagagaacacttcacctacatagaggcatttcttccatagagcctt  767

Seq_1  420   TGTGTTCAAACTGTTTTTTTCCTTTTTTCTTTTTTTCCTTTTTTTTTCATTTTTTCTTTT  479
             ||||||||||||||||||||||||||||||||||||||||||||||||||||||||||||
Seq_2  766   tgtgttcaaactgttttttccttttttctttttttccttttttttcatttttctttt  707

Seq_1  480   TTTAAGATTTCAAACTGGGTTACACACTGGAAAAGGCTGGGTTAAGGGCCGAAATTTAAT  539
             ||||||||||||||||||||||||||||||||||||||||||||||||||||||||||||
Seq_2  706   tttaagatttcaaactgggttacacactggaaaaggctgggttaagggccgaaatttaat  647

Seq_1  540   AAATCTGTACTGATAACTAAAGGCTACAGAGATTTCATATATTTTTTTTAACTTTTAGAA  599
             ||||||||||||||||||||||||||||||||||||||||||||||||||||||||||||
Seq_2  646   aaatctgtactgataactaaaggctacagagatttcatatatttttttaactttagaa  587

Seq_1  600   ATCAGAGTGCTTATAAAATGGCTGGCTCATGGCTCTGTCACCCAGCACCTCTGACGCCGC  659
             ||||||||||||||||||||||||||||||||||||||||||||||||||||||||||||
Seq_2  586   atcagagtgcttataaaatggctggctcatggctctgtcacccagcacctctgacgccgc  527

Seq_1  660   CTCCTAGCCTTCGTTGGTGAGATAACCAGGAATAGTGATTCCATGCGTAAACAACAAGAA  719
             ||||||||||||||||||||||||||||||||||||||||||||||||||||||||||||
Seq_2  526   ctcctagccttcgttggtgagataaccaggaatagtgattccatgcgtaaacaacaagaa  467

Seq_1  720   TACTAAACCAATAAAACTAGCTTATCATGCAAATATTAAGGCATCTAGAAAGTCAGTTAA  779
             ||||||||||||||||||||||||||||||||||||||||||||||||||||||||||||
Seq_2  466   tactaaaccaataaaactagcttatcatgcaaatattaaggcatctagaaagtcagttaa  407

Seq_1  780   AATATATTGTCATAGAGACAGAACATCTATTTCCCAGCGGACTTCATGTAACAAAGGCTA  839
             ||||||||||||||||||||||||||||||||||||||||||||||||||||||||||||
Seq_2  406   aatatattgtcatagagacagaacatctatttcccagcggacttcatgtaacaaaggcta  347

Seq_1  840   CGTTGCAGGGGCTGCGATCTACCATCAGTGAAATATCATCGACCCTTTTTATGTCATTAC  899
             ||||||||||||||||||||||||||||||||||||||||||||||||||||||||||||
Seq_2  346   cgttgcaggggctgcgatctaccatcagtgaaatatcatcgacccttttatgtcattac  287

Seq_1  900   AGTTTCAACCTTAAGGGAATTAGTGATTGTAAGTGCTGCAATTGCTGGTCTATTATCTTC  959
             ||||||||||||||||||||||||||||||||||||||||||||||||||||||||||||
Seq_2  286   agtttcaaccttaagggaattagtgattgtaagtgctgcaattgctggtctattatcttc  227

Seq_1  960   TTTCTTCAGTTTCTTTCCTTTCTGCCTTTGTGTTGTTTTGTCCAGTCTTCCTCTTTTCCT  1019
             ||||||||||||||||||||||||||||||||||||||||||||||||||||||||||||
Seq_2  226   tttcttcagtttctttcctttctgcctttgtgttgttttgtccagtcttcctcttttcct  167

Seq_1  1020  TTTTTTTTATTTAAAAAAAAAATTTCTTAAACTATTGGTTGGGTTTCTTTTTCCCTCAGT  1079
             |||||||||||||||||||||||||||||||| ||| ||||||||||||||||||||
Seq_2  166   ttttttttatttaaaaaaaaaatttcttaaactattg-ttgtgtttctttttccctcagt  108
```

```
Seq_1  1080  TGCTTGTTTCTGCTTGAAAGGAAAGGTTCTCCAATTATGTTCAAACCCGTAATTTTGGAC  1139
             |||||||||||||||||| |||||||||||||||||||||||||||| ||||||||||||
Seq_2  107   tgcttgtttctgcttgaa-ggaaaggttctccaattatgttcaaacc-gtaattttggac  50

Seq_1  1140  ATTGGGCCGGGAAAAATGGGGGGAAAGGGCGGAATTCCACGCACACTGGGCGGCCGTTTC  1199
             |||||
Seq_2  49    attgg-----------------------------------------------------  45
```

Sequencing result of **TOPO-NFIB 3'UTR_B** (sample name: **D6_1**) aligned to NFIB 3'UTR.

```
Seq_1  901   AGGGGAATCATGATTATAAGTCCTTCAGCCCTTGGACTCTAAATTGAGGGGATTAAAAAG  960
                                                                  ||||||
Seq_2  1258  ----------------------------------------------------AAAAAG  1253

Seq_1  961   AATTTAAAATAA--TTTTGAACGAATTTATTTTCCCCTCAGTTTTTGAGGGCATTAAAAA  1018
             ||||||||||    ||| ||   | ||||||| ||| |||||||| | ||||||||||||
Seq_2  1252  AATTTAAAAT-TTTTTTGGAGGAATTTTATTTCCCCTTCAGTTTTGGGGGGCATTAAAAA  1194

Seq_1  1019  GGCA-TTAAATCAAGACAAATCATGTGCTTGAGAAAAA-TAAAATTAATGAAAACA-CAG  1075
             |||  | ||  ||    || || |||| |||||||||| ||||||||||||||||  |||
Seq_2  1193  GGCCTTAAATCCAGCCAAATTCTTGTGGTTGAGAAAAATTAAAATTAATGAAAACCCCAG  1134

Seq_1  1076  CACTTATGTTGGTTTAGCTGCAGCCTCCTTGGAGGTAGAATTTATTTATTTAAAATTACT  1135
             || ||||||||||||||||||||||||||||||||||||||||||||||||||||||||
Seq_2  1133  CATTTATGTTGGTTTAGCTGCAGCCTCCTTGGAGGTAGAATTTATTTATTTAAAATTACT  1074

Seq_1  1136  GGTTGCATCAAGAACCCATAGGGTGTACAAAAGGTTCTATAAAATCTGCATTATAGAGAC  1195
             ||||||||||||||||||||||||||||||||||||||||||||||||||||||||||||
Seq_2  1073  GGTTGCATCAAGAACCCATAGGGTGTACAAAAGGTTCTATAAAATCTGCATTATAGAGAC  1014

Seq_1  1196  AAAGAGGCAGGCAAATCCATGTCACAAGGGTAAAGCTTACAGTTTACAAACTGGGAACGC  1255
             ||||||||||||||||||||||||||||||||||||||||||||||||||||||||||||
Seq_2  1013  AAAGAGGCAGGCAAATCCATGTCACAAGGGTAAAGCTTACAGTTTACAAACTGGGAACGC  954

Seq_1  1256  CAGGGTGTAGGATATAAAAACGCACTCTTGAGAAAACAAATGTAATCAGGGTGCTGAAAA  1315
             ||||||||||||||||||||||||||||||||||||||||||||||||||||||||||||
Seq_2  953   CAGGGTGTAGGATATAAAAACGCACTCTTGAGAAAACAAATGTAATCAGGGTGCTGAAAA  894

Seq_1  1316  CTTGCATGGTGCTTTCAGACATTAGCCTTGTTCAACAAATTTCTTGTATTGACAGATCCA  1375
             ||||||||||||||||||||||||||||||||||||||||||||||||||||||||||||
Seq_2  893   CTTGCATGGTGCTTTCAGACATTAGCCTTGTTCAACAAATTTCTTGTATTGACAGATCCA  834

Seq_1  1376  TAGTGTGCATGGGCAGACACATTTTGCCTCTATGTCTCTTAAAATTTTAATTAAAAATAC  1435
             ||||||||||||||||||||||||||||||||||||||||||||||||||||||||||||
Seq_2  833   TAGTGTGCATGGGCAGACACATTTTGCCTCTATGTCTCTTAAAATTTTAATTAAAAATAC  774

Seq_1  1436  TCTTTCCAGTAATCCTAATTTGCACGAAGATATAATGTCCACATTACGTGCCTTGCCTTG  1495
             ||||||||||||||||||||||||||||||||||||||||||||||||||||||||||||
Seq_2  773   TCTTTCCAGTAATCCTAATTTGCACGAAGATATAATGTCCACATTACGTGCCTTGCCTTG  714

Seq_1  1496  AAATCTAAAAAACAAAAAACAAAAAAAAAAAAAACAAAAAAATACAACAAAGTGACATCAC  1555
             ||||||||||||||||||||||||||||||||||||||||||||||||||||||||||||
Seq_2  713   AAATCTAAAAAACAAAAAACAAAAAAAAAAAAACAAAAAAATACAACAAAGTGACATCAC  654

Seq_1  1556  TACACTTGTTTTGCTGCATTTATTATCATTTTAAATCTTTACCATTTTTATGACAAAATA  1615
             ||||||||||||||||||||||||||||||||||||||||||||||||||||||||||||
Seq_2  653   TACACTTGTTTTGCTGCATTTATTATCATTTTAAATCTTTACCATTTTTATGACAAAATA  594

Seq_1  1616  TTTTGTACTCCAGACGAAGAAAAATGTGTGACATCATGGATTTTTTAGACAGTTATACCT  1675
             ||||||||||||||||||||||||||||||||||||||||||||||||||||||||||||
Seq_2  593   TTTTGTACTCCAGACGAAGAAAAATGTGTGACATCATGGATTTTTTAGACAGTTATACCT  534

Seq_1  1676  TTATCTCACATTTATAAAGCATATCATGGCTGTGTATAGTTGCCGCTTAAAAATTGTAAT  1735
             ||||||||||||||||||||||||||||||||||||||||||||||||||||||||||||
Seq_2  533   TTATCTCACATTTATAAAGCATATCATGGCTGTGTATAGTTGCCGCTTAAAAATTGTAAT  474

Seq_1  1736  CGACCAGCAATATTTTCAGTATTTTGGTGTTTTTTTCTATTAACCTTTCATGTTTTTCAT  1795
             ||||||||||||||||||||||||||||||||||||||||||||||||||||||||||||
Seq_2  473   CGACCAGCAATATTTTCAGTATTTTGGTGTTTTTTTCTATTAACCTTTCATGTTTTTCAT  414

Seq_1  1796  CTTCCAATTAATATTTGGGGGGGAGGGGTTTCAAATTTATACGAATTATGCAATACCAAG  1855
             ||||||||||||||||||||||||||||||||||||||||||||||||||||||||||||
Seq_2  413   CTTCCAATTAATATTTGGGGGGGAGGGGTTTCAAATTTATACGAATTATGCAATACCAAG  354

Seq_1  1856  TTTTGCCTATGTAGGTAGTGCTTTTAGCTGTATTGGTTATTATAGGTAAGTACACAGATT  1915
```

```
                ||||||||||||||||||||||||||||||||||||||||||||||||||||||||||||
Seq_2  353   TTTTGCCTATGTAGGTAGTGCTTTTAGCTGTATTGGTTATTATAGGTAAGTACACAGATT  294

Seq_1  1916  TAAAAAAAAAATAATGTATGCTTTTTTGTTTGTTTGTTTGTTTTAATTGACCAAAGTGGG  1975
              ||||||||||||||||||||||||||||||||||||||||||||||||||||||||||||
Seq_2  293   TAAAAAAAAAATAATGTATGCTTTTTTGTTTGTTTGTTTGTTTTAATTGACCAAAGTGGG  234

Seq_1  1976  TACTGCTATTTTTGCAGTGTGATGAGGTCCTTTTGTGTACTGAGAGATGGACAGGGGATT  2035
              ||||||||||||||||||||||||||||||||||||||||||||||||||||||||||||
Seq_2  233   TACTGCTATTTTTGCAGTGTGATGAGGTCCTTTTGTGTACTGAGAGATGGACAGGGGATT  174

Seq_1  2036  TTTTTTAATATACATATATATATATTCTGGGGTGGGTGGGAGGATTTTTAACACTTTGCA  2095
              ||||||||||||||||||||||||||||||||||||||||||||||||||||||||||||
Seq_2  173   TTTTTTAATATACATATATATATATTCTGGGGTGGGTGGGAGGATTTTTAACACTTTGCA  114

Seq_1  2096  GTGTAGCTGTGAAGCAGTGCACCCTGAGATGGGCCTGGGCTGCAAAGCGACTGTTCTGCC  2155
              ||||||||||||||||||||||||||||||
Seq_2  113   GTGTAGCTGTGAAGCAGTGCACCCTGAGAT------------------------------  84
```

Sequencing result of **TOPO-NFIB 3'UTR_C** (sample name: G1_1 sequenced with M13_F primer) aligned to NFIB 3'UTR.

```
Seq_1  85    ------TGTCGAAGCACCACTGTCTTTTTATTAGTATATACGGCCTTTAGCAAAAGTTTT  138
                   ||||||||||||||||||||||||||||||||||||||||||||||||||||||||
Seq_2  4319  tcagaatgtcgaagcaccactgtcttttattagtatatacggcctttagcaaaagtttt  4378

Seq_1  139   TGTGATTGTTACGTGATGGTATTTAAGGTTAAGTTTCACAGAGCATTCAGGATAGGCAGA  198
              ||||||||||||||||||||||||||||||||||||||||||||||||||||||||||||
Seq_2  4379  tgtgattgttacgtgatggtatttaaggttaagtttcacagagcattcaggataggcaga  4438

Seq_1  199   AAACTAAAACAGTGCTATGTCTCACATAACGTGTCCTCAGGGAGCAGAATCTTGGATTTG  258
              ||||||||||||||||||||||||||||||||||||||||||||||||||||||||||||
Seq_2  4439  aaactaaaacagtgctatgtctcacataacgtgtcctcagggagcagaatcttggatttg  4498

Seq_1  259   TGACTTGTAGCTTCATAAGGACTCAACGAAAGAGATTGCACAGGGACATCTTCAGCGGTG  318
              ||||||||||||||||||||||||||||||||||||||||||||||||||||||||||||
Seq_2  4499  tgacttgtagcttcataaggactcaacgaaagagattgcacagggacatcttcagcggtg  4558

Seq_1  319   TGACAGCAGGACATGTTCTTTACCTAGATTCAAATTCTATGTACTGTGTGAAATGATGAA  378
              ||||||||||||||||||||||||||||||||||||||||||||||||||||||||||||
Seq_2  4559  tgacagcaggacatgttctttacctagattcaaattctatgtactgtgtgaaatgatgaa  4618

Seq_1  379   GGCTGCAGAAAGTTATCCCATATTCAGTGTACAGTATTCATTTTTAATGAAACAACTCTA  438
              ||||||||||||||||||||||||||||||||||||||||||||||||||||||||||||
Seq_2  4619  ggctgcagaaagttatcccatattcagtgtacagtattcatttttaatgaaacaactcta  4678

Seq_1  439   CAATATTGCTGGCAGATAGGCCCCAAGCATGACATTCAATATAGTTTACATGTTCCTGTC  498
              ||||||||||||||||||||||||||||||||||||||||||||||||||||||||||||
Seq_2  4679  caatattgctggcagataggccccaagcatgacattcaatatagtttacatgttcctgtc  4738

Seq_1  499   AAGGTCTTTTGTTAACATTAACCAGCTGCATGCTTTCTGGACTTTAAGAAATTGGGTTTC  558
              ||||||||||||||||||||||||||||||||||||||||||||||||||||||||||||
Seq_2  4739  aaggtcttttgttaacattaaccagctgcatgctttctggactttaagaaattgggtttc  4798

Seq_1  559   TATAGAAAACTTTTTTTTTTTTTTTTTTT-AATGTGCAGGCTATTCAAGTTCAATAGTA  617
              |||||||||||||||||||||||||||||| ||||||||||||||||||||||||||||||
Seq_2  4799  tatagaaaacttttttttttttttttttttaatgtgcaggctattcaagttcaatagta  4858

Seq_1  618   AAAGCTCAAAAATGAATGTTCTACTCCATGCTGAAGGAGCTGAAAGCTGCCTTCTTCATA  677
              ||||||||||||||||||||||||||||||||||||||||||||||||||||||||||||
Seq_2  4859  aaagctcaaaaatgaatgttctactccatgctgaaggagctgaaagctgccttcttcata  4918

Seq_1  678   TTTTGCACTTTCTGGTAGTTCCCCTGTTTTTTCTAATTCCCTAAAATTGTGTGGGTGGAG  737
              ||||||||||||||||||||||||||||||||||||||||||||||||||||||||||||
Seq_2  4919  ttttgcactttctggtagttcccctgtttttttctaattccctaaaattgtgtgggtggag  4978

Seq_1  738   TGGAGCCCTGCAGTTGGGGGGTAACATGGACCACTGATTTTGCCCTTTGACCCTGCACAA  797
              ||||||||||||||||||||||||||||||||||||||||||||||||||||||||||||
Seq_2  4979  tggagccctgcagttgggggggtaacatggaccactgattttgcccctttgaccctgcacaa  5038

Seq_1  798   TGACCTTTGCATCAGCCAAACTCATTGCCATGACAACTCTTTGTACTGTGTCCGTGTCAC  857
              ||||||||||||||||||||||||||||||||||||||||||||||||||||||||    |
Seq_2  5039  tgacctttgcatcagccaaactcattgccatgacaactctttgtactgtgtccgtg---c  5095
```

Sequencing result of **TOPO-NFIB 3'UTR_C** (sample name: G1_1 sequenced with M13_R primer) aligned with NFIB 3'UTR.

```
Seq_1  129   ----------------------CCACATCAGTCCCTGTAGCACAGTTTTCAAAACCATTC  166
                                   |||||||||||||||||||||||||||||||||||||
Seq_2  5506  tctgcataaagagatatatttgccacatcagtccctgtagcacagttttcaaaaccattc  5447

Seq_1  167   TGTCAAAAATACAGTAATACAAGACTGGCTTTAGTGTCACTAGCTTACACTGCTTTTCAT  226
             ||||||||||||||||||||||||||||||||||||||||||||||||||||||||||||
Seq_2  5446  tgtcaaaaatacagtaatacaagactggctttagtgtcactagcttacactgcttttcat  5387

Seq_1  227   GTATTTAGGCCACCTGTTGTTCCTGGTACTGTATCATGCAATAAGTTATCTAGGGCTTAG  286
             |||||||||||||||||||||||||||||||||||||||||||||| ||| |||||||||
Seq_2  5386  gtatttaggccacctgttgttcctggtactgtatcatgcaataagtcatcaagggcttag  5327

Seq_1  287   TCCAGCGCACCGGTAAGCTAGTGGCACTGAAGCGCTTTTCACAATCTCA-C-ATATATTT  344
             || || | |||||||||||||||||||||||||||||||||||||||| |      ||
Seq_2  5326  tctagtgtaccggtaagctagtggcactgaagcgcttttcacaatctcaacatacatttg  5267
```

Sequencing result of **TOPO-NFIB 3'UTR_D** (sample name: F2_1 sequenced with M13_F primer) aligned to NFIB 3'UTR.

```
Seq_1  87    --------------------TACCAGGAACAACAGGTGGCCTAAATACATGAAAAGCAGT  126
                                 |||||||||||||||||||||||||||||||||||||||
Seq_2  5339  tgacttattgcatgatacagtaccaggaacaacaggtggcctaaatacatgaaaagcagt  5398

Seq_1  127   GTAAGCTAGTGACACTAAAGCCAGTCTTGTATTACTGTATTTTTGACAGAATGGTTTTGA  186
             ||||||||||||||||||||||||||||||||||||||||||||||||||||||||||||
Seq_2  5399  gtaagctagtgacactaaagccagtcttgtattactgtatttttgacagaatggttttga  5458

Seq_1  187   AAACTGTGCTACAGGGACTGATGTGGCAAATATATCTCTTTATGCAGAAGGAAGTCTTTT  246
             ||||||||||||||||||||||||||||||||||||||||||||||||||||||||||||
Seq_2  5459  aaactgtgctacagggactgatgtggcaaatatatctctttatgcagaaggaagtctttt  5518

Seq_1  247   TTTTTCTTTTTTTTTTTTT-AAGAAGTATGGCTTTTTATGCATCCTTCATCGAGGGCATT  305
             |||||||||||||||||| ||||||||||||||||||||||||||||||||||||||||
Seq_2  5519  ttttctttttttttttttaagaagtatggcttttatgcatccttcatcgagggcatt  5578

Seq_1  306   GAAGTTGCATGGACTGATAAAAGTTGATGCAAAACAAGAAAGAAACAAACAAAAAAAAAA  365
             ||||||||||||||||||||||||||||||||||||||||||||||||||||||||||||
Seq_2  5579  gaagttgcatggactgataaaagttgatgcaaaacaagaaagaaacaaacaaaaaaaaaa  5638

Seq_1  366   AACCAGCAAAATGTTTACCAAAAAACTCAAACAAATGAGCAGTGCCTGTTCAATTTCACA  425
             ||||||||||||||||||||||||||||||||||||||||||||||||||||||||||||
Seq_2  5639  aaccagcaaaatgtttaccaaaaaactcaaacaaatgagcagtgcctgttcaatttcaca  5698

Seq_1  426   GTCTCTGTTGAGTTCAGTTGTAAATATGTTTCAAATGACATTTTCTTGGGAAAAAAAATC  485
             ||||||||||||||||||||||||||||||||||||||||||||||||||||||||||||
Seq_2  5699  gtctctgttgagttcagttgtaaatatgtttcaaatgacattttcttgggaaaaaaaatc  5758

Seq_1  486   TCTACAACATTGTAGAATGTGAGGGGTAACTACATCCCAGGCATAGGTTTCTCAAAGCTG  545
             ||||||||||||||||||||||||||||||||||||||||||||||||||||||||||||
Seq_2  5759  tctacaacattgtagaatgtgaggggtaactacatcccaggcataggtttctcaaagctg  5818

Seq_1  546   CAGTAGATTATGTCTTCATCAAGCTGTTAATTTGTGCTTATATCATATAGAACTTTTAGC  605
             ||||||||||||||||||||||||||||||||||||||||||||||||||||||||||||
Seq_2  5819  cagtagattatgtcttcatcaagctgttaatttgtgcttatatcatatagaacttttagc  5878

Seq_1  606   ATCCTGGGAAGAGCTGCCCCCACCTCAATGATATTTCTCTGAGAACAACTTTTGTAGGAC  665
             ||||||||||||||||||||||||||||||||||||||||||||||||||||||||||||
Seq_2  5879  atcctgggaagagctgcccccacctcaatgatatttctctgagaacaacttttgtaggac  5938

Seq_1  666   TGTGTGTTTCTTTAGATACATTTAGTACAACTGTAGGTGACGAGTAGTCAGTTATTGCTT  725
             ||||||||||||||||||||||||||||||||||||||||||||||||||||||||||||
Seq_2  5939  tgtgtgtttctttagatacatttagtacaactgtaggtgacgagtagtcagttattgctt  5998

Seq_1  726   GCTAGCTACACACCAGGGTTGATCCATTTTAAAACTTTTGGCATTTTGTCCTCATGGGCC  785
             ||||||||||||||||||||||||||||||||||||||||||||||||||||||||||||
Seq_2  5999  gctagctacacaccagggttgatccattttaaaacttttggcattttgtcctcatgggcc  6058

Seq_1  786   ATAAATACAGAACCTTGTATTTTAATTAAATTTTTTTACAAAAGGAGGCACATGCACAAT  845
             ||||||||||||||||||||||||||||||||||||||||||||||||||||||||||||
Seq_2  6059  ataaatacagaaccttgtattttaattaaatttttttacaaaaggaggcacatgcacaat  6118

Seq_1  846   CTCCATGTAACAAACCTTTAGCAGTAGGATGTATTATACGACAGTTACTTAATTTCTAGA  905
             ||||||||||||||||||||||||||||||||||||||||||||||||||||||||||||
```

```
Seq_2  6119  ctccatgtaacaaacctttagcagtaggatgtattatacgacagttacttaatttctaga  6178

Seq_1  906   GTTCAGGCCTCTGGGATCAACCCCAGACTGGGCCAGAATGTTAGTGAAGGTTTTATTGTG  965
              ||||||||||||||||||||||||||||||||||||||||||||||||||||||||||||
Seq_2  6179  gttcaggcctctgggatcaaccccagactgggccagaatgttagtgaaggttttattgtg  6238

Seq_1  966   CCCGGTTGGAGGATAACGTTCTTTGGGTACTTTTTGTGGGTTGCAAATGAACTCAATTGC  1025
              ||||||||||||||||||||||||||||||||||||||||||||||||||||||||||||
Seq_2  6239  cccggttggaggataacgttctttgggtacttttgtgggttgcaaatgaactcaattgc  6298

Seq_1  1026  CACAAGTTTTAAACTGGTGTAAATCAAGCTTGACTTAATGTGATTGTTACTGGTATATCC  1085
              |||||||||||||||||||||||||||||||||||||||||||||||||||||||||||
Seq_2  6299  cacaagttttaaactggtgtaaatcaagcttgacttaatgtgattgttactgttatatcc  6358

Seq_1  1086  AGCCTATACTGCTAGCAGCTGCTCATACTGCAGTCAATTACTGGAAACGGATATATTTCC  1145
              |||||||||||||||||||||||||||||||||||||||||||||||||||||||||||
Seq_2  6359  agcctatactgctagcagctgctcatactgcagtcaattactggaagcggatatatttcc  6418

Seq_1  1146  TATGCAAAAACTGTTTAAACAATAAAATGAGCTATGCTCCAAACTCTGAAGGGGGAATTC  1205
              |||||||||||||||||||||||||||||||||||||||||||||||||||||||||||
Seq_2  6419  tatgcaaaaactgtttaaacaataaaatgagctatgctacagactctg------------  6466
```

Sequencing result of **TOPO-NFIB 3'UTR_D** (sample name: F2_1 sequenced with M13_R primer) aligned to NFIB 3'UTR.

```
Seq_1  121   CCTTCAGAGTCTGTAGCATAGCTCATTTTATTGTTTAAACAGTTTTTGCATAGGAAATAT  180
                  ||||||||||||||||||||||||||||||||||||||||||||||||||||||||||||
Seq_2  6466  ----cagagtctgtagcatagctcattttattgtttaaacagttttgcataggaaatat  6411

Seq_1  181   ATCCGCTTCCAGTAATTGACTGCAGTATGAGCAGCTGCTAGCAGTATAGGCTGGATATAA  240
              ||||||||||||||||||||||||||||||||||||||||||||||||||||||||||||
Seq_2  6410  atccgcttccagtaattgactgcagtatgagcagctgctagcagtataggctggatataa  6351

Seq_1  241   CAGTAACAATCACATTAAGTCAAGCTTGATTTACACCAGTTTAAAACTTGTGGCAATTGA  300
              ||||||||||||||||||||||||||||||||||||||||||||||||||||||||||||
Seq_2  6350  cagtaacaatcacattaagtcaagcttgatttacaccagtttaaaacttgtggcaattga  6291

Seq_1  301   GTTCATTTGCAACCCACAAAAAGTACCCAAAGAACGTTATCCTCCAACCGGGCACAATAA  360
              ||||||||||||||||||||||||||||||||||||||||||||||||||||||||||||
Seq_2  6290  gttcatttgcaacccacaaaaagtacccaaagaacgttatcctccaaccgggcacaataa  6231

Seq_1  361   AACCTTCACTAACATTCTGGCCCAGTCTGGGGTTGATCCCAGAGGCCTGAACTCTAGAAA  420
              ||||||||||||||||||||||||||||||||||||||||||||||||||||||||||||
Seq_2  6230  aaccttcactaacattctggcccagtctggggttgatcccagaggcctgaactctagaaa  6171

Seq_1  421   TTAAGTAACTGTCGTATAATACATCCTACTGCTAAAGGTTTGTTACATGGAGATTGTGCA  480
              ||||||||||||||||||||||||||||||||||||||||||||||||||||||||||||
Seq_2  6170  ttaagtaactgtcgtataatacatcctactgctaaaggtttgttacatggagattgtgca  6111

Seq_1  481   TGTGCCTCCTTTTGTAAAAAAATTTAATTAAAATACAAGGTTCTGTATTTATGGCCCATG  540
              ||||||||||||||||||||||||||||||||||||||||||||||||||||||||||||
Seq_2  6110  tgtgcctccttttgtaaaaaaatttaattaaaatacaaggttctgtatttatggcccatg  6051

Seq_1  541   AGGACAAAATGCCAAAAGTTTTAAAATGGATCAACCCTGGTGTGTAGCTAGCAAGCAATA  600
              ||||||||||||||||||||||||||||||||||||||||||||||||||||||||||||
Seq_2  6050  aggacaaaatgccaaaagttttaaaatggatcaaccctggtgtgtagctagcaagcaata  5991

Seq_1  601   ACTGACTACTCGTCACCTACAGTTGTACTAAATGTATCTAAAGAAACACACAGTCCTACA  660
              ||||||||||||||||||||||||||||||||||||||||||||||||||||||||||||
Seq_2  5990  actgactactcgtcacctacagttgtactaaatgtatctaaagaaacacacagtcctaca  5931

Seq_1  661   AAAGTTGTTCTCAGAGAAATATCATTGAGGTGGGGGCAGCTCTTCCCAGGATGCTAAAAG  720
              ||||||||||||||||||||||||||||||||||||||||||||||||||||||||||||
Seq_2  5930  aaagttgttctcagagaaatatcattgaggtggggcagctcttcccaggatgctaaaag  5871

Seq_1  721   TTCTATATGATATAAGCACAAATTAACAGCTTGATGAAGACATAATCTACTGCAGCTTTG  780
              ||||||||||||||||||||||||||||||||||||||||||||||||||||||||||||
Seq_2  5870  ttctatatgatataagcacaaattaacagcttgatgaagacataatctactgcagctttg  5811

Seq_1  781   AGAAACCTATGCCTGGGATGTAGTTACCCCTCACATTCTACAATGTTGTAGAGATTTTTT  840
              ||||||||||||||||||||||||||||||||||||||||||||||||||||||||||||
Seq_2  5810  agaaacctatgcctgggatgtagttacccctcacattctacaatgttgtagagatttttt  5751

Seq_1  841   TTCCCAAGAAAATGTCATTTGAAACATATTTACAACTGAACTCAACAGAGACTGTGAAAT  900
              ||||||||||||||||||||||||||||||||||||||||||||||||||||||||||||
Seq_2  5750  ttcccaagaaaatgtcatttgaaacatatttacaactgaactcaacagagactgtgaaat  5691
```

```
Seq_1  901   TGAACAGGCACTGCTCATTTGTTTGAGTTTTT-GGTAAACATTTTGCTGGGTTTTTTTTT  959
             |||||||||||||||||||||||||||||||| ||||||||||||||||| |||||||||
Seq_2  5690  tgaacaggcactgctcatttgtttgagtttttggtaaacatttgctggtttttttttt  5631

Seq_1  960   TTGTTGGTTCCTTCCTGG-TTTGCATCAACTTTTATCAATCCATGCAACTTCAATGCC-T  1017
             ||||| ||| ||| || | |||||||||||||||||| |||||||||||||||||| |
Seq_2  5630  ttgtttgtttctttcttgttttgcatcaacttttatcagtccatgcaacttcaatgccct  5571
```

APPENDIX J:

Alignment of sequencing results after In-Fusion cloning reaction for NFIB 3'UTR_C and NFIB 3'UTR_D.

Sequencing result of **Luc-NFIB 3'UTR_C** (sample name: L7_2 sequenced with **pmiRGLO-F primer**)

```
Seq_1  103   -------TGTCGAAGCACCACTGTCTTTTTATTAGTATATACGGCCTTTAGCAAAAGTTT  155
              |||||||||||||||||||||||||||||||||||||||||||||||||||||||||||
Seq_2  4318  TTCAGAATGTCGAAGCACCACTGTCTTTTTATTAGTATATACGGCCTTTAGCAAAAGTTT  4377

Seq_1  156   TTGTGATTGTTACGTGATGGTATTTAAGGTTAAGTTTCACAGAGCATTCAGGATAGGCAG  215
              |||||||||||||||||||||||||||||||||||||||||||||||||||||||||||
Seq_2  4378  TTGTGATTGTTACGTGATGGTATTTAAGGTTAAGTTTCACAGAGCATTCAGGATAGGCAG  4437

Seq_1  216   AAAACTAAAACAGTGCTATGTCTCACATAACGTGTCCTCAGGGAGCAGAATCTTGGATTT  275
              |||||||||||||||||||||||||||||||||||||||||||||||||||||||||||
Seq_2  4438  AAAACTAAAACAGTGCTATGTCTCACATAACGTGTCCTCAGGGAGCAGAATCTTGGATTT  4497

Seq_1  276   GTGACTTGTAGCTTCATAAGGACTCAACGAAAGAGATTGCACAGGGACATCTTCAGCGGT  335
              |||||||||||||||||||||||||||||||||||||||||||||||||||||||||||
Seq_2  4498  GTGACTTGTAGCTTCATAAGGACTCAACGAAAGAGATTGCACAGGGACATCTTCAGCGGT  4557

Seq_1  336   GTGACAGCAGGACATGTTCTTTACCTAGATTCAAATTCTATGTACTGTGTGAAATGATGA  395
              |||||||||||||||||||||||||||||||||||||||||||||||||||||||||||
Seq_2  4558  GTGACAGCAGGACATGTTCTTTACCTAGATTCAAATTCTATGTACTGTGTGAAATGATGA  4617

Seq_1  396   AGGCTGCAGAAAGTTATCCCATATTCAGTGTACAGTATTCATTTTTAATGAAACAACTCT  455
              |||||||||||||||||||||||||||||||||||||||||||||||||||||||||||
Seq_2  4618  AGGCTGCAGAAAGTTATCCCATATTCAGTGTACAGTATTCATTTTTAATGAAACAACTCT  4677

Seq_1  456   ACAATATTGCTGGCAGATAGGCCCCAAGCATGACATTCAATATAGTTTACATGTTCCTGT  515
              |||||||||||||||||||||||||||||||||||||||||||||||||||||||||||
Seq_2  4678  ACAATATTGCTGGCAGATAGGCCCCAAGCATGACATTCAATATAGTTTACATGTTCCTGT  4737

Seq_1  516   CAAGGTCTTTTGTTAACATTAACCAGCTGCATGCTTTCTGGACTTTAAGAAATTGGGTTT  575
              |||||||||||||||||||||||||||||||||||||||||||||||||||||||||||
Seq_2  4738  CAAGGTCTTTTGTTAACATTAACCAGCTGCATGCTTTCTGGACTTTAAGAAATTGGGTTT  4797

Seq_1  576   CTATAGAAAACTTTTTTTTTTTTTTTTTT--AATGTGCAGGCTATTCAAGTTCAATAGT  633
              ||||||||||||||||||||||||||||  ||||||||||||||||||||||||||||
Seq_2  4798  CTATAGAAAACTTTTTTTTTTTTTTTTTTTTAATGTGCAGGCTATTCAAGTTCAATAGT  4857

Seq_1  634   AAAAGCTCAAAAATGAATGTTCTACTCCATGCTGAAGGAGCTGAAAGCTGCCTTCTTCAT  693
              |||||||||||||||||||||||||||||||||||||||||||||||||||||||||||
Seq_2  4858  AAAAGCTCAAAAATGAATGTTCTACTCCATGCTGAAGGAGCTGAAAGCTGCCTTCTTCAT  4917

Seq_1  694   ATTTTGCACTTTCTGGTAGTTCCCCTGTTTTTTCTAATTCCCTAAAATTGTGTGGGTGGA  753
              |||||||||||||||||||||||||||||||||||||||||||||||||||||||||||
Seq_2  4918  ATTTTGCACTTTCTGGTAGTTCCCCTGTTTTTTCTAATTCCCTAAAATTGTGTGGGTGGA  4977

Seq_1  754   GTGGAGCCCTGCAGTTGGGGGGTAACATGGACCACTGATTTTGCCCTTTGACCCTGCACA  813
              |||||||||||||||||||||||||||||||||||||||||||||||||||||||||||
Seq_2  4978  GTGGAGCCCTGCAGTTGGGGGGTAACATGGACCACTGATTTTGCCCTTTGACCCTGCACA  5037

Seq_1  814   ATGACCTTTGCATCAGCCAAACTCATTGCCATGACAACTCTTTGTACTGTGTCCGTGCCA  873
              |||||||||||||||||||||||||||||||||||||||||||||||||||||||||||
Seq_2  5038  ATGACCTTTGCATCAGCCAAACTCATTGCCATGACAACTCTTTGTACTGTGTCCGTGCCA  5097

Seq_1  874   CAGATCTGTTGGTCACATTGTTAATAGTAAAGGGGACAAGTTGGAGACGGTCAATTTTTA  933
              |||||||||||||||||||||||||||||||||||||||||||||||||||||||||||
Seq_2  5098  CAGATCTGTTGGTCACATTGTTAATAGTAAAGGGGACAAGTTGGAGACGGTCAATTTTTA  5157

Seq_1  934   CATTTTTTGTTGCAATTTTTTCTTCAATGGGTGTAAGTAGTTTTTTTTTTTTT---AATAA  990
              |||||||||||||||||||||||||||||| ||||||||||||||||||||   |||||
Seq_2  5158  CATTTTTTGTTGCAATTTTTTCTTCAATGGTTGTAAGTAGTTTTTTTTTTTTTTTTAATAA  5217

Seq_1  991   TAAAAGGG-TCACTAGTTAATACTCTAGAAATATCTGTGTGTTGCAATTCAAATGTATGT  1049
              |||||||| ||||||||||||||||||||||||||||||||||||||||||||||||||
Seq_2  5218  TAAAAGGGTTCACTAGTTAATACTCTAGAAATATCTGTGTGTTGCAATTCAAATGTATGT  5277
```

```
Seq_1  1050  TGAGATTGTGAAAAGCGCTTCAGTGGCACTAGCTTACCGGTACACTAGACTAAGCCCTTG  1109
             |||||||||||||||||||||||| ||||||||||||||||||||||||||||||||||
Seq_2  5278  TGAGATTGTGAAAAGCGCTTCAGTGCCACTAGCTTACCGGTACACTAGACTAAGCCCTTG  5337

Seq_1  1110  ATGACTTATTGCATGATACAGTACCAGGACCAACAGGTGGCCTAA
             |||||||||||||||||||||||||||| ||||||||||||||
Seq_2  5338  ATGACTTATTGCATGATACAGTACCAGGAACAACAGGTGGCCTAA
```

Sequencing result of **Luc-NFIB 3'UTR_D** (sample name: K5_1 sequenced with EBV-RP primer) aligned to NFIB 3'UTR.

```
Seq_1  121   GCAGGTCGACTCTAGACTCGAGTGCTGGAATTCGCCCTTCAGAGTCTGTAGCATAGCTCA  180
                                                 ||||||||||||||||||||
Seq_2  6466  ------------------------------------CAGAGTCTGTAGCATAGCTCA  6446

Seq_1  181   TTTTATTGTTTAAACAGTTTTTGCATAGGAAATATATCCGCTTCCAGTAATTGACTGCAG  240
             ||||||||||||||||||||||||||||||||||||||||||||||||||||||||||||
Seq_2  6445  TTTTATTGTTTAAACAGTTTTTGCATAGGAAATATATCCGCTTCCAGTAATTGACTGCAG  6386

Seq_1  241   TATGAGCAGCTGCTAGCAGTATAGGCTGGATATAACAGTAACAATCACATTAAGTCAAGC  300
             ||||||||||||||||||||||||||||||||||||||||||||||||||||||||||||
Seq_2  6385  TATGAGCAGCTGCTAGCAGTATAGGCTGGATATAACAGTAACAATCACATTAAGTCAAGC  6326

Seq_1  301   TTGATTTACACCAGTTTAAAACTTGTGGCAATTGAGTTCATTTGCAACCCACAAAAAGTA  360
             ||||||||||||||||||||||||||||||||||||||||||||||||||||||||||||
Seq_2  6325  TTGATTTACACCAGTTTAAAACTTGTGGCAATTGAGTTCATTTGCAACCCACAAAAAGTA  6266

Seq_1  361   CCCAAAGAACGTTATCCTCCAACCGGGCACAATAAAACCTTCACTAACATTCTGGCCCAG  420
             ||||||||||||||||||||||||||||||||||||||||||||||||||||||||||||
Seq_2  6265  CCCAAAGAACGTTATCCTCCAACCGGGCACAATAAAACCTTCACTAACATTCTGGCCCAG  6206

Seq_1  421   TCTGGGGTTGATCCCAGAGGCCTGAACTCTAGAAATTAAGTAACTGTCGTATAATACATC  480
             ||||||||||||||||||||||||||||||||||||||||||||||||||||||||||||
Seq_2  6205  TCTGGGGTTGATCCCAGAGGCCTGAACTCTAGAAATTAAGTAACTGTCGTATAATACATC  6146

Seq_1  481   CTACTGCTAAAGGTTTGTTACATGGAGATTGTGCATGTGCCTCCTTTTGTAAAAAAATTT  540
             ||||||||||||||||||||||||||||||||||||||||||||||||||||||||||||
Seq_2  6145  CTACTGCTAAAGGTTTGTTACATGGAGATTGTGCATGTGCCTCCTTTTGTAAAAAAATTT  6086

Seq_1  541   AATTAAAATACAAGGTTCTGTATTTATGGCCCATGAGGACAAAATGCCAAAAGTTTTAAA  600
             ||||||||||||||||||||||||||||||||||||||||||||||||||||||||||||
Seq_2  6085  AATTAAAATACAAGGTTCTGTATTTATGGCCCATGAGGACAAAATGCCAAAAGTTTTAAA  6026

Seq_1  601   ATGGATCAACCCTGGTGTGTAGCTAGCAAGCAATAACTGACTACTCGTCACCTACAGTTG  660
             ||||||||||||||||||||||||||||||||||||||||||||||||||||||||||||
Seq_2  6025  ATGGATCAACCCTGGTGTGTAGCTAGCAAGCAATAACTGACTACTCGTCACCTACAGTTG  5966

Seq_1  661   TACTAAATGTATCTAAAGAAACACACAGTCCTACAAAAGTTGTTCTCAGAGAAATATCAT  720
             ||||||||||||||||||||||||||||||||||||||||||||||||||||||||||||
Seq_2  5965  TACTAAATGTATCTAAAGAAACACACAGTCCTACAAAAGTTGTTCTCAGAGAAATATCAT  5906

Seq_1  721   TGAGGTGGGGGCAGCTCTTCCCAGGATGCTAAAAGTTCTATATGATATAAGCACAAATTA  780
             ||||||||||||||||||||||||||||||||||||||||||||||||||||||||||||
Seq_2  5905  TGAGGTGGGGGCAGCTCTTCCCAGGATGCTAAAAGTTCTATATGATATAAGCACAAATTA  5846

Seq_1  781   ACAGCTTGATGAAGACATAATCTACTGCAGCTTTGAGAAACCTATGCCTGGGATGTAGTT  840
             ||||||||||||||||||||||||||||||||||||||||||||||||||||||||||||
Seq_2  5845  ACAGCTTGATGAAGACATAATCTACTGCAGCTTTGAGAAACCTATGCCTGGGATGTAGTT  5786

Seq_1  841   ACCCCTCACATTCTACAATGTTGTAGAGATTTTTTTTCCCA-GAAAATGTCATTTGAA-C  898
             |||||||||||||||||||||||||||||||||||||||| ||||||||||||||||| |
Seq_2  5785  ACCCCTCACATTCTACAATGTTGTAGAGATTTTTTTTCCCAAGAAAATGTCATTTGAAAC  5726

Seq_1  899   ATATTTACAACTGAACTCTACAGAGACTGTGAAATTGAACAGGCACTGCTCATTTGTTTG  958
             |||||||||||||||||| ||||||||||||||||||||||||||||||||||||||||
Seq_2  5725  ATATTTACAACTGAACTCAACAGAGACTGTGAAATTGAACAGGCACTGCTCATTTGTTTG  5666
```

APPENDIX K:

Alignment of sequencing results after site-direccted mutagenesis for Luc-NFIB 3'UTR_B-124M and Luc-NFIB 3'UTR_D-153M.

Sequencing result of **Luc-NFIB 3'UTR_B-124M** (sample name: B124-2). (Highlighet region shows mutated sequences).

```
Seq_1  183   ----------------ATCTCAGGGTGCACTGCTTCACAGCTACACTGCAAAGTGTTAAA  226
                             |||||||||||||||||||||||||||||||||||||||||||
Seq_2  2141  tttgcagcccaggcccatctcagggtgcactgcttcacagctacactgcaaagtgttaaa  2082

Seq_1  227   AATCCTCCCACCCACCCCAGAATATATATATATGTATATTAAAAAAAATCCCCTGTCCAT  286
             ||||||||||||||||||||||||||||||||||||||||||||||||||||||||||||
Seq_2  2081  aatcctcccacccaccccagaatatatatatatgtatattaaaaaaaatcccctgtccat  2022

Seq_1  287   CTCTCAGTACACAAAAGGACCTCATCACACTGCAAAAATAGCAGTACCCACTTTGGTCAA  346
             ||||||||||||||||||||||||||||||||||||||||||||||||||||||||||||
Seq_2  2021  ctctcagtacacaaaaggacctcatcacactgcaaaaatagcagtacccactttggtcaa  1962

Seq_1  347   TTAAAACAAACAAACAAACAAAAAAGCATACATTATTTTTTTTTTAAATCTGTGTACTTA  406
             ||||||||||||||||||||||||||||||||||||||||||||||||||||||||||||
Seq_2  1961  ttaaaacaaacaaacaaacaaaaaagcatacattatttttttttaaatctgtgtactta  1902

Seq_1  407   CCTATAATAACCAATACAGCTAAAAGCACTACCTACATAGGCAAAACTTGGTATTGCATA  466
             ||||||||||||||||||||||||||||||||||||||||||||||||||||||||||||
Seq_2  1901  cctataataaccaatacagctaaaagcactacctacataggcaaaacttggtattgcata  1842

Seq_1  467   ATTCGTATAAATTTGAAACCCCTCCCCCCCCAAATATTAATTGGAAGATGAAAAACATGAA  526
             ||||||||||||||||||||||||||||||||||||||||||||||||||||||||||||
Seq_2  1841  attcgtataaatttgaaaccccctcccccccaaatattaattggaagatgaaaaacatgaa  1782

Seq_1  527   AGGTTAATAGAAAAAAACACCAAAATACTGAAAATATTGCTGGTCGATTACAATTTTTAA  586
             ||||||||||||||||||||||||||||||||||||||||||||||||||||||||||||
Seq_2  1781  aggttaatagaaaaaaacaccaaaatactgaaaatattgctggtcgattacaattttaa  1722

Seq_1  587   GCGGCAACTATACACAGCCATGATATGCTTTATAAATGTGAGATAAAGGTATAACTGTCT  646
             ||||||||||||||||||||||||||||||||||||||||||||||||||||||||||||
Seq_2  1721  gcggcaactatacacagccatgatatgctttataaatgtgagataaaggtataactgtct  1662

Seq_1  647   AAAAAATCCATGATGTCACACATTTTTCTTCGTCTGGAGTACAAAATATTTTGTCATAAA  706
             ||||||||||||||||||||||||||||||||||||||||||||||||||||||||||||
Seq_2  1661  aaaaaatccatgatgtcacacatttttcttcgtctggagtacaaaatattttgtcataaa  1602

Seq_1  707   AATGGTAAAGATTTAAAATGATAATAAATGCAGCAAAACAAGTGTAGTGATGTCACTTTG  766
             ||||||||||||||||||||||||||||||||||||||||||||||||||||||||||||
Seq_2  1601  aatggtaaagatttaaaatgataataaatgcagcaaaacaagtgtagtgatgtcactttg  1542

Seq_1  767   TTGTATTTTTTTTGTTTTTTTTTTTTTTGTTTTTTGTTTTTTAGATTTCAAGGCATCCGA  824
             ||||||||||||||||||||||||||||||||||||||||||||||||||||||||    |
Seq_2  1541  ttgtatttttttgttttttttttttttgttttttgttttttagatttcaaggcaaggca  1484

Seq_1  825   CGTAATGTGGACATTATATCTTCGTGCAAATTAGGATTACTGGAAAGAGTATTTTTAATT  884
             ||||||||||||||||||||||||||||||||||||||||||||||||||||||||||||
Seq_2  1483  cgtaatgtggacattatatcttcgtgcaaattaggattactggaaagagtatttttaatt  1424

Seq_1  885   AAAATTTTAAGAGACATAGAGGCAAAATGTGTCTGCCCATGCACACTATGGATCTGTCAA  944
             ||||||||||||||||||||||||||||||||||||||||||||||||||||||||||||
Seq_2  1423  aaaattttaagagacatagaggcaaaatgtgtctgcccatgcacactatggatctgtcaa  1364

Seq_1  945   TACAAGAAATTTGTTGAACAAGGCTAATGTCTGAAAGCACCATGCAAGTTTTCAGCACCC  1004
             ||||||||||||||||||||||||||||||||||||||||||||||||||||||||||||
Seq_2  1363  tacaagaaatttgttgaacaaggctaatgtctgaaagcaccatgcaagttttcagcaccc  1304

Seq_1  1005  TGATTACATTTGTTTTCTCAAGAGTGCGTTTTTATATCCTACACCCTGGCGTTCCCAGTT  1064
             ||||||||||||||||||||||||||||||||||||||||||||||||||||||||||||
Seq_2  1303  tgattacatttgttttctcaagagtgcgttttatatcctacaccctggcgttcccagtt  1244

Seq_1  1065  TGTAAACTGTAAGCTTTACCCTTGTGACATGGATTTGCCTGCCTCTTTGTCTCTATAATG  1124
             ||||||||||||||||||||||||||||||||||||||||||||||||||||||||||||
Seq_2  1243  tgtaaactgtaagctttacccttgtgacatggatttgcctgcctctttgtctctataatg  1184
```

Sequencing result of **Luc-NFIB 3'UTR_D-153M** (sample name: A153-6) aligned to NFIB 3'UTR. (Highlighet region shows mutated sequences).

```
Seq_1  121   CTGCAGGTCGACTCTAGACTCGAGTGCTGGAATTCGCCCTTCAGAGTCTGTAGCATAGCT  180
             ##########################################|||||||||||||||
Seq_2  6461  ------------------------------------------tctgtagcatagct  6448

Seq_1  181   CATTTTATTGTTTAAACAGTTTTTCGTAAGGAAATATATCCGCTTCCAGTAATTGACTG  239
             |||||||||||||||||||||||    ||||||||||||||||||||||||||||||
Seq_2  6447  catttattgtttaaacagttttgcataggaaatatatccgcttccagtaattgactg  6389

Seq_1  240   CAGTATGAGCAGCTGCTAGCAGTATAGGCTGGATATAACAGTAACAATCACATTAAGTCA  299
             ||||||||||||||||||||||||||||||||||||||||||||||||||||||||||||
Seq_2  6388  cagtatgagcagctgctagcagtataggctggatataacagtaacaatcacattaagtca  6329

Seq_1  300   AGCTTGATTTACACCAGTTTAAAACTTGTGGCAATTGAGTTCATTTGCAACCCACAAAAA  359
             ||||||||||||||||||||||||||||||||||||||||||||||||||||||||||||
Seq_2  6328  agcttgatttacaccagtttaaaacttgtggcaattgagttcatttgcaacccacaaaaa  6269

Seq_1  360   GTACCCAAAGAACGTTATCCTCCAACCGGGCACAATAAAACCTTCACTAACATTCTGGCC  419
             ||||||||||||||||||||||||||||||||||||||||||||||||||||||||||||
Seq_2  6268  gtacccaaagaacgttatcctccaaccgggcacaataaaaccttcactaacattctggcc  6209

Seq_1  420   CAGTCTGGGGTTGATCCCAGAGGCCTGAACTCTAGAAATTAAGTAACTGTCGTATAATAC  479
             ||||||||||||||||||||||||||||||||||||||||||||||||||||||||||||
Seq_2  6208  cagtctggggttgatcccagaggcctgaactctagaaattaagtaactgtcgtataatac  6149

Seq_1  480   ATCCTACTGCTAAAGGTTTGTTACATGGAGATTGTGCATGTGCCTCCTTTTGTAAAAAAA  539
             ||||||||||||||||||||||||||||||||||||||||||||||||||||||||||||
Seq_2  6148  atcctactgctaaaggtttgttacatggagattgtgcatgtgcctcctttgtaaaaaaa  6089

Seq_1  540   TTTAATTAAAAATACAAGGTTCTGTATTTATGGCCCATGAGGACAAAATGCCAAAAGTTTT  599
             ||||||||||||||||||||||||||||||||||||||||||||||||||||||||||||
Seq_2  6088  tttaattaaaatacaaggttctgtatttatggcccatgaggacaaaatgccaaaagtttt  6029

Seq_1  600   AAAATGGATCAACCCTGGTGTGTAGCTAGCAAGCAATAACTGACTACTCGTCACCTACAG  659
             ||||||||||||||||||||||||||||||||||||||||||||||||||||||||||||
Seq_2  6028  aaaatggatcaaccctggtgtgtagctagcaagcaataactgactactcgtcacctacag  5969

Seq_1  660   TTGTACTAAATGTATCTAAAGAAACACACAGTCCTACAAAAGTTGTTCTCAGAGAAATAT  719
             ||||||||||||||||||||||||||||||||||||||||||||||||||||||||||||
Seq_2  5968  ttgtactaaatgtatctaaagaaacacacagtcctacaaaagttgttctcagagaaatat  5909

Seq_1  720   CATTGAGGTGGGGGCAGCTCTTCCCAGGATGCTAAAAGTTCTATATGATATAAGCACAAA  779
             ||||||||||||||||||||||||||||||||||||||||||||||||||||||||||||
Seq_2  5908  cattgaggtgggggcagctcttcccaggatgctaaaagttctatatgatataagcacaaa  5849

Seq_1  780   TTAACAGCTTGATGAAGACATAATCTACTGCAGCTTTGAGAAACCTATGCCTGGGATGTA  839
             ||||||||||||||||||||||||||||||||||||||||||||||||||||||||||||
Seq_2  5848  ttaacagcttgatgaagacataatctactgcagctttgagaaacctatgcctgggatgta  5789

Seq_1  840   GTTACCCCTCACATTCTACAATGTTGTAGAGATTTTTTTTCCCAAGAAAATGTCATTTGA  899
             ||||||||||||||||||||||||||||||||||||||||||||||||||||||||||||
Seq_2  5788  gttacccctcacattctacaatgttgtagagatttttttcccaagaaaatgtcatttga  5729

Seq_1  900   AACATATTTACAACTGAACTCAACAGAGACTGTGAAATTGAACAGGCACTGCTCATTTGT  959
             ||||||||||||||||||||||||||||||||||||||||||||||||||||||||||||
Seq_2  5728  aacatatttacaactgaactcaacagagactgtgaaattgaacaggcactgctcatttgt  5669
```

APPENDIX L:

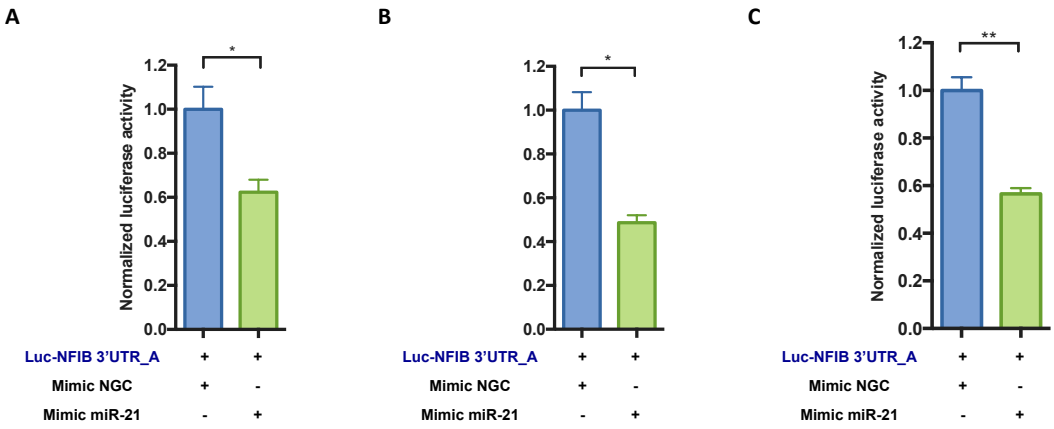


Figure L.1 : miR-21 represses Luc-NFIB 3'UTR_A. We assayed firefly luciferase activity relative to *Renilla* luciferase activity in HEK293T cells ($2x10^4$ number of cells/well) 48 h after transfected with reporter construct in the presence of 20 nM miR-21 mimics, or mimic negative control (NGC). Bars represent luciferase activity normalized to the mean activity of samples transfected with the mimic negative control. x-axis depicts treatment conditions. Data were expressed as mean±S.D. from 3 replicates and the significance of differences was determined using t-test analysis (**p<0.001; *p<0.05). Results show the first **(A)** and second **(B)** and third **(C)** independent experiments.

APPENDIX M:

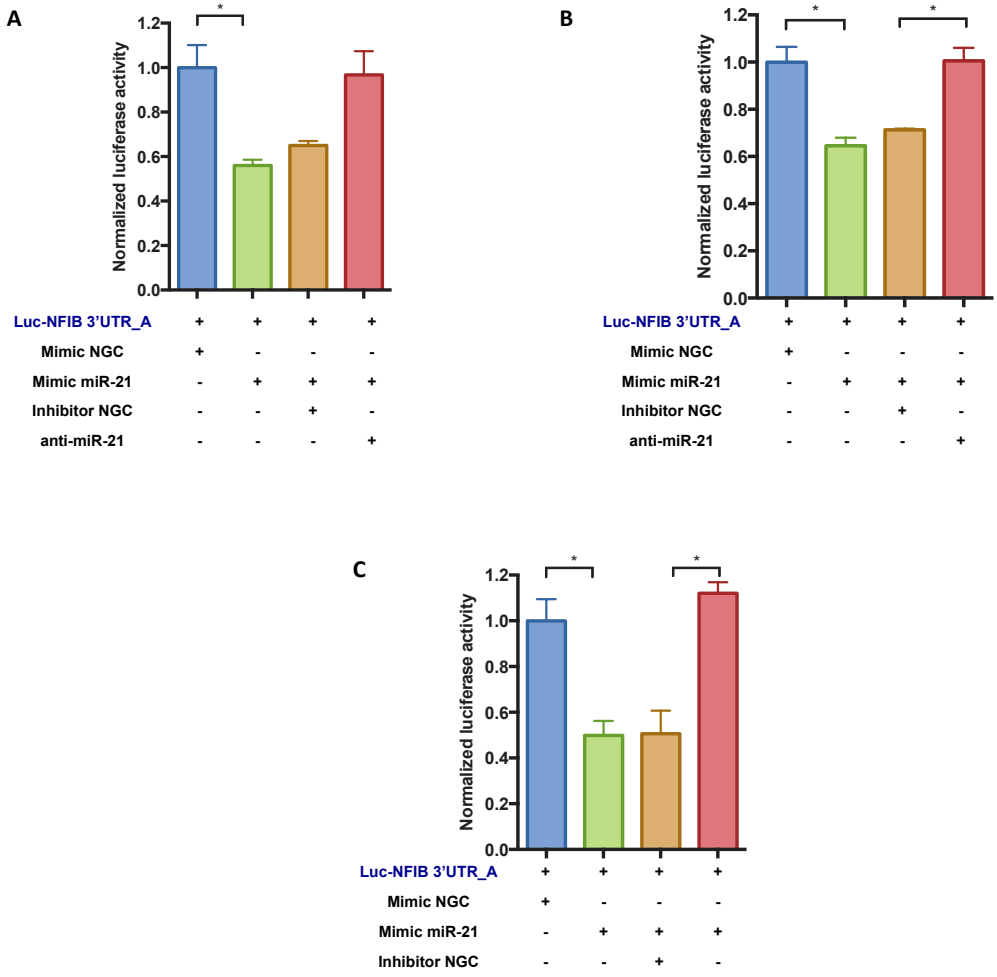


Figure M.1 : Binding of miR-21 on Luc-NFIB 3'UTR_A is reversed by anti-pre-miR-21. The average calculated signal ratios of *Renilla* and firefly luciferase from three different experiments 48h after co-transfection of vector construct (Luc-NFIB 3'UTR_A; 150 ng) and 20 nM miR-21 mimic with 100 nM anti-miR-21, relative to 100 nM inhibitor negative control to HEK293T cells ($2x10^4$ number of cells/well). Bars represent luciferase activity normalized to the mean activity of samples transfected with the mimic negative control. x-axis depicts treatment conditions. Data were expressed as mean±S.D. from 3 replicates and the significance of differences was determined using t-test analysis (*$p<0.05$). Results show the first **(A)** and second **(B)** and third **(C)** independent experiments.

APPENDIX N:

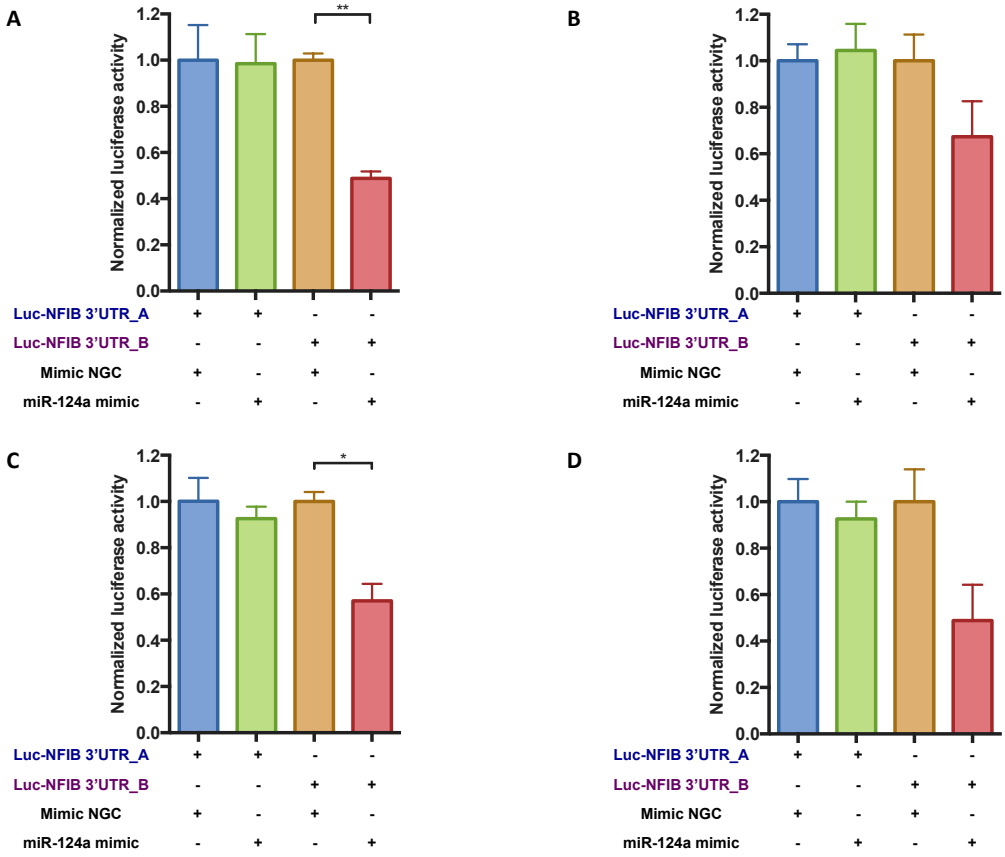


Figure N.1 : miR-124a represses Luc-NFIB 3'UTR_B, but not Luc-NFIB 3'UTR_A. We assayed firefly luciferase activity relative to *Renilla* luciferase activity in HEK293T cells ($2x10^4$ number of cells/well) 48 h after transfected with reporter construct in the presence of 20 nM miR-124a mimics, or mimic negative control (NGC). Bars represent luciferase activity normalized to the mean activity of samples transfected with the mimic negative control. x-axis depicts treatment conditions. Data were expressed as mean±S.D. from 3 replicates and the significance of differences was determined using t-test analysis (**p<0.001; *p<0.05). Results show the first **(A)**, second **(B)**, third **(C)** and fourth **(D)** independent experiments.

APPENDIX O:

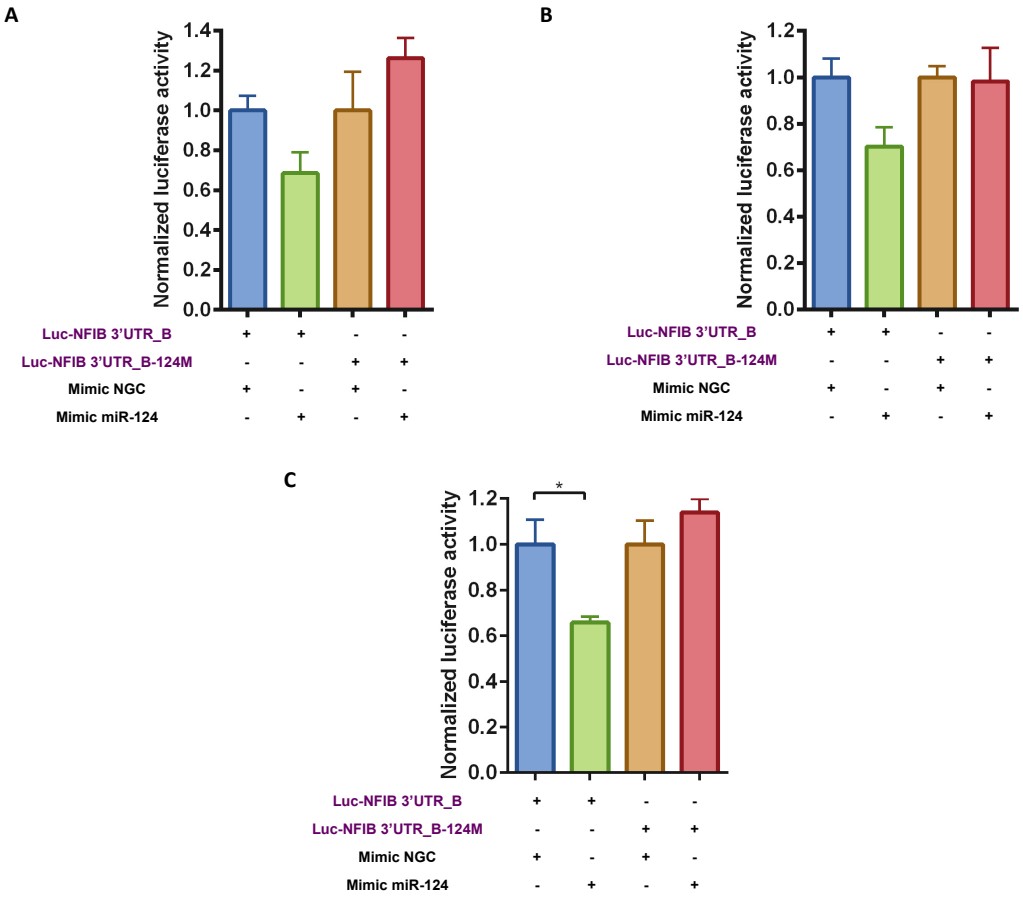


Figure O.1 : Binding of miR-124a does not repress Luc-NFIB 3'UTR_B-124M. The average calculated signal ratios of *Renilla* and Firefly luciferase from three different experiments 48h after co-transfection of vector constructs (Luc-NFIB 3'UTR_B and Luc-NFIB 3'UTR_B-124M; 150 ng) and 20 nM miR-124a mimics to HEK293T cells ($2x10^4$ number of cells/well). Bars represent luciferase activity normalized to the mean activity of samples transfected with the mimic negative control. x-axis depicts treatment conditions. Data were expressed as mean±S.D. from 3 replicates and the significance of differences was determined using t-test analysis (*$p<0.05$). Results show the first **(A)**, second **(B)**, third **(C)** independent experiments.

APPENDIX P:

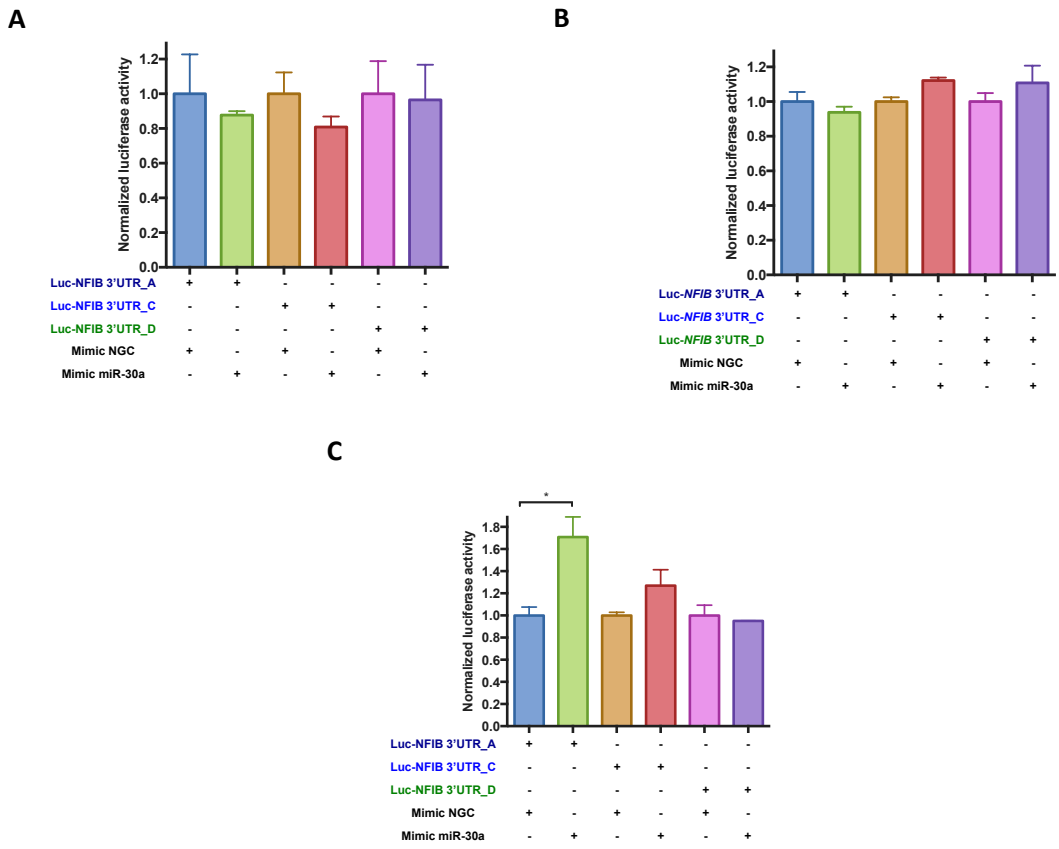


Figure P.1 : miR-30a cannot repress translation from Luc-NFIB 3'UTR_A, Luc-NFIB 3'UTR_C or Luc-NFIB 3'UTR_D. We assayed firefly luciferase activity relative to *Renilla* luciferase activity in HEK293T cells ($2x10^4$ number of cells/well) 48 h after transfected with reporter constructs in the presence of 20 nM miR-30a mimic, or mimic negative control (NGC). Bars represent luciferase activity normalized to the mean activity of samples transfected with the mimic negative control. x-axis depicts treatment conditions. Data were expressed as mean±S.D. from 3 replicates and the significance of differences was determined using t-test analysis (*$p<0.05$). Results show the first **(A)**, second **(B)** and third **(C)** independent experiments.

APPENDIX R:

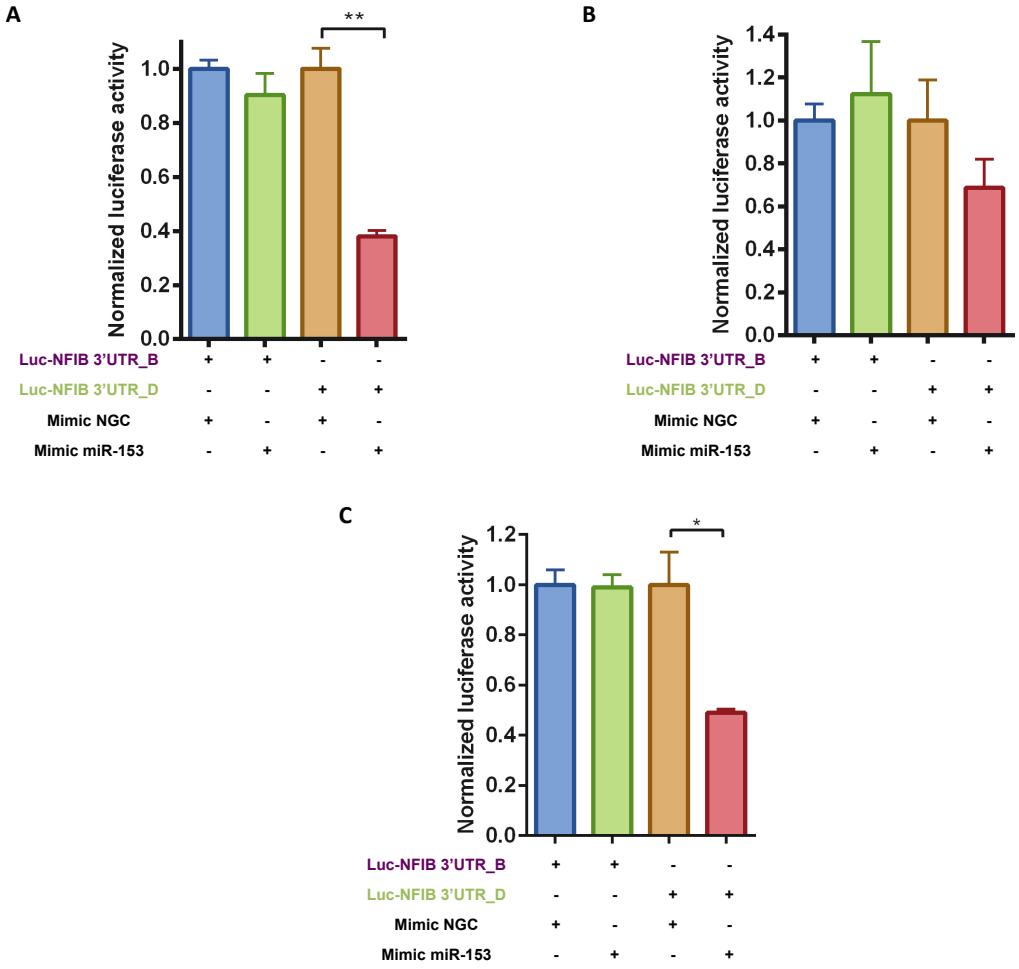


Figure R.1 : miR-153 repressed Luc-NFIB 3'UTR_D but not Luc-NFIB 3'UTR_B. We assayed firefly luciferase activity relative to *Renilla* luciferase activity in HEK293T cells ($2x10^4$ number of cells/well) 48 h after transfected with reporter construct in the presence of 20 nM miR-153 mimic, or mimic negative control (NGC). Bars represent luciferase activity normalized to the mean activity of samples transfected with the mimic negative control. x-axis depicts treatment conditions. Data were expressed as mean±S.D. from 3 replicates and the significance of differences was determined using t-test analysis (**p<0.001; *p<0.05). Results show the first **(A),** second **(B)** and third **(C)** independent experiments.

APPENDIX S:

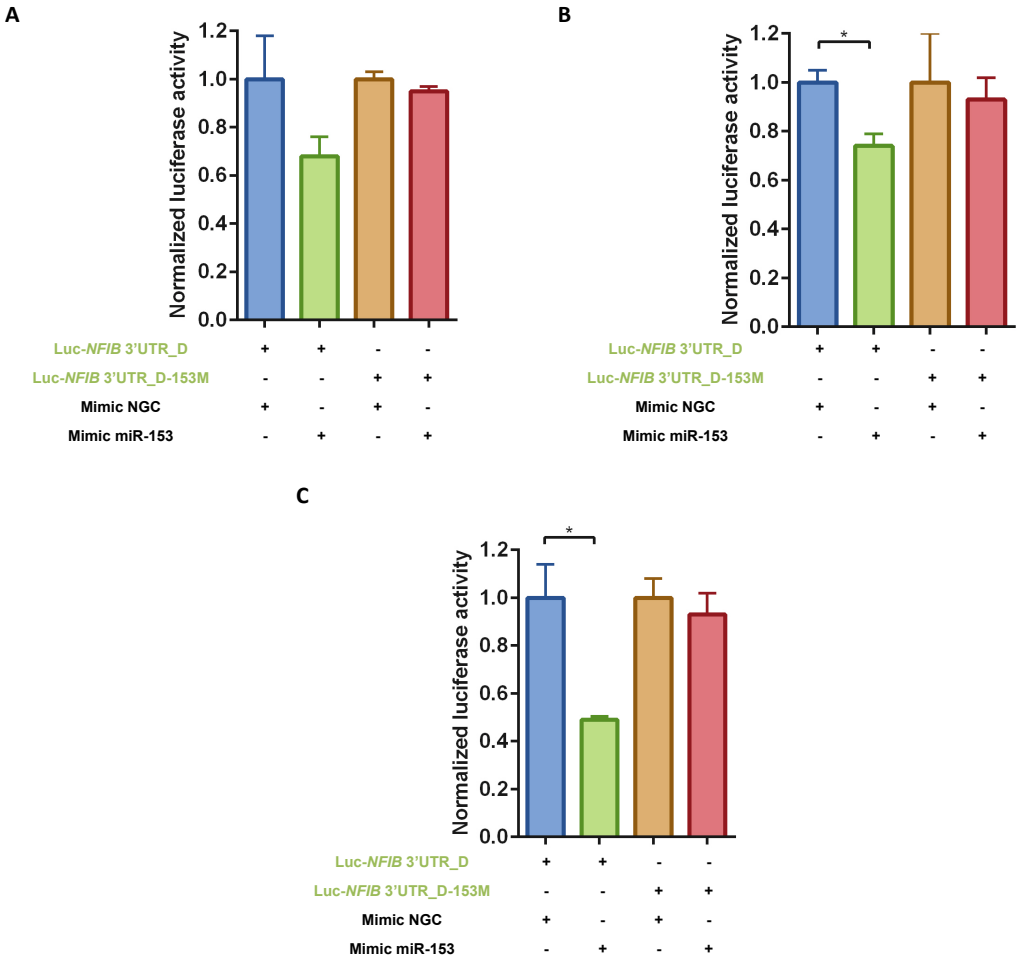


Figure S.1 : Binding of miR-153 does not repress Luc-NFIB 3'UTR_D-153M. The average calculated signal ratios of *Renilla* and firefly luciferase from three different experiments 48h after co-transfection of vector constructs (Luc-NFIB 3'UTR_D and Luc-NFIB 3'UTR_D-153M; 150 ng) and 20 nM miR-153 mimics to HEK293T cells ($2x10^4$ number of cells/well). Bars represent luciferase activity normalized to the mean activity of samples transfected with the mimic negative control (NGC). x-axis depicts treatment conditions. Data were expressed as mean±S.D. from 3 replicates and the significance of differences was determined using t-test analysis (**p<0.001; *p<0.05). Results show the first **(A)**, second **(B)** and third **(C)** independent experiments.

APPENDIX T:

Sequence alignment of mouse, rat and human NFIB 3'UTR sequences (by CLUSTAL-W2).

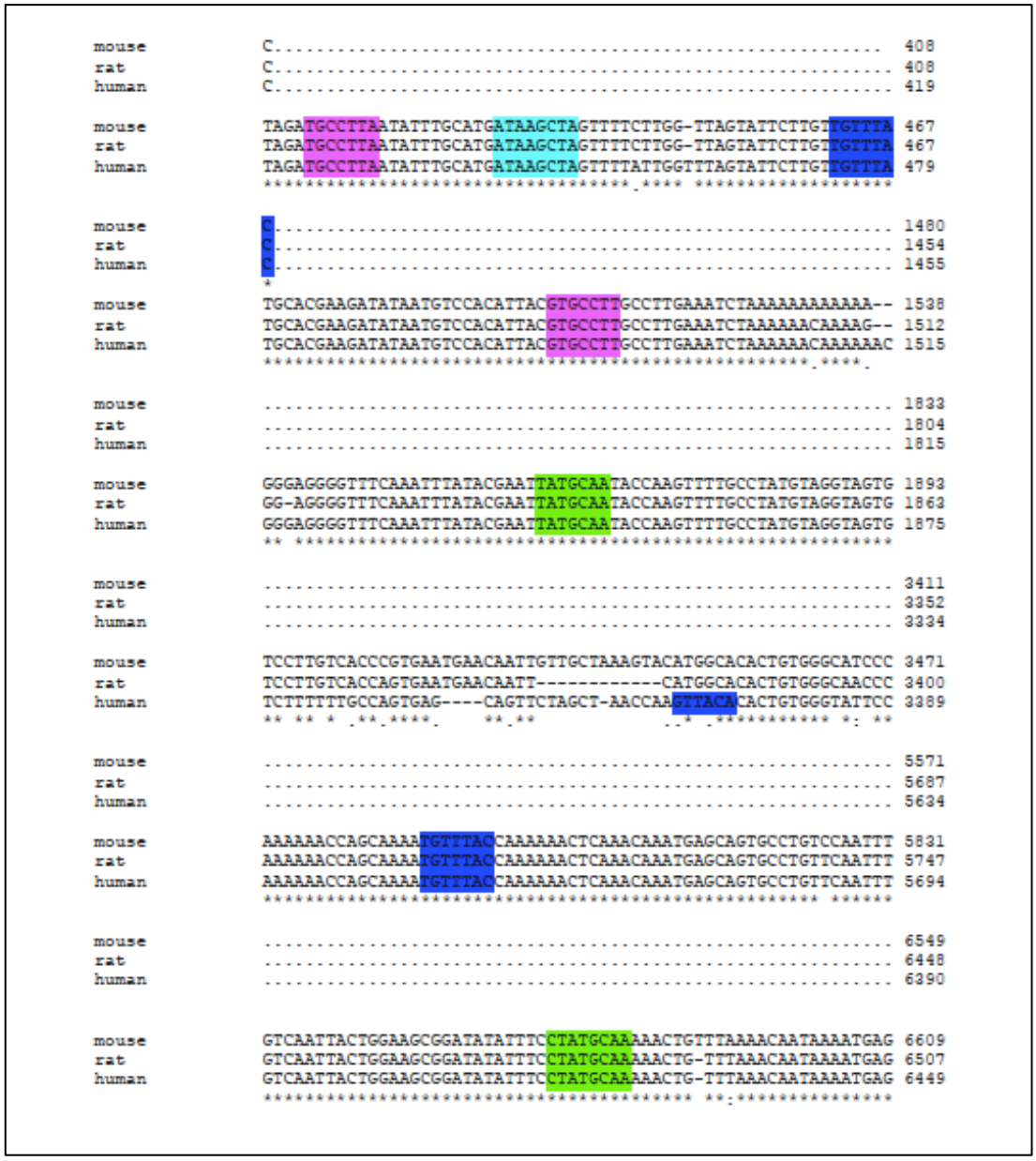


Figure T.1 : Predicted binding sites of potential NFIB targeting miRNAs in human, mouse and human. Binding sites are highlighted in the alignment of sequences above (miR-21 is blue; miR-30a is dark blue; miR-153 is green and miR-124a binding sites are pink).

CURRICULUM VITAE



Name Surname: **Gökçe CESUR**

Place and Date of Birth: Çanakkale, 10.09.1989

E-Mail: gokcesurr@gmail.com

EDUCATION:

B.Sc.: Istanbul Technical University, Faculty of Science & Letters, Department of Molecular Biology & Genetics, 2012

POSTER PRESENTATIONS ON THE THESIS:

Cesur, G., Uluca, B., Kumbasar, A., "Regulation of NFI and NFI-dependent Gene Expression in Human Neural Stem Cells", 3rd International Congress of the Molecular Biology Association of Turkey, 2014, Izmir, Turkey.

OTHER POSTER PRESENTATIONS:

Yılmaz, E. A., **Cesur, G.,** Güler, V., Kumbasar, A. "Identification of Novel Binding Partners of Nuclear Factor One B", 2nd International Congress of the Molecular Biology Association of Turkey, 2013, Istanbul, Turkey.